MECHANOSENSORY CELLS AND SWIMMING BEHAVIOUR OF EMBRYOS OF THE SEA URCHIN STRONGYLOCENTROTUS PURPURATUS

by

Maria Volnoukhin
B.Sc., Simon Fraser University, 2004

THESIS SUBMITTED IN PARTIAL FULFILLMENT OF
THE REQUIREMENTS FOR THE DEGREE OF

MASTER OF SCIENCE

In the
Department
of
Molecular Biology and Biochemistry

SIMON FRASER UNIVERSITY

Summer 2010

Approval

Name: **Maria Volnoukhin**

Degree: **Master of Science**

Title of Thesis: **Mechanosensory cells and swimming behaviour of embryos of the sea urchin *Strongylocentrotus purpuratus*.**

Examining Committee:

Chair: **Dr. Jenifer Thewalt**
Professor, Department of Molecular Biology and Biochemistry, SFU

Dr. Bruce P. Brandhorst
Senior Supervisor
Professor, Department of Molecular Biology and Biochemistry, SFU

Dr. Michel Leroux
Supervisor
Professor, Department of Molecular Biology and Biochemistry, SFU

Dr. Lynne Quarmby
Supervisor
Professor, Department of Molecular Biology and Biochemistry, SFU

Dr. Michael Hart
Internal Examiner
Associate professor, Department of Biological Sciences, SFU

Date Defended/Approved: August 18, 2010

Declaration of
Partial Copyright Licence

Abstract

Recent sequencing of the genome of the sea urchin Strongylocentrotus purpuratus identified Usher syndrome genes involved in photo- and mechanosensation in vertebrate retina and inner ear as well as the TRPA1 ion channel often involved in mechanosensation. Sensory cells have not been definitively identified in sea urchins despite the known photo- and mechanosensory capabilities of adults, larvae and embryos. To identify sensory cells in embryos and early larvae expression of Usher and TRPA1 genes was investigated, but did not identify candidate sensory cells. Some Usher genes were expressed in neurogenic ectoderm of embryos. Screening for cells having putative mechanosensory channels was performed using cationic fluorescent dyes and identified several types, including blastocoelar cells. Temporal expression of the TRPA1 gene and inhibition of swimming activity by ion channel inhibitors suggest its involvement in control of swimming. This study provides evidence that mechanosensory channels modulate swimming behaviour of embryos and early larvae.

Keywords: sea urchin; Usher syndrome; TRPA1; sensory cells; FM1-43; TO-PRO-3

Acknowledgements

I am very grateful to Dr. Bruce P. Brandhorst for his guidance and support. I wish to thank Dr. Michel Leroux and Dr. Lynne Quarmby, for the time they have devoted to being on my supervisory committee and for their invaluable advice on my project. I offer my gratitude to Dr. Michael Hart for taking on a role of the internal examiner for my Thesis and for his insightful comments on my work. I also wish to thank Dr. Tim Heslip for microscopy consultations, for his technical help and suggestions on experimental design.

A special thank you goes out to the Brandhorst Lab team, Karl-Frederik Bergeron and Barton Xu, for sharing their expertise, providing their honest constructive criticism of my project, and also much appreciated assistance with my experiments.

Lastly, I wish to thank my family and my friends for all of their help and encouragement throughout this endeavour.

Table of Contents

List of Figures

List of Tables

List of Abbreviations

µg	Micrograms
µl	Microlitres
µM	Micromolar
µm	Micrometres
5HT	5-hydroxytryptamine
aa	amino acid
Ab	Antibody
Ac	Achaete acute
AP	alkaline phosphatase
ASW	artificial seawater
b	Base
BCIP/NBT	5-Bromo-4-Chloro-3'-Indolyphosphate p-Toluidine Salt/Nitro-Blue Tetrazolium Chloride
BLAST	Basic Local Alignment Search Tool
blastn	nucleotide BLAST
blastp	protein BLAST
bp	base pair
BSA	Bovine Serum Albumin
Ca^{2+}	Calcium ion

Cat. No.	catalog number
cDNA	complementary DNA
cm	Centimetres
CSPD	chloro-5-substituted xiidamantly-1,2-dioxetane phosphate
Cy3	Cyanine 3
DEPC	Diethylpyrocarbonate
DEPC-H_2O	diethylpyrocarbonate treated deionized water
DIC	Differential Interference Contrast
DIG	Digoxigenin
DlgA	Drosophila disc large tumor suppressor
DMSO	dimethyl sulfoxide
DNA	deoxyribonucleic acid
DNase	Deoxyribonuclease
dNTP	Deoxyribonucleotide triphosphate
dT20	Primer containing 20 deoxythymidylic acid residues
DTT	Dithiothreitol
ECL	Enhanced chemiluminescence
EcoRV	*Escherichia coli* J62 pLG74 restriction endonuclease
ECPN	Encephalopsin
EDTA	ethyleneediaminetetraacetic acid
EGTA	ethylene glycol tetraacetic acid
EMBL	European Molecular Biology Laboratory
Fig.	Figure

FSW	filtered seawater
GABA	gamma-aminobutyric acid
Gd^{3+}	gadolinium ion
GPR98	G protein-coupled receptor 98
H_2O	deionized water
Hbn	Homeobrain
Hnf	Hepatocyte nuclear factor
Hp	*Hemicentrotus pulcherrimus*
hpf	hours post fertilization
hr(s)	hour(s)
HRP	horse radish peroxidase
InaD	Inactivation no afterpotential D
kb	Kilobase
KB	Kilobytes
L	Litres
LB	Luria Bertani Broth
MASO	morpholino antisense oligonucleotide
MB	Megabytes
MBL	Marine Biological Laboratory
MET	mechano-electric transducer
mg	Milligrams
min	Minutes
ml	Millilitres

mm	Millimetres
mM	Millimolar
M-MLV-RT	Moloney Murine Leukemia Virus Reverse Transcriptase
MOPS	3-morpholinopropane-1-sulfonic acid
mRNA	messenger RNA
NCBI	National Centre for Biotechnology Information
NEPCC	North East Pacific Culture Collection
ng	Nanograms
NIDCR	National Institute of Dental and Craniofacial Research
nm	Nanometres
No.	Number
NompC	No mechanoreceptor potential C (channel)
nr/nt	non-redundant /nucleotide
O/N	overnight (16-18 hrs)
ºC	degrees Celsius
PBS	Phosphate buffered saline
PBS-T	PBS containing 0.1% v/v Triton X-100
pBS-T	pBluescript II KS+ T-tailed vector
pCPA	p-chlorophenylalanine
PCR	Polymerase Chain Reaction
PDZ	PSD95, DlgA, zo-1
pH	potential of hydrogen
PI	Propidium iodide

PMC(s)	Primary mesenchyme mell(s)
POD	Peroxidase
PRE	Retinal pigment epithelium
PSD95	Post synaptic density protein 95
PSI-BLAST	Position Specific Iterative BLAST
PVC	Polyvinyl chloride
RNA	Ribonucleic acid
RNase	Ribonuclease
RNAseOUT	recombinant ribonuclease inhibitor
RT	room temperature (ambient temperature)
Rx	Retinal anterior homeobox
SAM	Sterile alpha motif
SDS	sodium dodecyl sulphate
SDS-PAGE	sodium dodecyl sulfate polyacrylamide gel electrophoresis
sec	Seconds
SMART	Simple Modular Architecture Research Tool
SMC(s)	secondary mesenchyme cell (s)
SOC	Super Optimal broth with Catabolite repression
Sp	*Strongylocentrotus purpuratus*
SPU	*Strongylocentrotus purpuratus*
Spur	*Strongylocentrotus purpuratus*
SRN	Serotonin Receptor cell Network
SSC	Saline Sodium Citrate

SW	Seawater
T	Treated
Ta	Annealing Temperature
Taq	*Thermus aquaticus*
TBS	Tris buffered saline
TBS-T	TBS containing 0.1% v/v Triton X-100
Tris-HCl	Tris(hy droxymethyl) amino methane hydrochloride
TRP	Transient Receptor Potential (channel)
TRPA	TRP Ankyrin (channel)
TRPC	TRP Canonical (channel)
TRPM	TRP Melastatin (channel)
TRPML	TRP Mucopilin (channel)
TRPN	TRP No mechanoreceptor potential C (channel)
TRPP	TRP Polycystin (channel)
TRPV	TRP Vanilloid (channel)
TSA	Tyramide Signal Amplification
TTP	Thymidine triphosphate
U	Units
UT	Untreated
UV	Ultraviolet
v	Volume
V	Volts
WMIFS	Whole Mount Immunofluorescent Staining

WMISH	Whole Mount In Situ Hybridization
x	Times
x*g*	Gravitational acceleration
zo-1	zonula occludens-1

1: Introduction

1.1 Sea urchin phylogeny and their use in research

The sea urchin is a marine invertebrate having a radially symmetric adult form and bilaterally symmetric larvae, which shares a common deuterostome ancestor with chordates. The sea urchins are considered to be some of the closest relatives of chordates (refer to Fig. 1 in Sea Urchin Genome Sequencing Consortium et al. (2006)) . Sea urchin development is indirect, whereby larvae metamorphose into adults with a radically different body plan and behaviour.

Historically, sea urchin has been an important model organism for studies of embryonic development. Its embryos can be easily obtained by external fertilization and cultured in large numbers. The embryos are nearly transparent making them especially suitable for microscopy. Experimental approaches are available to knock down and overexpress genes in embryos. A gene regulatory network involved in specification of cell fates during embryonic development has been well characterized (Oliveri and Davidson, 2004).

According to annotations of the recently sequenced genome of sea urchin *Strongylocentrotus purpuratus* (Sea Urchin Genome Sequencing Consortium et al., 2006) the sea urchin has 28,944 predicted coding genes, including orthologues of 7077 genes in humans, 7021 in mice and 6366 in ascidians. Fewer gene orthologues are shared with protostomes: 5344 genes in *Drosophila* and 4475 genes in *Caenorhabditis elegans* (refer to Fig. 2 in Sea Urchin Genome Sequencing Consortium et al. (2006)).

Homologues of almost all vertebrate gene families have been found in the sea urchin genome. Some of the most important findings include human disease genes which were previously thought to be restricted to chordates or vertebrates (Sea Urchin Genome Sequencing Consortium et al., 2006). These findings have made the sea urchin a valuable model organism for studying evolutionary relationships between the invertebrates, chordates and vertebrates and their genes.

1.2 Orthologues of hearing, vision and balance genes in *S. purpuratus*

The finding of orthologues of human Usher syndrome genes in the genome of *S. purpuratus* was surprising as they had been previously considered to be vertebrate specific. Usher genes are involved in vision, hearing and balance in humans and other vertebrates (Whittaker et al., 2006). Genes for proteins involved in phototransduction like photorhodopsins and retinal transcription factors were found expressed in developing larvae and adult tube feet (Burke et al., 2006). A member of TRPA subfamily involved in mechanotransduction in vertebrate hearing and balance, TRPA1, was also annotated (Sea Urchin Genome Sequencing Consortium et al., 2006).

The presence of genes involved in vertebrate hearing, vision and balance in the sea urchin genome suggests previously unknown sensory capabilities in larvae and adults (Burke et al., 2006). These findings were surprising given that sea urchin adults and larvae lack of obvious sensory organs. Nevertheless, these findings suggest that sea urchins are able to receive light and mechanical signals from the environment. The discovery of these genes in sea urchins presents an opportunity to gain insight into evolution of vertebrate sensory genes and organs.

1.2.1 Usher genes in *S. purpuratus*.

1.2.1.1 Overview of Usher syndrome and functions of Usher proteins

Usher syndrome is a human recessive autosomal disorder, which affects hearing, balance and vision (Ahmed et al., 2003). It is the most common cause of combined deafness and blindness, and it is responsible for approximately one half of total cases diagnosed (Saihan et al., 2009).

Three clinical subtypes for Usher syndrome have been identified: I, II (Smith et al., 1994; Tsilou et al., 2002; Wagenaar et al., 1999) and III (Sankila et al., 1995). Different subtypes result in varying degrees of hearing loss, vestibular dysfunction and retinal degeneration. Subtype I causes the most severe symptoms that are manifested early in life, and subtype III causes the least severe symptoms, which appear later in life (Kremer et al., 2006; Reiners et al., 2006). Currently nine Usher genes have been identified. Usher genes are classified according to the subtypes of the syndrome which their mutations cause (Table 1.1) (Kremer et al., 2006; Reiners et al., 2006; Saihan et al., 2009; Williams, 2008). Mutations in Usher genes affect sensory epithelia in the inner ear and the retina.

In the inner ear, Usher genes are required for the development and function of mechanotransducer hair cells. Hair cells are ciliated cells that have a tuft of stereocilia at the cell apex and connect to the central nervous system via ribbon synapses (refer to Fig.3A in Kremer et al. (2006)). Mechanical displacement of the bundle by sound or by head movements causes opening of mechano-electrical transducer (MET) channels at the tips of stereocilia (Corey et al., 2004). This leads to hair cell depolarization, and generation of a signal that allows hearing and balance to occur (Gillespie and Walker, 2001; Hudspeth, 1997; Muller, 2008; Saihan et al., 2009; Steel and Kros, 2001).

In the retina, analysis of effects of Usher gene mutations in photoreceptor cells found no definite causes for the progressive blinding retinal degeneration (Saihan et al., 2009). Photoreceptor cells are ciliated cells with metabolically active inner segments and photoreceptive outer segments. They are connected to the nervous system via ribbon synapses (refer to Fig. 3B in Kremer et al. (2006)). Evidence suggests that Usher proteins may have a function in the photoreceptor cilium, the adjacent retinal pigment epithelium (RPE) cells (Hasson et al., 1995; Liu X. et al., 1997; Williams, 2008), photoreceptor synapse (Reiners et al., 2005) and in the Crumbs complex, which is required for retinal cell polarity establishment (Gosens et al., 2007; Jacobson et al., 2008; Overlack et al., 2008).

Cilia are common structural features of hair cells and photoreceptor cells. Usher syndrome is associated with ciliary dysfunction in other types of tissues (Reiners et al., 2006). All Usher syndrome subtype 1 and 2 proteins, with exception of Harmonin, have been localized to the olfactory epithelium (Wolfrum et al., 1998b) and the spermatozoa in testis (Hunter et al., 1986). MyosinVIIa has been detected in olfactory neurons, kidney distal tubules, and lung bronchi (Wolfrum et al., 1998b). Impaired olfaction (Zrada et al., 1996), decreased sperm motility (Hunter et al., 1986), abnormal nasal cilia, bronchitis (Arden and Fox, 1979; Bonneau et al., 1993), and asthma (Baris et al., 1994) have been reported in Usher patients. Usher syndrome subtype I has been suggested to be a primary ciliary disorder (Bonneau et al., 1993).

Usher proteins consist of three classes of proteins (Table 1.1): 1) Actin based motor protein, MyosinVIIa; 2) Transmembrane and cell-cell adhesion proteins Cadherin23, Protocadherin15, Usherin (isoform b), and VLGR1 (Very Large G-Protein Coupled receptor 1 isoform b, also known as G protein-coupled receptor 98, GPR98); 3)

Membrane glycoprotein, Clarin1; 4) Scaffold proteins, Harmonin and Whirlin that contain PDZ domains (post synaptic density protein (PSD95), Drosophila disc large tumour suppressor (DlgA), and zonula occludens-1 protein (zo-1) domain) and SANS that contains ankyrin repeats and SAM (sterile alpha motif) domain.

Protein–protein interaction studies *in vitro* and colocalization of most Usher proteins at synapses of hair cells and photoreceptors suggest an existence of an Usher protein interactome (refer to Fig. 7 in Reiners et al. (2006)) and Fig. 2 in Kremer et al. (2006)). Within this interactome transmembrane proteins are organized via binding with their cytoplasmic domains to the scaffolding proteins, which are in turn linked to the cytoskeleton via MyosinVIIa (refer to Fig. 7 in Reiners et al. (2006)). The ability of Usher proteins to assemble into complexes explains why mutations in different classes of proteins cause similar effects in Usher patients. An Usher interactome which is comprised of a full set of Usher proteins has not yet been identified. However, studies in hair cells and photoreceptor cells show that Usher protein complexes of varying composition are involved in a range of different functions of these sensory cells (Saihan et al., 2009).

In the inner ear, Usher proteins form tip, lateral, kinociliary and ankle links required for morphogenesis, cohesion and polarity of the stereociliary bundle (refer to Fig. 3A in Kremer et al. (2006)). Ankle and lateral links are transient while the tip links remain in adult cells.

Table 1.1 Usher syndrome genes and functions of their protein products

Usher syndrome subtype	Locus	Gene	Protein	Protein function
I	B	MYO7A	MyosinVIIa	Actin based motor protein
	C	USH1C	Harmonin	PDZ domain scaffolding protein
	D	CDH23	Cadherin23	Transmembrane cell adhesion protein
	F	PCDH15	Protocadherin15	Transmembrane cell adhesion protein
	G	USH1G	SANS	Scaffolding protein
II	A	USH2A	Usherin (isoform b)	Transmembrane cell adhesion protein
	C	GPR98	VLGR1b	Transmembrane cell adhesion protein; G-protein coupled receptor
	D	DFNB31	Whirlin	PDZ domain scaffolding protein
III	A	CLRN1	Clarin1	Membrane glycoprotein; unknown function

Abbreviations: PDZ, post synaptic density protein, Drosophila disc large tumour suppressor , zonula occludens-1 protein; VLGR1b, Very Large G-Protein Coupled Receptor 1 isoform b; SANS, scaffold protein containing ankyrin repeats and SAM domain (sterile alpha motif). See text for references.

The kinocilium is important for organization of hair cell stereociliary bundle during hair cell development (Kelley et al., 1992; Sobkowicz et al., 1995). Mammalian cells lose their kinociliary links during development (Reiners et al., 2006). Extracellular domains of Cadherin23 and Protocadherin15 form stereociliary tip links which have been proposed to gate hair cell MET channels (Lagziel et al., 2005; Michel et al., 2005; Muller, 2008; Rzadzinska et al., 2005; Siemens et al., 2004). Cadherin23 is also localized to lateral links, and kinociliary links (Boeda et al., 2002; Lagziel et al., 2005; Michel et al., 2005; Rzadzinska et al., 2005; Siemens et al., 2002; Siemens et al., 2004; Sollner et al., 2004). SANS participates in regulation of Usher protein traffic and is a part of kinocilial links (McGee et al., 2006). Usherin, VLGR1b and Whirlin form the ankle links (Adato et al., 2005a; McGee et al., 2006; Michalski et al., 2007; van Wijk et al., 2006). According to the current model, all links are anchored intracellularly via the scaffold proteins Harmonin and Whirlin that in turn link the complexes to the actin cytoskeleton via MyosinVIIa, MyosinXV, Myo1c, and/or vezatin (Adato et al., 2005b; Boeda et al., 2002; Delprat et al., 2005; Kussel-Andermann et al., 2000; Michalski et al., 2007; Muller, 2008). Whirlin organizes molecular complexes which control coordinated actin polymerization and membrane growth of stereocilia (Mburu et al., 2003). MyosinVIIa is thought to act as a general transporter of Usher proteins in the stereocilia (Boeda et al., 2002; Michalski et al., 2007; Senften et al., 2006). Clarin1 is thought to participate in actin polymerization in hair cell stereocilia (Tian et al., 2009) and in sensory transduction (Geng et al., 2009).

In the retina, all proteins of Usher syndrome types I and II, with exception of Harmonin, colocalize within the ciliary and periciliary region of the photoreceptor cells (Adato et al., 2002; Barrong et al., 1992; Maerker et al., 2007; Reiners et al., 2006). The

ectodomains of Usherin and VLGR1b extend between the plasma membrane of the periciliary collar of the apical inner segment and the plasma membrane of the connecting cilium. Both proteins form fibrous links between these two membranes, which are analogous to the ankle links between adjacent stereocilia in cochlear hair cells. Scaffolding proteins SANS and Whirlin have also been localized to this region where they are thought to interact with the cytoplasmic domains of Usherin and VLGR1b (Reiners and Wolfrum, 2006). In photoreceptor cells, molecular components required for phototransduction are synthesized in the inner segment and then transported via the connecting cilium to the outer segment (Maerker et al., 2007; Wolfrum and Schmitt, 2000). MyosinVIIa is thought to participate in opsin transport in the connecting cilium and is required for proper disk membrane morphogenesis (Liu et al., 2007b). Whirlin, Usherin and VLGR1b are also localized to adherens junctions in photoreceptor cells and may function in apico-basal polarity determination (Kremer et al., 2006).

In the retinal pigment epithelium (RPE), MyosinVIIa participates in transport of phagosomes (Gibbs et al., 2003) and melanosomes (Futter et al., 2004; Gibbs et al., 2004; Klomp et al., 2007; Lopes et al., 2007). Outer segment phagocytosis is required for proper membrane turnover. Lack of turnover leads to photoreceptor degeneration (Gibbs et al., 2003).

In the synapses of hair cells and photoreceptor cells, Whirlin and Harmonin have been proposed to control synapse strength and plasticity (van Wijk et al., 2006). MyosinVIIa may participate in synaptic molecule transport and endocytosis (Kremer et al., 2006), while VLGR1b may function in signalling and ion homeostasis (Reiners et al., 2005). Other transmembrane Usher proteins could be required for cohesion of synaptic membranes (van Wijk et al., 2006). Regardless of colocalization of most Usher proteins

at synapses, synapses are most likely not the main sites of the Usher syndrome disorder, since the Usher gene mutations cause photoreceptor degeneration but not synaptic pathogenesis (Saihan et al., 2009).

1.2.1.2 Evolutionary conservation of Usher protein functions

In mouse (*Mus musculus*) and zebrafish (*Danio rerio*) models (Table 1.2), mutations in Usher gene homologues are associated with characteristic vestibular abnormalities, hearing impairment and retinal degeneration, suggesting a significant conservation of Usher gene functions across vertebrate phyla (Wolfrum et al., 1998b).

Hearing and vestibular dysfunction have been detected in mouse models for Usher syndrome type I genes: MyosinVIIa (Gibson et al., 1995), Harmonin (Johnson et al., 2003), Cadherin23 (Di Palma et al., 2001), Protocadherin15 (Alagramam et al., 2001), and SANS (Kikkawa et al., 2003). The mouse Whirlin model for Usher syndrome type II (Mburu et al., 2003) has vestibular dysfunction, which is not detected in humans with mutations in this gene (Williams, 2008). Clarin1 knockout mice have been reported to have hearing loss and vestibular dysfunction (Geng et al., 2009).

The retinal degeneration phenotype has not been observed for any of the Usher gene mouse models. MyosinVIIa (Gibson et al., 1995), Cadherin23 (Di Palma et al., 2001), Protocadherin15 (Alagramam et al., 2001), Harmonin (Johnson et al., 2003) and VLGR1b (McGee et al., 2006) models show reduced electroretinogram amplitudes. Presently, the only Usher gene model that possesses convincing retinal degeneration is the Usherin knockout mouse (Liu et al., 2007b).

Zebrafish MyosinVIIa mutant (Ernest et al., 2000), like the mouse model, has vestibular abnormalities, morphologically and functionally defective sensory hair cells,

and defects in RPE melanosome transport. Mutations in Protocadherin15 and morpholino knockdowns of Harmonin, Usherin and VLGR1b result in abnormal auditory, vestibular and retinal function (Seiler et al., 2005; Phillips et al., 2007). The Cadherin23 mutant has either reduced or absent hair cell mechanotransduction, but no vision defects (Sollner et al., 2004).

Few Usher gene homologues have been found in protostome invertebrates where their functions do not appear to be conserved. Genomic screens and sequence analysis reveal that Harmonin genes are not present in protostomes, but are highly conserved in vertebrates (Reiners et al., 2003). Homologues of two Usher genes have been identified in *Drosophila melanogaster* and eight genes in urochordate *Ciona intestinalis* (Table 1.3). Usher genes have not been identified in *Caenorhabditis elegans*.

In *D. melanogaster*, the orthologue of MyosinVIIa (Table 1.2) is important for maintenance of integrity in scolopidia in the *Drosophila* auditory organ, the Johnston's organ (JO) (Kiehart et al., 2004) that is developmentally and functionally related to the vertebrate inner ear (Todi et al., 2004). Mutation in MyosinVIIa results in fly deafness (Todi et al., 2005). Cad99C, fly orthologue of Protocadherin15 (Table 1.2), is a component of microvilli which promotes microvillar elongation (D'Alterio et al., 2005). However, Cad99C has no reported function in auditory mechanotransduction.

Table 1.2 Vertebrate and invertebrate Usher gene models

Gene	Protein	Animal Model
MYO7A	MyosinVIIa	Shaker (mouse) (Gibson et al., 1995)
		Mariner (zebrafish) (Ernest et al., 2000)
		Crinkled (fly) (Kiehart et al., 2004)
USH1C	Harmonin	Deaf circler (mouse) (Johnson et al., 2003)
		Inad (fly) (Hardie and Raghu, 2001)
CDH23	Cadherin23	Waltzer (mouse) (Di Palma et al., 2001)
		Sputnik (zebrafish) (Sollner et al., 2004)
PCDH15	Protocadherin15	Ames waltzer (mouse) (Alagramam et al., 2001)
		Orbiter (zebrafish) (Nicolson et al., 1998; Seiler and Nicolson, 1999)
		Pcdh15a (zebrafish) (Seiler and Nicolson, 1999)
		Cad99C (fly) (D'Alterio et al., 2005)
USH1G	SANS	Jackson shaker (mouse) (Kikkawa et al., 2003)
USH2A	Usherin	Knockout (mouse) (Cosgrove et al., 2004)
GPR98	VLGR1	Vlgr1/del7TM (mouse) (McGee et al., 2006)
DFNB31	Whirlin	Whirler (mouse) (Mburu et al., 2003; Mogensen et al., 2007)
CLRN1	Clarin1	Clrn1 knockout (mouse) (Geng et al., 2009; Tian et al., 2009)

InaD (Inactivation no after potential D) is a PDZ domain protein that is the *Drosophila* analog of Harmonin (Hardie and Raghu, 2001). In the rhabdomeric photoreceptors, InaD scaffolds the components of the visual signal transduction cascade into a signal complex (Montell, 1999).

Recent molecular phylogenic analyses suggest that urochordates, including *C. intestinalis*, are a group most closely related to vertebrates (Delsuc et al., 2006) and will probably provide excellent genomic model organisms for human diseases (Virata and Zeller, 2010). *C. intestinalis* genome was recently annotated. MyosinVIIa, Usherin, Whirlin, Cadherin23, Protocadherin15, SANS, and VLGR1 were annotated in genome assembly V2.0 (Table 1.3). Harmonin has not been annotated. InaD-like genes Ci-scribble, and Ci-magi1b, and GW1.05Q.1072.1 may be alternatives to Harmonin. To date, no investigations have been carried of the expression or functions of any of these genes in *C. intestinalis*.

1.2.1.3 Usher gene predictions in *S. purpuratus* and their embryonic expression

A nearly complete set of Usher genes has been annotated in the *S. purpuratus* genome (Table 1.3) (Whittaker et al., 2006). A total of eleven Usher gene predictions have been annotated. The presence of Harmonin in the sea urchin genome is intriguing given that Harmonin is not found in protostome invertebrates, and may be a feature of deuterostomes. No orthologous sequences to *Drosophila* Cad99c or InaD have been annotated, suggesting that the sensory function of Harmonin may be conserved in sea urchins. Absence of Clarin1 in sea urchins and urochordates suggests that this gene may be vertebrate specific.

Most Usher genes have been regarded as vertebrate specific and no investigations of their functions have been performed in sea urchins. Functional conservation of Usher genes has been observed in vertebrates. It would be interesting to determine whether this extends to the sea urchin phylum as well. Characterization of Usher gene functions in sea urchins could provide a valuable insight into the evolution of vertebrate sensory genes and organs.

Table 1.3 Annotations of Usher genes in *S. purpuratus* genome and *C. intestinalis* genome

Gene Name	Annotations in *C. intestinalis* Genome	Annotations in *S. purpuratus* Genome
MyosinVIIa	yes	Yes
Harmonin	no	Yes
Cadherin23	yes	Yes
Protocadherin15	yes	Yes
SANS	no	Yes
Usherin	yes	Yes
VLGR1	yes	Yes
Whirlin	yes	Yes
Clarin1	no	No

Usher gene annotations were found in the *C. intestinalis* and *S. purpuratus* genome databases. DOE Joint Genome Institute *C. intestinalis* V2.0 annotation database: http://genome.jgi-psf.org/Cioin2/Cioin2.home.html. Baylor College of Medicine *S. purpuratus* Spur 2.1 annotation database: http://annotation.hgsc.bcm.tmc.edu/Urchin/cgi-bin/pubLogin.cgi.

1.2.2 Transient Receptor Potential Channel A1 in *S. purpuratus*

1.2.2.1 Overview of TRP channels

Members of the transient receptor potential (TRP) channel family are found in a wide range of vertebrate and invertebrate organisms including mammals, zebrafish, tunicates, nematodes, fruit flys and yeast (Montell, 2005). There is 1 known TRP gene in yeast, 16 in fly *D. melanogaster*, 17 in nematode *C. elegans*, 27 in sea squirt *C. intestinalis*, 25 in fish *Fugu rubripes* and zebrafish *D.rerio* , 28 in mouse *M. musculus*, and 27 in human, *Homo sapiens*. TRP channels are well conserved among different organisms (Flockerzi, 2007). TRP channel genes have not been identified in eubacteria, archaebacteria, protistas, or in plants. In fungi, a single TRP-related gene has been found which cannot be assigned to any of the known TRP subfamilies in animals (Damann et al., 2008). Evolutionarily, the first TRP genes appear in the unicellular choanoflagellates (*Monosiga brevicollis*) which are considered to be the closest living relatives of the animals (Cai, 2008).

TRP channels are preferentially distributed in sensory organs in agreement with their critical and diverse roles in signal reception and sensory transduction (Yin and Kuebler, 2010). Studies in mammals, *D. melanogaster* and *C.elegans* show that TRP channels participate in detection of light, osmotic, thermal, chemical, and mechanical stimuli, pain perception, and cell volume regulation (Bandell et al., 2007; Clapham, 2003; Christensen and Corey, 2007; Caterina, 2007; Flockerzi, 2007; Kung, 2005; Montell and Caterina, 2007; Sukharev and Corey, 2004; Voets et al., 2005). TRP channels have been proposed to have a role in mechanosensory control of neuronal

migration in development (Cui and Yuan, 2007). TRP channels are also present in non sensory cells where they are required in endothelium dependent relaxation and smooth muscle dependent contractility. TRP channels may have roles in cell cycle control, and even roles as possible tumour suppressors (Flockerzi, 2007).

TRP channels are generally non-selective cation channels (Clapham, 2003; Voets et al., 2005). They are classified into seven subfamilies (refer to Fig. 3 in Yin and Kuebler (2010)) based on similarities in their amino acid sequences (Montell, 2005). The subfamilies are listed as follows (Flockerzi, 2007):

1. Canonical TRPs or TRPCs, considered to be classical TRP channels because they show sequence similarity to the *Drosophila* TRP which was identified first and is required for signal transduction in *Drosophila* photoreception.
2. Vanniloid receptor TRPs or TRPVs.
3. Melastatin TRPs or TRPMs.
4. Mucopilin TRPs or TRPMLs.
5. Polycystin TRPs or TRPPs.
6. Ankyrin TRPs or TRPAs
7. No mechanoreceptor potential C TRPs or TRPNs.

Since this classification is based on sequence rather than channel function, members of different families may have multimodal properties and may share functions (Schaefer, 2005).

TRP channels are assumed to be tetramers based on their protein sequence and similarities to other channel proteins (refer to Fig. 1 in Flockerzi (2007)). There is a limited amount of direct evidence that indicates that such tetrameric structures exist (Hoenderop et al., 2003; Erler et al., 2004; Kedei et al., 2001). Structurally, TRP proteins have six transmembrane domains, and TRP channels closely resemble voltage gated potassium channels (Flockerzi, 2007). The linker between the predicted transmembrane domains 5 and 6 is thought to form the TRP channel pore (Nilius et al., 2001; Oberwinkler et al., 2005; Owsianik et al., 2006). Both N- and C-termini are predicted to be intracellular (Hoenderop et al., 2003).

Members of the same TRP subfamilies may form heteromeric TRP channels *in vivo* (Flockerzi, 2007). It is still presently unclear whether functional TRP channels heteromultimerize from TRP proteins from different subfamilies. Such heterotetramerization could be biologically relevant as it allows for control of various properties of the channel like gating and ion permeability (Schaefer, 2005).

1.2.2.2 Overview of TRPA1 structure and function

TRPA1 is a member of TRPA subfamily that has members in various phyla, including vertebrates and invertebrates. TRPA1 is expressed in a variety of sensory cells and sensory neurons in different organisms where it is implicated in detection of chemical, thermal and noxious mechanical stimuli (Damann et al., 2008).

A distinguishing feature of TRPA1, compared to other TRP proteins is a long N-terminal region of ankyrin repeats, up to 18 in total (Garcia-Anoveros and Nagata, 2007). Other TRP proteins possess between 0 and 8 ankyrin repeats, with exception of TRPN1 which has 29 predicted ankyrin repeats (Li et al., 2006; Sidi et al., 2003; Walker

et al., 2000) (refer to Fig. 3 in Yin and Kuebler (2010)). Ankyrin repeats are elastic and have been proposed to form molecular gating springs in TRPA1, TRPN1 and other TRP channels (Howard and Bechstedt, 2004; Sotomayor et al., 2005). Ankyrin repeats have also been proposed to function as candidates for gating of mechanotransducers in vertebrate hair cells and in *Drosophila* bristles (Corey et al., 2004; Howard and Bechstedt, 2004; Sotomayor et al., 2005). They may also cluster and organize ion channels and receptors at specialized regions of cells (Bennett and Chen, 2001; Lee et al., 2006). In TRPV1, ankyrin repeats have been shown to be important in regulating channel sensitivity through binding of ligands to the multi-ligand binding site (Lishko et al., 2007).

TRPA1 can be activated directly or indirectly though a multitude of external and internal factors. A large number of plant derived compounds which cause neurogenic inflammation and pain are external agonists of TRPA1. These compounds are the isothiocyanates from wasabi, mustard, horseradish, Brussels sprouts and capers (Bandell et al., 2004; Jordt et al., 2004; Nagata et al., 2005), cinnamaldehyde from cinnamon (Bandell et al., 2004), allicin from garlic (Bautista et al., 2005; Macpherson et al., 2005), acrolein in tear gas (Bautista et al., 2006), methyl salicylate from mouthwashes such as Listerine, gingerol from ginger, eugenol from clove, icilin or A-G-35 (Bandell et al., 2004), α- and β-unsaturated aldehydes from cigarette smoke, several general anesthetics used in surgery (Andre et al., 2008; Bandell et al., 2004; Bautista et al., 2005; Jordt et al., 2004; Macpherson et al., 2005; Matta et al., 2008), and environmental irritants like exhaust fumes and isocyanates (Bandell et al., 2004; Bessac et al., 2008; Jordt et al., 2004). The allyl isothiocyanate from mustard and allicin from garlic are thought to be specific agonists of TRPA1 (Bautista et al., 2006).

Endogenous mediators of inflammation and pain also interact with TRPA1. TRPA1 may be activated downstream of Phospholipase C coupled receptors by inflammatory mediators like endocannabinoids and bradykinin (Bandell et al., 2004) suggesting TRPA1 activation via second messengers (Bandell et al., 2004; Jordt et al., 2004; Kwan et al., 2006). Prostaglandins, hydroxynonenal, and reactive oxygen species have all been shown to act as TRPA1 agonists (Cruz-Orengo et al., 2008; Taylor-Clark et al., 2008; Trevisani et al., 2007).

One specific group of TRPA1 agonists, referred to as reactive electrophiles, activates TRPA1 via covalent modification. Electrophiles are pungent and irritating chemicals which cause damage to cells by covalently binding and disrupting functions of proteins, nucleic acids and other molecules (Hinman et al., 2006; Macpherson et al., 2007). Examples of such compounds are thiol-reactive substances, like allyl isothiocyanate and diallyl disulfide from garlic, cinnamaldehyde, or products of oxidative stress, like hydrogen peroxide and endogenous alkenyl aldehydes. Reactive electrophiles, although different in their chemical structures, all activate TRPA1 via a common mechanism. They activate TRPA1s by forming covalent bonds with conserved cysteine and lysine residues, present almost exclusively at the N-terminus of TRPA1 proteins (Cebi and Koert, 2007; Hinman et al., 2006; Macpherson et al., 2007). There are six residues in total per TRPA1 protein, five cysteines and one lysine. Mutations in these residues decrease electrophile sensitivity of TRPA1s (Hinman et al., 2006; Macpherson et al., 2007).

1.2.2.3 Evolutionary conservation of TRPA1 protein functions

Recent phylogenetic analysis of TRPA1 homologues from different species separated them into two clades, electrophile sensitive TRPA1s and electrophile

insensitive basal TRPAs (refer to Fig. 4D in Kang et al. (2010)). TRPA1s are derived from a common electrophile sensitive ancestor, in both vertebrates and invertebrates, suggesting that reactive electrophile detection has been conserved for at least 500 million years of animal evolution. The ancestral TRPA1 contained all six critical residues associated with electrophile detection. All TRPA1 clade members contain these six residues, suggesting common mechanisms for reactive electrophile sensing by invertebrate and vertebrate TRPA1s. Basal TRPAs may conserve more than one of the five cysteines (Kang et al., 2010).

Apart from electrophile sensitivity, most other functions of TRPA1 clade members have diverged. For example, in *Drosophila*, dTRPA1 is sensitive to heating, while the mammalian TRPA1 is thought be activated by cold (Viswanath et al., 2003). Even though mouse and human TRPA1s are closely related, they can respond differently to menthol or caffeine through either channel activation or deactivation respectively (Klionsky et al., 2007; Nagatomo and Kubo, 2008; Xiao et al., 2008). Menthol does not activate TRPA1 through covalent modification (Karashima et al., 2007; Macpherson et al., 2006), which again shows that TRP channels have multimodal properties.

Most of what is known about invertebrate TRPA1s comes from studies in *D. melanogaster* and *C.elegans*. Until recent phylogenetic analysis, performed by Kang et al. (2010), it was assumed that some of the TRPA genes in flys and worms were orthologues of mammalian or vertebrate TRPA1s. It has been demonstrated that instead those genes represent a clade of basal TRPAs. The study demonstrates that deuterostomes, including sea urchins, have lost their basal TRPA and have only one or two copies of electrophile sensitive TRPA1s. Basal TRPAs appear to be a signature of protostomes and have diverged to 1 to 6 genes per organism. The only protostomes

analyzed, which have retained electrophile sensitive TRPA1, are *Drosophila* and a mollusc (refer to Fig. 4E in Kang et al. (2010)).

In flys, nematodes and zebrafish electrophile sensitive TRPA1s do not appear to have functions in mechanosensation. According to evidence from the literature, these functions are fulfilled by basal TRPAs or TRPN subfamily members which are structurally analogous to TRPAs.

Of the 4 members of TRPA subfamily in *D. melanogaster*, only dTRPA1 is electrophile sensitive and orthologous to vertebrate TRPA1. dTRPA1 is expressed in thermosensory neurons and is required for thermotaxis (Hamada et al., 2008). dTRPA1 is also expressed in mouthpart neurons where it mediates ingestion dependent responses including aversion to electrophilic compounds (Kang et al., 2010). *Drosophila* Painless, Pyrexia and Waterwitch are the remaining members of TRPA subfamily which are basal TRPAs. Painless is required for responses to elevated temperatures, chemosensation and mechanosensation (Tracey Jr. et al., 2003) and was previously considered a fly orthologue of mammalian TRPA1. Painless has been previously reported as the mediator of fly aversion to allyl isothiocyanate (Al-Anzi et al., 2006). More investigation is required to resolve this discrepancy (Kang et al., 2010). Pyrexia is implicated in heat sensation (Lee et al., 2005; Rosenzweig et al., 2005; Sokabe et al., 2008; Tracey Jr. et al., 2003), and Waterwitch is required for hydrosensation (Liu et al., 2007a). TRP channels involved in cold sensation have not yet been identified in *Drosophila* (Damann et al., 2008). *Drosophila* TRPN subfamily member "no mechanoreceptor potential C" (NompC) is required for mechanosensation in bristle organs of flies (Walker et al., 2000).

During evolution, nematodes appear to have lost their electrophile sensitive TRPA1 (Kang et al., 2010). There are two basal TRPAs in *C.elegans*. One of them, called TRPA1, close in sequence to anemone and choanoflagellate basal TRPAs. This TRPA is required for mechanosensory behaviours like nose touch responses and for foraging behaviour, and is expressed and functions in mechanosensory neurons required for these behaviours (Kindt et al., 2007). *C. elegans* TRPA2 is another basal TRPA, with no predicted ankyrin domains and of unknown function (Kindt et al., 2007). *C.elegans* TRPN1 is a *D. melanogaster* NompC analog (Walker et al., 2000) which functions in mechanosensation in ciliated mechanosensory neurons and in stretch activated neurons (Li et al., 2006; Sidi et al., 2003).

The tunicate *C. intestinalis* has only one TRPA subfamily member, TRPA1, which is classified as electrophile sensitive (Kang et al., 2010). No investigation of *C. intestinalis* TRPA1 has been reported. TRPN1 was also annotated in *C. intestinalis* genome assembly V2.0, and its function is also currently unknown.

In the zebrafish, *D. rerio*, two orthologues of TRPA1 exist that have been classified as electrophile sensitive, TRPA1a and TRPA1b (Kang et al., 2010). Morpholino antisense knockdown of zebrafish TRPA1 suggests that *D.rerio* TRPA1 may form part of the hair cell mechanotransduction channel that is required for inner ear and lateral line hair cell function (Corey et al., 2004). A recent study contradicts these results: both *D. rerio* TRPA1 paralogues, TRPA1a and TRPA1b, are expressed in sensory neurons and are activated by several chemical irritants in vitro. Behavioural analyses of TRPA1a and TRPA1b null mutant larvae indicate that TRPA1b is necessary for behavioural responses to chemical irritants. Neither of the TRPA1 paralogues has been found to be required for behavioural responses to temperature changes or for mechanosensory hair cell function

in the inner ear or lateral line. Therefore, zebrafish TRPA1s appear to be involved in chemical but not thermal or mechanical responses (Prober et al., 2008). *D. rerio* TRPN1, a *D. melanogaster* NompC analog (Walker et al., 2000) is expressed selectively in sensory hair cells in the inner ear and the lateral line of zebrafish, and is critical for hair cell mechanotransduction. Morpholino knockdown of zebrafish TRPN1 results in larval deafness and imbalance. It has been suggested that TRPN1, in association with other proteins like TRPA1, contributes to mechanosensitive channels in *D. rerio* hair cells (Corey, 2006; Howard and Bechstedt, 2004).

Only a single member of TRPA subfamily, TRPA1, is present in mammals, and it has been classified as electrophile sensitive (Kang et al., 2010). TRPN1 has not been identified in mammals. Therefore, TRPA1 is the only mammalian TRP channel that contains an extended ankyrin repeat domain at the N-terminus (Flockerzi, 2007). Due to structural similarities of TRPA1 to TRPN1 and its expression in mammalian mechanosensory organs, TRPA1 was proposed to be a candidate mechanosensory channel protein in mammals (Corey et al., 2004; Nagata et al., 2005).

In mammals, TRPA1 protein is reliably localized within two types of sensory tissues, the receptors of the peripheral somatosensory system and in the mechanosensory epithelia of the inner ear, the hair cells and supporting cells (Damann et al., 2008; Garcia-Anoveros and Nagata, 2007).

The mammalian peripheral somatosensory system detects a wide variety of stimuli (Tsunozaki and Bautista, 2009). Free sensory nerve endings of this system are localized in the skin, muscles, joints, and viscera. The information received by these sensory nerve endings is sent to and interpreted by the central nervous system (Kindt et al., 2007). Approximately 20% to 56% of all somatosensory neurons express TRPA1

(Bautista et al., 2005; Jaquemar et al., 1999; Kobayashi et al., 2005; Nagata et al., 2005; Story et al., 2003). Physical and chemical stimuli are thought to directly activate TRPA1 in the sensory nerve endings causing an increase in their intracellular calcium ion concentration leading to generation of action potentials (Damann et al., 2008; Doerner et al., 2007; Jordt et al., 2004; Nagata et al., 2005).

The exact role of TRPA1 in mechanotransduction in mammals has not been determined (Kerstein et al., 2009). Mice with a deletion in the pore domain of TRPA1 have decreased behavioural responses to intense in noxious mechanical force (Kwan et al., 2006). TRPA1 has been localized by immunostaining to keratinocytes, where it may function to modify tactile responses of sensory neurons in the skin (Anand et al., 2008; Kwan et al., 2009). However, currently no direct evidence exists demonstrating activation of mammalian TRPA1 by mechanical force. If TRPA1 is knocked out or blocked pharmacologically, different types of somatosensory fibers appear to respond differently to mechanical stimulation (Kerstein et al., 2009; Kwan et al., 2009). These results suggest that mammalian TRPA1 is not intrinsically mechanically sensitive, but instead serves as a signal amplifier or integrator that is downstream of an unknown mechanoreceptor. Alternatively, TRPA1 could be a part of an unknown larger protein complex that mediates mechanotransduction (Kerstein et al., 2009; Kwan et al., 2009). It was suggested that to determine the exact function of TRPA1 in mechanical nociception, TRPA1 function should be examined in the different tissues and fiber types separately (Tsunozaki and Bautista, 2009).

In mechanosensory epithelia of the mammalian inner ear, TRPA1 protein is located in the vestibular and auditory sensory hair cells at the cuticular plate, in the kinocilia and the mechanosensory stereocilia (Corey et al., 2004; Nagata et al., 2005).

TRPA1 is a candidate channel protein in the hair cell MET channel (Walker et al., 2000), the molecular identity of which is still under investigation.

Presently, the function of TRPA1 in the inner ear is unclear. Studies of TRPA1 function in mammalian hair cells show contradicting results. Inhibition of TRPA1 mRNA expression in mouse hair cells resulted in reduced mechanotransducing currents (Corey et al., 2004). Allyl isothiocyanate, an exclusive agonist of TRPA1 which activates currents in peripheral nerve fibers, is able to activate currents in hair cells *in vitro* (Stepanyan et al., 2006). However, in mice with a deletion of the pore domain of TRPA1, no obvious vestibular or auditory defects were observed (Bautista et al., 2006). Also, TRPA1 knockout mice showed unimpaired auditory function (Kwan et al., 2006). TRPA1 may be participating in hair cell mechanotransduction but is not essential for it. MET channels appear to be functionally heterogeneous, with different conductance levels (Ricci et al., 2003). Multimerization of TRPA protein and other TRP channel subfamily proteins found in hair cells could accomplish this difference in conductance. TRPML3 is a candidate for such TRP protein. Mutations in TRPML3 result in abnormalities in stereocilia and deafness in mice (Di Palma et al., 2002). Alternatively, TRPA1 could function in hair cell supporting cells, since expression of TRPA1 is weak in hair cells and is more prominent in the adjacent supporting cells (Castiglioni and Garcia-Anoveros, 2007; Garcia-Anoveros and Nagata, 2007).

Overall, similarities in pharmacology and pore properties of mammalian TRPA1 channel to hair cell MET, its structural and/or phylogenetic similarities to mechanosensory channels from invertebrates like TRPN1, its expression in mechanosensory nociceptors, and reduction of withdrawal thresholds to mechanical stimulation in TRPA1 knockout animals all suggest that the mammalian TRPA1 channel

functions in mechanonociception (Castiglioni and García-Añoveros, 2007). Apart from its role in mechanoniception, mammalian TRPA1 participates in chemosensation (Al-Anzi et al., 2006; Bandell et al., 2004; Bautista et al., 2005; Bautista et al., 2006; Jordt et al., 2004; Kwan et al., 2006; Macpherson et al., 2005; McNamara et al., 2007; Trevisani et al., 2007), inflammatory pain detection (Bautista et al., 2006; Caceres et al., 2009; McNamara et al., 2007), and possibly noxious cold detection (Bandell et al., 2004; Fajardo et al., 2008; Klionsky et al., 2007; Kwan et al., 2006; Sawada et al., 2007; Story et al., 2003), although its participation in detection of noxious cold has been questioned (Doerner et al., 2007; Zurborg et al., 2007).

1.2.2.4 Fluorescent cationic dyes and their use in studying mechanosensory channels

FM1-43 is a fluorescent styryl pyridinium dye with divalent cationic head group and a long lipophilic tail (refer to Fig.1 in van Netten and Kros (2007)). FM1-43 reversibly partitions into the outer leaflets of cell membranes and is commonly used to label cell membranes (Betz et al., 1992; Henkel et al., 1996). Upon incorporation into the outer leaflet of the membrane, FM1-43 fluorescence increases by two or many orders of magnitude (Betz et al., 1996; Schote and Seelig, 1998). Due to its structure FM1-43 cannot cross the lipid bilayer or transfer between the membrane leaflets. Once FM1-43 is internalized by endocytosis, it becomes trapped in the inner leaflet of endocytosed vesicles. FM1-43 is non-toxic and is commonly used to track endocytosis, exocytosis, endosome trafficking and synaptic vesicle recycling in living cells (Betz and Bewick, 1992; Betz et al., 1996; Betz et al., 1992; Cochilla et al., 1999; Henkel et al., 1996; Ryan, 2001).

Styryl pyridinium cationic dyes such as FM1-43, DASPEI, and 4-Di-2-ASP are used to selectively label the cytoplasm of sensory hair cells in the lateral lines and inner ears of vertebrates (Balak et al., 1990; Collazo et al., 1994; Gale et al., 2001; Jorgensen, 1989; Nishikawa and Sasaki, 1996; Seiler and Nicolson, 1999). It has been suggested and demonstrated repeatedly that styryl dyes enter hair cells by passing directly through mechanically gated transduction channels at the tips of the stereocilia (Balak et al., 1990; Gale et al., 2001; Meyers et al., 2003; Nishikawa and Sasaki, 1996). FM1-43 rapidly fills the cytoplasm of hair cells within 30 seconds of treatment, where it labels the endoplasmic reticulum and the mitochondria. The dye does not remain within the stereocilia and is quickly transported to the cell body (Meyers et al., 2003). FM1-43 also labels the plasma membranes of the adjacent supporting cells (Nishikawa and Sasaki, 1996).

In live mice, subcutaneous injection of FM1-43, with incubation of two weeks, specifically selectively labels many different types of sensory cells and neurons, leaving non-sensory cells unlabelled. FM1-43 intensely labels the cell bodies of primary sensory neurons including proprioceptive, thermoreceptive and nociceptive neurons. Most of the tissues labelled by FM1-43 have mechanoreceptive functions, suggesting that the dye permeation is a property of mechanosensory cells. Non-mechanoreceptive structures labelled by FM1-43 include the taste receptors and their nerve fibers. FM1-43 was shown to be internalized into primary sensory neurons in mice through their peripheral sensory terminals and got transported to their cell bodies (Meyers et al., 2003). *In vitro*, FM1-43 dye permeates through non-selective cation channels found in nociceptors like TRPV1 and P2X2 purinoreceptor (Meyers et al., 2003). TRPA1 is hypothesized to be a component of hair cell MET channel and participates in mechanotransduction in

mammalian nociceptors. Therefore FM1-43 can be internalized through TRPA1 channels and possibly other types of TRP channels.

YO-PRO and its analog TO-PRO are nuclear cationic fluorescent dyes which are cell membrane impermeant but can pass through large non-selective channels, such as P2X7 receptors (Chung et al., 2008; Khakh et al., 1999; Santos et al., 2006; Virginio et al., 1999) (refer to Fig. 1 for structures in Petty et al. (2000)). Both dyes selectively label hair cell nuclei, and have been used to screen for viable hair cells in conjunction with FM1-43 (Santos et al., 2006). No neuronal labelling by either dye has been reported to date. YO-PRO and TO-PRO belong to a family of cyanine monomer nucleic acid stains which intercalate into DNA. Dyes like YO-PRO were first used as a replacement for ethidium bromide in agarose gels since they have a very high signal to noise ratio (Glazer and Rye, 1992). The YO-PRO dye has also been used to measure cellular DNA content after permeabilization with methanol as well as for the detection, of dead cells, which take it up ((Haughland, 1992-1994).

It is believed that due to their cationic nature and small size dyes like FM1-43 are able to pass through the pore of hair cell MET and other non-selective cation channels. According to a recently proposed model of the MET pore, the minimum channel pore diameter is approximately 1.25nm (Farris et al., 2004). FM1-43 is an elongated molecule with a maximum end on diameter of about 0.78nm and a length of about 2.2nm (van Netten and Kros, 2007). The entry of small cationic molecules like FM1-43 into the hair cells from the extracellular side is thought to resemble diffusion because of a small extracellular energy barrier. A large intracellular energy barrier prevents the exit of these molecules and traps them intracellularly (van Netten and Kros, 2007). YO-PRO and TO-PRO are both similar in structure and dimensions to FM1-43

(refer to Fig. 1 for structures in Petty et al. (2000)). It has been hypothesized that these dyes enter the hair cells through the MET, although the exact mechanism of their internalization in hair cells is unknown (Santos et al., 2006). Longer incubation protocols of 30 minutes have been used for YO-PRO and TO-PRO (Santos et al., 2006) possibly because they are bulkier than FM1-43 and do not diffuse as fast through the MET pore.

As FM1-43 selectively labels sensory cells and primary sensory neurons, it has been suggested that FM1-43 can be used to screen for functional transducer channels and mechanoreceptors in live organisms. FM1-43 screening allows one to search for cells having sensory transducer channels with structural similarities to hair cell MET channel (Meyers et al., 2003). An advantage of using FM1-43 for sensory cell screening is that FM1-43 has no route of exit once it gets internalized in sensory cells. The only route of exit for the dye is back though the channels, but the inward driving force of the divalent cations would make the exit negligible. Another advantage of FM1-43 screening is the persistence of labelling. *In vitro*, the staining of the hair cells is retained after FM1-43 washout, and the staining persists in hair cell culture for at least 3 weeks. Similarly, hair cell and sensory neuron staining is retained *in vivo* for at least 2 weeks (Meyers et al., 2003). Finally, FM1-43 labelling intensity provides a quantitative measure of ion channel activity and can be used to study the effects of mutations, antagonists or agonists on the channel function (Meyers et al., 2003). For example, FM1-43 has been used to screen for loss of function in hair cell MET channel (Gale et al., 2001; Kros et al., 2002; van Netten and Kros, 2007), studying hair cell MET channel during development (Geleoc and Holt, 2003; Si et al., 2003), and monitoring the recovery of hair cell function following ototoxic damage by aminoglycoside antibiotics (Taura et al., 2006). YO-PRO

and TO-PRO selectively label hair cell in zebrafish (Santos et al., 2006). Structural similarities of YO-PRO and TO-PRO to FM1-43, and their colocalization with FM1-43 in hair cells, suggest that those dyes may also be used in screening for sensory cells like FM1-43.

Although FM1-43 is small enough to permeate through the active MET channel (van Netten and Kros, 2007), FM1-43 can be a blocker of mechanotransducer currents in hair cells (Gale et al., 2001; Nishikawa and Sasaki, 1996). It has been suggested that FM1-43 is able to physically block ion internalization in hair cells by competing with calcium for binding sites in the MET selectivity filter (Farris et al., 2004; Gale et al., 2001). FM1-43 can also block mechanotransducer currents in mechanosensory neurons in mammals (Drew and Wood, 2007). In mice, local application of FM1-43 inhibited responses in two behavioural assays of mechanosensitivity. FM1-43 increased paw withdrawal thresholds in response to punctate stimulation with von Frey hairs and high levels of pressure in the Randall-Selitto device (Drew and Wood, 2007). Therefore the dye can be used not only to specifically label sensory structures, but may also be used to inhibit the mechanotransducer channel functions associated with those structures, and the effects of this inhibition can be assayed in model organisms through behavioural assays.

1.2.2.5 Studies of TRPA1 using fluorescent dyes and TRPA1 inhibitors

TRPA1 can be blocked by either specific pharmacological or non-specific cation channel blockers.

Four classes of specific pharmacological TRPA1 antagonists are currently known. The oxime antagonist AP18 which is related in structure to cinnamaldehyde (Petrus et

al., 2007), trichlorosulfide antagonists from Amgen, like AMG7160 6, which is related in structure to mustard gas (Klionsky et al., 2007), diaminohexane derivative ((Patapoutian and Jegla, 2007) and purine acetamides, like HC030031, from Hydra Biosciences (Eid et al., 2008;Moran et al., 2007;Ng et al., 2009).

AP18 or ((Z)-4-(4-chlorophynyl)-3-methylbut-3-en-2-oxime (refer to Fig.1A in Petrus et al. (2007)) was identified through screening 43,648 small molecules for their ability to block cinnamaldehyde-activation of human and mouse TRPA1 in a Chinese Hamster Ovary (CHO) cell line (Petrus et al., 2007).The mechanism of AP18 induced TRPA1 inactivation has been recently suggested. According to a recently proposed model, AP18 covalently modifies TRPA1 cysteine residues at the N-terminal domain of the receptor, but then prevents TRPA1 from adopting an active conformation due to the presence of the methyl groups in AP18 structure (DeFalco et al., 2010). The antagonist AMG7160 is also thought to be a covalent modifier of TRPA1, but no study on its mechanism of action has been reported.

HC030031 is a specific reversible blocker of TRPA1 with unknown mode of action. It was identified by screening for ability to block formalin and allyl isothiocyanate induced activation in humans and mouse TRPA1 (Kerstein et al., 2009). In mice, TRPA1 inhibition by HC030031 leads to a decrease the responsiveness of nociceptors to mechanical force. HC030031 blocks formalin-evoked activation and markedly reduces mechanically-evoked action potential firing in fibers of the peripheral neurons (Kerstein et al., 2009).

Both AP-18 and HC030031 block internalization of cationic fluorescent dye YO-PRO *in vitro*, through TRPA1 channel (Chen et al., 2009). This suggests that

pharmacological antagonists can be used to specifically block cationic fluorescent dye internalization through TRPA1.

Various cations can act as non-specific blockers of TRPA1 channel and can be used to inhibit fluorescent dye internalization. Elevation of calcium ion concentration blocks MET currents in hair cells (Kros et al., 1992; Kros, 1996; Nishikawa and Sasaki, 1996) and FM1-43 internalization in hair cells (Nishikawa and Sasaki, 1996). Elevation of calcium concentration also blocks neuronal mechanosensitive ion channels (Drew et al., 2002; Lumpkin et al., 1997). Ruthenium red and gadolinium chloride are simple cation channel pore blockers which block TRPA1 in mice and *C.elegans* (Garcia-Anoveros and Nagata, 2007; Garcia-Martinez et al., 2000; Kanzaki et al., 1999; Kindt et al., 2007; Liedtke, 2008; Yang and Sachs, 1990). Gadolinium chloride blocks the hair cell MET (Kimitsuki et al., 1996) and reversibly inhibits FM1-43 internalization into hair cells (Meyers et al., 2003). Ruthenium red has been used to inhibit FM1-43 labelling of cells expressing TRPV1 *in vitro* (Meyers et al., 2003).

Aminoglycoside antibiotics, like neomycin, gentamycin and dihydrostreptomycin, are candidate blockers of TRPA1. These large polycationic molecules are non-specific permeant blockers of MET (refer to Fig. 1 in van Netten and Kros (2007)). They interact with the negatively charged selectivity filter in the MET pore blocking transducer currents (Kroese et al., 1989; Ohmori, 1985). Aminoglycosides can enter the hair cells by permeating through MET pore thereby promoting hair cell degeneration which leads to permanent hearing loss (Forge and Schacht, 2000; Marcotti et al., 2005; Waguespack and Ricci, 2005; Wersall et al., 1973). The ability of antibiotics to enter hair cells through MET is a general property of aminoglycosides. The antibiotics are bulkier molecules than FM1-43. A typical size of an aminoglycoside antibiotic is close to dihydrostreptomycin,

DHS, with a diameter of about 1 nm and a length of about 1.5 nm (van Netten and Kros, 2007). Aminoglycosides have been used to inhibit FM1-43 dye internalization in hair cells (Nishikawa and Sasaki, 1996). Neomycin, can induce analgesia in various animal models, and has been reported to potently block TRPV1-mediated membrane currents in sensory neurons (Raisinghani and Premkumar, 2005).

1.2.2.6 TRP gene predictions and their embryonic expression in *S. purpuratus*

Members of the following subfamilies of mammalian TRP channels have been implicated at least in some form of cellular mechanosensation and mechanotransduction: TRPA1, TRPC1, TPRC6, TRPV1, TRPV2, TRPV4, TRPM4, TRPM7 and TRPP2 (Christensen and Corey, 2007; Kahn-Kirby and Bargmann, 2006; Liedtke and Kim, 2005; Liedtke, 2008; Mutai and Heller, 2003; O'Neil and Heller, 2005; Pedersen and Nilius, 2007; Sharif-Naeini et al., 2008; Tobin and Bargmann, 2004; Yin and Kuebler, 2010). Representatives of TRPA, TRPC, TRPM and TRPP subfamilies have been annotated in *S. purpuratus* genome and most of them are expressed embryonically (Table 1.5).

One of these annotations, Sp-TRPA1 (SPU_010335), is the only member of TRPA subfamily identified in *S. purpuratus* genome. In sequence, Sp-TRPA1 is closely related to tunicate TRPA1, and has been grouped with the insect electrophile sensitive TRPA1s (Kang et al., 2010). *S. purpuratus* does not have TRPN1. Therefore, Sp-TRPA1 is the only TRP channel in *S. purpuratus* with the long ankyrin repeat domain and can function in mechanical gating of potential unidentified mechanotransducer. Another TRP channel was annotated in the genome, Sp-TRP channel (SPU_021148), which was not assigned a TRP channel subfamily and could be related to Sp-TRPA1.

Conservation of cysteine and lysine residues in the N-terminus of Sp-TRPA1 predicted protein sequence implies the ability of Sp-TRPA1 to be activated by electrophiles, and to be inhibited by the specific pharmacological antagonist AP-18. Treatment with AP-18 and other TRPA1 inhibitors presents a unique opportunity to explore the function of TRPA1 in embryonic, larval and adult behaviour. It would be of interest to determine whether Sp-TRPA1 is required for mechanosensation in sea urchins as it is in mammals.

Fluorescent dyes, like FM1-43 or TO-PRO, may be used to specifically screen for sensory cells and structures in embryos, larvae and adults having functional mechanotransducer channels that may contain TRPA1 protein. Fluorescent dyes may also be used as indicators of TRPA1 channel activity in response to TRPA1 inhibitor treatments, TRPA1 mutations or morpholino-antisense knockdowns.

Table 1.4 TRP channels in *S. purpuratus*

Channel Family	Channels predicted in *S. purpuratus* genome	Total # of gene predictions	Channels expressed in embryos (egg-72hpf)	# gene predictions expressed in embryos
Transient Receptor Potential (TRP) channels	TRPA1	1	TRPA1	1
	TRPC	2	TRPC	1
	TRPC3	2	TRPC3	2
	TRPC5	8	TRPC5	4
	TRPC6	2	TRPC6	2
	TRPC7	1	TRPC7	0
	TRPM	4	TRPM	4
	TRPM3	9	TRPM3	9
	TRPP1 (PKD1)	1	TRPP1(PKD1)	1
	TRPP2 (PKD2)	3	TRPP2(PKD2)	3
	PKD1L2	1	PKD1L2	1
	TRP-channel	1	TRP-channel	1

1.3 Sensory cells in embryos and early plutei of *S. purpuratus*

Sea urchin embryos, larvae and adults have no sensory structures similar to those of vertebrates (Burke et al., 2006). Genomic evidence has provided clues to the types of sensory structures which may exist in embryos or larvae (Burke et al., 2006; Sea Urchin Genome Sequencing Consortium et al., 2006). Morphological and behavioural studies have identified candidate cells and organs in embryos and larvae with sensory capabilities.

1.3.1 Overview of sea urchin embryonic development

S. purpuratus embryos develop into feeding free swimming pluteus larvae within 4 days if cultured at 12ºC (refer to Fig. 1 in Angerer L.M. and Angerer R.C. (2003)). After approximately two months of feeding and growth larvae undergo metamorphosis to produce a juvenile sea urchins.

Sea urchin eggs have a maternal animal-vegetal axis, and upon fertilization undergo radial holoblastic cleavage to produce a 128 cell blastula (refer to Fig. 8.8 and 8.16 in Gilbert (2000)). After ninth and tenth cleavages, the mid-blastula transition occurs when the cells start dividing asynchronously, zygotic genes are more actively expressed, and all cells develop motile cilia on their surfaces (Masuda and Sato, 1984). The ciliated blastula begins to rotate within the fertilization envelope, secretes zygotically produced hatching enzyme (Lepage et al., 1992) and hatches from the fertilization envelope as a ciliated free swimming "hatched blastula" (Angerer and Angerer, 2003; Ettensohn and Ingersoll, 1992). After hatching, the cells of the blastula

thicken at the vegetal pole and flatten to produce a thickened vegetal plate. The late blastula contains approximately 1000 cells.

All embryonic territories are specified by the 60-cell stage although all cells retain their pluripotency (refer to Fig. 8.12 in Gilbert (2000)). The animal half gives rise to ectoderm and neurons. The Veg1 layer produces ectoderm or endoderm. The Veg2 layer produces endoderm cells, the body wall, and secondary mesenchyme cells. Large micromeres produce primary mesenchyme cells which later form the larval skeleton, and the small micromeres contribute to the body wall (Angerer and Angerer, 2000; Davidson et al., 1998; Ettensohn and Sweet, 2000; Logan and McClay, 1999; Logan and McClay, 1997; Wray, 1999) (refer to Fig. 1 in Angerer L.M. and Angerer R.C. (2000)).

At approximately 20 hours after fertilization, at mesenchyme blastula stage, skeletogenic primary mesenchyme cells (PMCs) leave the vegetal plate and ingress into the blastocoel (Ettensohn and McClay, 1986; Okazaki, 1975; Peterson and McClay, 2003). Approximately 10 hours after the PMC ingression, at early gastrula stage, the archenteron (gut) starts invagination and extends about one third of the way into the blastocoel from the centre of the vegetal plate (Gustafson and Wolpert, 1967). The gut is further extended via: convergent extension (Keller et al., 1985), cell division (Martins et al., 1998), involution movements, and the action of secondary mesenchyme cells (SMCs) which are located at the gut tip (Hardin, 1990). During the late stages of gastrulation SMCs guide the archenteron invagination by attaching to a site near the animal pole and pulling the archenteron to its final length using their contractile filopodia (Dan and Okazaki, 1956; Hardin and McClay, 1990; Hardin, 1988; Schroeder, 1981) . PMCs fuse to form a syncitial ring around the base of the archenteron, and within the ring PMC nuclei form two clusters on the ventral/oral side of the embryo (Peterson and

McClay, 2003). PMCs produce spicule matrix and biomineralize to form the calcite spicules, which will then extend to form a skeleton (Ettensohn, 1992; Ettensohn and Sweet, 2000; McClay et al., 1992). At late gastrula, the archenteron fuses with the stomodeum of the ectoderm wall to form a mouth (Angerer and Angerer, 2003; Ettensohn and Ingersoll, 1992). SMCs ingress from the tip of the archenteron into the blastocoel before the fusion of gut and ectoderm (Gustafson and Wolpert, 1963) (refer to Fig. 8.16 in Gilbert (2000)). When gastrulation is complete, the endoderm differentiates as a tripartite gut separated into distinct fore-, mid-, and hind-gut by sphincters formed from primitive myoepithelial cells (McClay et al., 2004).

During gastrulation, subpopulations of SMCs differentiate and emigrate from the tip of the archenteron (Gustafson and Toneby, 1971). The first subpopulation of SMCs are the pigment cell progenitors, which leave the archenteron at early gastrula stage and embed in the basal side of the ectoderm by pluteus stage (Gibson and Burke, 1985; Gustafson and Wolpert, 1967; Kominami et al., 2001). Pigment cells continue to migrate within the basal side of the ectoderm to space themselves throughout the aboral/dorsal ectoderm using avoidance behaviour that prevents pigment cell clustering (McClay et al., 2004). The remaining SMC sublinneages reside at the tip of future archenteron until gastrulation is completed. These cells participate in the last third of the archenteron elongation and give a rise to the blastocoelar cells, circumesophageal muscle and coelomic pouch cells (Cameron et al., 1991; Ruffins and Ettensohn, 1996).

At prism stage, the oral and aboral regions of the embryo are separated by a band of specialized ciliated cells. These cells align linearly into two or three rows to form a ciliated belt that surrounds the surface of the embryo (Nakajima, 1986b). As development progresses, the cells of the ciliated band increase in thickness and become

columnar or pear shaped. At early or 2-arm pluteus stage, two postoral arms form along the ciliated band (refer to Fig. 1A in Nakajima (1986b)).

When morphogenesis is complete, a pyramidal shaped, 4-arm pluteus is produced, which contains a total of approximately 2000 cells (Angerer and Angerer, 2003; Ettensohn and Ingersoll, 1992). Structurally, the 4-arm pluteus is bilaterally symmetrical, has a pair of triradiate skeletal spicules, two postoral and two anterolateral arms which are rimmed by the ciliated band (refer to Fig. 1A in Burke (1978) and Fig. 1A, B in Smith et al. (2008)). The entire integument of a 4-arm pluteus consists of a monolayer of cells joined by septate junctions covered by hyaline layer externally and lined by basal lamina on the inner side. Each epithelial cell has a motile cilium that extends vertically through the hyaline layer that is surrounded by a ring of microvilli (Nakajima, 1986a). Ciliated epithelium extends throughout the length of the oesophagus (Burke, 1978) and into the stomach of the pluteus (Amemiya et al., 1979). The aboral ectoderm of the pluteus is a simple squameous epithelium, while oral ectoderm is more cuboidal. The ciliated band consists of spindle shaped cells which taper at their apical and basal ends (Burke, 1978). In the ciliated band, each motile cilium is surrounded by a ring of 8-10 microvilli (Burke, 1978), and there are three rows of ciliated cells, the number of which increases as larval development progresses (Burke, 1978). The ciliated band shows little regional specialization, but the portion of the band that overhangs the mouth or the oral hood is notably thicker (Burke, 1978) (refer to Fig. 2A, B in Smith et al. (2008)). The ciliated band surrounding the mouth of the larva separates into two parts: the preoral and perioral ciliated bands (refer to Fig.1A in Nakajima (1986b)). The pluteus begins actively capturing food and feeding at this stage. The ciliated band and ectodermal cilia are used for locomotion and feeding by directing food particles to the

mouth (Burke, 1978; Strathmann, 1971; Strathmann, 1975). The apical organ, a serotonergic sensory structure implicated in feeding and swimming, is positioned at the oral hood between the two anterolateral arms of the pluteus (Byrne et al., 2007).

1.3.2 Overview of sea urchin nervous system structure and development

The understanding of development and structure of the larval and the adult echinoderm nervous systems remains incomplete to this day. Identification of neurons in echinoderms, especially in larvae, has been challenging due to lack of distinguishing features. Structurally, echinoderm neurons have unusual synapses without direct synaptic contacts or pre-post synaptic specializations (Cobb and Pentreath, 1977). To date, no neurophisiological investigation of larval neurons has been accomplished (Burke et al., 2006).

In echinoderm larvae, the nervous system is thought to control ciliary beating, contractions of the esophagus, and arm flexing (Bisgrove and Burke, 1986) required for coordinated behaviour during swimming and feeding (Strathmann, 1971). The circumesophageal muscles, dilator muscles of mouth, and cells of the ciliated band are considered to be the effectors of the larval nervous system (Burke, 1978). It has been hypothesized that the ciliated band of echinoderm larvae is a functional precursor of the neural tube or central nervous system of vertebrates (Garstang, 1894; Lacalli et al., 1994). The larval apical organ of echinoderms has been proposed to be the precursor of the vertebrate brain (Hay-Schmidt, 2000).

The nervous system in echinoderm larvae is comprised of the major neuronal systems present in vertebrates, such ascholinergic (Gustafson and Toneby, 1971; Ozaki, 1974; Ryberg, 1973; Ryberg, 1977), dopaminergic (Burke, 1983), serotonergic (Bisgrove

and Burke, 1986; Bisgrove and Burke, 1987; Burke et al., 1986; Yaguchi et al., 2000; Yaguchi and Katow, 2003), catecholaminergic (Nakajima, 1987), GABAergic (Bisgrove and Burke, 1987), SALMF-amidergic (Beer et al., 2001; Moss et al., 1994; Thorndyke et al., 1992). No melatonin or adrenalin is used in sea urchin larvae or adults (Burke et al., 2006). Apart from neural functions, the neurotransmitter serotonin functions in embryonic development. Preneural serotonin acts as a multifunctional regulator of gastrulation and spiculogenesis (Buznikov et al., 2005; Cameron et al., 1994; Toneby, 1973; Toneby, 1977).

Sequencing and annotation of the *S. purpuratus* genome has provided more insight into the nervous system. According to analyses of annotations of nervous system related genes, sea urchins likely have neurons with ion channel proteins. Genes encoding proteins involved in synaptic function have been annotated. Sea urchin neurons appear to lack gap junction proteins, suggesting that they lack electrical coupling via gap junctions and may communicate thorough chemical synapses without ionic coupling (Burke et al., 2006).

Nearly all genes encoding known neurogenic transcription factors are present in the sea urchin genome (Burke et al., 2006). In embryos, animal plate ectoderm is a site of expression of a transcription factors involved in neural specification in vertebrates and other systems, although their expression is not always confined to this region. Two of them are Sp-Sc-Ac (achaete-scute) and Sp-Hbn (homeobrain), homologues of genes known to be involved in early neural specification in other systems. Sp-Ac is expressed in the scattered cells of the animal plate ectoderm at prism stage. Sp-Hbn is expressed in oral ganglia and scattered cells near the animal plate of plutei (Burke et al., 2006).

Present knowledge of the larval nervous system organization has been accumulated through use of electron microscopy, and histochemical assays, antibodies specific for neural components and neurotransmitters, and in-situ hybridization (Beer et al., 2001; Bisgrove and Burke, 1986; Bisgrove and Burke, 1987; Burke, 1978; Katow et al., 2004; Nakajima, 1986a; Nakajima, 1986b; Nakajima et al., 2004; Ryberg and Lundgren, 1977; Ryberg, 1977; Yaguchi and Katow, 2003). Only early larval nervous system structure and development will be discussed in detail in this section. More information about the organization of late larval and adult nervous system can be found in the following publications (Bisgrove and Burke, 1986; Bisgrove and Burke, 1987; Burke et al., 2006).

Two types of neurons have been identified during embryonic development and in 4-arm plutei of *S. purpuratus*: the serotonergic neurons and the synaptotagmin positive neurons (refer to Fig.1 and 3 in Nakajima et al. (2004)). Studies in a different species of sea urchin, *Strongylocentrotus droebachiensis*, demonstrated that apart from developing a serotonergic system, the 4-arm plutei also develop a dopaminergic and GABAergic system that both increase in complexity as the plutei develop (refer to Fig. 2, 5 and 7 in Bisgrove and Burke (1987)). In *S. purpuratus*, dopaminergic and GABAergic neurons are thought to appear after the 4-arm pluteus stage (Nakajima et al., 2004). Serotonergic and dopaminergic systems function together to control cilia based swimming behaviour in larvae (Bisgrove and Burke, 1987; Wada et al., 1997; Yaguchi and Katow, 2003). In 4-arm plutei of sea urchins *Pseudocentrotus depressus* and *Hemicentrotus pulcherrimus*, dopamine and serotonin were found to influence the beating of cilia by modifying beating cycle length and decreasing or increasing ciliary beating frequency respectively (Wada et al., 1997).

Serotonergic neurons are first to form during embryonic development (Bisgrove and Burke, 1986; Bisgrove and Burke, 1987; Yaguchi and Katow, 2003). In *S. purpuratus*, the first neuronal cells arise at the boundary of animal plate ectoderm and aboral ectoderm. These cells are the presumptive apical organ cells, and are immunoreactive to serotonin antibody. At late gastrula, two pairs of synaptotagmin positive cells arise ventrally from the oral ectoderm at the border of presumptive ciliated band ectoderm, with one pair to the left and the other to the right of the animal-vegetal axis (refer to Fig.3A in Nakajima et al. (2004)).

By early prism stage, more synaptotagmin immunoreactive cells appear. Synaptotagmin positive cells in the presumptive ciliated band project neurites underneath the band. Two bilaterally symmetrical clusters of synaptotagmin positive cells, which formed at the border of oral and aboral ectoderm at gastrula stage, extend neurites towards the aboral side of the embryo (refer to Fig. 3B in Nakajima et al. (2004)). They later develop into the lateral ganglia at pluteus stage, located between the anterolateral and postoral arms on either side of the pluteus body (refer to Fig.3C Nakajima et al. (2004)).

In the 4-arm pluteus, a network of synaptotagmin positive neurites is found beneath the ciliated band ectoderm that extends to all parts of the pluteus (refer to Fig. 1 and 5 in Nakajima et al. (2004). Flask shaped or angular shaped synaptotagmin positive cells are found regularly spaced within the ciliated band ectoderm. These cells connect with their processes to the tracts of neurites extending beneath the ciliated band ectoderm (refer to Fig.1A, B, C and D in Nakajima et al. (2004)). The apical organ contains 4-6 serotonin immunoreactive cells which are bilaterally positioned on either side of the organ, and 10-12 synaptotagmin immunoreactive cells positioned

between the serotonin immunoreactive cells. Both types of cells in the apical organ project processes to the tract of neurites below (refer to Fig.1D, E, and F in Nakajima et al. (2004)). The lateral ganglia contain a cluster of 4-6 cells that project neurites towards the larval posterior (refer to Fig.1A in Nakajima et al. (2004)). A pair of oral ganglia are positioned on either side of the lower lip of the mouth and contain 6-8 column shaped synaptotagmin positive cells (refer to Fig.1A and 5 in Nakajima et al. (2004)). The synaptotagmin positive network of cells also surrounds the oesophagus and the intestine forming the oesophageal plexus and the intestinal plexus respectively (refer to Fig. 1I and G Nakajima et al. (2004)). The 4-arm plutei of sea urchin *Strongylocentrotus droebachiensis* have dopaminergic and GABAergic neurons apart from the serotonergic neurons. The lateral ganglia and the oral ganglia have dopaminergic neurons (refer to Fig. 2A in Bisgrove and Burke (1987)). The GABAergic neurons are positioned on the dorsal wall of the oesophagus. These neurons extend neurites laterally to either side of the oesophagus (Bisgrove and Burke, 1987).

Synaptotagmin antibody staining has provided the most insight into the structure of the *S. purpuratus* nervous system in embryos and 4-arm plutei. However, it has been noted that synaptotagmin antibody might not label all nerve cells (Nakajima et al., 2004). Synaptotagmin positive projections which extend towards the pluteus posterior are thought to extend along the basal side of the ectoderm (Nakajima et al., 2004) (refer to Fig. 1A in Nakajima et al. (2004). The identification of a network in the pluteus posterior at the base of the aboral ectoderm by synaptotagmin antibody supports the findings of previous ultrastructural studies of the pluteus nervous system. Studies of early plutei of sea urchin *Psammechinus miliaris* by Ryberg (1977) and Ryberg and Lundgren (1977) have described a plexus of interconnected neurite-like processes at the

basal side of the ectoderm which interconnect the ectodermal cells (refer to Fig. 2, 3 and 9 in Ryberg (1977) and Fig. 1 in Ryberg and Lundgren (1977)).

It is still not clear if neurite projections in aboral ectoderm are axonal projections to the effector cells or dendritic projections to sensory cells (Nakajima et al., 2004). Previous studies suggest that a second deeper-lying network of cells within the blastocoel made of SMC derived blastocoelar cells makes direct contacts with the basal ectodermal network and therefore may participate in signal propagation in response to ectodermal stimulation (Ryberg and Lundgren, 1977; Ryberg, 1977). However, due to lack of neuronal character attributed to blastocoelar cells, according to ultrastructural and histochemical studies, this theory has been questioned (Bisgrove and Burke, 1987; Burke, 1978). Recently, a serotonin receptor protein was found expressed within the blastocoelar cell network, and it has been suggested that the apical organ may control ciliary beating through the blastocoelar network via secretion of serotonin into the blastocoel (Katow et al., 2007; Katow et al., 2004). These findings will be discussed in more detail in section 1.3.5.5.

The nervous system grows more complex during late larval stages. The number of neurons increases during larval development to include complex array of sensory neurons, interneurons, tracts of axons and ganglia closely associated with larval ciliated bands and muscles (Beer et al., 2001; Bisgrove and Burke, 1986). The larval and adult nervous systems appear to have no direct connections, and during metamorphosis the larval nervous system is largely lost (Burke et al., 2006; Chia and Burke, 1978). In adults, the nervous system is segmented and lacks cephalisation (Burke et al., 2006).

1.3.3 Evidence of a mechanosensory system in sea urchin embryos, larvae and adults

Plutei are able to reverse their ciliary locomotion in response to tactile and electrical stimuli on their surface (Mackie et al., 1969). Pluteus larvae also respond to touch by moving their arms. They exhibit negative geotactic behaviours and can maintain a fixed orientation with their arms pointing upwards in culture (Yoshida, 1966). Pluteus larvae are capable of actively capturing and directing food particles to their mouth by reversal of ciliary beating in the ciliated band (Strathmann, 1975; Strathmann, 2007). Mechanical stimulation of the thickened region of the ciliated band rimming the upper lip of the larval mouth stimulates swallowing (Gustafson et al., 1972b).

Adult sea urchins detect touch stimuli and are negatively geotactic. The adult spines, tube feet and pedicellariae are extensively enervated, and are all proposed to be mechanosensory structures (Burke et al., 2006). Cells with sensory hairs and the ciliated epithelium found on the test surface may have a mechanosensory role as well (Hyman, 1955). Sphaeridia, small enervated skeletal appendages found on the test surface, have been proposed to act as balance organs (Fell and Pawson, 1966; Hyman, 1955).

1.3.4 Evidence of a photosensory system in sea urchin embryos, larvae and adults

The sea urchin genome contains genes encoding homologues of proteins involved in phototransduction including retinal transcription factors and several opsins (Burke et al., 2006). Rx (retinal anterior homeobox) is a crucial transcription factor in vertebrate eye development which may function in the proliferation of cells in the retina and the ventral hypothalamus and in specification of the retinal progenitors (Bailey et al., 2004). In *S. purpuratus* blastulae, Sp-Rx mRNA accumulates in animal plate ectoderm and at a low level in vegetal cells of blastulae. In gastrulae, Sp-Rx mRNA is

restricted to the animal plate ectoderm. At pluteus stage, Sp-Rx mRNA is found in the animal plate and around the gut (Burke et al., 2006). Multiple other retinal transcription factors are expressed in *S. purpuratus* starting as early as 72hpf at prism stage (Burke et al., 2006; Ooka et al., 2010; Raible et al., 2006).

A total of six opsin genes have been found in *S. purpuratus* genome. Expression of Sp-opsin-1 homologue, Hp-ECPN, was characterized in the embryos of sea urchin *Hemicentrotus pulcherrimus*. Spatial protein expression of this opsin was detected in SMC derivatives in 4-arm plutei (Ooka et al., 2010). Results of this study will be discussed in detail in further sections. Older larvae of *S. purpuratus* express four out of six opsins present in the genome (Raible et al., 2006). Spatial Sp-opsin-4 gene expression was detected in *S. purpuratus* two-week-old larvae in a specific subset of 1–2 cells close to the ciliated band at the tips of the postoral arms. This study reports that, structurally, cells expressing this opsin resemble rhabdomeric photoreceptor cells (Raible et al., 2006).

Little is known about the photosensitivity of sea urchin embryos and larvae. Phototactic responses of sea urchin plutei have been detected (Neya, 1965; Pennington and Emlet, 1986; Yoshida, 1966), but specific photoreceptors of sea urchin larvae have not been identified (Burke et al., 2006). More evidence for photosensitivity of sea urchins has been accumulated from studies on adults. They exhibit behavioural responses to light, and their reproductive cycle is influenced by the photoperiod (Boolootian, 1966; Giese and Farmanfarmanian, 1963; Reese, 1966;Yoshida, 1966). Sea urchin test, pigmented radial nerves and tube feet are photosensitive (Burke et al., 2006; Sea Urchin Genome Sequencing Consortium et al., 2006). In adult tube feet of *S. purpuratus*, cells adjacent to the longitudinal muscle fibers express a homologue of Pax6

(Czerny and Busslinger, 1995), a critical transcriptional regulator of vertebrate and invertebrate eye development (Gehring, 2005). Tube feet express three homologues of opsins, and several other key mammalian retinal transcription factors suggesting that tube feet may function as photosensory organs. Pedicellariae express five opsins (Burke et al., 2006; Raible et al., 2006). Sea urchins adults were proposed to have spatial vision (Blevins and Johnsen, 2004), and they may be using their test as a compound eye (Aizenberg et al., 2001; Woodley, 1982). A recent study shows that *S. purpuratus* is capable of detecting a target within its environment and respond to that target by either fleeing or approaching it (Yerramilli and Johnsen, 2010).

1.3.5 Sensory cell candidates in sea urchin embryos and 4-arm plutei

1.3.5.1 Apical tuft

During development, before the gut invagination, embryos obtain a tuft of long non-motile cilia at the animal plate ectoderm (refer to Fig. 8.16B in Gilbert (2000)). An apical plate with tufted non-motile cilia is a common feature in many aquatic invertebrate embryos (Hyman, 1955). In echinoid larvae, the apical tuft area develops into the apical organ at later stages (Burke, 1983; Burke, 1978). Specific cells of the apical plate give a rise to the larval nervous system (refer to section 1.3.2).

The appearance of apical tuft coincides with the acquisition of swimming directionality by embryos. The apical tuft has been proposed to play a mechanosensory role and is possibly required for swimming directionality. Structurally the apical tuft cilia are indistinguishable from the motile cilia used for swimming, but are longer (Stephens, 2008).

1.3.5.2 Apical organ

The animal plate ectoderm that harbours the apical tuft cilia at earlier embryonic stages later develops into the apical organ. The serotonergic cells of the apical organ are considered to be sensory neurons and the apical organ is a sensory organ that participates in swimming and feeding (Bisgrove and Burke, 1987; Gustafson and Toneby, 1971; Horstadius, 1973; MacBride, 1903; Ryberg, 1974). The apical organ is highly sensitive to mechanical stimulation (Gustafson et al., 1972a). Expression of Sp-Rx in the animal plate at earlier stages in *S. purpuratus* (Burke et al., 2006) suggests that the cells of the apical organ may have photosensory functions.

In the sea urchin *H. pulcherrimus*, starting at the 4-arm pluteus stage, the apical organ area between the anterolateral arms, contains epithelial cells with coiled non-motile cilia that project axonal processes to the underlying neurite tracts. The coiled cilia are submerged within the hyaline layer on the ectoderm surface. These cilia always lie horizontally to the surface in the hyaline layer and are invisible unless the hyaline layer is removed. Their function is most likely sensory, as they structurally resemble sensory cells in other invertebrates (Nakajima, 1986a) . Such cells may be present in the 4-arm plutei of *S. purpuratus*.

1.3.5.3 Cells of the ciliated band

The ciliated band of the pluteus is enervated. Axonal tracts extend along the basal side of the ciliated band ectoderm. In *S. purpuratus*, up to 20 axons are found within this tract at 4-arm pluteus stage (Burke, 1978).

In *H. pulcherrimus* 4-arm plutei, a subtype of cells with sensory cell characteristics has been found within the ciliated band. The cell bodies of these cells

are located between the rows of ciliated band cells (refer to Fig. 5 in Nakajima (1986b)). These cells have immotile cilia, which lie within the grooves between the rows. Axonal projections, containing vesicles, extend from these cells and join the underlying axonal tract. The immotile cilia of these cells are covered by a hyaline layer and do not extend away from the ectoderm surface. Mechanosensory and chemosensory functions have been proposed for these cells. Other cells of the ciliated band that lack axonal projections contain vesicles and make direct contacts with the basal axonal tract (refer to Fig. 5 in Nakajima (1986b)) and may also have sensory functions as well.

Another subtype of cells within the ciliated band was detected in *S. purpuratus* 4-arm plutei. These cells are located on the oral side of ciliated band and extend their branched microvillar processes to the exterior of the larva. The cytoplasm of the processes is filled with vesicles. These cells have axons, with vesicles, that extend to the basal axonal tract of the ciliated band. Branched microvilli that surround the oral ectoderm of the larva may function as sensory receptors detecting water current when larvae swim forward, or as mechanoreceptors involved in larval feeding mechanism (Burke, 1978).

Although obvious similarities exist in structures and positions of the aforementioned ectoneural cells to the flask shaped or angular synaptotagmin cells of the ciliated band of *S. purpuratus* 4-arm pluteus (Nakajima et al., 2004), the direct relationship of between these cells has not been described.

Spatial expression of Sp-opsin-4 has been detected at the arm tips two-week-old 4-arm plutei of *S. purpuratus* (Raible et al., 2006). Thus, it is possible that specific cells of the ciliated band at the arm tips of 4-arm plutei have photosensory functions.

1.3.5.4 Ciliated cells of the oral and aboral ectoderm

The oral ectoderm of the *H. pulcherrimus* 4-arm pluteus has cells with immotile cilia and fine radial processes extending on the surface of epithelium. Both the cilia and the processes are submerged within the hyaline layer (Nakajima, 1986b). These cells have axonal projections extending toward the ciliated band between the epithelial cells and the basal lamina (refer to Fig. 9 in Nakajima (1986b)). The nerve bundles originating from these cells often lie in close vicinity to the filopodia of blastocoelar cells. These cells were proposed to function in chemoreception, mechanoreception and photoreception (Nakajima, 1986b).

The aboral ectoderm has been suggested to be a sensory field responsive to touch and electrical stimulation controlling ciliary beating reversals (Mackie et al., 1969). The ciliary reversal behaviour was blocked by magnesium chloride (Mackie et al., 1969), a substance known to suppress nervous activity in vertebrates (Burke, 1978). Since all cells in the aboral ectoderm are ciliated and make close contact with synaptotagmin positive projections of the larval nervous system (Nakajima et al., 2004) it is reasonable to speculate that some or all of them are mechanosensitive.

Larval aboral epithelium was suggested to be able to perform non-nervous conduction in response to extraembryonic stimuli (Mackie et al., 1969). Non-nervous conduction arose in evolution to serve as an alternative to nervous (Leys et al., 1999). In small animals, the non-nervous conduction can be efficient because of the short conduction route (Spencer, 1974). Non-nervous conduction in epithelia in animals plays a role of protective and escape responses. In hydromedusae, sponges and amphibian tadpoles the epithelia are able to sense mechanical force. Conductive epithelia are extensions of the sensory nervous system and are able to spread excitation to effectors

where there is no need for each effector to be enervated independently (Spencer, 1974).

1.3.5.5 Blastocoelar cells

Blastocoelar cells are dendritic shaped cells derived from secondary mesenchyme cells (SMCs). They form a network within the blastocoel of embryos and larvae. The cells of the network exist in clusters, which contact each other through branched thin processes and interconnect all the parts of the larva within the blastocoel (Burke, 1978). The cells are concentrated around the apical organ, the ciliated band, the digestive tract, and along the skeletal rods of the larva (Katow et al., 2004; Katow et al., 2007; Ryberg, 1977). The function of the blastocoelar cells is not established. Suggestions have been made through the years about their function, including immune and sensory functions.

In sea stars mesenchyme cells appear at the tip of archenteron during gastrulation, similar to the sea urchin embryos. Later in development, they are found widely dispersed throughout the blastocoel (Chia, 1977). These cells form a network similar to the sea urchin blastocoelar network (Kaneko et al., 1995). Blastocoelar cells of the starfish larva have an ability to migrate, encapsulate and adopt a multi-nucleated form in response to foreign materials injected in the blastocoel (Metchnikoff, 1891). Bacteria and foreign materials can also can cross the blastocoelar walls of larvae, presumably when septate junctions within the wall transiently disassemble without loss of epithelial integrity. It was suggested this penetration may be a natural occurrence, and marine bacteria could be a target of mesenchyme cells in the defence system of the sea star larva, where mesenchyme cells act as scavenger cells to sustain an immaculate blastocoel (Furukawa et al., 2009). As in sea star embryos, sea urchin blastocoelar cells are also capable of phagocytosis and bacterial degradation (Hibino T. and Rast J.

unpublished data) (Hibino et al., 2006). It has been suggested that most of the sea urchin blastocoelar cells are dendritic cells having a role in the innate immune response, similar to the dendritic cells in vertebrates that regulate immune responses, and appear to connect the immune system to the nervous system (John Rast , unpublished data). Sea star mesenchyme cells have also been suggested to sustain embryonic shape by exerting mechanical tension against the fibrous component of the extracellular matrix (Crawford et al., 1997; Kaneko et al., 2005), although in sea urchins larvae skeletal spicules appear to fulfil this role.

In a study of 4-arm pluteus of sea urchin *Psammechinus miliaris*, blastocoelar cells were suggested to have a neuronal character and function in signal propagation. The blastocoelar cell network was found to connect to a superficial hydra-like ectodermal plexus of processes extending under and between the ectodermal cells of the pluteus ectoderm. In the ectodermal plexus, processes interconnected between each other. They were also seen interconnecting the cell bodies in the ectoderm (refer to Fig. 2, 3 and 9 in Ryberg (1977)). The ectodermal plexus was suggested to have a sensory function in detection of external stimuli. Histochemical and electron microscope evidence showed that blastocoelar cells had a neuronal ultrastructure similar to adult neurons from tube feet of the sea stars *Asterias rubens* and *Astropecten irregularis*. The cytoplasm of blastocoelar cells contained vesicles, polysomes and ER, and the cell junctions between these cells appeared to have closely apposed membranes (Ryberg, 1977). Although some aspects of the structure of blastocoelar cells were similar to nerve cells, propagation of action potential in these cells was thought to be unlikely (Burke, 1978).

Recently, analysis of the sea urchin *H. pulcherrimus* embryos and plutei by immunohistochemistry showed that the serotonin receptor protein is expressed on the surface of blastocoelar cells (Katow et al., 2004; Katow et al., 2007). Expression of other nervous system related genes such as "glial cell missing" has also been reported in secondary mesenchyme cells (Davidson et al., 2002).

In vertebrates, serotonin receptors have been found in neurons of both the central and the peripheral nervous systems and in non-neuronal tissues such as gut and cardiovascular system (Hoyer and Martin, 1997). Serotonin receptors have been grouped into seven families based on structural, functional and transductional properties (Hoyer et al., 2002). So far 14 serotonin receptors have been identified in mammals (Hoyer and Martin, 1997) and 13 in invertebrates like *Drosophila*, molluscs, and nematodes (Tierney, 2001). Invertebrate serotonin receptors have diverged from those of vertebrates and now have different pharmacological properties (Tierney, 2001). Homologues of four serotonin receptors have been identified in the *S. purpuratus* genome (Burke et al., 2006): 5HT-1A (GLEAN3_18826), 5HT-1F (GLEAN3_25436), 5HT-2C (GLEAN3_25436) and 5HT-7 (GLEAN3_05097). Only one of the four predicted serotonin receptors, 5HT-1A, is expressed at embryonic stages (Katow et al., 2007).

In *H. pulcherrimus* embryos, cells immunoreactive to 5HT-1A antibody first appear at prism stage, restricted to the region around the archenteron tip. The 5HT-1A antibody stain then expands to more secondary mesenchyme cells as development progresses. This expansion does not involve proliferation of immunoreactive cells and occurs by an unknown mechanism. The stain expands posteriorly in prisms and early larvae in a clockwise direction from the right side of the apical tuft. The stain then spreads anteriorly on the left side by early 2-arm pluteus stage to complete the ventral

network formation. Immunoreactive cells start to form a network starting from prism stage. Initially, at prism stage, this network is not associated with the skeletal spicules, but as development progresses to the 2-arm pluteus stage, the signal spreads along the cell tracts of the larval skeletal rods (Katow et al., 2004).

At 4-arm pluteus stage, there are seven 5HT-1A immunoreactive blastocoelar cell tracts, some spicule-associated and some spicule-independent. These seven tracts of blastocoelar cells are collectively referred to as the serotonin receptor cell network (SRN) (Katow et al., 2007). The SRN cells are derived from the SMCs. It is not known whether all of the blastocoelar cells belong to the SRN, or if the SRN constitutes a subpopulation of blastocoelar cells (Katow et al., 2004; Katow et al., 2007)..

The SRN is comprised of left and right anterolateral rod tracts, left and right body rod tracts, an oral transverse tract, and two SRN plexuses that include dorsal oesophagus plexus and dorsal stomach plexus (refer to Fig. 3H in Katow et al. (2007)). The cell processes of the SRN insert into the ectoderm in several areas of the pluteus larva. Seven areas of insertion were identified by Katow et al. (2004) and Katow et al. (2007):

1. Around the apical organ, with fibers extending from the oral lobe transverse tract; some of these fibers reach the apical surface of the larva and associate closely with serotonin-positive cells suggesting a functional relationship between SRN and the serotonin cells of the apical organ.
2. At the tips of left and right anterolateral arms, with multiple branching fibers extending from oral rod tracts.

3. At the tips of left and right postoral arms, with multiple branching fibers extending from postoral rod tracts; these fibers closely associate with the spicules and appear to reach apical surface of the ectoderm.
4. Some fibers of the SRN enter the ectoderm in the middle of the larval arms and bend at the apical surface of the ectoderm.
5. In the middle of the left and right sides of pluteus posterior, with single fibers extending from body rod tracts.
6. In the ciliated band between the two postoral larval arms, with processes extending from the body rod tracts.
7. In the posterior tip of the pluteus, with multiple branched fibers extending from the body rod tracts.

The SRN has been suggested to be a component of the nervous system produced by the SMCs downstream of neuronal system transduction pathways initiated by serotonin cells (Katow et al., 2004; Yaguchi et al., 2000). In 4-arm plutei, the SRN has been proposed to control "spatial swimming" (Katow et al., 2007). Serotonin is proposed to be secreted into the blastocoelar cavity by the apical organ, where it binds to the 5HT-1A receptors of the SRN and transmits signals to ectodermal cells via the SRN processes inserted in the ectoderm (Katow et al., 2007). It is proposed that the response of ectodermal cells is elevation of calcium ion concentration that may "stabilize the rhythm of ciliary beating" (Wada et al., 1997). In this way the apical organ may orchestrate the ciliary beating and elicit its control over swimming behaviour of the pluteus allowing "spatial swimming" to occur (Katow et al., 2007). Treatment of developing embryos with serotonin synthesis inhibitor, p-Chlorophenylalanine (pCPA),

altered the SRN resulting in fewer SRN cells, fewer connections between SRN cells, fewer insertions into the ectoderm and inhibition of spatial swimming. Larval cilia were still able to beat but the larvae were observed crawling at the bottom of the culture dish and were incapable of swimming upwards. The pCPA treatment did not alter the structure of the synaptotagmin-defined neural network, suggesting that this system is not sufficient for spatial larval swimming. However, the possibility of control of swimming by other systems than the SRN was not excluded. The pCPA-treated larvae had abnormal morphology with small digestive tract and severely decreased levels of gut calcium ion concentration (Katow et al., 2007).

Serotonin mediated intracellular calcium ion elevation affects ciliary beating in other invertebrates. Ciliary beating increases through serotonin stimulated cytoplasmic calcium elevation in invertebrates including the pond snail *Helisoma trivolvis* (Christopher et al., 1996; Doran et al., 2004), mussel *Mytilus edulis* (Murakami, 1983; Murakami, 1987), and clam *Spisula solidissima* (Stephens and Prior, 1992). Similar to invertebrates, ciliary beating increases through serotonin stimulated cytoplasmic calcium elevation in vertebrates (Jahnel et al., 1993; Nguyen et al., 2001; Saino et al., 2002). In mammals, serotonergic neurons transmit signals through synapses or by secretion to the target cells that have serotonin receptors (Deutch and Roth, 1999).

An alternative function has been proposed for the SRN. The SRN fibers that insert into the ectoderm may be involved in the extra-embryonic signal reception (Katow et al., 2004). This theory is considerable given that the SRN fibers insert into all of the areas of the pluteus that contain candidate sensory cells described in section 1.3.5. Also, Ryberg (1977) described the blastocoelar cell network contacting a superficial plexus of cell processes at the basal side of the ectoderm (refer to Fig. 9 in Ryberg (1977)), which

may have synaptotagmin positive processes (Nakajima et al., 2004). This plexus may communicate extra-embryonic signals to the SRN. Alternatively, the processes of the SRN may detect extra-embryonic signals and modulate ciliary beating through this superficial plexus.

1.3.5.6 Pigment cells

The function of pigment cells in sea urchin embryos and larvae has not been fully characterized. One of the proposed functions of sea urchin pigment cells is immune defence (Metchnikoff, 1891; Silva, 2000). The sea urchin echinochrome is synthesized in pigment cells (Griffiths, 1965; Kuhn and Wallenfells, 1940; McLendon, 1912). The echinochrome has the characteristics of a polyketide compound (Calestani et al., 2003). In bacteria, fungi and plants polyketide compounds function as antibiotics in defence against pathogens (Calestani et al., 2003; Schroder et al., 1998; Winkel-Shirley, 2002). In plants, the polyketides also function in response to UV and visible light exposure (Schroder et al., 1998; Winkel-Shirley, 2002). In algae, sponges and molluscs polyketides are toxic compounds that function in defence against predators (Garson, 1989). The *S. purpuratus* echinochrome has been proposed to function as an antibiotic. The echinochrome is thought to be made by *S. purpuratus* polyketide syntheases, which are closely related to bacterial and fungal polyketide syntheases (Calestani et al., 2003; Service and Wardlaw, 1984).

The morphology and behaviour of pigment cells was noted to be similar to those of macrophages. Pigment cells have a stellate shape with two or three pseudopodia which can be rapidly extended and contracted, and they have the ability to migrate within the larval epithelium and through the basal lamina (Gibson and Burke, 1987). Pigment cells were proposed to be involved in defence of sea urchin larval ectoderm

(Smith, 2005). They are capable of phagocytosis and appear to participate in wound healing in larvae (Hibino and Rast, unpublished data). Pigment cells migrate to the gut and release their pigment content when larvae are placed in high concentrations of bacteria (Jon Rast, unpublished data).

Photosensation is another proposed function of pigment cells. Pigment cells were observed to change shape and pigment cell granules are displaced in response to light in pseudopodia of sea urchin *Centrostephanus longispinus* (Gras and Weber, 1977; Weber and Dambach, 1974; Weber and Gras, 1980) similar to the melanophores and dermal photoreceptors, in fish and amphibians (Schliwa and Bereiter-Hahn, 1973; Wise, 1969).

A recent study proposes that a sea urchin opsin protein is localized in cells that function together with pigment cells to control spatial swimming in response to light (Ooka et al., 2010). Encephalopsin is thought to be required for encephalic photoreception in mammals, an extra-retinal form of photoreception known to be important for circadian rhythms in non-mammalian vertebrates (Blackshaw and Snyder, 1999). *Hemicentrotus pulcherrimus* Hp-ECPN protein, a sea urchin homologue of mammalian encephalopsin and analogue of *S. purpuratus* Sp-Opsin1, was found expressed in a subset of cells derived from SMCs in *H. pulcherrimus* embryos and larvae. According to the study, the origin and distribution of Hp-ECPN cells during development closely resembles that of the pigment cells (Katow and Aizu, 2002; Kominami et al., 2001; Takata and Kominami, 2003; Takata and Kominami, 2004).

Hp-ECPN mRNA expression was detected starting at swimming blastula stage and until 4-arm pluteus stage. No spatial mRNA expression data was reported in the study. Hp-ECPN protein expression was detected by Western Blotting at swimming blastula stage and persisted until the 4-arm pluteus stage. Spatial protein expression

was not detected until early gastrula stage, when the protein localized to the cells of the archenteron. By mid-gastrula stage, the protein was present in the cells at and around the tip of the archenteron. In late gastrulae, immunoreactive cells increased in numbers and spread within the blastocoel and around the ectoderm. By prism, these cells distributed extensively within the blastocoel and ectoderm and were irregular or bipolar in shape. At 2-arm pluteus stage, the cells acquired a round shape, and became restricted to the aboral ectoderm in the blastocoel. At 4-arm pluteus stage, the number of these cells was reduced in the aboral ectoderm. They concentrated at the tips of the larval arms and in the blastocoelar space at the posterior end of the embryo (Ooka et al., 2010).

Vertical or spatial swimming in larvae was inhibited with a morpholino-antisense oligonucleotide against Hp-ECPN mRNA. After injection of morpholino at the 2-arm pluteus stage, 12 hours later, larvae sank to the bottom of the bio-assay cuvettes. As development progressed to 4-arm pluteus stage, the number of settling plutei increased. Injected plutei were alive and retained ability to swim horizontally. The number of Hp-ECPN cells in these larvae was reduced but the pigment cells were not lost. The study showed no rescue experiments for morpholino effects. When plutei were cultured in the dark they failed to develop a normal number of Hp-ECPN positive cells, and their swimming activity was not assessed. Also, no experiments to assess the ability of larvae to swim vertically in response to light were conducted in the study (Ooka et al., 2010).

It was suggested that the pigment cells and the Hp-ECPN positive cells at arm tips were required for vertical or spatial swimming in larvae, and that Hp-ECPN protein was required for larval phototaxis. The Hp-ECPN cells at the arm tips were proposed to

be photoreceptors controlling swimming direction in response to light, presumably through axonal contacts with the ciliated band (Ooka et al., 2010).

1.4 Specific aims of the project

This introduction has summarized the state of knowledge concerning the nervous system of sea urchin embryos and early larvae. Clearly, more information is required about the sensory system and how swimming behaviour is controlled in response to external stimuli. Considering this backdrop and taking advantage of the recently annotated sea urchin genome, the goals of my Thesis project were:

1. Characterize spatial and temporal expression of Usher genes and the TRPA1 gene in embryos and early (4-arm plutei) of *S. purpuratus* possibly identifying putative mechanosensory and photosensory cells.
2. Screen for possible mechanosensory cells using fluorescent dyes FM1-43 and TO-PRO.
3. Assess the effects of non-specific inhibitors of mechanosensory channels and specific inhibitors of TRPA1 on internalization of FM1-43 and TO-PRO dyes, and on the swimming behaviour of embryos and early pluteus larvae.

2: Usher genes

2.1 Introduction

Usher syndrome is a human recessive autosomal disorder that is the most common cause of combined deafness and blindness in humans. Mutations in the set of Usher genes affect function of ciliated sensory cells, including the hair cells in the inner ear and the photoreceptors in the retina. Usher genes have been considered to be vertebrate specific, and their functions do not appear to be conserved in invertebrates. With the recent annotation of an almost complete set of Usher genes in the genomes of *S. purpuratus* and *C. intestinalis*, it has become apparent that these genes are not vertebrate specific, raising questions about their function in invertebrates (refer to sections 1.2.1.2 and 1.2.1.3).

A considerable amount of genomic and behavioural evidence suggests the ability of sea urchin embryos and larvae to sense their external environment (refer to sections 1.3.3 and 1.3.4). The embryonic apical tuft is proposed to be a mechanosensory structure that may be required for embryo swimming directionality. Mechanosensory or photosensory roles have been proposed for a variety of ciliated cells in 4-arm plutei including cells of the apical organ, cells of the ciliated band, ectoneural cells of the oral ectoderm, and cells of the aboral ectoderm (refer to section 1.3.5). But these proposed roles remain tentative, awaiting more definitive investigations.

In an attempt to identify sensory cells in embryos and 4-arm plutei, I performed temporal and spatial mRNA expression analyses for all *S. purpuratus* Usher gene predictions as well as temporal and spatial analyses of the Whirlin protein expression.

2.2 Materials and Methods

All reagents were obtained from Sigma-Aldrich unless otherwise specified.

2.2.1 Animals

Adult *Strongylocentrotus purpuratus* sea urchins were collected during the mid-winter to early spring period, on the west coast of Vancouver Island, British Columbia, Canada. Animals were kept in circulating tanks in natural seawater (SW) at 9^{o}C. A winter light cycle was used to preserve them in gravid state.

2.2.2 Culture of embryos

Gametes were collected by electrical stimulation. The animals were partially submerged in SW in a shallow glass dish, with their aboral surfaces facing up, leaving the aboral surfaces above SW level. During the procedure the SW rested at 1-2cm below the gonopores, so that the exposed test surface was moist. A pair of electrodes was used to apply 10sec 30 Volt pulses to radially opposed gonopores, by lightly touching the animal surface with an electrode, approximately 1cm below either gonopore. The pulses were repeated until the animal started shedding. Approximately 50µl of sperm was collected using a glass Pasteur pipette and stored in 1.5ml microcentrifuge tube on ice. Great care was taken to ensure that the sperm had no contact with the SW before collection. Eggs were collected by rinsing the aboral surface of the animal with SW and separated from debris by filtration through 153µm nylon mesh. Eggs were then washed 3 times at 12ºC, by settling for 1hr, pouring of excess SW to final volume of 300ml, and adding more SW to a total of 2L. Approximately 5µl of sperm was diluted in 1.5ml of SW, mixed, and the immediately added to 300ml of washed egg suspension in a 2L beaker. The sperm solution was added in small increments using a Pasteur pipette, by

exponentially increasing the added sperm amount from 1 drop to approximately 1ml. All of the sperm dilution was added within one minute. As the sperm was being added, the egg suspension was constantly and vigorously mixed by swirling. Fertilization efficiency and embryo numbers were estimated using Zeiss upright microscope with 10x magnification lens. To determine fertilization efficiency, approximate percentage of embryos with fertilization envelopes was estimated. Only 95-100% fertilization efficiencies were acceptable for embryo cultures used. A second round of fertilization was acceptable, in some cases, if it was performed immediately. Fertilized eggs were washed once in 2L of SW by settling the eggs for 1-2hrs and pouring off excess SW. A haemocytometer (Depth 0.100mm; 1/400 square mm) was used to estimate fertilized egg concentration. Embryo cultures were set up by adding the appropriate amount of fertilized egg suspension to culture plates to a final concentration of 25 embryos/ml. Embryos were cultured in 1.5L or 1.0L flat bottom glass plates for up to 96 hours post fertilization (hpf). During the first 24hrs each embryo had a space around it once settled to the culture dish bottom to allow proper aeration. The plates were loosely covered with saran wrap to prevent contamination and to allow air exchange to occur. The dishes were kept in a ventilated incubator without stirring in the dark at 12ºC. Alternatively, embryos were cultured at 300-2000 embryos/ml in 2L beakers with constant stirring using turning paddles. The speed of the paddle device was 1 full rotation/min, and the bottom edge of the paddle was at least 1cm away from the bottom of the beaker. When cultured with stirring, embryos were washed after hatching (at 24hpf) by reverse filtration through a 10cm diameter filter with 25µm nylon mesh, as described in Wray et al. (2004). Developmental progress and embryo behaviour were monitored using a Leica MZ95 dissecting microscope.

2.2.3 Larval culture

Larvae were cultured as recommended by Wray et al. (2004). Larvae were grown in 3L beakers, without stirring, in a ventilated incubator at 12ºC in the dark. The beakers were loosely covered with saran wrap to prevent contamination and to allow air exchange to occur. Feeding regimen for embryo cultures started at 4-5 days post fertilization, at early 4-arm pluteus stage. As development of larvae progressed, the concentration of larval culture was gradually adjusted to 1 larva/10ml. Once a week, the SW was changed in larval cultures by reverse filtration through a 10cm diameter filter with 25µm nylon mesh. While in the filter, the larvae were rinsed with a light flow of SW. After washing, the larvae were collected using a Pasteur pipette and added to a clean beaker with fresh SW. Generally, eight-armed larvae were obtained within 4-5 weeks.

Larvae were fed 3 times a week, by adding *D. tertiolecta* concentrate to achieve a constant daily concentration of 5000 cells/ml. Algal concentrate was prepared by centrifuging algal culture for 5min at 3000*xg* at RT. The supernatant algal medium was discarded (toxic to embryos and larvae), and the algal pellet was dissolved in fresh SW. Algal cell concentration was estimated using a haemocytometer (Depth 0.100 mm; 1/400 square mm).

2.2.4 Algal medium

Algal medium was prepared according to recommendations in Harris et al. (1980) and Price et al. (1987). A Combined Stock Solution was prepared by mixing 0.2 volumes of each of the five Nutrient Enrichment Stock Solutions. Nutrient Enrichment Stock Solutions: No.1 (549.09µM $NaNO_3$), No.2 (21.79µM Na_2glycerophosphate), No. 3 (105.60µM $Na_2SiO_3 \cdot 9H_2O$), No. 4 (9.81µM $Na_2EDTA \cdot 2H_2O$, 5.97µM

$Fe(NH_4)_2(SO_4)_2 \cdot 6H_2O$, 5.92 x 10^{-1} µM $FeCl_3 \cdot 6H_2O$), No. 5 (2.42µM $MnSO_4 \cdot 4H_2O$, 2.54 x 10^{-1} µM $ZnSO_4 \cdot 7H_2O$, 5.69 x 10^{-2} µM $CoSO_4 \cdot 7H_2O$, 5.2 x 10^{-1} µM $Na_2MoO_4 \cdot 2H_2O$, 5.05µM $Na_2EDTA \cdot 2H_2O$, pH 6.0), and No.6 (61.46µM H_3BO_3). To prepare the algal medium, 0.005 volumes of Combined Stock Solution, 2ml/L Vitamin Stock solution (2.97 x 10^{-1}mM Thiamine, 1.47 x 10-3mM Vitamin B12, 4.09x 10-3mM Biotin), 0.12g/L Sodium Bicarbonate, and 0.96ml/L 1N HCl were combined with natural SW in an Erlenmeyer flask. The algal medium was mixed thoroughly by light shaking for 10min at RT. Then, the algal medium was autoclaved for 20min at 121ºC. After autoclaving, the algal medium was allowed to sit for 24hrs at RT so that a precipitate formed at the bottom of the flask. This precipitate was removed by aseptic vacuum-filtration through a sterile filter. The filter was assembled from glass wool placed between two 9cm diameter paper filters (Whatman, Inc., 202 grade). After the medium had been filtered into an Erlenmeyer flask, it was stored at RT.

2.2.5 Algal culture

Dunaliella tertiolecta (NEPCC strain 001) was obtained from North East Pacific Culture Collection (NEPCC), at University of British Columbia. Algae were cultured in sterile 0.5L Erlenmeyer flasks, covered with aluminum foil, with constant bubbling via polyvinyl chloride (PVC) tubing connected to a 1ml plastic sterile serological pipette (Sarstedt, Cat. No. D51558). The air was filtered through a 0.45µm filter (Millipore, Cat. No. HPWP02500). Algal culture was passaged every 2 weeks, or when the culture started to accumulate a precipitate at the bottom of the flask. Passaging was done by aseptically transferring 10ml of old culture to a new sterile flask containing 400ml of fresh algal medium. Used flasks were cleaned by incubation in glacial acetic acid (EMD, Cat.No.AX0073-6) for 2hrs at RT. After cleaning, flasks were rinsed with distilled water

and autoclaved. All equipment, including flask cleaning utensils, was washed with distilled water only, without any detergent or soap.

2.2.6 Probe and primer design

Full coding sequences for *S. purpuratus* gene annotations were obtained from Baylor College of Medicine *S. purpuratus* annotation database: http://annotation.hgsc.bcm.tmc.edu/Urchin/cgi-bin/pubLogin.cgi. Embryonic expression data from microarray analyses (egg to 96hpf) was confirmed using two databases, *S. purpuratus* Gene Expression Database, National Institute of Dental and Craniofacial Research (NIDCR), http://urchin.nidcr.nih.gov/blast/exp.html, and the Transcriptome of Sea Urchin *S. purpuratus*, Systemix Institute, http://www.systemix.org/content/transcriptome-sea-urchin-strongylocentrotus-purpuratus-v-05. Annotated coding sequences were in-silico translated using Biological Sequence Alignment Editor (BioEdit), Ibis Biosciences, http://www.mbio.ncsu.edu/BioEdit/bioedit.html. Protein secondary domains were predicted using Simple Modular Architecture Research Tool (SMART), European Molecular Biology Laboratory (EMBL), http://smart.embl-heidelberg.de/. Probe sequences were designed to be approximately 800-1000bp long. The probe sequences were selected to be unique identifiers of the gene predictions. The unique identity of probe sequences was confirmed by searching *S. purpuratus* taxid 7668 Nucleotide Collection (nr/nt) using NCBI Nucleotide Basic Local Alignment Search Tool (blastn), (http://blast.ncbi.nlm.nih.gov/Blast.cgi?). Primer pairs for PCR amplification of probe sequences from cDNA were selected using Primer Premier 5.0, Premier Biosoft International, http://www.premierbiosoft.com/primerdesign/index.html.

2.2.7 Synthesis of single stranded cDNA for probe sequence PCR amplification

Prism stage embryos (72hpf) were collected by concentrating 500ml of embryo culture per sample by reverse filtration on a 6cm diameter filter with 0.25µm nylon mesh. Concentrated embryos were transferred into a 15ml tube and centrifuged for 2min at 80x*g* at RT.

All steps were performed using RNAse free reagents. RNA was isolated using a Trizol Reagent (Invitrogen, Cat.No.15596-026). Ten volumes of Trizol Reagent were added to one volume of packed embryos. The sample was homogenized, by repeated passage through a pipette tip and vortexing, and then incubated for 5min at RT. RNA was then extracted by adding 0.2 volumes of chloroform per 1 volume of Trizol homogenate and shaking by hand for 15sec at RT. The sample was then centrifuged for 10min at 12,000x*g* at 4ºC. The supernatant was transferred to a new tube, and 0.83 volumes of isopropyl alcohol were added per 1 volume of supernatant. The sample was incubated for 10min at RT and centrifuged for 10min at 12,000x*g* at 4ºC. Supernatant was discarded and the resulting pellet was washed in 70% ethanol by vortexing for 3sec and centrifuging for 5min at 7,500xg at 4ºC. The supernatant was discarded again, and the pellet was dried for 5min at RT. The pellet was dissolved in DEPC-H_2O by pipetting up and down and subsequent 10min incubation at 55ºC.

To isolate poly (A) mRNA from the sample, the Oligotex mRNA Mini Kit was used (QIAGEN, Cat.No.70022). The isolation was performed according to the manufacturer's protocol (Oligotex mRNA Spin Column Protocol, Oligotex Handbook, 05/2002, pg.20) with the following modifications. The elution was performed by adding 30µl OEB at 70ºC, to obtain 25µl of purified mRNA.

To set up the cDNA synthesis reaction, 1-2µg purified mRNA was added to a 10µl reaction containing 1µl of 50µM poly dT_{20}, and 1µl 10U/µl RNAse OUT (Invitrogen, Cat.No. 10777-019). The reaction was incubated for 10min at 70ºC and then immediately for 1min on ice. Then, 2µl 10x First Strand Buffer (Ambion, 8704G), 1µl 10mM dNTP mix (Amersham Pharmacia Biotech, Inc., 27-2035-01), 2µl 100mM DTT (Invitrogen,Y00147) , 1µl 10U/µl RNAse OUT, and 1µl M-MLV RT 100U/µl (Ambion, AM2043) were added to the reaction to a final volume of 20µl. The reaction was incubated for 2hrs at 37ºC. Then, 1µl 5U/µl RNAse H (USB, Cat. No. 70054Y) was added, and the reaction was incubated for 1hr at RT. The resulting cDNA was stored at -20ºC or used immediately in PCR.

2.2.8 PCR and touchdown PCR

PCR was performed in Light Thermocycler (Idaho Technology, Inc.) using 50µl Capillary Tubes, according to manufacturer's instructions. Each 25µl PCR reaction was set up using 16.3µl H_20, 2.5µl 10x PCR buffer with 30mM $MgCl_2$ (Idaho Technology, Inc., Cat.No. 1782), 2.5µl 2mM dNTP mix (Amersham Pharmacia Biotech, Inc., Cat.No. 27-2035-01), 1.25µl 10µM sense and antisense primer dilutions in H_20, 0.2µl cDNA, and 0.2µl 0.5U/µl Taq DNA polymerase (Invitrogen, Cat.No. 18038-018). Regular or touchdown PCR amplification protocols were performed. Regular protocol followed the following scheme: hold 15sec at 94ºC; cycle 35 times (0sec at 94ºC; 0sec at Ta; 20sec/kb at 72ºC); hold 5-10min at 72ºC. Touchdown protocol followed the following scheme: hold 15sec at 94ºC; cycle 5 times at Ta+8ºC, 5 times at Ta+6ºC, 5 times Ta+4ºC, 5 times at Ta+2ºC, and 20 times at Ta; hold for 5-10min at 72ºC. The time of the last step, in both PCR protocols, was extended to promote addition of single adenosine nucleotides to the 3' ends of PCR products to generate adenosine (A)-tailed

PCR products. PCR efficiency was determined using agarose gel electrophoresis with 1% ethidium bromide and visualization under UV.

2.2.9 Purification of PCR products from agarose gel for cloning

Amplified fragments were purified from the agarose gel using a QIAquick Gel Extraction Kit (QIAGEN, Cat. No.28704). Purification was performed according to manufacturer's instructions (QIAquick gel extraction kit protocol, QIAquick Spin Handbook, 11/ 2002, pg.25) with the following modifications. Agarose gel was dissolved for 15min at 50ºC in 330ul QG buffer per 100mg gel. Purified DNA was eluted by adding 30µl H_20 to the column filter and incubating the column for 1min at RT before the final centrifugation step.

2.2.10 Synthesis of pBluescript KS+ T-tailed vector (pBS-T)

A linearized vector, with thymine base 3' end overhangs (or thymine (T)-tailed vector), was synthesized to clone A-tailed PCR products. The protocol for vector synthesis was followed as described in Marchuk et al. (1991). pBluescript II KS+ Phagemid Vector (Agilent Technologies, Cat.No.212207) was linearized with blunt cutter restriction enzyme EcoRV (Gibco BRL, Cat.No.15425-010), according to manufacturer's instructions, for a minimum of 3hrs at 37ºC. Then, 5µg blunt-ended vector was added to a 100µl reaction containing 10µl 10x PCR buffer with 30mM $MgCl_2$ (Idaho Technology, Inc., Cat.No. 1782), 5µl Taq DNA polymerase (Invitrogen, Cat.No. 18038-018), and 6µl 25mM TTP (Amersham Pharmacia Biotech, Inc., 27-2035-01). This reaction was incubated for 2hrs at 70ºC. The vector was purified using QIAquick PCR Purification Kit (QIAGEN, Cat.No. 28104) according to manufacturer's instructions (QIAquick PCR

Purification Kit protocol, QIAquick Spin Handbook, 11/2006, pg.19). The vector was stored at 20ºC or used immediately for cloning PCR fragments.

2.2.11 Cloning of PCR fragments into pBS-T

PCR fragments, purified in 2.2.9, were ligated into pBS-T vector, using Promega pGEM-T Easy Vector System Kit (Promega, Cat.No. A1360) Manufacturer's instructions were followed with the following modifications. pGEM-T T-tailed vector was substituted with pBS-T vector at 50ng per ligation reaction. The ligation reaction was incubated O/N at 4 ºC.

Transformation of subcloning efficiency DH5α competent cells (Invitrogen, Cat. No. 18265-017) was performed as described in the manufacturer's protocol with the following modifications. SOC medium (0.5% Yeast Extract, 2% Tryptone, 10mM NaCl, 2.5mM KCl, 10mM $MgCl_2$, 10mM $MgSO_4$, 20mM Glucose) was used post–heat shock for 1hr incubation at 37ºC. The transformation reaction was spread on LB-agar plates containing 50µg/ml X-galactose and 100µg/ml ampicillin, and the plates were incubated O/N at 37ºC. Colonies containing transformed cells were inoculated and grown O/N at 37ºC. Plasmid DNA was purified using QIAprep Spin Miniprep Kit (QIAGEN, Cat.No. 27104) according to manufacturer's instructions (QIAprep Miniprep Handbook, 12/2006, pg.22). Presence of insert of the correct size in purified plasmid DNA was confirmed by restriction digestion. Plasmids containing the inserts of expected size were sequenced at the CMMT/CFRI and CGDN Vancouver DNA Sequencing Core Facility. To confirm the identity of cloned probe sequences the *S. purpuratus* taxid 7668 Nucleotide Collection (nr/nt) was searched using NCBI Nucleotide Basic Local Alignment Search Tool (blastn).

2.2.12 DIG RNA probe synthesis

To determine the orientation of the cloned probe sequences with respect to T7/T3 promoters in pBS-T, sequencing data was processed and analyzed using BioEdit software. A restriction enzyme was selected using the BioEdit software Restriction Map feature to cut as close as possible to the probe sequence but did not cut within that sequence. The restriction enzyme was selected to cleave between the EcoRV site, where the probe sequence was inserted, and the T7 or T3 promoter, to synthesize a T3 or T7 probe, respectively.

To linearize the plasmid for probe synthesis, 5µg of plasmid DNA was first digested with 10U of the appropriate restriction enzyme for 3hrs at 37 ºC. To purify the linearized plasmid DNA, the digest was diluted in water to 90µl volume, then extracted with an equal volume of phenol/chlolophorm/isoamyl alcohol 25:24:1 (Fluka, Cat. No. 77617) by vortexing twice for 3 sec at RT, and centrifuged for 10min at 9660x*g* at RT. Approximately 90µl supernatant were transferred to a fresh tube, and 10µl 3M Na-acetate pH 5.2 were added. The sample was vortexed twice for 3 sec at RT. All subsequent steps were performed using RNAse free reagents. 200µl 100% ethanol were added to the sample, and the sample was vortexed twice, for 3 sec at RT, and centrifuged for 10min at 9660x*g* at RT. The resulting pellet was washed by aspirating the supernatant, adding 100µl 70% ethanol, vortexing the tube for 1 sec at RT, and centrifuging for 15min at 9660x*g* at RT. The supernatant 70% ethanol was aspirated, and the pellet was dried for 5min at RT. The pellet was dissolved in 10µl of DEPC- H_20.

To synthesize the probe, 2µg purified plasmid DNA were added to a 20µl reaction containing 2µl 10xTranscription Buffer (Ambion, Cat. No.8151G), 1µl RNAse OUT inhibitor (Invitrogen, Cat. No.10777-019), 2µl 10xDIG RNA Labelling Mix (Roche, Cat.

No.11277073910), and 2µl 20U/µl T7 RNA polymerase (Ambion, Cat. No.AM2082), or 2µl 20U/µl T3 RNA polymerase (Ambion, Cat. No.AM2060). The reaction was incubated for 2.5 hrs at 37 ºC. DNA was removed by adding 1µl DNAseI (Roche, Cat. No.776785) and incubating the reaction for 30min at 37ºC. The probe was purified from the reaction using a Micro Bio-Spin 30 Chromatography Column (Bio-Rad, Cat. No.732-6202), according to the manufacturer's instructions.

All probe names and sequences are listed in Supplemental table 1, Supplemental figure 2, and Supplemental figure 3. Probes for Onecut/Hnf and Spec1a were provided by Karl-Frederik Bergeron and Barton Xu, of the Brandhorst Lab, SFU.

2.2.13 Artificial seawater preparation

ASW was prepared according to Cavanaugh, G.M. (1975) (Cavanaugh, 1975). ASW formula was calculated by J.D. Ostrow from the table of major constituents of seawater (Lyman and Fleming, 1940), and tested by E.B. Harvey.

ASW was prepared from two stock solutions, MBL1 and MBL2. To prepare MBL1, 464g NaCl (58.44 g/mol), 73g Na_2SO_4 (142.04 g/mol), 14g KCl (74.56 g/mol), and 4g $NaHCO_3$ (84.00 g/mol) were dissolved in 2L H_2O. To prepare MBL2, 26.4g $CaCl_2 \cdot 2H_2O$ (147.01 g/mol) and 198.0g $MgCl_2 \cdot 6H_2O$ (203.33 g/mol) were dissolved in 2L H_2O. Both stock solutions were stored at 4ºC.

To make ASW, 0.1 volumes of MBL1 (3.97M NaCl, 257mM Na_2SO_4, 93.9mM KCl, and 23.8mM $NaHCO_3$) were dissolved in 0.8 volumes of H_2O in an Erlenmeyer flask, followed by addition of 0.1 volumes of MBL2 (89.8 $CaCl_2 \cdot 2 H_2O$, 487mM of $MgCl_2 \cdot 6H_2O$). The resulting ASW was aerated by bubbling air through a PVC tube for 2hrs to O/N at RT. The pH of the ASW was adjusted to 8.0-8.2 if necessary.

2.2.14 Deciliation

Deciliation of embryos was performed according to Merlino et al. (1978) with the following modifications. To deciliate prism stage embryos, 0.12 volumes of 4.45M NaCl were added to the embryo culture. The culture was stirred to distribute the salt solution evenly for 5sec at RT. The culture was incubated for 1min at 12°C. To re-establish isotonicity, 1.08 volumes of original culture volume of special ASW was added, which contained 10% greater concentration of all salts, but lacked NaCl.

2.2.15 Northern Blotting

Embryos and larvae were collected by concentrating 500ml of embryo culture per sample via reverse filtration on 6cm diameter filter with 0.25µm nylon mesh. Concentrated embryos were transferred into 15ml tubes on ice and centrifuged for 2min at 80x*g* at RT.

RNA was extracted using RNeasy Mini Kit (QIAGEN, Cat.No. 74104) according to manufacturer's instructions (RNeasy Mini handbook, 04/2006, pg.25) with the following modifications. Buffer RLT, supplemented with 10µl/ml β-Mercaptoethanol, was added to packed embryos at 600µl per sample. The sample was immediately homogenized in RLT buffer by pipetting up and down with a 1000µl pipette tip. Then, it was either immediately processed further or flash frozen in liquid nitrogen and stored for later extraction at -80ºC.

Stored samples were thawed on ice before continuing extraction. While homogenizing multiple samples, all tubes were kept on ice at all times. To continue extraction, the sample was homogenized further using a 1ml syringe with a 0.9mm diameter blunt-ended needle. The sample was aspirated and expelled from the syringe

up to 10 times within 10sec. Care was taken to wash the liquid collected at the inner sides of the sample tube with each expulsion. In the final step of the RNeasy Mini handbook protocol, 30µl DEPC-H_2O was added to elute the RNA from the column. RNA concentration were estimated using a spectrophotometer. The RNA yield from 500ml of 25embryo/L culture varied between 5 to 75µg.

All reagents and materials used in the Northern Blotting procedure were RNase-free. All equipment was treated with RNase Zap (Sigma, Cat. No. R2020), according to manufacturer's protocol. To prepare an RNA sample for electrophoresis, 1µg of RNA was diluted in DEPC-H_2O to a total volume of 4µl. RNA ladder sample was prepared by adding 0.2µl DIG-labelled RNA Molecular Weight Marker II (Roche, Cat.No. 11526537910) to 4µl of DEPC-H_2O. Then, 8µl 1.5x Northern Blot Loading Buffer (1x MOPS electrophoresis buffer, 50% v/v deionized formamide, 6 % w/v formaldehyde, 10% v/v glycerol, 0.05% w/v bromophenol blue, 5µg/ml ethidium bromide) were added to each sample, and the samples were mixed by pipetting up and down. The samples were then incubated for 10 min at 65°C, followed by 1 min on ice, and centrifugation for 10 sec at 2000x*g* at RT. The samples were loaded on a 1% agarose-formaldehyde gel (1x MOPS electrophoresis buffer, 1% w/v agarose, 7% formaldehyde) and electrophoresed in 1x MOPS electrophoresis buffer (1/10 dilution of 10x MOPS electrophoresis buffer (200mM MOPS pH 7.0, 50mM Na-acetate, 20mM EDTA (pH 8.0), pH 7.0) in DEPC-H_2O). Electrophoresis was performed at 80V for 2hrs, or until the dye front had travelled 4.5cm from the wells. Ribosomal RNA was visualized under UV trans-illuminator to ensure equal RNA loading between different wells, and a picture was taken for further reference.

The gel was washed 2 times for 15min in 20x SSC (3M NaCl, 300mM Na-citrate, pH 7.0). RNA was transferred from the gel O/N in 20x SSC to a positively charged nylon membrane (Roche, Cat. No.11209299001). After transfer, the membrane was placed, face up, on 3mm chromatography paper (Whatman, Cat.No.3030917) soaked in 2xSSC (1/10 dilution of 20xSSC in DEPC-H_2O), and immediately UV crosslinked. After crosslinking, the membrane was washed in DEPC-H_2O for 5min at RT. The membrane was air-dried on 3mm chromatography paper for 30min at RT and stored sealed at 4ºC. Alternatively, the membrane was immediately processed as described further.

The following steps were performed using a Robbins Scientific hybridization glass tube and hybridization oven. The membrane was incubated in pre-heated Prehybridization Solution ((5x SSC 0.1% w/v N-lauryl sarcosine, 2% w/v Blocking reagent (Roche Cat. No. 1096176), 50% v/v deionized formamide, 0.02% SDS)) for 30 min at 55 ºC. The probe was denatured in DEPC-H_2O for 5 min at 100ºC, followed by incubation for 1min on ice and centrifugation for 10sec at 2000x*g* at RT. Hybridization Solution was made by adding the denatured probe immediately to fresh pre-heated prehybridization solution to a final concentration of 0.1µg/ml. The membrane was then incubated in Hybridization Solution O/N at 55 ºC. After incubation, the hybridization solution was removed and stored at -80ºC to be reused. The membrane was washed 2 times in Low Stringency Buffer (2x SSC, 0.1% SDS) for 10min at RT, and then 2 times in pre-heated High Stringency Buffer (0.5x SSC, 0.1% SDS) for 45min at 70ºC. Then, the membrane was washed once in Washing Buffer (0.1M Maleic acid, 0.15M NaCl, pH7.5, 0.3% (v/v) Tween 20) for 2min at RT. The membrane was then blocked in Blocking Solution (1% w/v Blocking reagent (Roche, Cat. No. 11096176001), 0.1M Maleic acid, 0.15M NaCl, pH 7.5) for 30min at RT, followed by incubation in Antibody solution

(1:10,000 of 0.75U/µl anti-DIG Ab (Roche, Cat.No.1093274) in Blocking solution) for 30 min at RT. After the antibody incubation, the membrane was washed 2 times in Washing Buffer for 15min at RT and equilibrated in Detection Buffer (0.1M Tris-HCl,0.1M NaCl, pH 9.5) for 5min at RT. The membrane was placed face up on saran wrap, and CSPD Solution (1% v/v CSPD (25mM, Roche, Cat.No.1655884) in Detection buffer) was applied to the membrane surface. The membrane was incubated with CSPD Solution for 5min at RT. Excess CSPD solution was drained, and the membrane was incubated between two fresh pieces of saran wrap for 10 min at 37ºC. Chemiluminescence was detected by exposing the membrane to Bioflex Econo Film (Clonex Co., Cat.No. CLEC810), from 30sec up to O/N, depending on probe signal strength.

Approximate transcript sizes were estimated by semi-logarithmic plotting. The $\log_{10}$ values of DIG-labelled RNA Molecular Weight Marker II band sizes versus the distance migrated by the bands from the wells were plotted. The resulting linear equation was used to estimate the size of gene transcripts by using the distance travelled from the wells by the transcript of interest.

2.2.16 Whole mount in situ hybridization (WMISH)

Embryos and larvae were collected by concentrating 500ml of embryo culture per sample via reverse filtration on 6cm diameter filter with 0.25µm nylon mesh. Concentrated embryos were transferred into 15ml tubes on ice and centrifuged for 2min at 80x*g* at RT.

Supernatant SW was aspirated to leave the embryos in 1ml of SW. Then, 10ml of WMISH fixative (4.0% paraformaldehyde,32.5% SW, 32.5mM MOPS pH 7.0, 162.5mM NaCl) was added to each tube, and the samples were incubated O/N at 4 ºC

,with tubes lying flat or with constant rotation. The samples were washed 2 times in 10 volumes of Post-fix wash buffer (100mM MOPS pH 7.0, 1.0M NaCl) for 1hr at RT. The samples were then either immediately processed further or dehydrated for storage. Sample dehydration was performed by consecutive 1-3hrs incubations of embryos in 10, 20, 40 and 70% ethanols at RT. Dehydrated samples were stored in 70% ethanol at -20 ºC.

All reagents and materials used in the following procedure were RNase-free. All subsequent steps were performed in 120µl micro well plates (GeNunc Modules, InterMed, Cat.No. 232549). All DIG probes used in the procedure were identical to the probes used in the Northern blotting. Embryos were deposited in the wells and rehydrated by incubating them 3 times in 10 volumes of MOPS buffer (100mM MOPS pH7.0, 500mM NaCl, 0.1% Tween 20) for 15 min at RT. The samples were then incubated in Prehybridization Buffer (70% deionized formamide, 100mM MOPS pH7.0, 500mM NaCl, 0.1% Tween 20, 1mg/ml BSA) for 15min at RT and again for 3hrs at 50 ºC. Then samples were incubated in Hybridization Buffer (0.2ng/µl DIG-labelled RNA probe in Prehybridization buffer) for one week at 50ºC. Following hybridization, one of the two probe detection protocols was used, either chromogenic or fluorescent.

To perform chromogenic detection, samples were washed 5 times with MOPS buffer for 15min at RT, in Prehybridization buffer for 3hrs at 50ºC, and 3 times in MOPS buffer for 15min at RT. The samples were blocked with MOPS buffer containing 10 mg/ml BSA for 20 min at RT and then with MOPS buffer containing 10% goat serum and 1 mg/ml BSA for 30 min at 37ºC. Antibody incubation was performed in MOPS buffer containing 1% goat serum (Sigma, Cat.No. G9023), 0.1mg/ml BSA (Sigma, Cat.No. A2153) and 0.5U/ml anti-DIG Ab (Roche, Cat.No.1093274) O/N at RT. Samples were

washed 5 times in MOPS buffer for 1hr at RT and again O/N at RT. Finally, samples were washed 2 times in Alkaline Phosphatase Buffer (100mM Tris-HCl pH 9.5, 50mM $MgCl_2$, 100mM NaCl, 1mM Levamisole (Sigma, Cat.No.L9756), for 30min at RT, and incubated in BCIP /NBT (Sigma, Cat.No. B1911) up to 24hrs at RT in the dark until colour development became visible. Staining reaction was stopped by washing samples 3 times in MOPS buffer for 15min at RT. Samples were viewed using 20x or 40x objective lenses on Vanox (Olympus, AHBS3) microscope. Images were acquired at brightfield settings using a Sony Power HAD Camera (Sony) and Northern Eclipse V6.0 software, http://www.empix.com/.

To perform fluorescent detection, a Tyramide Signal Amplification (TSA) system was used. Samples were incubated in Blocking Solution (10% goat serum , 5mg/ml BSA in MOPS buffer) O/N at RT. Samples were then incubated in Antibody Solution (0.5U/ml anti-DIG-POD (horse radish peroxidase) (Roche, Cat.No. 11207733910), 10% goat serum, 5mg/ml BSA in MOPS buffer) for 30min at RT. Samples were then washed 8 times in MOPS buffer for 15min at RT, followed by an incubation in Cy3-Tyramide solution (1:100 Cyanine 3 Amplification Reagent (Perkin-Elmer Life Sciences, Inc., FP1170), 1x Plus Amplification Diluent (Perkin-Elmer Life Sciences, Inc., FP1135) for 8min at RT. Finally, samples were washed 5 times in MOPS buffer for 15min at RT.

Samples were then mounted in Vectashield (Vector Laboratories , Inc., Cat.No. H-1000) and visualized using 25x or 40x objective lenses on a WaveFX Spinning Disc Confocal Microscope (Quorum Technologies, Ltd.). Tyramide signal was detected using 561nm laser line and a Cy3 595/50 filter. Images were acquired using Hamamatsu 9100-13 EMCCD camera (Hamamatsu Photonics) and Volocity software V5.0, http://www.cellularimaging.com/products/volocity/.

2.2.17 Western blotting

Embryos and larvae were collected by concentrating 500ml of embryo culture per sample via reverse filtration on 6cm diameter filter with 0.25µm nylon mesh. Concentrated embryos were transferred into 15ml tubes on ice and centrifuged for 2min at 80x*g* at RT.

Samples were immediately homogenized in 1000µl RIPA Buffer (150mM NaCl, 50mM Tris-HCl pH8.0, 5mM EDTA (pH 8.0), 1% v/v Nonidet P-40 (Sigma, Cat.No. 3516), 0.5% w/v sodium deoxycholate (Sigma, D6750), 0.1% w/v SDS, 1 tablet/10ml of Complete Mini Protease Inhibitor Cocktail (Roche, Cat.No.1836153)) and centrifuged at 12,000x*g* for 15min at 4°C. The protein concentration of the collected supernatant was estimated using a Bradford protein assay and a spectrophotometer. Protein samples were resolved using SDS-PAGE. Each gel sample contained 50µg of total protein. To prepare gel samples, purified protein was mixed 1:1 ratio with 2x SDS Gel Loading Buffer (100mM Tris-HCl (pH 6.8), 10% v/v β-mercaptoethanol, 4% w/v SDS, 0.02% w/v bromophenol blue, and 20% v/v glycerol) and the samples were denatured for 5min at 100°C, or for 10min at 70°C. Samples were electrophoresed at 100V (15V/cm) on 6% Resolving gel and 5% stacking gel in 1x Tris-glycine electrophoresis buffer (1/5 dilution of 5x Tris-glycine electrophoresis buffer (100mM Tris base, 1M glycine, 10% SDS, pH 8.3) in H_2O), until the dye front reached the bottom of the gel. Before transfer, the gel was equilibrated in Towbin Buffer (25mM Tris, 192mM glycine, 20% v/v methanol), pre-chilled at 4°C. Protein transfer was performed in Trans Blot SD Semi Dry electrophoretic Transfer Cell (Biorad), according to manufacturer's protocol, in Towbin buffer, at 15V-25V from 15min to 1.5 hrs at 4°C. After transfer, the membrane was rinsed in TBS-T (10mM Tris-Cl, 150mM NaCl, pH7.5, 0.05% v/v Tween-20) for 5sec at RT and then

incubated in Blocking Solution (1%BSA, 5% milk in TBS-T) for 1hr at RT. The membrane was rinsed briefly in TBS-T for 5sec at RT and then incubated in Primary Antibody Solution (1:200 to 1:1000 of 200µg/ml Whirlin D-20 Ab (goat-polyclonal, Santa Cruz, 49785) or 1:200 to 1:1000 of 1.0 mg/ml DFNB31 Ab (mouse monoclonal, Abcam, Cat.No. ab57106) in TBS-T) O/N at 4°C. The blot was washed 4 times in TBS-T for 10min at RT, and then incubated in Secondary Antibody Solution (1:2000 donkey anti-goat HRP (Santa Cruz, sc-2020) or 1:2000 Goat anti-mouse HRP (Jackson Immuno Research Laboratories,Cat.No.115035044) in Blocking Solution) for 1hr at RT. The blot was then washed 4 times in TBS-T for 10min at RT.

Luminol-based chemiluminescent detection was used to visualize the HRP signal. The Pierce Enhanced Chemilumincence ECL Western Blotting Substrate kit (Pierce, Cat.No. 32209) was used, according to the manufacturer's protocol. Chemiluminescent signal was detected by exposing to Bioflex Econo Film (Clonex Co., Cat.No. CLEC810) to the membrane from 30sec up to O/N, depending on signal strength.

2.2.18 Whole mount immunofluorescent antibody staining (WMIFS)

Embryos and larvae were collected by concentrating 500ml of embryo culture per sample via reverse filtration on 6cm diameter filter with 0.25µm nylon mesh. Concentrated embryos were transferred into 15ml tubes on ice, and centrifuged for 2min at 80x*g* at RT.

Embryos were fixed in 10 volumes of freshly prepared Antibody Staining Fixative (4% paraformaldehyde, 50mM EGTA in FSW) for 1hr at RT. Alternatively, embryos were fixed in 10 volumes of pre-chilled methanol containing 50mM EGTA, for 20min at -20ºC.

After fixation, samples were washed 3 times in 10 volumes of FSW or PBS (50mM Potassium phosphate, 150mM NaCl, pH 7.2) for 1hr at RT.

To perform antibody staining, samples were washed 2 times in PBS-T (0.1% v/v Triton X-100 in PBS) for 10min at RT, and incubated in Blocking Solution (10% BSA (w/v), 10% (v/v) goat serum or 10%(v/v) sheep serum (Sigma, Cat.No. S3772) in PBS-T) for 2hrs at RT. Samples were then incubated in Primary Antibody Solution (1:50 to 1:500 of 200µg/ml anti-Whirlin D-20 (goat-polyclonal, Santa Cruz, 49785); or 1:100 to 1:2500 of 1.0 mg/ml anti-DFNB31 (mouse monoclonal, Abcam, Cat.No. ab57106) or 1:10 or 1:100 anti-α-Tubulin mouse monoclonal (Sigma, Cat. No. T9026) in Blocking Solution) O/N at 4°C. After primary antibody incubation, samples were washed 5 times in PBS-T for 10min at RT. Then samples were incubated in Secondary Antibody Solution (1:500 goat anti-mouse Alexa Fluor 660 (Invitrogen, Cat.No. A21054), 1:500 goat anti-mouse Alexa Fluor 448 (Invitrogen, Cat.No. A11001), or 1:500 donkey anti-goat 660 (Invitrogen, Cat.No. A21083) in PBS-T) for 2hrs at RT. When double antibody labelling was performed, the samples were washed 4 times in PBS-T 10 min at RT, and then the protocol was repeated starting from primary antibody incubation step. After the secondary antibody incubation step, samples were washed 2 times in PBS-T for 10min at RT and 3 times in PBS for 10min at RT. If nuclear staining was required, 1µg/ml of Hoechst 33258 dye (Polysciences, Inc., Cat.No. 09460) was added to one of the last two PBS-T washes.

Samples were mounted in Vectashield and were visualized using 25x, 40x or 60x objective lenses on a WaveFX Spinning Disc Confocal Microscope (Quorum Technologies, Ltd.). For Alexa Fluor 488, 491nm laser lines and 515/30 or 520/40 filters were used. For Alexa Fluor 660, 640nm laser lines and Cy5 690/50 or 700/75 filters were used.

Hoechst 33258 labelling was viewed using X-Cite 120 arc lamp (EXFO) and 470/24 or 480/40 filters Images were acquired using Hamamatsu 9100-13 EMCCD camera (Hamamatsu Photonics) and Volocity software V5.0, http://www.cellularimaging.com/products/volocity/.

2.3 Results

2.3.1 Evidence of Usher gene mRNA expression

Usher gene coding sequences were obtained from the *S. purpuratus* annotated database of genome assembly Spur 2.1. A total of 13 gene predictions were found (Table 2.1). A search of the NCBI nucleotide database revealed an additional Whirlin sequence "similar to Whirlin" (XM_788456).

To determine if *S. purpuratus* Usher genes were expressed in embryos, two embryonic mRNA expression databases were used: 1) Microarray database; 2) Tiling array database (Table 2.1). Information on expression of "similar to Whirlin" (XM_788456) was not available within these databases. The first database is a microarray database that shows temporal expression of *S. purpuratus* gene annotations at 2-cell morula (2hpf), early blastula (15hpf), early gastrula (30hpf), late gastrula (48hpf) and pluteus (72hpf) stages. This database gives information about the relative abundance of transcripts between different stages, although comparisons of transcript abundance between different genes are not possible. The second database is a tiling array database that shows combined expression data for predicted genes at egg, early blastula, gastrula and prism stages. This database does not offer a distinction between the expression data for transcripts at different stages. This database provides a direct answer to whether an annotation is expressed during embryonic stages or not.

According to the Database 1, all Usher gene predictions are expressed during embryonic stages with the following exceptions: Sp-Cadherin23-like-1 (SPU 004556), Sp-Protocadherin15-like (SPU 003730) and Sp-Harmonin partial (SPU 009191). All of these annotations have signal values below 100 arbitrary units, and they are most likely not expressed from 2-cell morula (2hpf) to pluteus stage (72hpf). Sp-Harmonin (SPU 028159) has signal values of 0 units at all stages examined, and it is not expressed from 2-cell morula (2hpf) to pluteus stage (72hpf) (Table 2.1, Supplemental Fig. 1). According to Database 2, Sp-Harmonin partial (SPU 009191) and Sp-Harmonin (SPU 028159) are most likely not expressed during embryonic development (Table 2.1).

Table 2.1 Embryonic expression of *S. purpuratus* Usher gene predictions

Gene Name	SPU#	Database 1	Database 2
		Expression	
Sp-Cadherin23-like1	SPU 004556	Maybe	Yes
Sp-Harmonin partial	SPU 009191	Maybe	Maybe
Sp-Harmonin	SPU 028159	No	Maybe
Sp-Myosin7a	SPU 022040	Yes	Yes
Sp-Protocadherin15-like	SPU 003730	Maybe	Yes
Sp-SANS-like	SPU 007551	Yes	Yes
Sp-SANS	SPU 022872	Yes	Yes
Sp-Usherin-like (N-term)	SPU 020012	Yes	Yes
Sp-Usherin-like (C-term)	SPU 017733	Yes	Yes
Sp-VLGR1	SPU 027371	Yes	Yes
Sp-Whirlin	SPU 002363	Yes	Yes
Sp-Whirlin	SPU 021200	Yes	Yes

Predicted gene names, their identification numbers, and their expression during embryonic stages are shown. Gene predictions were obtained from Baylor College of Medicine *S. purpuratus* annotation database of genome assembly Spur 2.1. Embryonic expression database 1: http://urchin.nidcr.nih.gov/blast/exp.html (Wei et al., 2006), a microarray database which shows expression data from 2-cell stage (2hpf) to pluteus stage (72hpf). Embryonic expression database 2: http://www.systemix.org/Data/Strongylocentrotus_purpuratus/Genome_tiling/ (Samanta et al., 2006), a tiling array database which shows expression data from egg to prism stage. SPU is the organism code for *Strongylocentrotus purpuratus*.

2.3.2 Design of Usher gene primers and amplification of target sequences for DIG probe synthesis

To amplify an approximately 1000bp sequence for each Usher gene prediction, RNA from prism stage (72hpf) embryos was used to prepare cDNA, and probe sequences were amplified from this cDNA using PCR. Multiple pairs of PCR primers were designed and tested for each prediction (Supplemental Fig. 2, Supplemental table 1).

Mutations of genes responsible for the Usher syndrome involve the long transmembrane isoforms of VLGR1 and Usherin (Kremer et al., 2006; Reiners et al., 2006; van Wijk et al., 2004; Weston et al., 2004). For other Usher genes no isoforms were distinguished as specific to Usher syndrome (Kremer et al., 2006; Reiners et al., 2006; Saihan et al., 2009). Primer pairs were selected for Sp-Usherin and Sp-VLGR1 with a goal to amplify probe sequences which would be detecting transcripts of their long transmembrane isoforms. Probe sequence USH_5 was targeted towards the transcripts of long transmembrane isoform B of Usherin, while probe sequence USH_3 was targeted towards transcripts of isoforms A and B (Supplemental Fig. 2). Usherin isoform A is not an Usher protein (Reiners et al., 2006). Probe sequence VLB_2 was targeted to the transcripts for long transmembrane isoform B (Supplemental Fig. 2), although it might also detect transcripts for isoform C. VLGR1 isoform C is not an Usher protein (Weston et al., 2004). Primer pair selection was performed using Primer Premier 5 program and was limited due to the nature of the predicted gene sequences. Therefore, selection of primer pairs for the desired isoforms was limited.

If a regular PCR protocol failed to produce an amplified product of predicted size, a touchdown protocol was used (Supplemental table 1). Probe sequences were cloned

and sequenced (Supplemental Fig. 3). At least one probe sequence was successfully amplified for each of the annotated Usher genes, with the exception of Sp-Harmonin (SPU 028159) and Sp-Harmonin partial (SPU 009191). This is consistent with information about Harmonin expression from two embryonic mRNA expression databases (Table 2.1). After PCR amplification, each probe sequence was cloned into a pBluescript KS+ T-tailed vector, and DIG-RNA probes were synthesized using T7 or T3 polymerase. DIG-probes were then used in mRNA expression analyses by Northern blots and Whole Mount In-Situ Hybridization (WMISH).

2.3.3 Temporal mRNA expression of Usher genes

To investigate the temporal expression of *S. purpuratus* Usher genes, RNA from embryos of eight developmental stages was extracted: egg, 16-cell morula (6hpf), early blastula (12hpf), hatched blastula (24hpf), mesenchyme blastula (36hpf), gastrula (48hpf), prism (72hpf) and early 4-arm pluteus (96hpf). The timing of developmental stages was different from the timing reported in the microarray database (Wei et al., 2006). The embryos in this study were cultured at 12ºC as opposed to 15ºC in Wei et al. (2006) accounting for their slower rate of development.

Northern blots showed that all detected Usher gene transcripts were maternal. They were all expressed throughout development at significantly varying levels from one another, and they had no co-relating patterns of expression across the developmental stages (Fig. 2.1, Table 2.2). SANS2_1, a probe for Sp-SANS (SPU 022872), failed to detect anything on Northern blots. Multiple bands were observed for SANS1_4 and Ubiquitin probes (a loading control) (Fig. 2.1), but the appearance of multiple bands was not consistent between different cultures. The only probes which consistently produced double bands across different cultures, were TUBB__2 (Sp-β-tubulin-1, another loading

control), VLB_2 and USH_5. The Ubiquitin probe consistently detected 3kb transcripts in different cultures, which were close in size to 3.2kb value reported previously in *S. purpuratus* embryos (Norrander et al., 1995). Similarly, Sp-β-tubulin-1 probe detected a 1.8kb and 2.2kb bands similar in size to the Sp- β-tubulin-1 1.8kb transcript, reported previously in *S. purpuratus* embryos (Harlow and Nemer, 1987). This demonstrated that the method of fragment size estimation was able to identify the approximate sizes of transcripts with relative accuracy.

2.3.4 Effects of deciliation on mRNA expression of Usher genes

Upregulation of synthesis of cilia related proteins occurs in response to deciliation (Casano et al., 2003; Stephens, 1995), when sea urchin embryos are immersed in hypertonic medium containing a high amount of NaCl (Auclair and Siegel, 1966). Upregulation of tubulin transcripts, in response to deciliation, has been reported in sea urchin embryos (Gong and Brandhorst, 1987).

To determine if deciliation caused an upregulation of Usher gene transcripts, deciliation at prism stage (72hpf) was performed. RNA samples were collected 30min and 1hr post deciliation. Northern blotting was used to compare transcript levels in deciliated samples to transcript levels in untreated samples. Transcript levels of Usher genes were not affected by the deciliation treatment. Sp-Ubiquitin was used as a negative control and its transcript levels were also not affected by deciliation (Fig. 2.2). Sp-β-tubulin-1 probe was used as a positive control to confirm that the deciliation upregulated Sp-β-tubulin expression (Fig. 2.2B).

Figure 2.1 Temporal mRNA expression of Usher genes

Northern blots showing expression profiles of Usher gene transcripts during embryonic development. RNA from egg, 6, 12, 24, 36, 48, 72, and 96hpf was loaded at 1µg per well. Ethidium bromide staining of the ribosomal RNA bands served as a loading control. The approximate sizes of detected transcripts are shown in kilobases (kb). A, B) Data from two different batches of embryos obtained by fertilization from two different pairs of adults. A) Ubiquitin; CAD23_4 (Cadherin23); PC15_5C (Protocadherin15); SANS1_5 (SANS1); USH_5 (Usherin SPU 020012); VLB_2 (VLGR1); WRL1_1 (Whirlin SPU 002363); WRL2_2 (Whirlin SPU 021200); WRL3_3 (Similar to Whirlin XM 788456). B) Ubiquitin; MYO7A_1 (MyosinVIIa); SANS1_4 (SANS1); TUBB_2 (β-tubulin-1); USH_3 (Usherin SPU 017733); WRL2_1 (Whirlin SPU 021200).

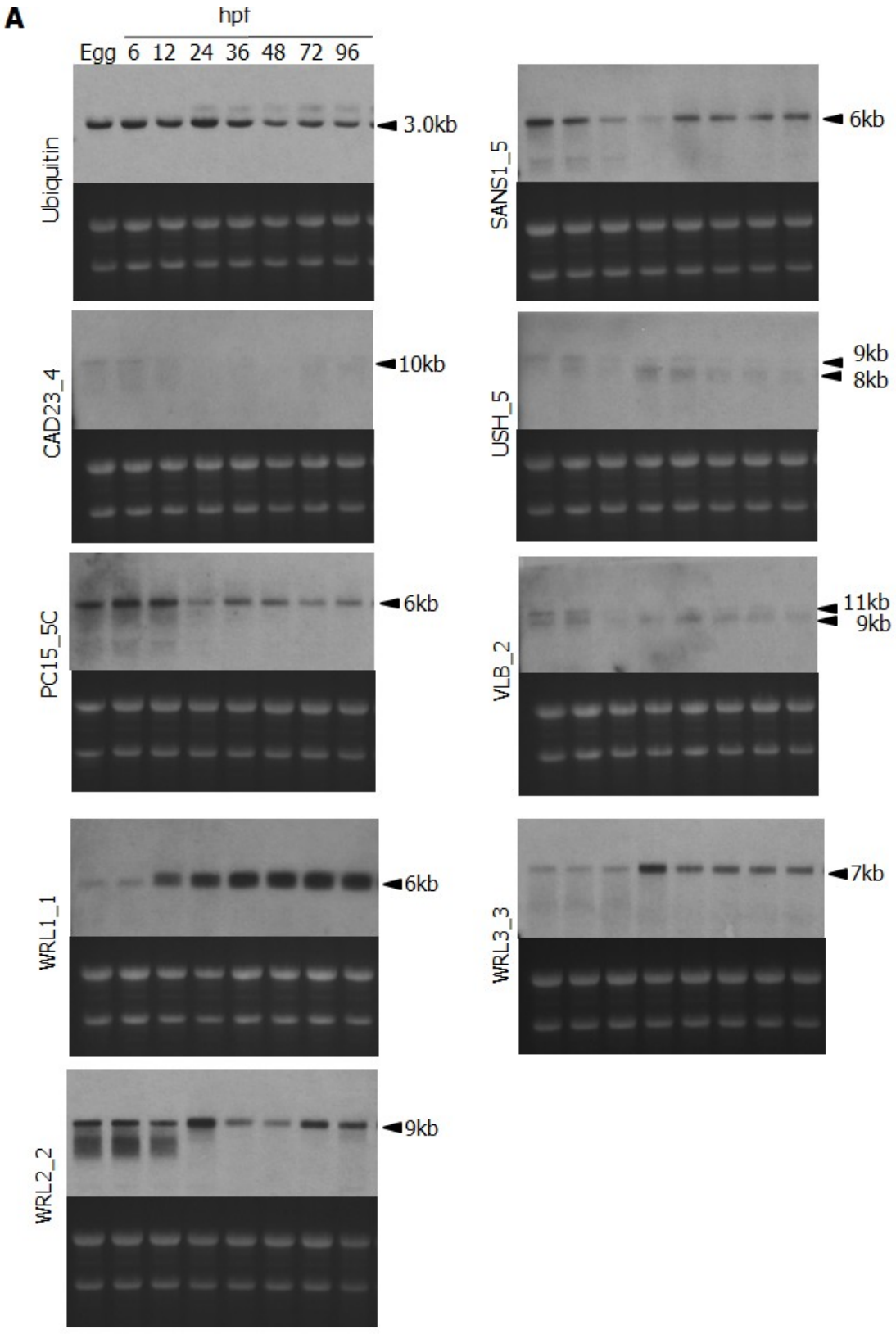
A
hpf
Egg 6 12 24 36 48 72 96
Ubiquitin
3.0kb
SANS1_5
6kb
CAD23_4
10kb
USH_5
9kb
8kb
PC15_5C
6kb
VLB_2
11kb
9kb
WRL1_1
6kb
WRL3_3
7kb
WRL2_2
9kb

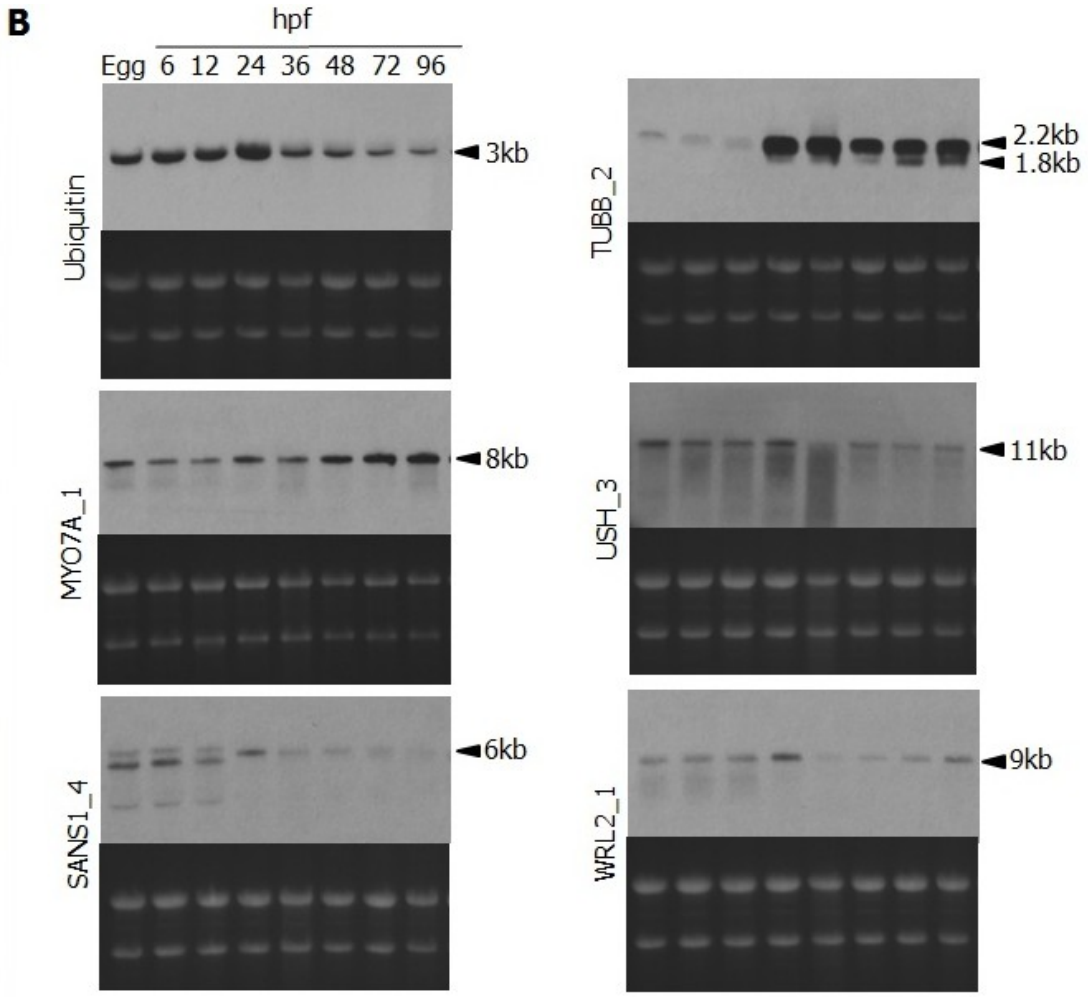
B
hpf
Egg 6 12 24 36 48 72 96
Ubiquitin
3kb
TUBB_2
2.2kb
1.8kb
MYO7A_1
8kb
USH_3
11kb
SANS1_4
6kb
WRL2_1
9kb

Figure 2.2 Effects of deciliation on Usher gene mRNA expression

Northern blots showing expression profiles of Usher genes before and after deciliation. RNA samples were loaded at 1µg per well. The approximate sizes of the transcripts are shown in kilobases (kb). An upregulation in transcript levels in response to deciliation is seen only in Sp-β-tubulin-1, with transcript levels increasing at 30 minutes and 60 minutes post deciliation treatment. A, B) Data from two different batches of embryos obtained by fertilization from two different pairs of adults. A) Ubiquitin; PC15_5C (Protocadherin15); SANS1_5 (SANS1); USH_5 (Usherin SPU 020012); WRL1_1 (Whirlin SPU 002363); WRL2_2 (Whirlin SPU 021200); WRL3_3 (Similar to Whirlin XM 788456). B) Ubiquitin; CAD23_4 (Cadherin23); MYO7A_1 (MyosinVIIa); SANS1_4 (SANS1); TUBB_2 (β-tubulin-1); USH_3 (Usherin SPU 017733); VLB_2 (VLGR1); WRL2_1 (Whirlin SPU 021200). Sample names: PT, pre-treatment control; 30T, 30 min treated; 30UT, 30min untreated; 60T, 60 min treated, deciliated; 60UT, 60min untreated. Abbreviations: T, treated and UT, untreated.

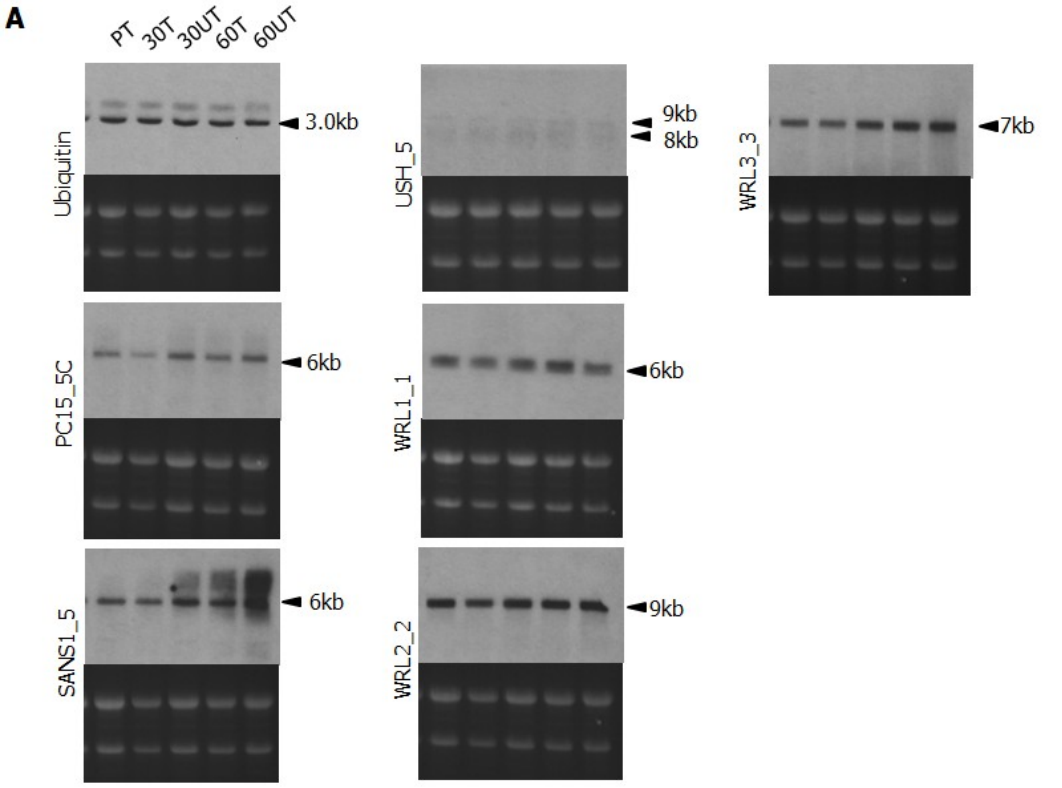
A
PT
30T
30UT
60T
60UT
Ubiquitin
3.0kb
USH_5
9kb
8kb
WRL3_3
7kb
PC15_5C
6kb
WRL1_1
6kb
SANS1_5
6kb
WRL2_2
9kb

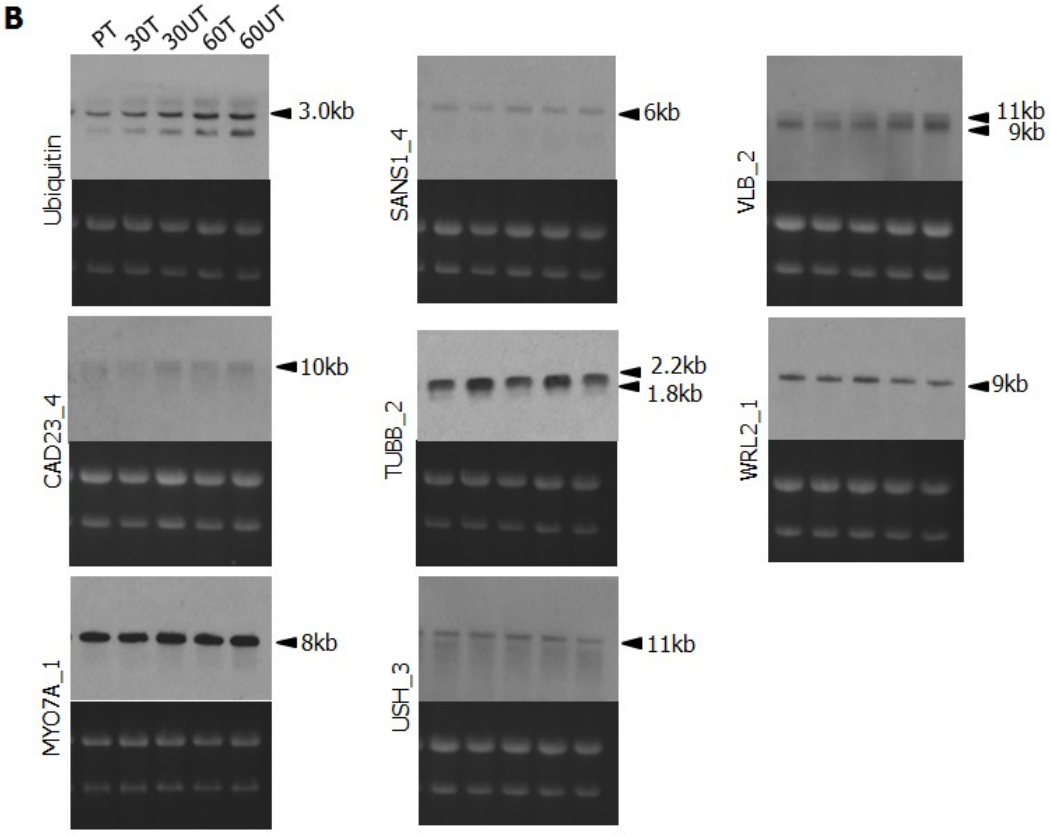
B
PT
30T
30UT
60T
60UT
Ubiquitin
3.0kb
SANS1_4
6kb
VLB_2
11kb
9kb
CAD23_4
10kb
TUBB_2
2.2kb
1.8kb
WRL2_1
9kb
MYO7A_1
8kb
USH_3
11kb

2.3.5 Spatial mRNA expression of Usher genes

To determine spatial expression of Usher genes, WMISH was performed using five developmental stages: hatched blastula (24hpf), mesenchyme blastula (36hpf), gastrula (48hpf), prism (72hpf) and early 4-arm pluteus (96hpf).

Three of the probes showed reproducible expression patterns: WRL2_1 and WRL2_2 for Sp-Whirlin (SPU 021200), and VLB_2 for Sp-VLGR1 (SPU 027371). Whirlin (SPU 021200) and VLGR1 (SPU 027371) had similar expression patterns throughout development. At mesenchyme blastula, gastrula and prism stages, the staining was observed in animal plate ectoderm. At prism stage, the staining also appeared in the ectoderm around the mouth. At pluteus stage, the staining was observed in the apical organ, the gut and in the ectoderm around the ciliated band between the postoral arms (Fig.2.3 and Fig. 2.4). A positive control, Onecut/Hnf6 probe, which identifies the area of the presumptive ciliated band, was used to demonstrate that WMISH procedure was working properly (Fig. 2.3A, B).

Other probes for Usher genes showed no reproducible or consistent patterns of expression. To address this problem, a highly sensitive Tyramide based detection protocol was attempted instead of the chromogenic protocol. Although this protocol worked for a positive control (Spec1a, an aboral ectoderm marker), it did not produce any staining for Usher gene probes. WMISH was repeated multiple times using different samples from different batches of embryos. Probes were resynthesized and reagents were remade several times, without any imporvements.

Figure 2.3 Spatial mRNA expression of Usher gene predictions at gastrula stage

WMISH with Usher gene probes showing expression of Onecut/Hnf, Sp-Whirlin (SPU 021200) and Sp-VLGR1 in gastrulae (48hpf). All the embryos are positioned with their animal poles facing upwards. A scale bar of 30µm applies to all panels. A,D,E,F,I) Side view; B,C,G,K,) Abanal view; L,M) Anal view. A-B) Onecut/Hnf (positive control) staining within the presumptive ciliated band ectoderm. C-E) WRL2_1, Sp-Whirlin (SPU 021200); staining in the animal plate ectoderm. F-G) WRL2_2, Sp-Whirlin (SPU 021200); staining in the animal plate ectoderm. I-M) VLB_2, Sp-VLGR1 (SPU 027371) staining in the animal plate ectoderm.

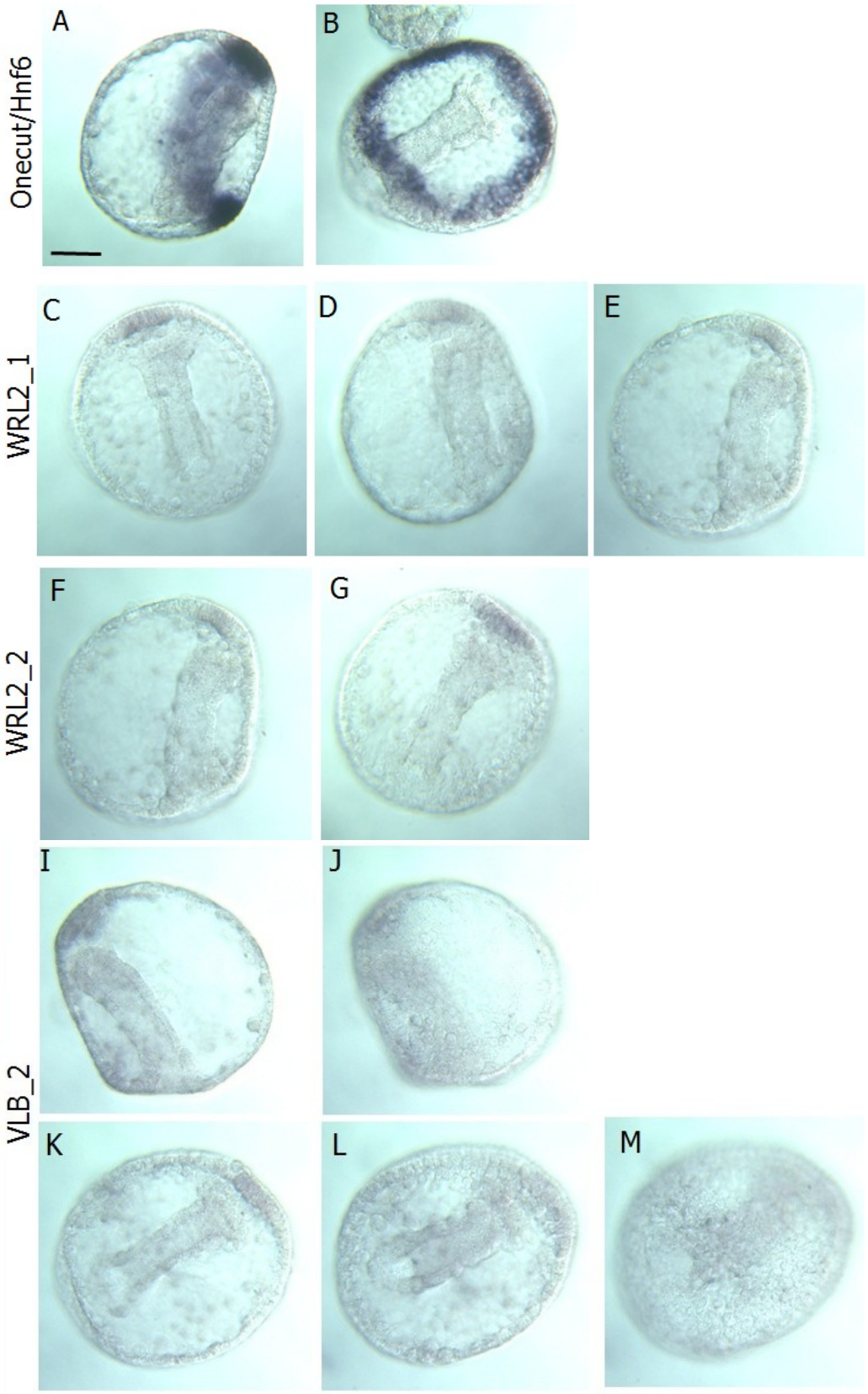
Onecut/Hnf6
A
B
WRL2_1
C
D
E
WRL2_2
F
G
VLB_2
I
J
K
L
M

Figure 2.4 Expression of Usher genes during embryonic development

WMISH with Usher gene probes shows overlapping staining patterns throughout development. All the embryos are positioned with their animal poles facing upwards. A scale bar of 30µm applies to all panels. A,G,L) hatched blastula (24hpf). B,H,M) mesenchyme blastula (36hpf). C,I,N) gastrula (48hpf). D,J,O) prism (72hpf). E,F,K,Q) early 4-arm pluteus (96hpf). Staining is seen in the animal plate ectoderm at mesenchyme blastula, gastrula and prism stages; in the apical organ of pluteus stage; in the ectoderm around the mouth at prism stage; in the gut and ectoderm around the ciliated band between postoral arms at pluteus stage. A-F) WRL2_1, WRL2_1, Whirlin (SPU21200). G-K) WRL2_2, Whirlin (SPU 021200). L-Q) VLB_2, VLGR1 (SPU 027371).

WRL2_1

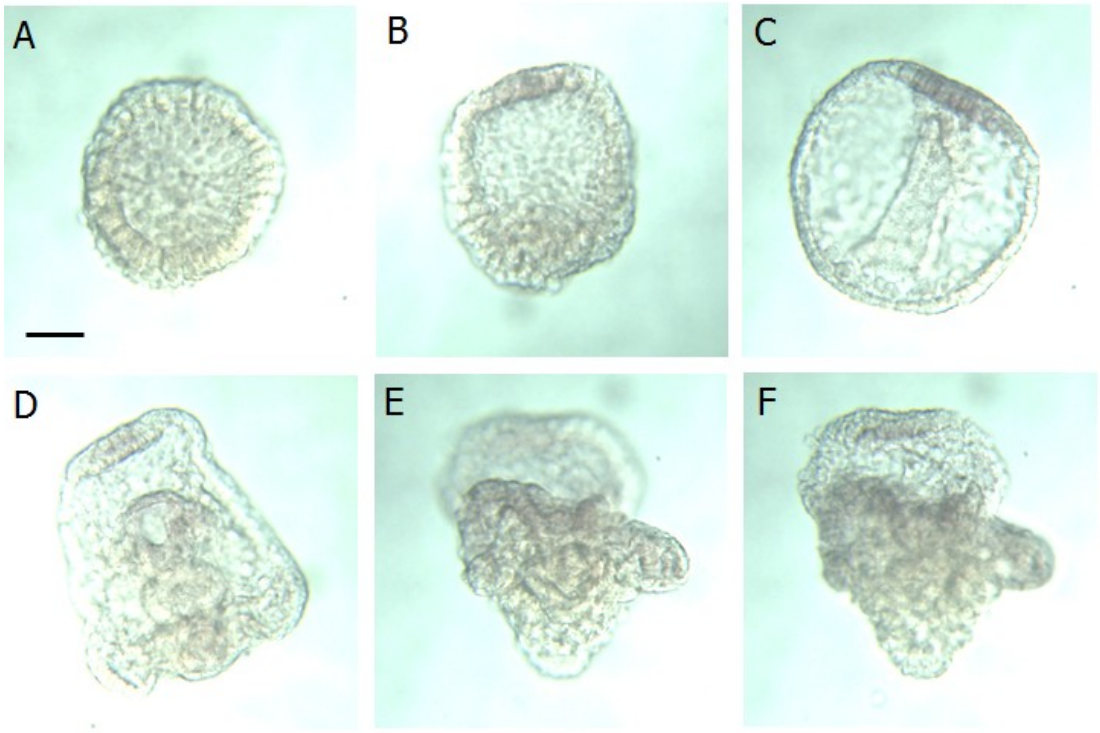

WRL2_2

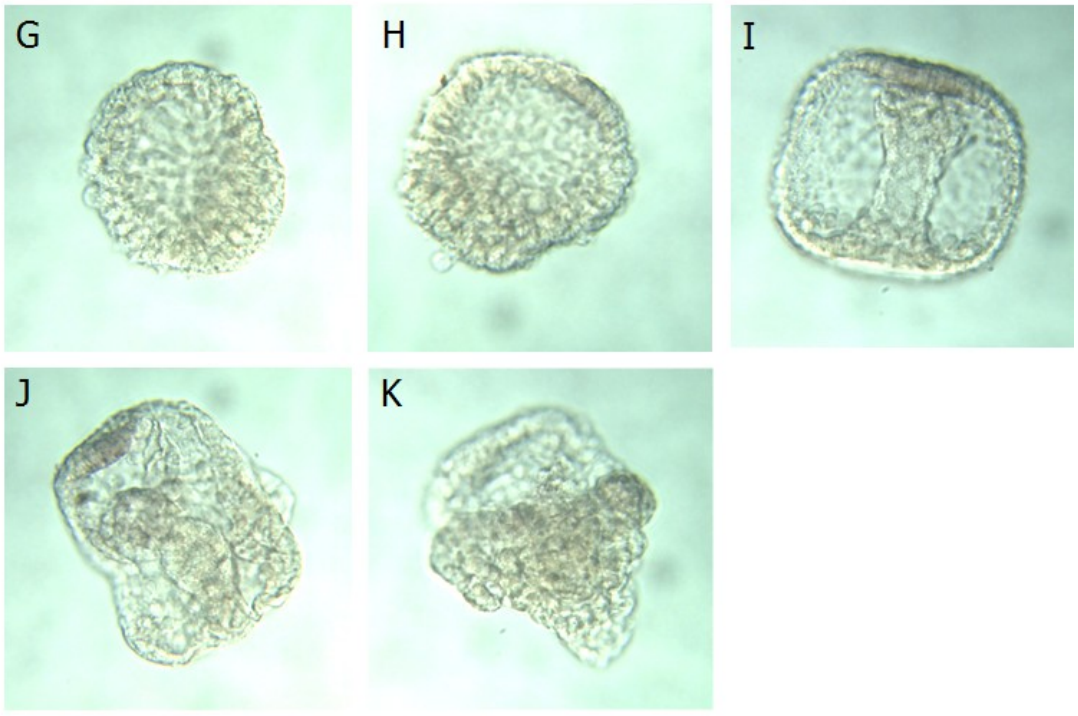

VLB_2

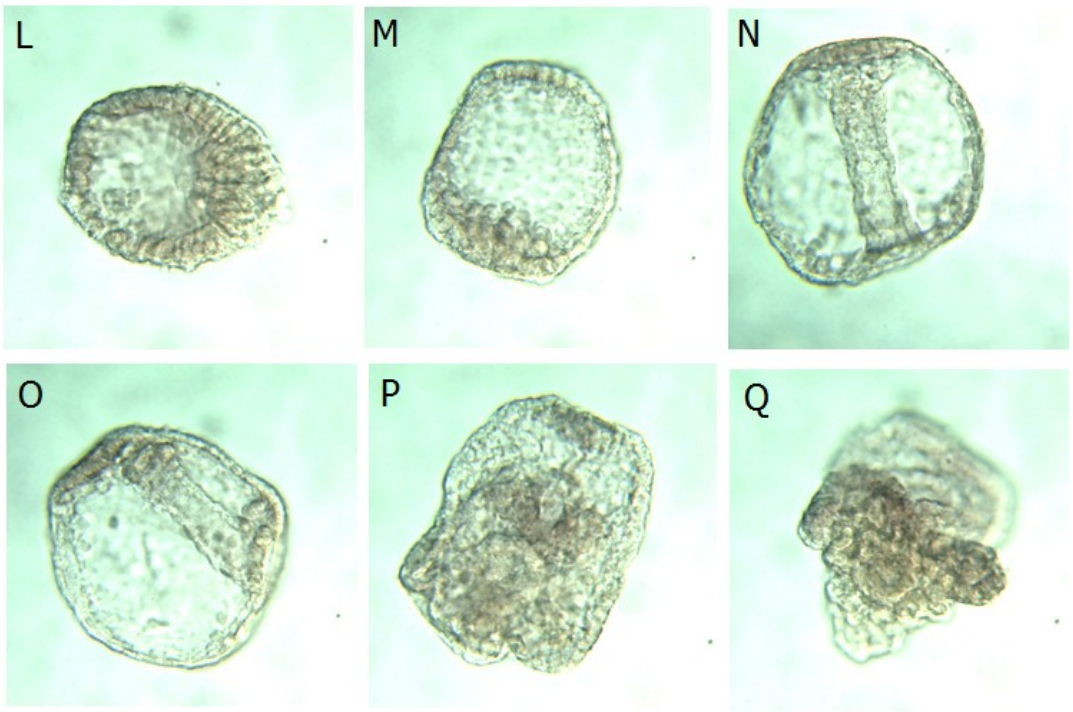

Table 2.2 Summary of Usher gene mRNA expression analysis results

Results summary for temporal expression analysis by Northern blotting, spatial expression analysis by WMISH and the deciliation experiments. Approximate transcript level was estimated by referring to the time of visible chemiluminescent signal appearance during the Northern blot development procedure. For high abundance transcripts (H), the signal appeared within 0-10min. For medium abundance transcripts (M), the signal appeared anywhere between 10min to 3hrs. For low abundance transcripts (L), the signal appeared anywhere from 3hrs to O/N. Temporal or spatial expression detection is referred to as "Detected", and lack of expression is referred to as "None detected". Sp-β-tubulin-1 spatial expression was not tested. Deciliation mediated upregulation of transcript levels is referred to as "Effect observed" and lack of upregulation is referred to as "No effect".

Gene name	Gene number	Probe sequence	Temporal expression	Approximate Transcript Level	Deciliation	Spatial Expression
Sp-Cadherin23-like1	SPU 004556	CAD23_4	Detected	L	No effect	None detected
Sp-Myosin7a	SPU 022040	MYO7A_1	Detected	M	No effect	None detected
Sp-Protocadherin15 15like	SPU 003730	PC15_5_C	Detected	M	No effect	None detected
Sp-SANS-like	SPU 007551	SANS1_4	Detected	M	No effect	None detected
		SANS1_5	Detected	M	No effect	None detected
Sp-SANS	SPU 022872	SANS2_1	None detected	NA	NA	None detected
Strongylocentrotus purpuratus mRNA fragment for beta-tubulin (SP-beta1)	X07502.1	TUBB_2	Detected	H	Effect observed	Not tested
Sp-Usherin-like (isoforms A and B)	SPU 020012	USH_3	Detected	M	No effect	None detected
Sp-Usherin-like (isoform B)	SPU 017733	USH_5	Detected	L	No effect	None detected
Sp-VLGR-1	SPU 027371	VLB_2	Detected	L	No effect	Detected
Sp-Whirlin	SPU 002363	WRL1_1	Detected	M	No effect	None detected
Sp-Whirlin	SPU 021200	WRL2_1	Detected	M	No effect	Detected
		WRL2_2	Detected	M	No effect	Detected
similar to Whirlin	XM 788456	WRL3_3_2D	Detected	M	No effect	None detected

2.3.6 Temporal and spatial protein expression of Sp-Whirlin

To detect temporal and spatial Sp-Whirlin protein expression, two commercially available antibodies to human Whirlin were used in Western blotting and Whole Mount Immunofluorescent Staining (WMFIS). A goat polyclonal antibody (Whirlin (D-20), Santa Cruz, Cat.No. sc-49785), is reportedly cross-reactive in different species. It was recommended by the manufacturer for detection of all isoforms of Whirlin in a broad range of applications. A mouse monoclonal antibody, DFNB31 (Abcam, Cat. No. ab57106), was raised against an immunogenic peptide sequence which had some resemblance to the "similar to Whirlin" (XM_788456) protein sequence of *S. purpuratus*.

Both antibodies failed to detect any specific proteins in Western blotting procedures. In an attempt to increase the sensitivity of the procedure, various adjustments were made to the Western blotting protocol. Those adjustments included changing sample preparation time and temperature and gel percentage, modifications of transfer time and transfer buffer composition, changing antibody concentrations and incubation times, and changing compositions of blocking solutions.

In WMFIS, both antibodies failed to produce a spatial pattern of protein expression. Various modifications were made to the fixation protocol including fixation in methanol instead of paraformaldehyde, addition of 50mM EGTA to the fixative to preserve cilia, and adjusting time and temperature of fixation in paraformaldehyde.

Positive controls with anti-α-tubulin antibody were used to successfully detect tubulin on Western blots and in WMFIS. These results indicated that the protocols for

both procedures were working, and that the commercial antibodies failed to detect Sp-Whirlin protein expression.

2.4 Discussion

The aim of this line of experiments was to characterize spatial and temporal expression of Usher genes in embryos and early 4-arm plutei of *S. purpuratus*, and to identify putative mechanosensory and photosensory cells.

Probe sequences for all *S. purpuratus* gene predictions, except for both predictions for Harmonin, were successfully amplified by PCR and cloned. The use of cDNA in PCR amplification of probe sequences ensured that probe sequences were amplified from actual transcribed messages. The absence of Harmonin transcripts in embryos was expected and correlated to the information in both mRNA expression databases. The cDNA was isolated from prism stage embryos. It is possible that Harmonin transcripts are present in plutei or other embryonic stages, and for that reason they were not detected.

Temporal expression analysis was performed to investigate relative expression levels of Usher genes from egg to early 4-arm pluteus stage. All the Usher gene probes except for SANS2_1 detected transcripts. Overall, transcript levels varied considerably in abundance for different genes; because of similarities in probe size and specific activities, relative intensities of bands provide a rough estimate of relative transcript prevalences. No co-relating patterns in levels of expression across the developmental stages were observed between different genes assessed. Tight coordination of expression of genes, which may function in common processes, often occurs in

eukaryotes (Niehrs and Pollet, 1999). The results suggest that Usher genes are not co-ordinately regulated and most likely do not form an Usher protein complex in embryos.

Expression of some genes is known to be upregulated in response to one round of deciliation, including tubulin. Deciliation did not visibly upregulate the transcript levels of any Usher genes. The apical tuft appears around the mesenchyme blastula stage and remains in the embryo until prism stage. Deciliation of prism stage should have removed the apical tuft cilia along with all the other cilia of the embryo (Stephens, 2008). The results did not provide any evidence for Usher proteins being localized to the apical tuft cilia and any motile cilia of the ectoderm at prism stage, but did not eliminate the possibility that their proteins may be localized to cilia. No deciliation of other stages or plutei was performed. More types of ciliated candidate sensory cells are proposed for pluteus stage (refer to section 1.3.5). Nevertheless, at pluteus stage, the cilia of the proposed sensory cells are buried beneath the hyaline layer and therefore most likely not accessible to the deciliation treatment. Also, repeated rounds of deciliation may be required to deplete the ciliary proteins and upregulate transcription of ciliary proteins in sea urchin embryos (Merlino et al., 1978). Repeated deciliation might have stimulated Usher gene transcription but this was not tested

In spatial expression analysis, Sp-Whirlin (SPU 021200) and Sp-VLGR1 transcripts were detected. Both Sp-Whirlin and Sp-VLGR1 had matching patterns of expression throughout development. Transcripts were localized within the main neurogenic territories of the embryos (Nakajima et al., 2004). Their expression was observed in the animal plate ectoderm at mesenchyme blastula, gastrula and prism stages; around the mouth prism stage; and around the gut and aboral ciliated band of plutei. The animal plate ectoderm is an early-specified neurogenic territory of the sea urchin embryo

(Yaguchi et al., 2006). It is a site of expression of a number of transcription factors involved in neurogenesis (Burke et al., 2006). In fact, expression of Sp-Whirlin and Sp-VLGR1 closely resembled the expression patterns of *Sp-Sc-Ac* and *Sp-Hbn*, homologues of genes known to be involved in early neural specification in other systems, and *Sp-Rx*, which is required for retinal development in vertebrates (Burke et al., 2006). *Sp-Hbn* is expressed in oral ganglia at prism stage, so it is possible that the staining observed around the mouth of prism stage embryos could be in oral ganglia. In mouse embryos, Whirlin expression is detected in the neural epithelium and matches the expression pattern of VLGR1b. It has been suggested that they could both have a role in neuronal proliferation and function in the same protein complex very early in neural development (van Wijk et al., 2006). Therefore, colocalization of spatial expression of Sp-Whirlin and Sp-VLGR1b in neurogenic areas suggests that their protein products may have a role in neuronal development in *S. purpuratus* embryos and that they could form a protein complex.

Spatial expression of other Usher genes was not detected. In humans and mice, apart from their expression in the sensory epithelia of the inner ear and retina, Usher gene transcripts are found ubiquitously in a wide range of organs and tissues. SANS is the only Usher gene expression of which is thought to be restricted to the inner ear and the retina (Reiners et al., 2006). It is conceivable that the Usher gene probes used in this study did not detect any localized expression for these genes because of their ubiquitous expression in embryos. This also suggests that in *S. purpuratus* embryos and plutei, Usher genes may involved in a variety of other processes than mechanosensation or photosensation. For example, MyosinVIIa is ubiquitously expressed and is a common component of cilia and microvilli. It is expressed in all ciliated or microvilli-bearing

epithelial tissues, where it is thought to participate in their morphogenesis (Hasson et al., 1997; Sahly et al., 1997; Wolfrum et al., 1998a). Apart from its role in cilia and microvilli, MyosinVIIa may participate in intracellular transport, cell-cell adhesion and endocytosis (Wolfrum, 2003). MyosinVIIa is also a common motor protein associated with lysosomes (Soni et al., 2005). Other functions suggested for the Usher proteins are regulation of actin cytoskeleton architecture in formation of cell processes, neuronal morphogenesis, formation of adherens junctions, and determination of apico-basal polarity (Kremer et al., 2006). Taken together, Usher genes could participate in various aspects of sea urchin embryo morphogenesis.

On the other hand, lack of localized expression could be a consequence WMISH protocol. Long hybridization times of the WMISH procedure might have not been suitable for detection of these transcripts. However, the protocol has been used successfully to detect many transcripts of various abundance in all cell types of the embryos (Arenas-Mena et al., 2000; Hinman et al., 2003; Minokawa et al., 2004). WMISH was attempted for later larval stages but produced no convincing or reproducible patterns.

Protein expression evaluation, with commercial antibodies to human Whirlin, failed to produce conclusive results. Failure of commercial antibodies to detect Sp-Whirlin expression suggests lack of sufficient structural similarity of Sp-Whirlin protein sequence to human Whirlin. Raising a specific antibody to Sp-Whirlin would have been a better approach to detect protein expression.

In conclusion, Usher gene mRNA and protein expression analysis did not identify specific cells having putative mechanosensory or photosensory functions in sea urchin embryos and early 4-arm plutei. In sea urchin embryos and early 4-arm plutei, Usher

genes most likely do not have sensory functions, but some may have a role in neuronal development. Usher proteins may have a sensory function in late larvae, which are much more complex in structure, and in adult sea urchins, which have specific structures identified as mechanosensory and photosensory (refer to sections 1.3.3 and1.3.4).

3: TRPA1 expression and identification of sensory cell candidates with fluorescent dyes

3.1 Introduction

Sea urchin embryos and pluteus larvae are sensitive to mechanical stimulation (refer to section 1.3.3). The embryonic apical tuft, which appears at mesenchyme blastula stage, has been proposed to be a sensory structure that may be required for embryo swimming directionality. Mechanosensory properties have also been proposed for a variety of cells in early 4-arm plutei including cells of the animal plate, apical organ, cells of the ciliated band, ectoneural cells of the oral ectoderm, cells of the aboral ectoderm, and the blastocoelar cells (refer to section 1.3.5)

TRPA1 has been proposed to be a candidate protein in a hypothetical mechanotrasduction channel in vertebrate hair cell stereocilia. TRPA1 is expressed by nociceptive neurons in mammals, where it is thought to participate in mechanotransduction (refer to section 1.2.2.3). Only one gene prediction for the TRPA1 channel has been annotated in the *S. purpuratus* genome, Sp-TRPA1 (SPU_010335). *S. purpuratus* apparently has only one TRPA1 gene, and no TRPN gene, which suggests that TRPA1 may have a mechanosensory function (refer to section 1.2.2.3). Another potential candidate for TRPA1 is a predicted Sp-TRP channel (SPU_021148) that has not been assigned to a TRP family.

Multiple studies have shown that the cationic fluorescent dyes FM1-43 and a YO-PRO are internalized into cells through mechanosensory channels, including

TRPA1. Staining with FM1-43 has been proposed as a screening method for mechanosensory cells and mechanosensory neurons. This may also apply to YO-PRO and its analogs (refer to section 1.2.2.4).

Here, temporal and spatial and expression of the Sp-TRPA1 gene was examined in embryos and early 4-arm plutei of *S. purpuratus* in an effort to identify putative mechanosensory cells. Live embryos and plutei were treated with FM1-43FX, a fixable analog of FM1-43, and TO-PRO-3, an analog of YO-PRO, in order to screen for mechanosensory cells.

3.2 Materials and Methods

All reagents were obtained from Sigma-Aldrich unless otherwise specified.

3.2.1 Animals

As described in 2.2.1.

3.2.2 Culture of embryos

As described in 2.2.2.

3.2.3 Probe and primer design

As described in 2.2.6.

3.2.4 Position Specific Iterated Blast (PSI –BLAST)

The position Specific Iterated Blast (PSI-BLAST) tool, in the National Centre of Biotechnology Information (NCBI) website, was used to identify proteins, similar to Sp-TRP-channel, in other organisms. A blastp search of non-redundant protein sequence database was performed using a PSI-BLAST algorithm,

http://blast.ncbi.nlm.nih.gov/Blast.cgi?PAGE=Proteins. The PSI-BLAST search settings were specified as described in the PSI-BLAST tutorial, http://www.ncbi.nlm.nih.gov.proxy.lib.sfu.ca/Education/BLASTinfo/psi2a.html. Search iterations were performed until no new sequences appeared in search results.

3.2.5 Synthesis of single stranded cDNA for probe sequence PCR amplification

As described in 2.2.7.

3.2.6 PCR and touchdown PCR

As described in 2.2.8.

3.2.7 Purification of PCR products from agarose gel for cloning

As described in 2.2.9.

3.2.8 Synthesis of pBluescript KS+ T-tailed vector (pBS-T)

As described in 2.2.10.

3.2.9 Cloning of PCR fragments into pBS-T

As described in 2.2.11.

3.2.10 DIG RNA probe synthesis

As described in 2.2.12.

All probe names and sequences are listed in Supplemental table 2 and Supplemental figures 5 and 6.

3.2.11 Artificial seawater preparation

As described in 2.2.13.

3.2.12 Deciliation

As described in 2.2.14.

3.2.13 Northern Blotting

As described in 2.2.15.

3.2.14 Whole mount in situ hybridization (WMISH)

As described in 2.2.16.

3.2.15 Whole mount immunofluorescent antibody staining (WMIFS)

As described in 2.2.18.

If the embryos were labelled with FM1-43FX prior to antibody staining (described in section 3.2.17), samples were kept in the dark during the washing steps after fixation. Right before antibody staining, the samples were washed 3 times in PBS-T for 10min at RT.

Primary Antibody Solutions used: 1:10 to 1:100 anti-α-Tubulin mouse monoclonal (Sigma, Cat. No. T9026) in Blocking Solution. Secondary Antibody Solutions used: 1:500 goat anti-mouse Alexa Fluor 660 (Invitrogen, Cat.No. A21054) in PBS-T.

3.2.16 *S. purpuratus* pluteus structural terminology

Early 4-arm pluteus structural terminology was adapted from Smith et al. (2008). Structural terminology, ectodermal terminology, and ciliated band localization are described in Figure 3.1.

Figure 3.1 *S. purpuratus* early 4-arm pluteus structural terminology

A, C) Pluteus viewed from the anal side. B, D) Pluteus viewed from left side. A) Pluteus anterior, posterior, left and right sides are shown. B) Pluteus anterior, posterior, anal and abanal sides are shown. Structures: A, anus; E, oesophagus; I, intestine; LA, left anterolateral arm; LAR, left anterolateral rod; LBR, left body rod; LPO, left postoral arm; LPOR, left postoral rod; M, mouth; PT, posterior tip; RA, right anterolateral arm; RAR, right anterolateral rod; RBR, right body rod; RPO, right postoral arm; RPOR, right postoral rod; S, stomach. C, D) Ectodermal areas: oral ectoderm (red); ciliated band (green); aboral ectoderm (blue).

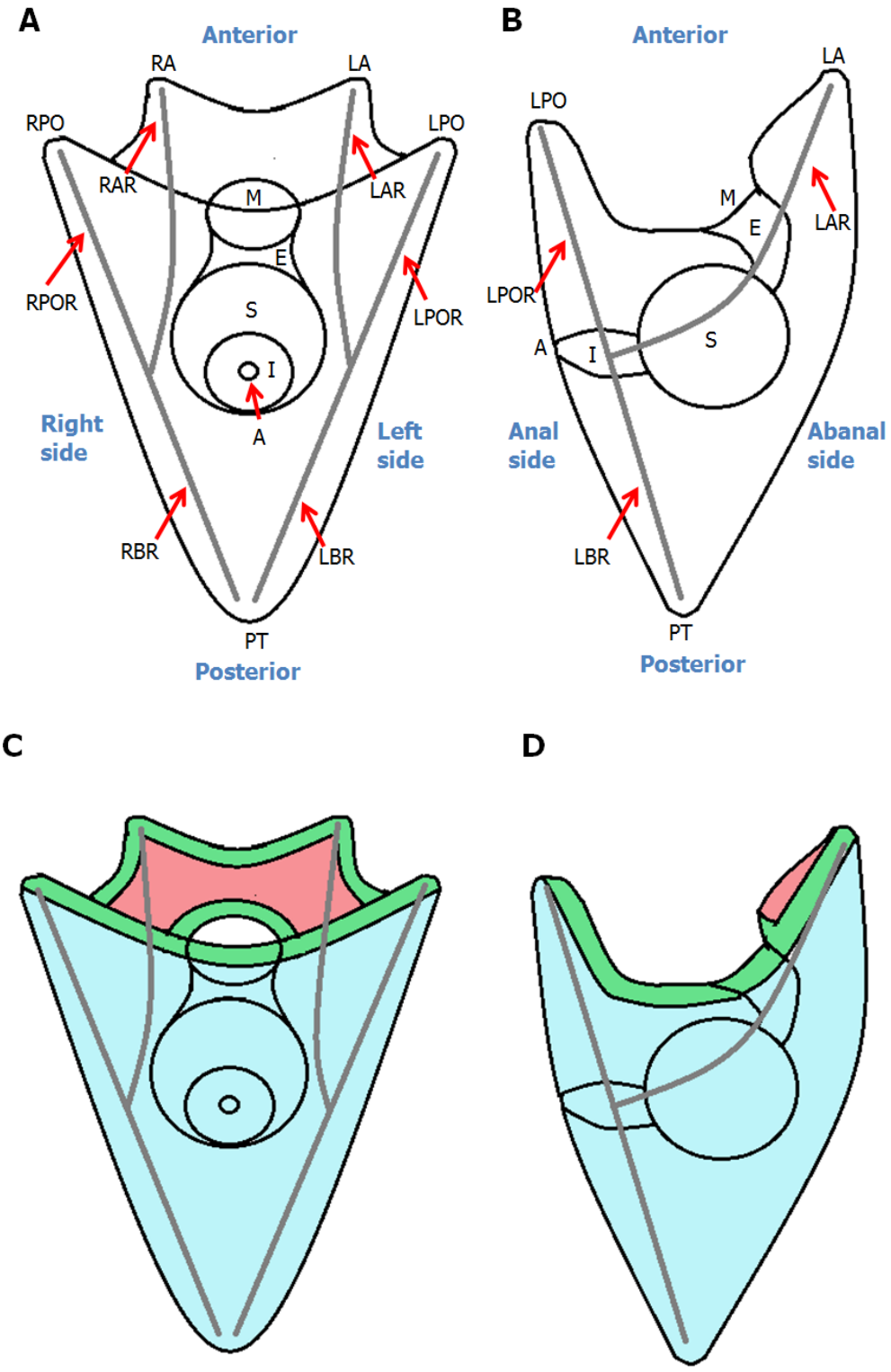
A
Anterior
RA
LA
RPO
LPO
RAR
LAR
M
E
S
RPOR
LPOR
I
A
Right side
Left side
RBR
LBR
PT
Posterior
B
Anterior
LA
LPO
M
E
LAR
LPOR
A
I
S
Anal side
Abanal side
LBR
PT
Posterior
C
D

3.2.17 Fluorescent dye labelling of embryos and larvae

A fixable analog of FM1-43 (n-(3-triethylammoniumpropyl)-4-(4-(dibutylamino)-styryl) pyridinium dibromide), FM1-43FX (Invitrogen, Cat.No.F35355) was used in all procedures which crosslinks to membranes when samples are fixed in paraformaldehyde. Other dyes were not fixable: TO-PRO-3 iodide (4-[3-(3-methyl-2(3H)-benzothiazolylidene)-1-propenyl]-1-[3-(trimethylammonio)propyl], diiodide) (Invitrogen, T3605) and Propidium iodide (PI) (3,8-diamino-5-[3-(diethylmethylammonio)propyl]-6-phenylphenanthridinium, diiodide) (Sigma, Cat.No.P1470).

To treat embryos with a fluorescent dye, the embryo culture was concentrated to 5000 embryos/ml by reverse filtration through a 6cm diameter filter of 25µm nylon mesh (Nitex). Treatments were performed using 2ml of concentrated samples in 35mmx19mm Petri dishes (Sarstedt, Cat.No. 82.1135) to minimize the amount of dye used. The wash out step for all dyes was performed using a specially constructed reverse filter apparatus to minimize sample loss during collection. The reverse filter was made from a 50ml Conical Tube with Flip-Top Cap (BD Falcon, Cat. No. 89048-930). The tube was cut at 25ml mark to create a barrel, and the flipping part of the cap was removed to make the detachable screw-on ring. A 25µm nylon mesh, 3x3 cm, was placed over the opening of the barrel, and this ring was used to attach the mesh to the barrel tightening the mesh in the process. The final diameter of the mesh filter was 2.5cm. The filter was placed in a glass dish, 5cm in diameter and 2cm high. The dish was then was filled with SW to cover the filter mesh by 1-2cm.

Dyes were added to samples in Petri dishes by pipetting an appropriate amount of dye stock solution to a desired final dye concentration using a 20µl pipette. Stock solution concentrations were as follows: FM143FX, 1µg/µl in H_2O; TO-PRO-3, 1mM in DMSO; PI, 1mg/ml in PBS-T. After dye addition, samples were immediately and thoroughly mixed to uniformly distribute the dye by swirling the plate contents counter clockwise and clockwise. Final concentrations of dyes in culture were as follows(unless otherwise specified): 3µM for FM143FX, 2µM for TO-PRO-3, or 2µM for PI. FM1-43FX samples were treated for 30sec in the dark at RT. TO-PRO-3 samples were treated for 1min the dark at RT, or for 5min, 7min, 10min, and 40min in the dark at 12ºC. PI samples were treated for 30min in the dark at 12ºC. At the end of the incubation, the embryo sample was quickly poured into a specially constructed reverse filter, and rinsed, while in the filter, with continuous light flow of approximately 300ml of fresh SW, which was applied fully within 10sec. The embryos were then collected with a Pasteur pipette into a 1ml volume into a 15ml sample tube. Embryos were then immediately visualized live. Alternatively, the samples were fixed, before visualization, in 15 volumes of Antibody Staining Fixative (4% paraformaldehyde, 50mM EGTA in FSW). Upon addition of the fixative, the samples were mixed thoroughly and incubated for 1hr in the dark at RT. The samples were then washed 3 times in 15 volumes of PBS or FSW for 1hr at RT. Antibody staining of embryos was sometimes performed after this step (refer to section 3.2.15).

Samples were viewed alive in SW or fixed in Vectashiled. To obtain Epifluorescent images, the samples were visualized using 20x or 40x objective lenses on a Vanox (Olympus, AHBS3) microscope at a GFP setting, and images were acquired Sony Power HAD Camera (Sony) and Northern Eclipse V6.0 software. To obtain confocal

images, the samples were visualized using 25x, 40x or 60x objective lenses on a WaveFX Spinning Disc Confocal Microscope (Quorum Technologies, Ltd.). FM1-43FX samples were viewed using the 440nm or 491nm laser lines and a 595/50 filter. For TO-PRO-3, the 640nm laser line and 655 690/50, 620/60 or 700/75 filters were used. For PI, the 561nm laser line and 618 595/50 or 620/60 filters were used. Images were acquired using Hamamatsu 9100-13 EMCCD camera (Hamamatsu Photonics) and Volocity software V5.0, http://www.cellularimaging.com/products/volocity/.

3.2.18 FM1-43 live labelling assay

This assay was performed in a specially constructed dye labelling chamber. To construct a dye labelling chamber, two 30mm x 5mm pieces of Scotch Permanent Double Sided tape (3M) were placed, parallel to each other, onto the surface of a 1mm thick glass microscope slide (75mmx25mm, Premier, Cat.No.9101) leaving 15mm gap in between the strips. Tape strips were attached to the slide by applying pressure, ensuring that no air bubbles were caught between the tape and the glass surface. Then, a 10µl drop of concentrated 5000 embryo/ml culture was applied to the slide in the space between the strips. A Microcover Glass coverslip (22mm x 22mm, 0.13 to 0.17mm thick, VWR, Cat.No.48366067)), was gently placed on top of the drop and pressure was applied to attach the coverslip to the double sided tape. The chambers with embryos were placed unsealed into a humidified chamber made of a 150X25mm Petri dish (BD Falcon, Cat.No. 351013) with a moistened Kimtech Science Precision Wipes (Kimberly Clark professional). The humidified chamber containing the slides was kept in the dark on ice before dye labelling, for no longer than 10min, to prevent dehydration or effects of low temperature on viability of embryos.

To prevent embryos from moving on the slide, coverslips were coated with Poly-L-lysine (Sigma, P1274). To make Poly-L-lysine coated coverslips, multiple pieces of Microcover Glass 22mmx22mm, 0.13 to 0.17mm thick (VWR, 48366067), were incubated in 1mg/ml of Poly-L-lysine, with light agitation, for 30 min at RT. Coverslips were then washed 10 times in H_2O for 5min at RT, rinsed in 100% ethanol and dried.

To label embryos with FM1-43FX, 10µl of 6µM FM1-43FX were added by inserting the end of a 20µl pipette tip into the space between the slide and the cover slip. Mixing of the two phases was allowed to occur by capillary action.

Embryos were observed before, during and after dye addition to the slide, using using 40x objective lens on a WaveFX Spinning Disc Confocal Microscope (Quorum Technologies, Ltd.). FM1-43FX labelling was visualized using the same settings as described in section 3.2.17. Images and live videos were acquired Hamamatsu 9100-13 EMCCD camera (Hamamatsu Photonics) and Volocity software V5.0, http://www.cellularimaging.com/products/volocity/.

3.2.19 pCPA treatment of embryos

DL-p-Chlorophenylalanine (pCPA) (Sigma, Cat.No. C6506) was applied directly to embryo culture plates, at 2µg/ml, at swimming blastula (24hpf) and prism (72hpf) stages. At 96hpf, pCPA treated embryos were labelled with FM1-43FX and fixed for visualization as described in section 3.2.17.

3.3 Results

3.3.1 Evidence for TRPA1 mRNA expression

The Baylor College of Medicine *S. purpuratus* annotated database of genome assembly Spur 2.1 was searched for gene predictions for TRPA1 (http://annotation.hgsc.bcm.tmc.edu/Urchin/cgi-bin/pubLogin.cgi). Only one gene prediction was found for TRPA1 (SPU 010335), and one prediction was found for a generic TRP channel (SPU 021148).

To determine if these *S. purpuratus* TRP genes were expressed in embryos, two embryonic mRNA expression databases were examined: 1) Microarray database; 2) Tiling array database (refer to section 2.3.1 for details). According to two databases, both gene predictions are expressed during embryonic stages. According to Database 1, Sp-TRPA1 (SPU 010335) is most likely not expressed at 2hpf, where the signal value is only 4 units, and it starts being expressed at 15hpf. Expression of the Sp-TRP channel gene (SPU 021148) was detected in early embryos, but no expression was detected at 30hpf, where the signal value is equal to 0 units (Supplemental Fig. 4).

The predicted Sp-TRP channel protein (SPU_021148) has not been assigned to a specific TRP family. However, according to a search with Position Specific Iterated Blast algorithm (PSI –BLAST) of NCBI non-redundant protein sequence database, Sp-TRP-channel is a TRPV family protein, most similar to mammalian TRPV6 channel. TRPV6 is a highly calcium selective epithelial channel involved in the maintenance of calcium ion homeostasis across intestinal and renal epithelia in mammals (Vennekens et al., 2008). Expression of TRPV6 has been reported in retinal pigment epithelium where the channel

can mediate subretinal space calcium ion composition (Kennedy et al., 2010). Therefore, the Sp-TRP-channel is does not belong to the TRPA1 family and presumably has different properties and functions than TRPA1.

3.3.2 Design of TRPA1 primers and amplification of probe sequences

To amplify an approximately 1000bp sequence for each TRP gene prediction, cDNA from prism stage (72hpf) embryos was isolated, and probe sequences were amplified from this cDNA sample using PCR. Multiple pairs of PCR primers were designed and tested for each prediction (Supplemental Fig. 5, Supplemental table 2).

Each pair of primers was tested using a regular PCR protocol (Supplemental table 2). At least one probe sequence was successfully amplified for each of the predictions.

Probe sequences were cloned and sequenced (Supplemental Fig. 6). After PCR amplification, each probe sequence was cloned into a pBluescript KS+ T-tailed vector, and DIG-RNA probes were synthesized using T7 or T3 polymerase.

Two different DIG probes were synthesized for Sp-TRPA1 (TRPA1_1_10E and TRPA1_3), and one for Sp-TRP channel (TRPCH_4_6E) (See Supplemental table 2, Supplemental Fig. 6 for details). DIG-probes were then used in mRNA expression analyses by Northern blots and Whole Mount In-Situ Hybridization (WMISH).

3.3.3 Temporal mRNA expression of Sp-TRPA1 and Sp-TRP-channel

To investigate the temporal expression of *S. purpuratus* TRP genes, RNA from eight developmental stages was extracted: egg, 16-cell morula (6hpf), early blastula (12hpf), hatched blastula (24hpf), mesenchyme blastula (36hpf), gastrula (48hpf), prism (72hpf) and early 4-arm pluteus (96hpf). Northern blotting showed that Sp-TRPA1

transcripts were not detected at the egg stage, 6hpf, or 12hpf. Sp-TRPA1 expression was substantial by 24hpf, and its transcript prevalence had increased significantly at 36hpf. Similarly, transcripts for the Sp-TRP-channel were not detected in the egg, but appeared between 6hpf and 12hpf, and their prevalence increased substantially by 36 hpf (Fig. 3.2).

3.3.4 Effects of deciliation on mRNA expression of Sp-TRPA1 and Sp-TRP-channel

To determine if deciliation caused an upregulation of TRP gene transcripts, deciliation at prism stage (72hpf) was performed (refer to section 2.3.4 for background information). RNA samples were collected 30min and 1hr post deciliation. Northern blotting was used to compare transcript levels in deciliated samples to transcript levels in untreated samples.

Transcript levels of Sp-TRPA1 and Sp-TRP-channel were not affected by the deciliation treatment. Sp-Ubiquitin was used as a negative control and its transcript levels were not affected by deciliation (Fig.3.3). Sp-β-tubulin probe was used as a positive control to demonstrate that the deciliation upregulated Sp-β-tubulin expression (Fig. 2.2B).

3.3.5 Spatial mRNA expression of Sp-TRPA1 and Sp-TRP-channel

To determine spatial expression of TRP genes, WMISH was performed using five developmental stages: hatched blastula (24hpf), mesenchyme blastula (36hpf), gastrula (48hpf), prism (72hpf) and early 4-arm pluteus (96hpf).

No localized patterns of expression were identified in the five stages analyzed. Troubleshooting was performed as described in section 2.3.5, without improvements.

Figure 3.2 Temporal mRNA expression of *S. purpuratus* TRP channels

Northern blots showing expression profiles of TRP gene transcripts during embryonic development. RNA from egg, 6, 12, 24, 36, 48, 72, and 96hpf was loaded at 1µg per well. Ethidium bromide staining of the ribosomal RNA bands served as a loading control. The approximate sizes of detected transcripts are shown in kilobases (kb). Data was obtained from a single batch of embryos. Probes: Ubiquitin; TRPCH_4, Sp-TRP channel (SPU 021148); TRPA1_1 and TRPA1_3, Sp-TRPA1 (SPU 010335).

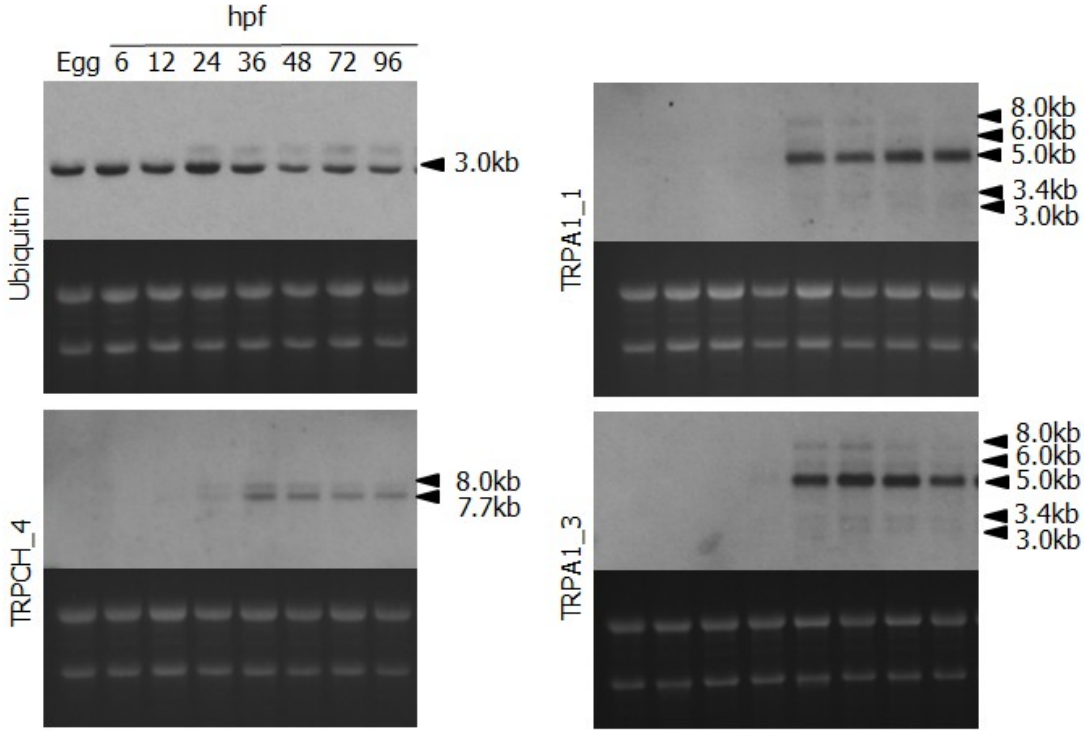
hpf
Egg 6 12 24 36 48 72 96
Ubiquitin
3.0kb
TRPA1_1
8.0kb
6.0kb
5.0kb
3.4kb
3.0kb
TRPCH_4
8.0kb
7.7kb
TRPA1_3
8.0kb
6.0kb
5.0kb
3.4kb
3.0kb

Figure 3.3 Effects of deciliation on TRP channel mRNA expression

Northern blots showing expression profiles of TRP genes before and after deciliation. RNA samples were loaded at 1µg per well. Ethidium bromide staining of the ribosomal RNA bands served as a loading control. The approximate sizes of the transcripts are shown in kilobases (kb). Data was obtained from a single batch of embryos. Probes: Ubiquitin; TRPCH_4, Sp-TRP channel (SPU 021148); TRPA1_1 and TRPA1_3, Sp-TRPA1 (SPU 010335). Abbreviations: PT, pre-treatment control, 30T- 30min treated,30UT – 30min untreated, 60T- 60min treated, 60UT – 60min untreated. Abbreviations: T, treated; UT, untreated.

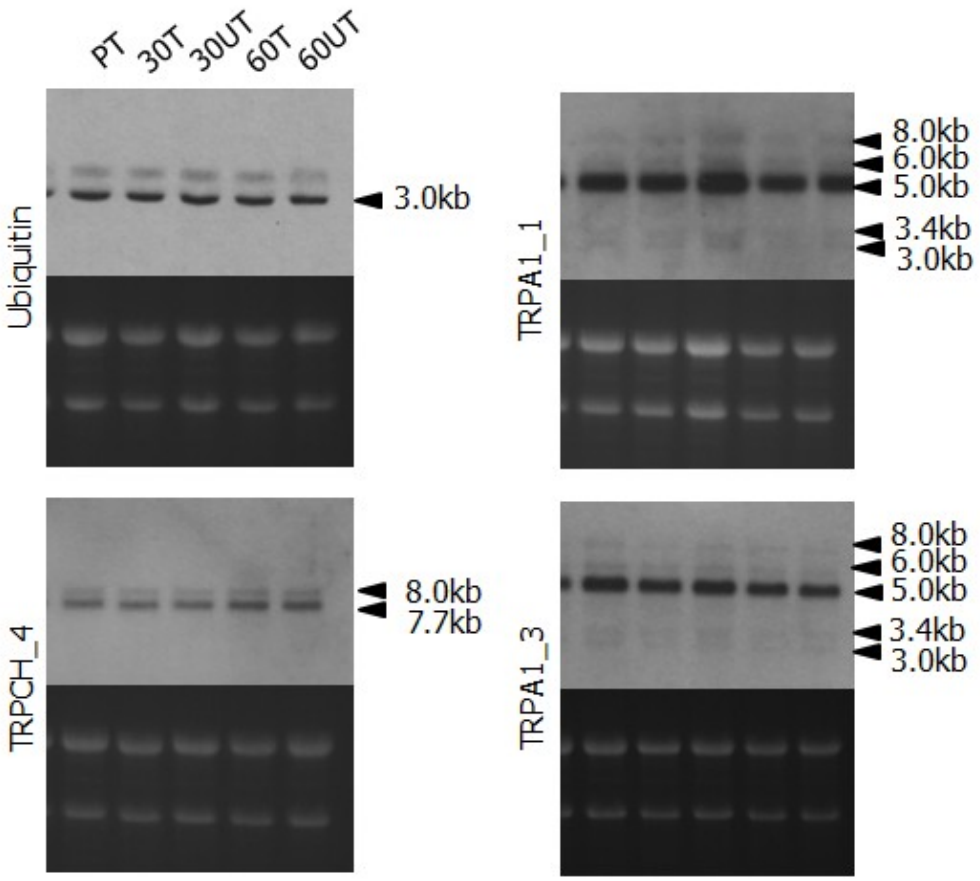
PT
30T
30UT
60T
60UT
Ubiquitin
3.0kb
TRPA1_1
8.0kb
6.0kb
5.0kb
3.4kb
3.0kb
TRPCH_4
8.0kb
7.7kb
TRPA1_3
8.0kb
6.0kb
5.0kb
3.4kb
3.0kb

3.3.6 FM1-43 labelling

3.3.6.1 FM1-43 labels specific cells in live early 4-arm plutei

For all the following experiments, the terminology used for structural features of the early 4-arm pluteus was in accordance with Smith et al. (2008). The structural and ectodermal terminology is described in Fig. 3.1 in section 3.2.19.

To identify mechanosensory cell candidates, live early 4-arm plutei (96hpf) were treated with FM1-43 for 30 seconds, washed and visualized live. FM1-43 labelled the ectoderm, the blastocoelar cell network, the gut and the pigment cells. The ectodermal labelling was punctate in nature. Tracts of blastocoelar cells labelled with FM1-43 were interconnected, forming a network. Some of these tracts associated with skeletal spicule body rods. Other tracts extended beneath the ciliated band and around the gut and the mouth. Processes, extending from these tracts, were seen inserted into the ectoderm at the apical organ, the ectoderm at the tips of anterolateral and postoral arms, and at the posterior tip (Fig. 3.4 and 3.5).

The blastocoelar cell network contained motile FM1-43 labelled vesicles (Supplemental Fig. 7; Supplemental video 1 and 2). Ciliated band cells contained motile FM1-43 labelled vesicles that moved towards and away from the apical cell surface (Supplemental Fig. 8, Supplemental video 3). Pigment cells also contained motile FM1-43 labelled vesicles (Supplemental Fig.9, Supplemental video 4). Blastocoelar cells, labelled with FM1-43, shifted in shape in live embryos (Supplemental Fig. 10, Supplemental video 5; Supplemental Fig. 11, Supplemental video 6).

Figure 3.4 Epifluorescent images of FM1-43 labelling in live plutei

Epifluorescent images of cells in plutei labelled with FM1-43 (green) for 30 seconds with washout. A) Blastocoelar cell network tracts beneath the ciliated band (arrowhead) (Scale bar 20µm). B) The left and right body rod tracts of blastocoelar cells (arrowheads) (Scale bar 20µm). C) Blastocoelar cell network processes insert into the ectoderm at the tip of the left anterolateral arm (Scale bar 20µm). C') Inset from C (Scale bar 5µm). D) Pigment cell of the aboral ectoderm (Scale bar 20µm). D') Inset from D (Scale bar 5µm) E) Blastocoelar cell network of the gut (arrow) and punctate labelling of the ciliated band ectoderm (arrowhead) (Scale bar 20µm). F) Punctate labelling of the ciliated band ectoderm (Scale bar 10µm).

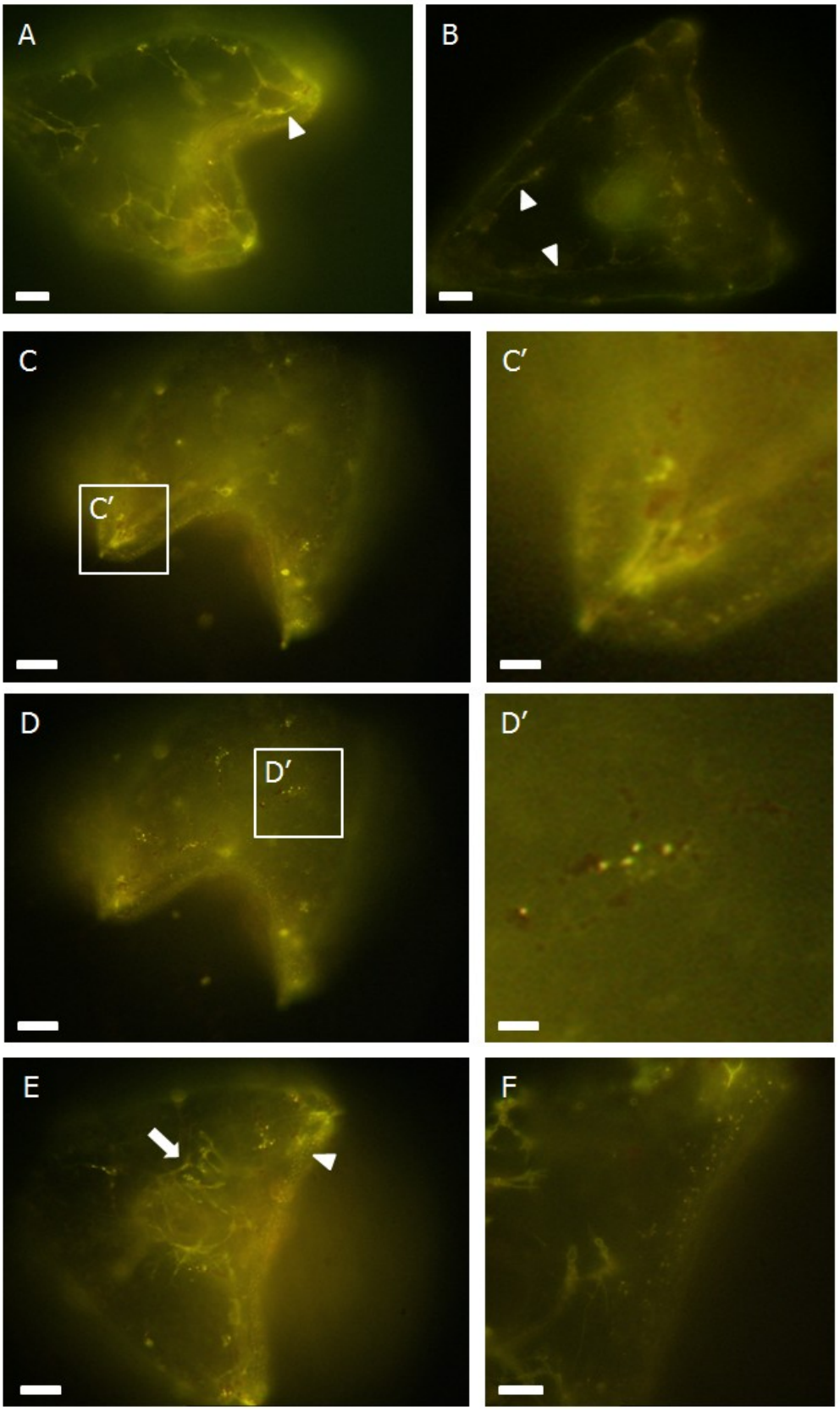
A
B
C
C′
C′
D
D′
D′
E
F

Figure 3.5 Confocal images of FM1-43 labelling in live plutei

Spinning disk confocal images of live plutei labelled with FM1-43 (green) for 30 seconds with washout and their corresponding brightfield images. Scale bar of 20µm applies to all panels. A) Blastocoelar cell tract extending at the base of the ciliated band, between the postoral arms (arrowhead), and vesicles within the cell cytoplasm of the ciliated band (arrow). B) Punctate labelling of the ciliated band ectoderm surface (arrowhead). C) Blastocoelar cell processes inserting into the ciliated band between the anterolateral arms or the apical organ (arrowhead). D) Blastocoelar cell tract extending between the anterolateral arms (arrow). E) Processes, from the blastocoelar cell tract in D, inserting into the ectoderm of the anterolateral arms (arrowheads). F) Blastocoelar cell tract inserting processes into the ectoderm of the right postoral arm (arrowhead) and connecting to the tract in A and the right postoral rod tract (arrow). G) Tracts associated with the right and left body rods (arrowheads). H) Processes of both tracts in G inserting into the ectoderm at the posterior tip (arrow). I) Punctate ectodermal labelling. J) Pigment cell labelling. Abbreviations: BF, Brightfield.

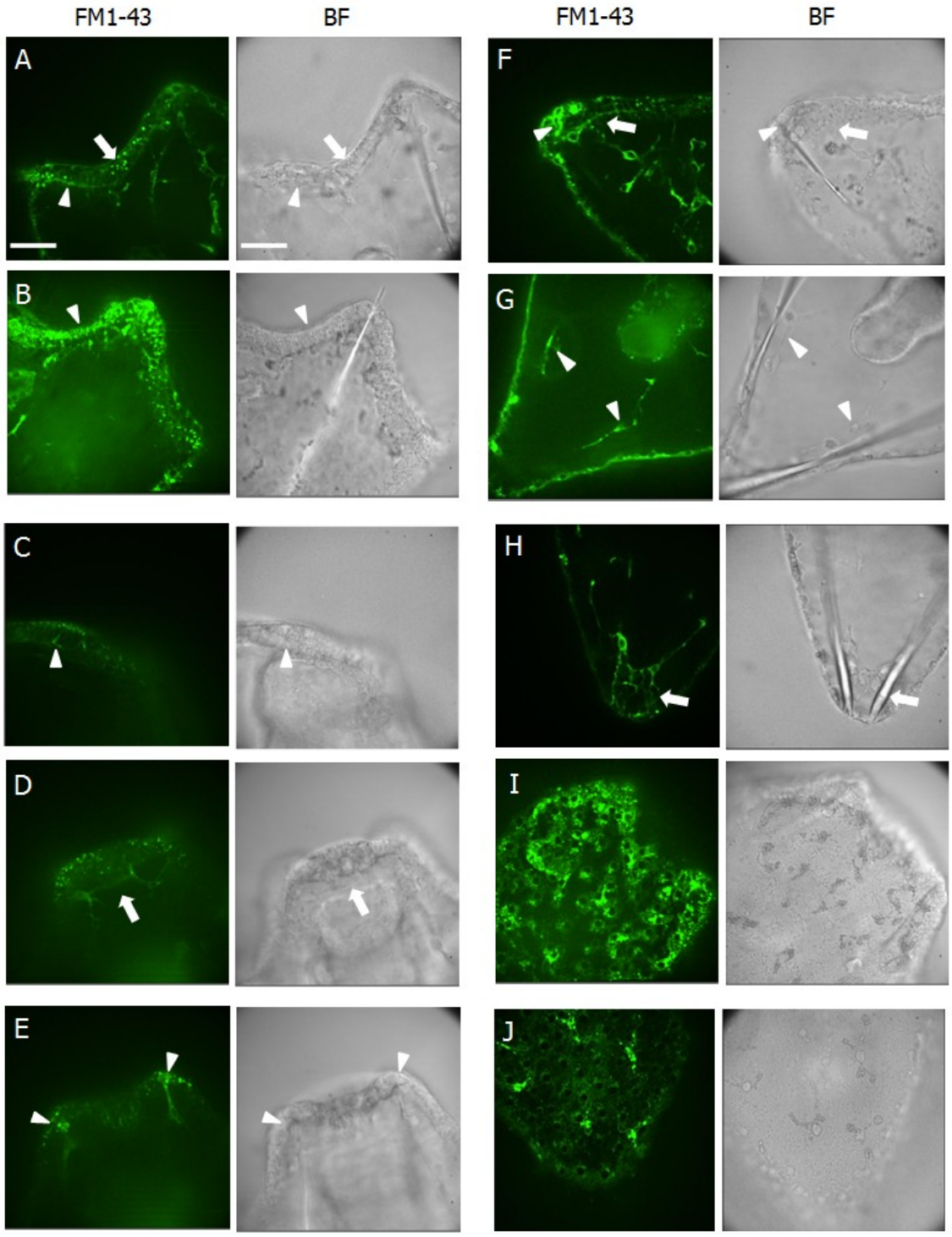
FM1-43
BF
FM1-43
BF
A
F
B
G
C
H
D
I
E
J

Rapid internalization of FM1-43 into cell cytoplasm is basis for identification of a candidate mechanosensory cells, and this FM1-43 labelling should persist after washout (refer to section 1.2.2.4). Therefore, to determine if the FM1-43 labelling in plutei was persistent, as described for *in vivo* labelling of sensory structures of mice (Meyers et al., 2003), plutei were labelled for 30 seconds with FM1-43, were washed out and then allowed to swim freely in culture for an extra 24 hours before fixation in paraformaldehyde and visualization. These plutei were visualized using the same laser settings used for observation of plutei that were fixed immediately after washout. Plutei cultured for 24hrs before fixation retained the blastocoelar cell fluorescent labelling intensity equivalent to plutei fixed at 0hrs. The plutei fixed at 24hrs also showed labelling of thin blastocoelar cell processes, not seen in plutei fixed at 0hrs, and significantly reduced ectodermal labelling. FM1-43 labelling of specific cells in the ciliated band ectoderm of the postoral arms was observed, which had not been previously noticed (Fig. 3.6).

The results suggest that the blastocoelar cells and specific cells within the ciliated band internalize FM1-43 into their cytoplasm, and that they are the best candidates for mechanosensory cells in early 4-arm plutei.

Figure 3.6 FM1-43 labelling in plutei fixed at 0 hrs vs. plutei fixed at 24 hrs post dye treatment

A-D) Confocal images showing reduction of ectodermal FM1-43 fluorescence intensity and retainment of fluorescence intensity in the blastocoelar cell network. Images were acquired using the same laser sensitivity and exposure to compare FM1-43 fluorescence intensity across samples. A, B) Plutei fixed at 0hrs post FM1-43 treatment (Scale bar 30µm). C, D) Plutei fixed at 24hrs after FM1-43 treatment; thin blastocoelar cell processes are visible (arrowhead) (Scale bar 30µm). E-H) Cells labelled with FM1-43 in the ciliated band ectoderm of postoral arms, after 24hrs post FM1-43 treatment (arrowheads). E) FM1-43 labelling, right postoral arm (Scale bar 20µm). F) Brightfield image corresponding to E. G) FM1-43 labelling, left postoral arm (Scale bar 20µm). H) Brightfield image corresponding to G. Abbreviations: BF, Brightfield.

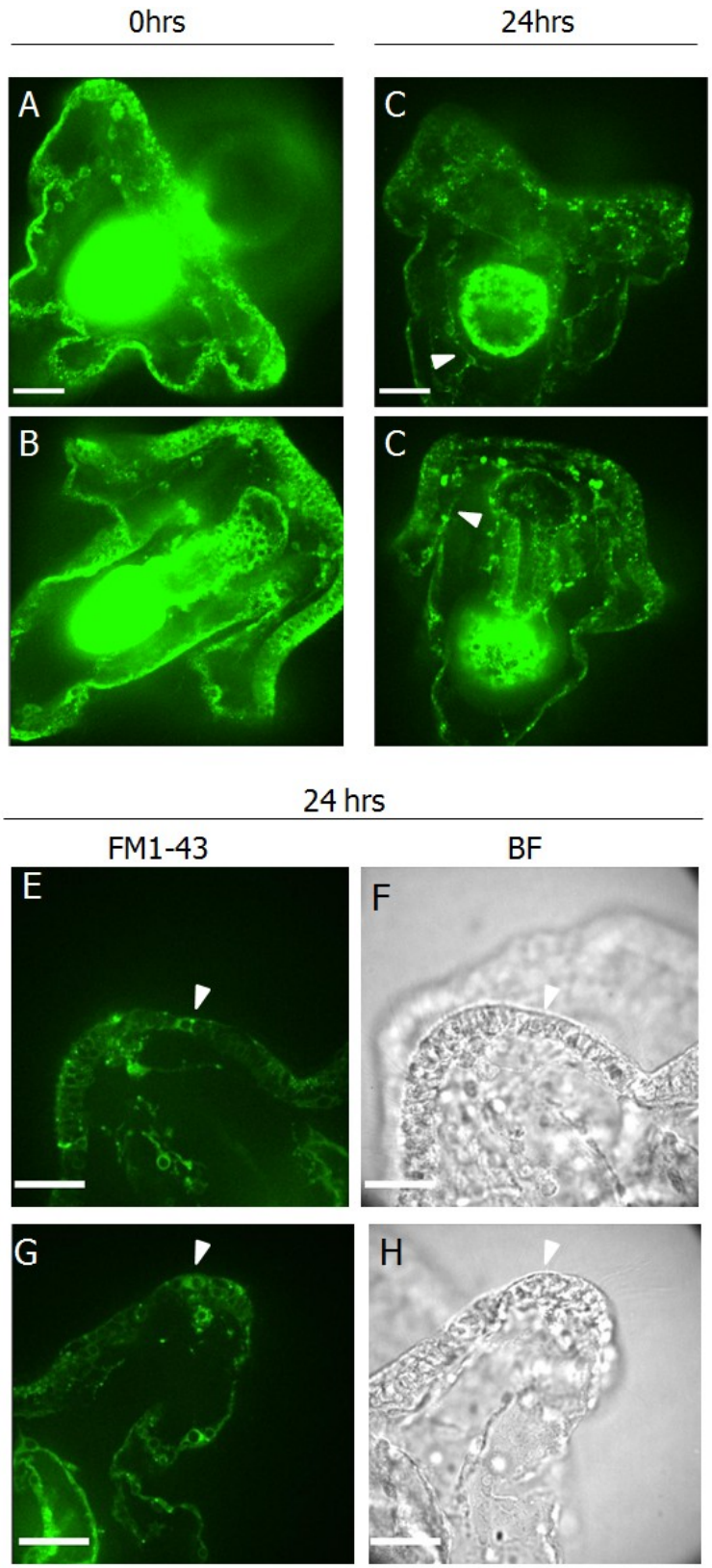
0hrs
24hrs
A
C
B
C
24 hrs
FM1-43
BF
E
F
G
H

3.3.6.2 Effects of pCPA treatment on FM1-43 internalization

Treatment of embryos with the inhibitor of serotonin synthesis, p-chlorophenylalanine (pCPA), disrupts formation of the serotonin receptor cell network (SRN), which is thought to be a major component of the blastocoelar cell network and may participate in spatial swimming control (Katow et al., 2004; Katow et al., 2007).

To determine if FM1-43 is internalized into the SRN, SRN formation was disrupted by adding pCPA to embryos at either swimming blastula stage (24hpf) (S-CPA) or prism stage (72hpf) (P-CPA). S-CPA and P-CPA embryos were labelled with FM1-43 at pluteus stage (96hpf) for 30 seconds, with washout, and were then fixed in paraformaldehyde. Their labelling was compared to untreated plutei, which were labelled and fixed in the same conditions, using the same laser exposure and sensitivity. Compared to untreated plutei, S-CPA and P-CPA embryos were labelled with less fluorescence intensity, and the labelling of their blastocoelar cells was reduced. The FM1-43 labelled blastocoelar network in treated embryos was not developed at 96hpf: lots of blastocoelar cells had round shapes lacking processes, and few connections were observed between the cells. The guts of P-CPA plutei were severely affected by the treatment: they had reduced fluorescence intensity and appeared to dissociate into separate cells (Fig. 3.7).

These results show that proper development of the SRN is required for the development of the FM1-43-labelled blastocoelar network. Therefore, FM1-43 internalization most likely occurs in the SRN.

Figure 3.7 FM1-43 labelling in pCPA treated embryos

Confocal images of fixed plutei labelled with FM1-43 (green). Images were acquired using the same laser sensitivity and exposure to compare FM1-43 fluorescence intensity across samples in A-F and G-L panels. Scale bar of 30µm applies to all panels. A-F) Optimal laser exposure and sensitivity was set using untreated plutei as a reference. A) Untreated pluteus, higher intensity gut labelling (arrow) compared to gut labelling of P-CPA pluteus in C. B) Untreated pluteus with higher intensity labelling of blastocoelar cells (arrowhead) compared to blastocoelar cell labelling in D, F and E. C) P-CPA pluteus with lower gut labelling intensity (arrow) compared to gut labelling of untreated pluteus in A. D) P-CPA pluteus with lower intensity labelling of blastocoelar cells (arrowhead) compared to blastocoelar cell labelling of untreated pluteus in B. E,F) S-CPA pluteus with lower intensity labelling of blastocoelar cells (arrowheads) compared to blastocoelar cell labelling of untreated pluteus in B. G-L) Optimal laser exposure and sensitivity was set using S-CPA and P-CPA plutei as a reference. G) Untreated pluteus, higher intensity gut labelling (arrow) compared to gut labelling of P-CPA pluteus in I. H) Untreated pluteus with higher intensity labelling of blastocoelar cells (arrowhead) compared to blastocoelar cell labelling in J, K and L. I) P-CPA pluteus with lower gut labelling intensity (arrow) compared to gut labelling of untreated pluteus in G. J) P-CPA pluteus with lower intensity labelling of blastocoelar cells (arrowhead) compared to blastocoelar cell labelling of untreated pluteus in H. K, L) S-CPA pluteus with lower intensity labelling of blastocoelar cells (arrowheads) compared to blastocoelar cell labelling of untreated pluteus in H.

Laser exposure and sensitivity set for untreated plutei

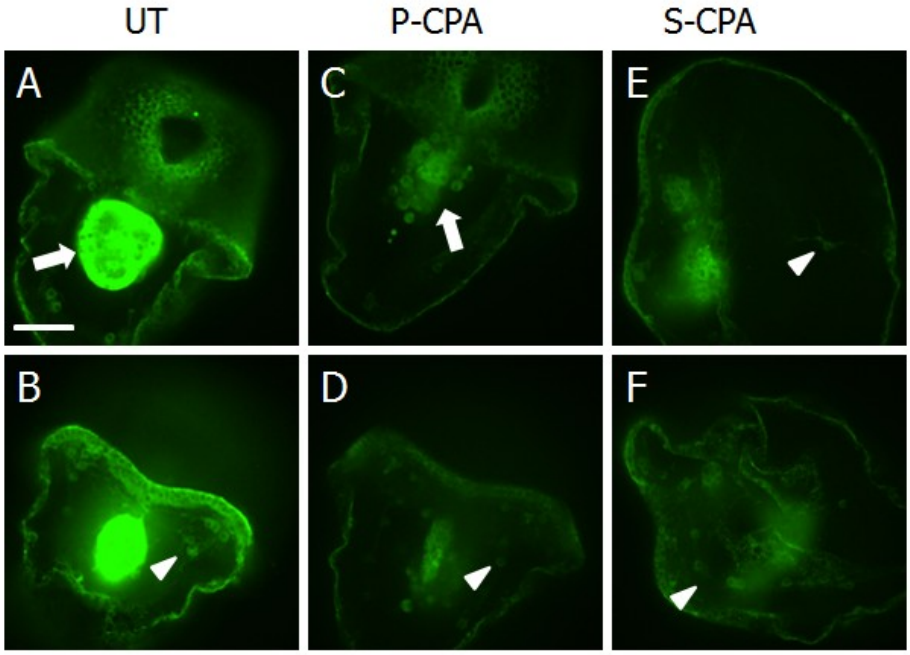

Laser exposure and sensitivity set for treated embryos

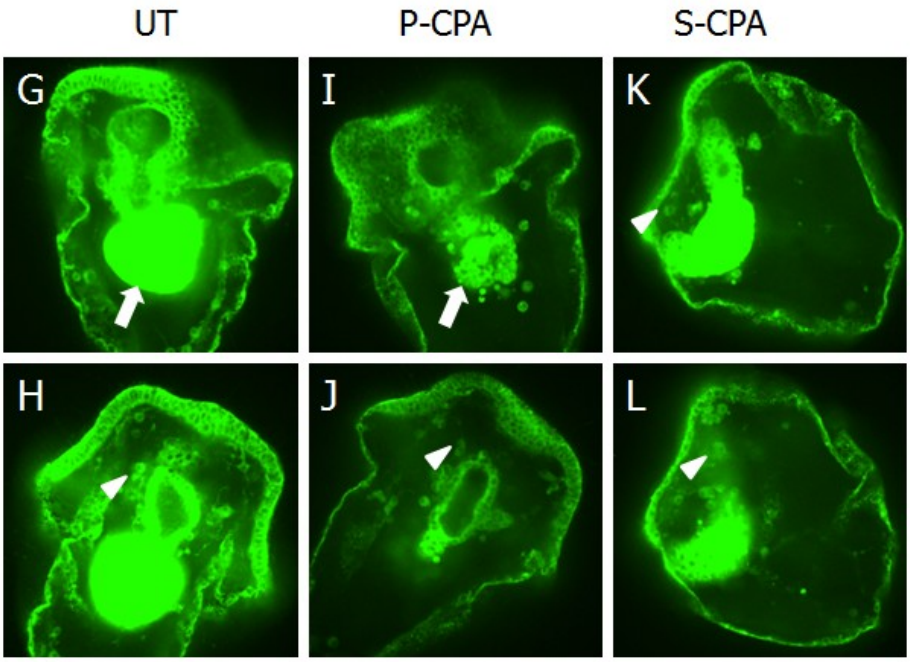

3.3.6.3 Analysis of punctate labelling of the ectoderm

To investigate the nature of the punctate labelling of cells of the ciliated band, oral and aboral ectoderm, fixed embryos, treated for 30 seconds with FM1-43 with washout, were stained with anti-α-tubulin antibody to visualize cilia. FM1-43 dye labelled the apical zone of ectoderm cells at the bases of their cilia (Fig. 3.8). At higher magnification of the cilia bases, each labelled spot was resolved into a ring of lobules (Fig. 3.9).

The labelled lobules resemble the components of the Golgi complex in ciliated ectodermal cells of *S. purpuratus* embryos reported previously (Eldon et al., 1990). Alternatively, the lobules may be endosomes. Thus, labelling with FM1-43 suggests that it may be taken up by endocytosis at the bases of cilia, though the short labelling time was used to avoid dye uptake by endocytosis.

Figure 3.8 FM1-43 punctate ectodermal labelling at the bases of cilia

Confocal images showing punctate FM1-43 ectodermal labelling at the bases of cilia in fixed plutei. Scale bar of 12μm applies to all panels. A-E) Ciliated band ectoderm surface between the postoral arms. F-J) Ciliated band ectoderm of the anterolateral arm; cross section along the anal/abanal axis. K-O) Aboral ectoderm surface. A, F, K) Brightfield images. B, G, L) FM1-43 punctate labelling (green). C, H, M) Anti-α-tubulin staining of cilia (red). D, I, N) Hoechst 33258 staining of nuclei (blue). E) Merge of panels B, C and D. J) Merge of panels G, H and I. O) Merge of panels L, M and N. Abbreviations: BF, Brightfield.

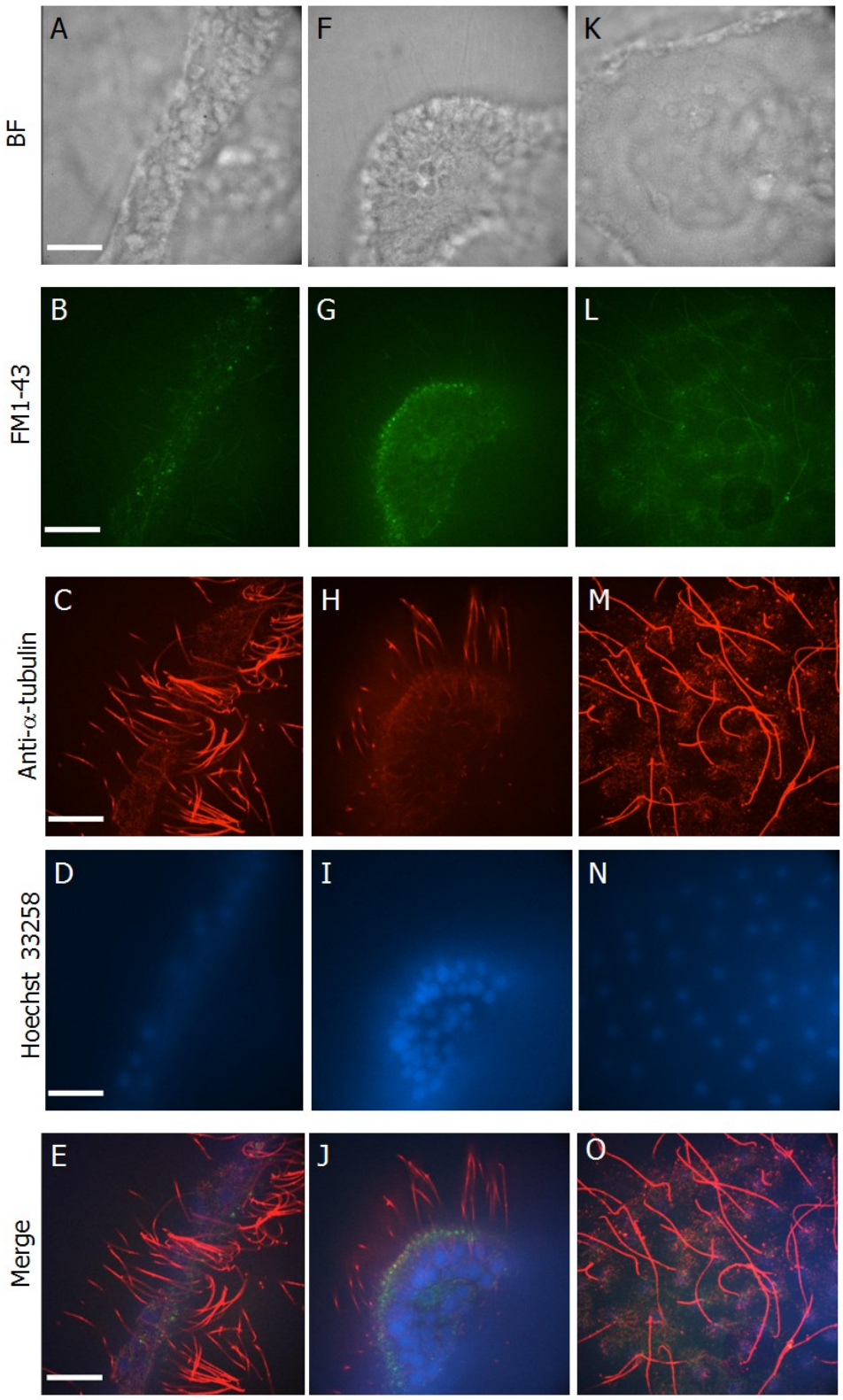
BF
FM1-43
Anti-α-tubulin
Hoechst 33258
Merge
A
F
K
B
G
L
C
H
M
D
I
N
E
J
O

Figure 3.9 FM1-43 labelling of rings of lobules at the bases of cilia

Confocal images of FM1-43 punctate labelling of ectodermal cells in a fixed pluteus. A-D) Oral ectoderm of the pluteus. A) Brightfield image corresponding to panels B, C and D (Scale bar 12µm). B) FM1-43 punctate labelling (green) (Scale bar 12µm). C) Hoechst 33258 staining of nuclei (blue) (Scale bar 12µm). D) Merge of panels B and C (Scale bar 12µm). D') Inset form panel D showing the ring of lobules labelled by FM1-43 (Scale bar 2µm).

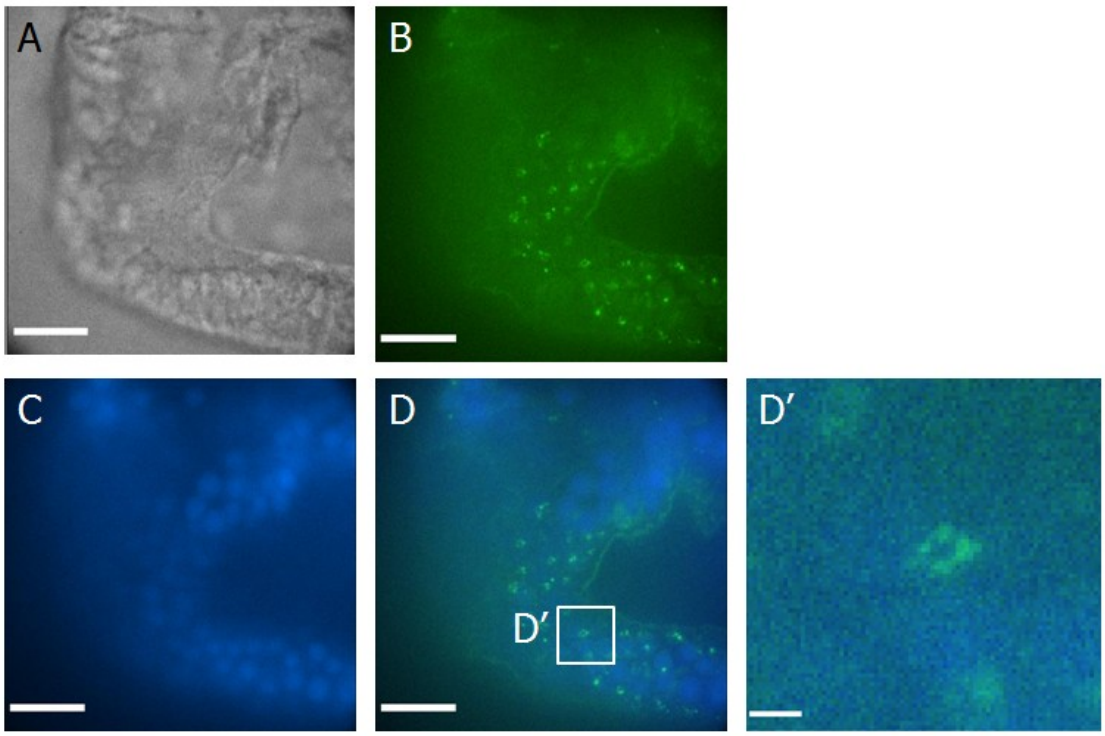
A
B
C
D
D′
D′

3.3.6.4 Live FM1-43 labelling assay

The 30 second treatment with FM1-43 resulted in labelling of several groups of cells identifying potential mechanosensory cells, but the plutei were viewed 5-10 minutes after labelling due to experimental design constraints. Thus, there was a possibility that the dye could have distributed from the cells that had internalized it initially, into other parts of the pluteus body, in that period. In addition, the dye uptake might have occurred through endocytosis; therefore, these observations did not identify with certainty the population of cells that internalizes the dye via cationic channels within the first 30 seconds.

To establish which cells internalized FM1-43 initially, dye labelling was recorded in real time using the spinning disc confocal microscope. Live plutei were mounted in seawater on a glass slide and covered with a coverslip, coated with poly-L-lysine, to inhibit their movement. An equal volume of seawater, containing double the regular FM1-43 concentration (6μM), was added to the slide. Plutei were monitored for appearance of internalized fluorescence. Most of the observations were performed in the aboral region at the pluteus posterior tip. This part of the pluteus was chosen for observation because it was technically easier to observe. The choice was made also because the literature had indicated that the SRN had long processes inserting into the ectoderm in that region (Katow et al., 2007) which could be the possible point of entry of FM1-43 into the blastocoelar cell network.

Within 1 minute of dye application to the slide, the exterior surface of the aboral ectoderm became rapidly labelled and immediately rapidly de-stained. Following the

destaining of the ectoderm surface, fluorescence started to appear within blastocoelar cells positioned in direct contact with the basal side of the aboral ectoderm. Fluorescence intensity was observed to increase on the side of the blastocoelar cells closest to the ectoderm and then quickly spread across the cells (Fig. 3.10A, Supplemental video 7). Imaging of multiple plutei showed that fluorescence increased in these blastocoelar cells for 2-3 minutes and then abruptly decreased within approximately 1 second. This rapid decrease in cellular labelling was accompanied by a wave of fluorescence spreading into the blastocoel. The fluorescence accumulation and release were accompanied by rapid increase and decrease in cell volumes respectively (Fig. 3.10, Supplemental videos 7 and 8). A fluorescence void, corresponding to the nucleus, was seen during accumulation of fluorescence and after its release (Fig. 3.11, Supplemental video 9). These rapidly labelled cells were observed exclusively within the aboral ectoderm, though it is not certain that they were absent in the oral ectoderm. In addition, none of these cells was observed to repeat the fluorescence uptake and release over the next 10 minutes. These cells had multiple interconnected spherically shaped cytoplasmic compartments that could lose fluorescence separately from each other, with or without changes in cell volume (Fig. 3.11; Supplemental Fig. 12 and 13; Supplemental videos 9, 10 and 11). The fluorescent staining of these cells spatially colocalized with pigment cells (Fig. 3.12), and resembled the pigment cell labelling seen previously in culture labelled plutei (Fig. 3.5J).

Figure 3.10 Live labelling with FM1-43

Snapshots from videos showing rapid FM1-43 labelling and release in blastocoelar cells at the basal side of the aboral ectoderm of plutei. A) Snapshots from Supplemental video 7, FM1-43 labelling (blue), and a brightfield image (grey scale) corresponding to preceding FM1-43 panels. A scale bar of 20µm applies to all panels. B) Snapshots from Supplemental video 8, FM1-43 labelling (blue) and a brightfield image (grey scale) corresponding to preceding FM1-43 panels. A scale bar of 20µm applies to all panels. A, B) Blastocoelar cells rapidly labelled with FM1-43 (arrowheads). B) Cell compartments of neighbouring cells acquiring fluorescence (arrows). Time is shown at the bottom of every panel (minutes: seconds. milliseconds).

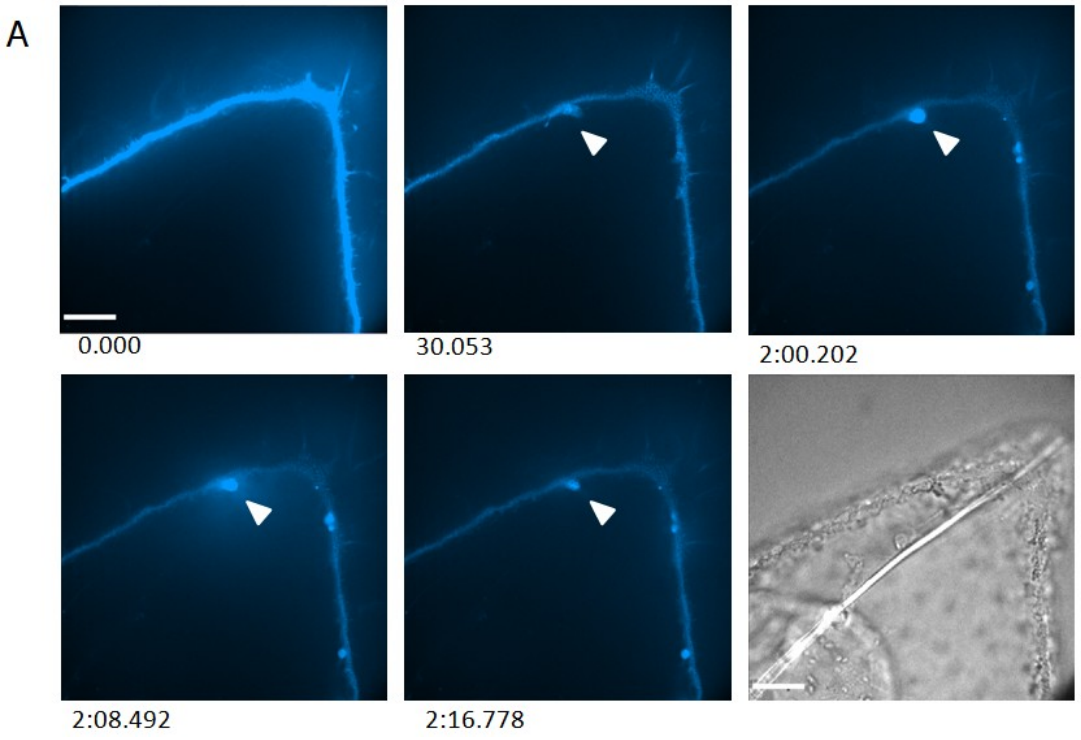
A
0.000
30.053
2:00.202
2:08.492
2:16.778
B
32.905
1:47.623
3:17.511
3:32.328
3:59.080
4:02.908

Figure 3.11 FM1-43 labelling of cell cytoplasm

Snapshots from Supplemental video 9 showing rapid FM1-43 labelling and release in blastocoelar cells of the aboral ectoderm at the abanal side of the pluteus, near the right oral arm. FM1-43 labelling (blue) and brightfield image (grey scale) corresponding to preceding FM1-43 panels. A scale bar of 20µm applies to all panels. A nuclear void of fluorescence is maintained during and after FM1-43 labelling (arrow). Spherical cell compartments destain separately from the main cell body (arrowheads). Time is shown at the bottom of every panel (minutes: seconds. milliseconds).

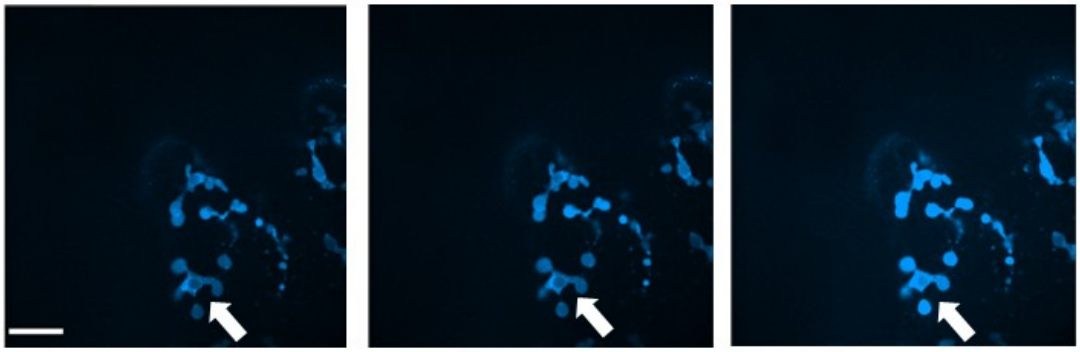

3.43.177 3.57.372 4.06.598

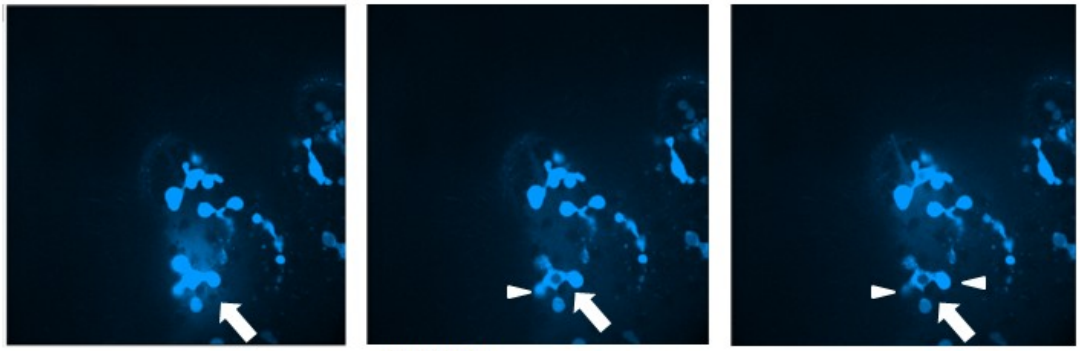

4.21.081 4.22.805 4.26.239

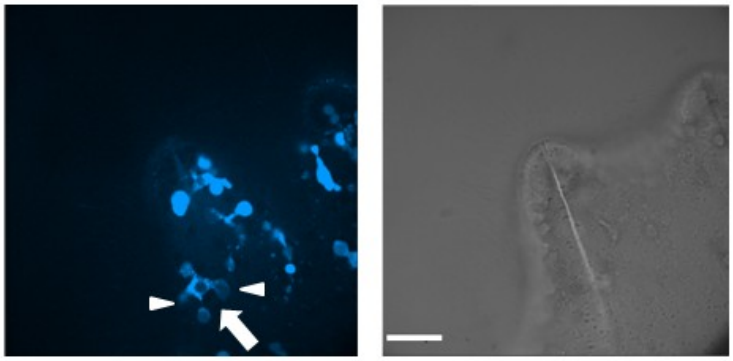

4.37.808

Figure 3.12 FM1-43 labelling colocalization with pigment cells

Confocal images of pluteus aboral ectoderm showing colocalization of rapidly labelled blastocoelar cells with pigment cells. A scale bar of 20µm applies to all panels. A) FM1-43 labelling (blue) of a pigment cell like shape (arrowhead). B) Brightfield image showing the pigment cell (arrowhead). C) Merge of panels A and B showing the colocalization of FM1-43 labelling and the pigment cell (arrowhead).

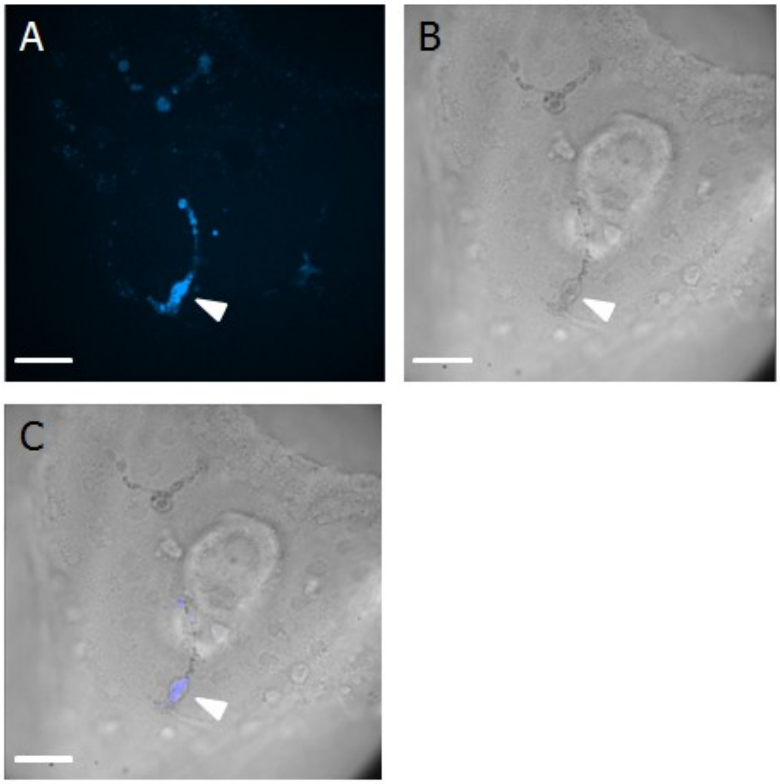
A
B
C

3.3.6.5 Differences in FM1-43 labelling on a slide vs. labelling in culture

The pattern of labelling with FM1-43 of live plutei on a slide (refer to section 3.3.6.4) was different from the labelling of live plutei in culture (refer to section 3.3.6.1). To compare the FM1-43 labelling pattern acquired in live FM1-43 labelling assay with the 30 second labelling in culture with washout, equal laser sensitivity and exposure were used to acquire images of plutei treated by two different methods.

Plutei labelled in culture with washout were labelled with significantly greater fluorescence intensity and their ectoderm and blastocoelar network were brightly labelled. However, in plutei treated on a slide, FM1-43 did not label the blastocoelar network, but instead labelled a limited number of pigment cells and possibly some blastocoelar cells in close contact with the aboral ectoderm. The ectodermal surface labelling was much fainter on a slide as well (Fig. 3.13).

The nominal dye concentration during labelling on a slide and in culture was the same. One of the main differences between slide labelled plutei and culture labelled plutei was the absence of a washout step. To determine if the lack of washout on slides resulted in labelling differences in Figure 3.13, plutei were incubated with FM1-43 for 30 seconds in culture and visualized without washout. Their labelling pattern was compared to the plutei, from the same batch of embryos, treated for 30 seconds in culture with washout. The plutei without washout showed the same labelling pattern as the plutei with washout. The intensity of fluorescence was very similar in the blastocoelar cell network and the ectoderm (Fig. 3.14).

Slow dye diffusion on slides may account for the relatively faint labelling of the ectoderm and lack of labelling of the blastocoelar network in the live FM1-43 labelling assay. Overall, the differences resulting from assay design suggest that the live FM1-43 labelling assay cannot be used with confidence to identify the cells that initially internalize the FM1-43.

3.3.7 TO-PRO-3 labelling in live early 4-arm plutei

The DNA binding dye TO-PRO-3 has been used as an alternative sensory cell marker to FM1-43 (Santos et al., 2006). To determine if sensory cell candidates, identified by uptake of FM1-43, can also be labelled by TO-PRO-3, plutei were treated with the 2μM TO-PRO-3 for 40min, washed out and immediately visualized live. The long incubation times were suggested by literature (Santos et al., 2006) and exposure of embryos to TO-PRO-3 for shorter periods of time resulted in rapid photo bleaching of the dye when plutei were visualized. After a 40-minute incubation, labelled nuclei were detected in a subpopulation of FM1-43 labelled blastocoelar cells around the mouth, the oesophagus, the stomach, and at the posterior tip. The nuclei were also detected within the ectoderm of the ciliated band, at the tips of the anterolateral and postoral arms (Fig. 3.15 and 3.16, Supplemental Fig. 14). TO-PRO-3 labelling was inconsistent between different cultures and was rarely symmetrical or consistent in separate plutei within the same cultures.

TO-PRO-3 has identified two groups of candidate mechanosensory cells, a specific subpopulation of blastocoelar cells and a specific population of ciliated band cells, both of which internalize FM1-43 in their cytoplasms. Although because of long incubation time with TO-PRO-3, the possibility of endocytosis into those cells cannot be excluded.

Figure 3.13 FM1-43 labelling differences: slide vs. culture labelling

Confocal images of FM1-43 labelling in live plutei showing differences in labelling methods. Images were acquired using the same laser sensitivity and exposure to compare FM1-43 fluorescence intensity across samples. A scale bar of 20µm applies to all panels. A-D) Anterolateral arm and part of the pluteus posterior. A) FM1-43 labelling (blue) performed on a slide without washout. FM1-43 exclusively labels pigment cells or blastocoelar cells at the base of the aboral ectoderm (arrowhead). B) Brightfield image corresponding to panel A. C) FM1-43 labelling (blue) performed in culture with washout. The blastocoelar cell network is labelled (arrowhead). D) Brightfield image corresponding to panel C.

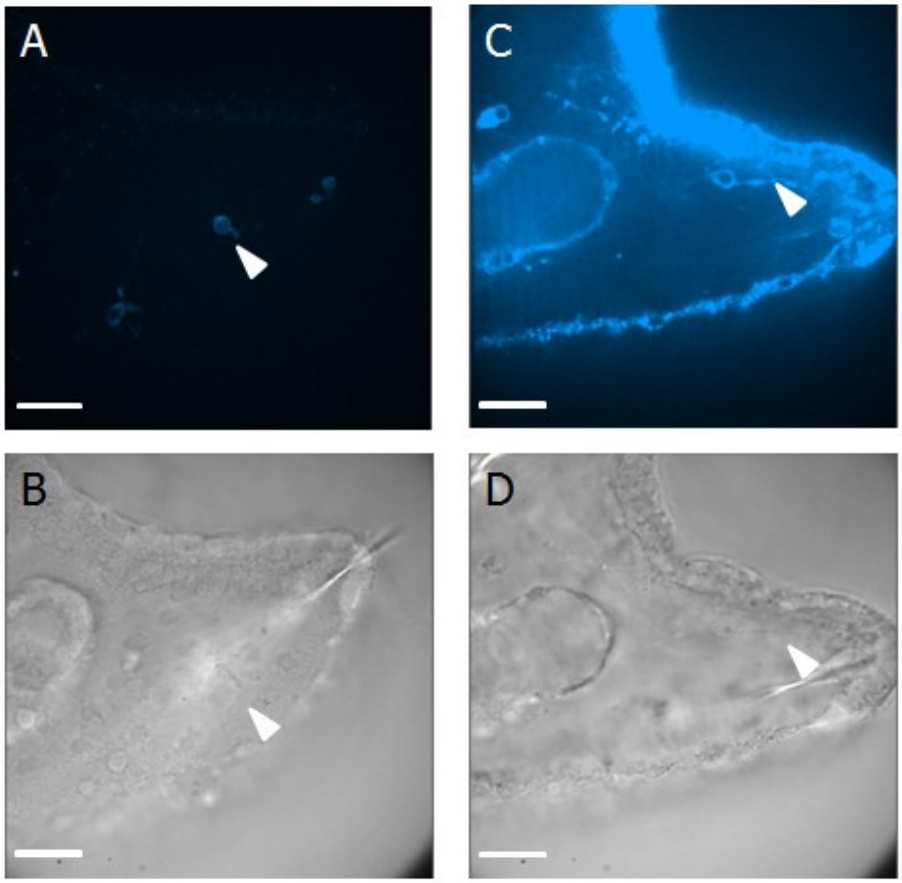
A
C
B
D

Figure 3.14 FM1-43 labelling differences: washout vs. no washout

Confocal images of live plutei showing similarity in labelling pattern and fluorescence intensity between plutei labelled in culture, with washout, and the same plutei labelled in culture, without washout. Images were acquired using the same laser sensitivity and exposure to compare FM1-43 fluorescence intensity across samples. A scale bar of 20μM applies to all panels. A, C) Left postoral arm. B, D) Posterior tip. A, B) Plutei washed out immediately after FM1-43 treatment. The blastocoelar network is labelled (arrowhead). C, D) Plutei without washout after FM1-43 treatment. The blastocoelar network is labelled (arrowhead).

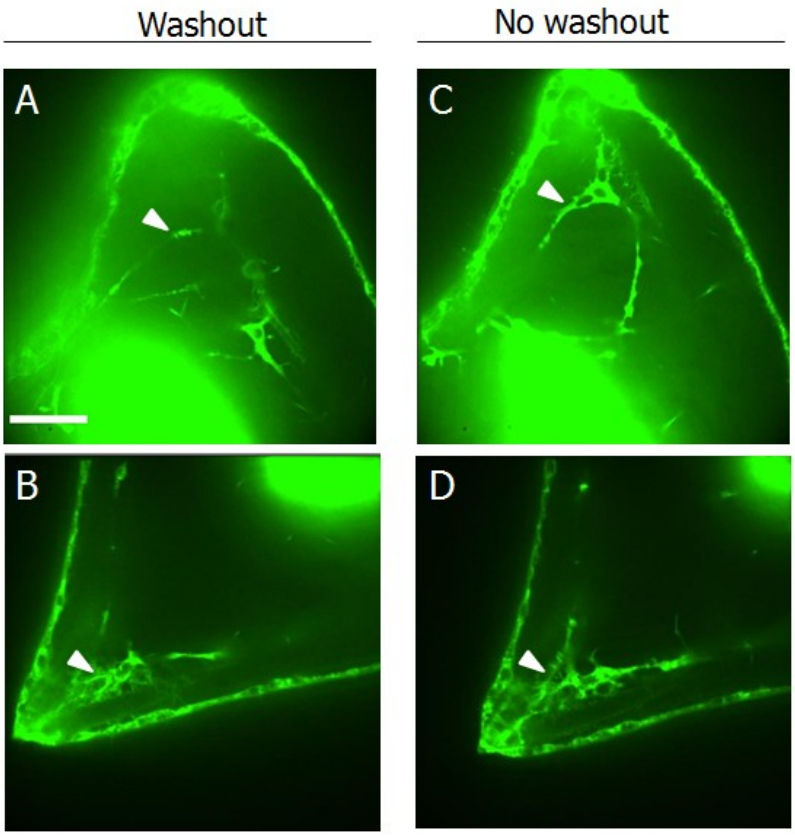
Washout
No washout
A
C
B
D

Figure 3.15 TO-PRO-3 nuclear labelling in live plutei

Confocal images showing colocalization of TO-PRO3 labelling and FM1-43 labelling in blastocoelar cells, and ciliated band cells. A scale bar of 20µm applies to all panels. A-E) Pluteus anterior. Blastocoelar cells co-label with TO-PRO-3 and FM1-43 (arrowheads). F-J) Left postoral arm. A single cell within the ciliated band co-labels with TO-PRO-3 and FM1-43 (arrowhead). K-O) Posterior tip. A single cell within a cluster of blastocoelar cells co-labels with TO-PRO-3 and FM1-43 (arrowhead). A, F, K) TO-PRO-3 (red). B, G, L) FM1-43 (green). C) Merge of panels A and B. H) Merge of panels F and G. M) Merge of the panels K and L. D) Brightfield image corresponding to panels A, B and C. I) Brightfield image corresponding to panels F,G and H. N) Brightfield image corresponding to panels K,L and M. E) Merge of panels C and D. J) Merge of panels H and I. O) Merge of panels M and N. Abbreviations: BF, Brightfield.

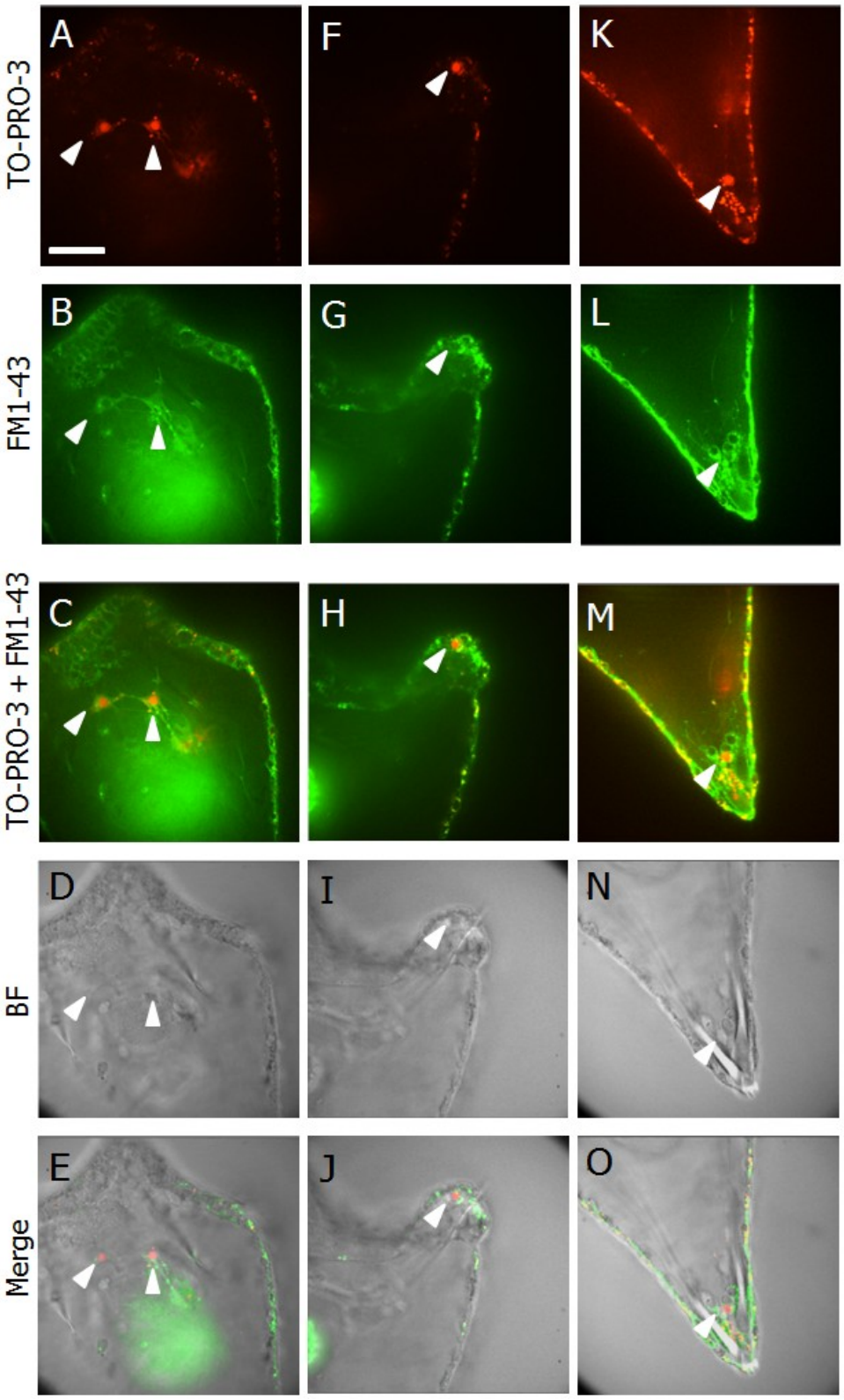
TO-PRO-3
FM1-43
TO-PRO-3 + FM1-43
BF
Merge
A
F
K
B
G
L
C
H
M
D
I
N
E
J
O

Figure 3.16 Locations of TO-PRO-3 labelled nuclei within the pluteus body

Summary of all detected TO-PRO-3 labelled nuclei and their positions within the body of an early 4-arm pluteus. Red circles represent separate nuclei, and grey circles represent the nuclei which were never detected yet were expected to be present because of bilateral symmetry of the pluteus. Confocal images of all nuclei including images showing nuclear TO-PRO-3 labelling, colocalized with FM1-43 labelling ,are found in Supplemental figure 14. Nuclei A-J and M-W are found within blastocoelar cells. Nuclei K, L and Q, P are found within the ciliated band ectoderm at the anterolateral and postoral arm tips respectively. Refer to Figure 3.1 for abbreviations and structural details.

Anal side

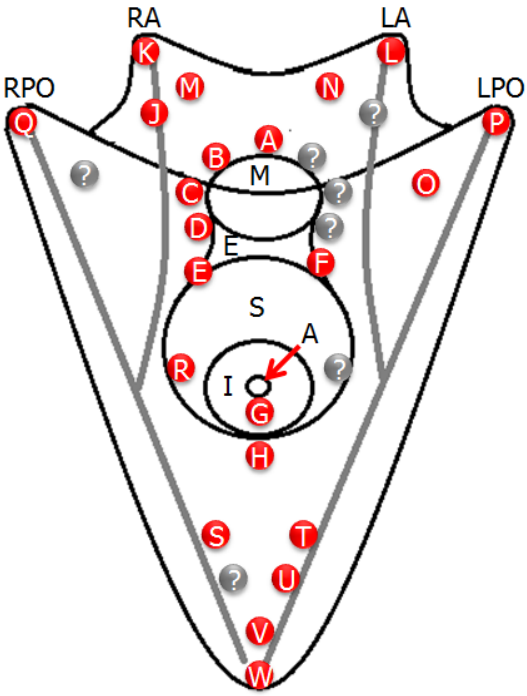

Left side

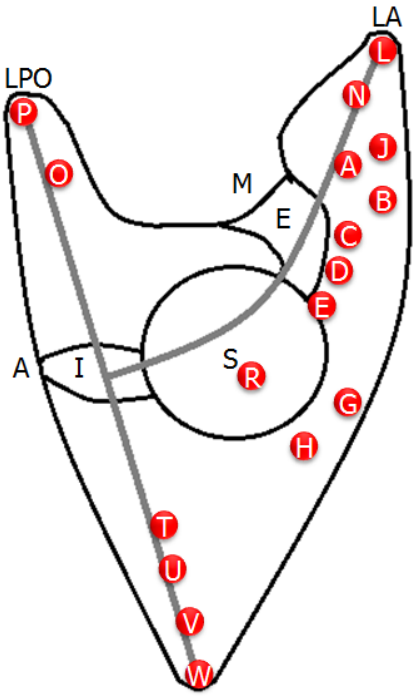

An artifactual TO-PRO-3 labelling was discovered in fixed embryos. If the plutei were treated with TO-PRO-3, washed, and fixed in paraformaldehyde, TO-PRO-3 labelled the nuclei of all cells in the pluteus body (Supplemental Fig. 15).

The result suggests that either residual TO-PRO-3, retained by plutei during the washing step, or TO-PRO-3 from labelled nuclei is able to diffuse after plutei are fixed, which results in artifactual nuclear labelling of all cells.

3.3.8 Colocalization of FM1-43 and TO-PRO-3 labelling during development

During development, FM1-43 and TO-PRO-3 started labelling blastocoelar cells at gastrula stage. Multiple TO-PRO-3 labelled vesicles were observed within the FM1-43 labelled blastocoelar cells at gastrula, prism and early 4-arm pluteus stages. TO-PRO-3 also labelled the ectoderm at blastula, gastrula, prism and pluteus stages, with a punctate pattern similar to FM1-43. TO-PRO-3 labelled vesicles were seen within the ciliated band of the plutei and in pigment cells. FM1-43 and TO-PRO-3 punctate ectodermal labelling patterns and vesicle labelling patterns did not colocalize completely. Interestingly, TO-PRO-3 nuclear labelling was never observed at gastrula or prism stages (Fig. 3.17, Supplemental Fig. 16).

The results suggest that both FM1-43 and TO-PRO-3 are internalized into the blastocoelar cell network starting from its appearance at gastrula stage. Also, TO-PRO-3 dye may be internalized into the ectoderm cells by endocytosis, like FM1-43. TO-PRO-3 nuclear labelling appears to be a specific property of blastocoelar cells and ciliated band cells at pluteus stage.

Figure 3.17 Co-labelling by FM1-43 and TO-PRO-3 of cellular components in live plutei

Confocal images showing colocalization of TO-PRO-3 and FM1-43 labelling in live plutei. FM1-43 (green), TO-PRO-3 (red), FM1-43 and TO-PRO-3 colocalization (yellow), Brightfield (grey scale). A scale bar of 20µm applies to all panels. A) Anterior blastocoelar space of the pluteus. B) Blastocoelar space around the ciliated band and the gut. C) Left postoral arm. D) Posterior tip. E) Ciliated band of the right postoral arm. F) Aboral ectoderm. G) Pigment cells. A, B, C, D) TO-PRO-3 vesicles in FM1-43 labelled blastocoelar cell tracts (arrows); some TO-PRO-3 labelled vesicles colocalize with FM1-43 labelled vesicles. E) TO-PRO-3 and FM1-43 labelled vesicles in the cells of the ciliated band ectoderm. F) TO-PRO-3 and FM1-43 punctate labelling in aboral ectoderm. G) TO-PRO-3 labelled vesicles colocalize with FM1-43 labelling in pigment cells (arrow). Abbreviations: BF, Brightfield.

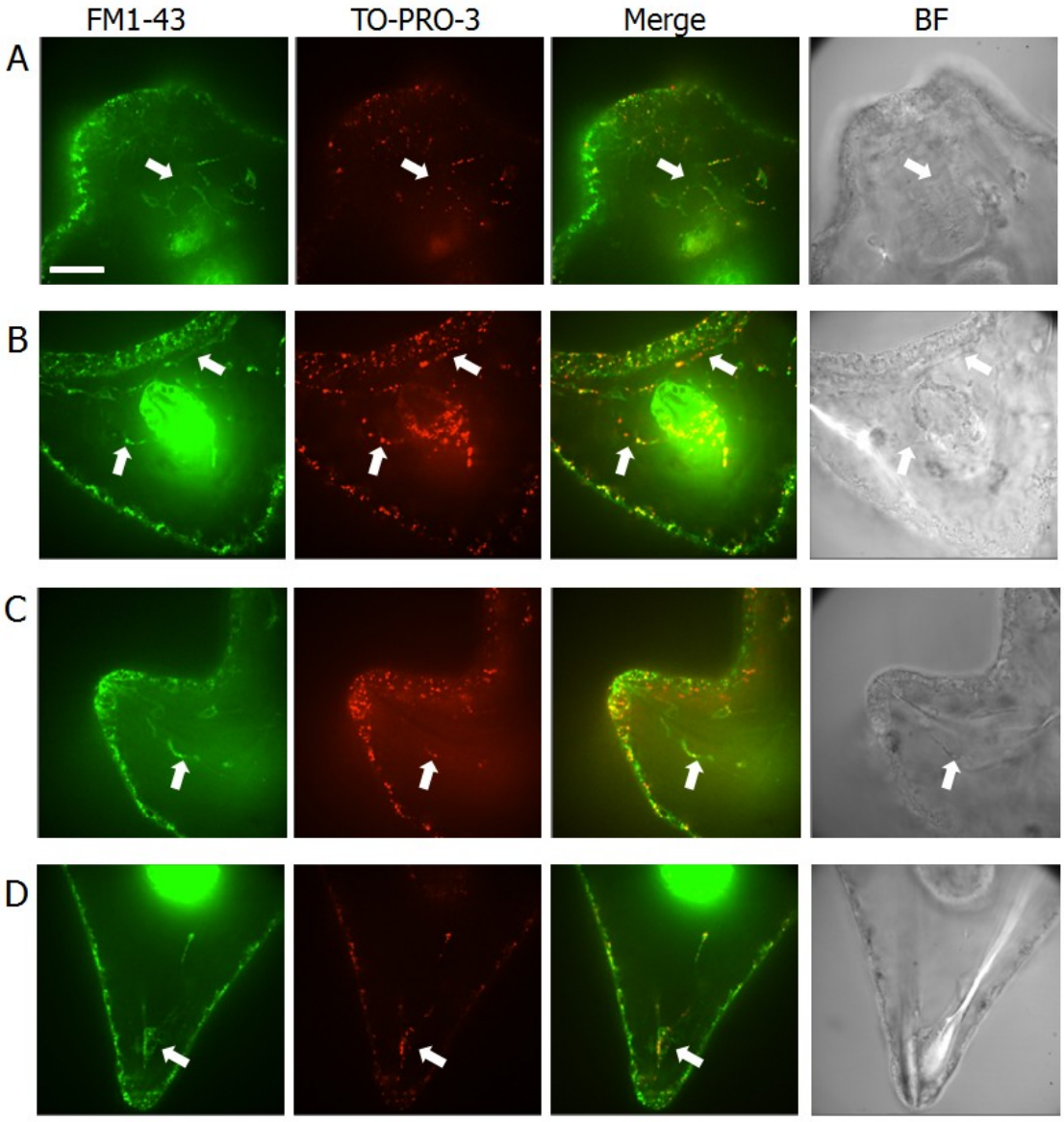
FM1-43
TO-PRO-3
Merge
BF
A
B
C
D

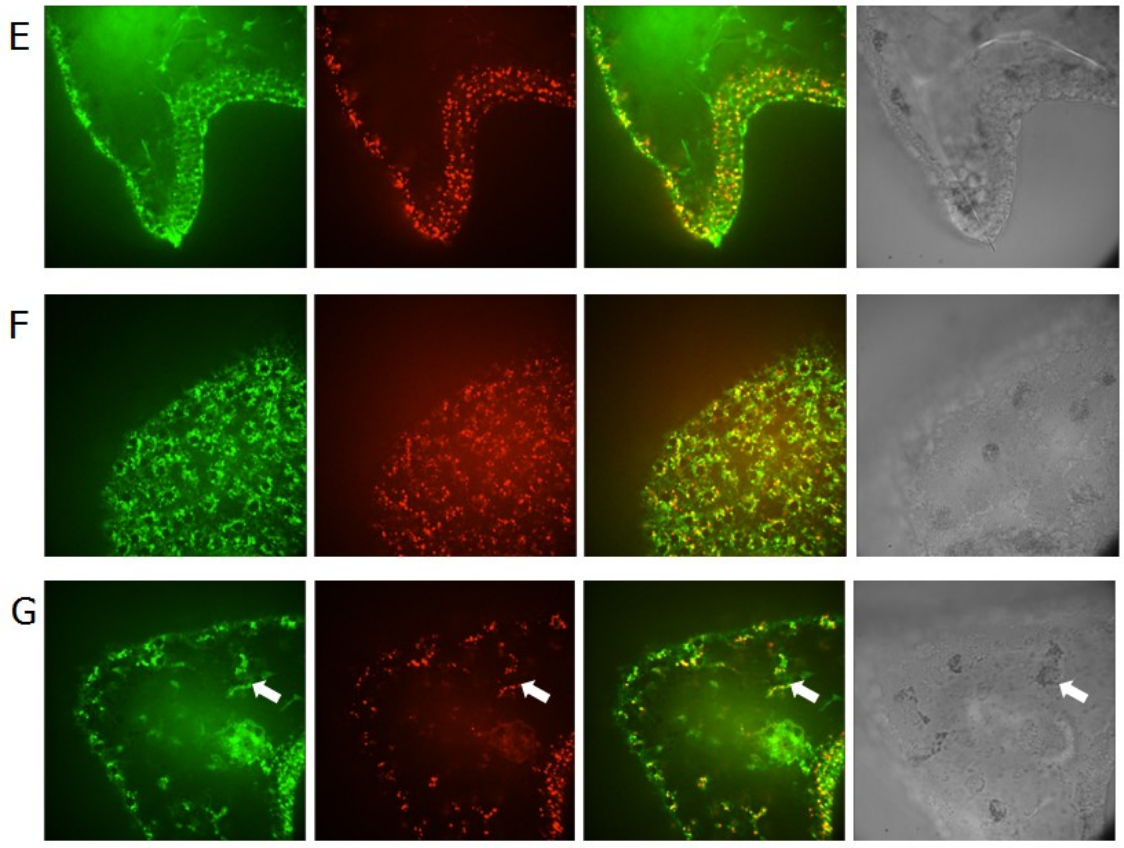
E
F
G

3.3.9 Dye exclusion assay

The incubation with TO-PRO-3 continued for 40 minutes. Therefore, it was possible that TO-PRO-3 internalization into the blastocoelar cells could occur by endocytosis. To address this issue the fluorescent cationic nuclear dye, propidium iodide (PI), was used in a dye exclusion assay. This dye has been estimated to be close to 1nm in diameter (Prevette et al., 2010) and is slightly wider than FM1-43 , which has an end-on diameter of 0.8nm (van Netten and Kros, 2007). TO-PRO-3 is very similar in structure to FM1-43 and is narrower than PI in its end-on diameter. Molecules which are wider than FM1-43, like its analog FM3-25, neither block nor permeate through a mechanotrasduction channels(Gale et al., 2001; Meyers et al., 2003). If TO-PRO-3 is indeed internalized into cells by endocytosis then PI should be internalized into cells with the same efficiency and speed as TO-PRO-3.

Live plutei were treated for 30 minutes with PI, fixed in paraformaldehyde and visualized. These plutei were then compared to fixed plutei from the same batch of embryos that were either untreated or treated with PI after paraformaldehyde fixation. Treatment of live plutei with PI for 30 minutes before fixation did not label any nuclei, or vesicles in the ectoderm. However, treatment of fixed plutei with PI, at the same concentration and for the same amount of time, resulted in bright nuclear staining of all cells in the plutei (Supplemental Fig.17).

The long 30-minute exposure of live plutei to PI was comparable to the 40-minute exposure of live plutei to TO-PRO-3. These results show that PI did not label live plutei, and this supports speculations that internalization of TO-PRO-3 in blastocoelar

cells and ciliated band cells in live plutei occurs through cation channels and not endocytosis. Also, lack of PI labelling suggests that TO-PRO-3 is not labelling dying or dead blastocoelar cells that should also be labelled by PI.

3.4 Discussion

The aim of this set of experiments was to use analysis of TRPA1 expression and fluorescent dye labelling to identify potential mechanosensory cell candidates in *S. purpuratus* embryos and plutei.

The temporal expression profile for Sp-TRPA1 (SPU 010335) corresponds to the results within both embryonic mRNA expression databases, while Sp-TRP channel (SPU 021148) expression profile does not, showing that some temporal expression patterns from the microarray database are not accurate. The transcript size of Sp-TRPA1 is approximately 5kb, close to the size to the protein-coding human TRPA1 transcript, reported to be 5190 bp in the NCBI (http://www.ncbi.nlm.nih.gov) and Ensembl (http://uswest.ensembl.org/index.html) databases. Other bands on the Northern indicate the presence of Sp-TRPA1 mRNAs of greater and smaller size than 5kb. These bands appeared inconsistently among different cultures and were always less intense than the 5kb band. The transcript sizes of for the Sp-TRP-channel gene were approximately 7.7 and 8kb. Human TRPV6 mRNA is 2918bp (NM_018646.2) according to NCBI database. The Ensembl database reports another human TRPV6 transcript of 10425bp (ENST00000485138), which has a retained intron and is not protein coding. This suggests that both Sp-TRP-channel transcripts observed on the Northern blots may have been produced by intron retention. The larger Sp-TRPA1 transcripts may also not be fully processed. Therefore, Sp-TRPA1 protein is most likely translated from the 5kb transcript expressed during embryonic stages, while the Sp-TRP-channel protein may

not be expressed. Intron retention is rare and is responsible for only 5% of alternative splicing in vertebrates and invertebrates, but is the primary form of alternative splicing in lower eukaryotes like plants, fungi and protozoa (Keren et al., 2010). Intron retention is more common in invertebrates (Sammeth et al., 2008). It is an important post-transcriptional regulatory mechanism of the biological protein activity and has been reported to be induced by temperature changes (Mastrangelo et al., 2005). Multiple bands of different sizes for both TRP genes may be a result of intron retention, and may be produced in response to environmental factors, which may explain the inconsistency of their appearance among different cultures.

Transcripts for both TRP channels were not detected in eggs but were upregulated at later embryonic stages. The lack of transcripts at the egg stage and upregulation at later stages of embryonic development is interesting, because this is nearly always associated with cell-type specificity of gene expression during cellular specification and/or differentiation. A dramatic upregulation of transcripts occurred at 36hpf, for both channel genes. Around 36hpf, at mesenchyme blastula stage, the apical ciliary tuft appears and the capacity for directional swimming develops in embryos. Later stage sea urchin embryos swim with their animal pole forward (Maruyama, 1981). It is possible that the mechanical displacement of the apical tuft cilia by water flow allows the embryo to sense the environment and swim directionally. Since the accumulation of transcripts for Sp-TRPA1 channel protein coincides with the appearance of the apical tuft cilia and development of directional swimming it was plausible to propose that Sp-TRPA1 protein may be expressed in the cells of the animal plate and/or localized to the cilia of the ciliated tuft. The TRPA1 channel protein might be present in motile cilia as well, where it may have a role detection of environmental stimuli and possibly regulation of

directional swimming. Evidence in other systems shows that TRP channels are important for sensing mechanical displacement of cilia. TRPN1 has been suggested to be required for sensing fluid flow by beating cilia of the *Xenopus* larval epidermis (Shin et al., 2005), as for TRPP2 in primary cilia of kidney cells (Pazour et al., 2002;Rosenbaum and Witman, 2002;Yoder et al., 2002).

Deciliation removes all the cilia within the embryo including the motile cilia of the ectoderm and the non-motile cilia of the apical tuft. Expression of some genes is known to be upregulated in response to one round of deciliation, including tubulin. Deciliation did not visibly upregulate the transcript levels of either channel. The results did not provide any evidence for TRP proteins being localized to the apical tuft cilia and any motile cilia of the ectoderm at prism stage, but did not eliminate the possibility that their proteins may be localized to cilia. Repeated rounds of deciliation may be required to deplete some ciliary proteins and to upregulate the transcription of some ciliary genes in sea urchin embryos (Merlino et al., 1978). Therefore, repeated deciliation may have been required to stimulate TRP channel transcription.

WMISH with TRP channel probes was performed to identify the mechanosensory candidate cells. No spatial-specificity of expression was detected. Northern Blotting data indicates medium transcript abundance for TRP channel transcripts; therefore, lack of localized expression implies the ubiquitous expression of these genes in embryos and early 4-arm plutei. Lack of localized expression could be a consequence of the WMISH protocol. Long hybridization times of the WMISH procedure which might have not been suitable for detection of these transcripts, although the procedure has been used successfully to detect many transcripts of various abundances in all cell types of the embryos (Arenas-Mena et al., 2000; Hinman et al., 2003; Minokawa et al., 2004).

WMISH was not attempted for later larval stages, where TRP channel expression could potentially be localized. Interestingly, although temporal expression of opsin mRNA has been detected at embryonic stages and in one week old 4-arm plutei, spatial mRNA expression data is only available for only one of the opsins (Ooka et al., 2010; Raible et al., 2006). This suggests that spatial mRNA expression of genes encoding sensory proteins may be in general difficult to detect in sea urchin embryos and early larvae. Protein expression of TRP channels was not investigated here.

Screening for mechanosensory cells with FM1-43 has identified several groups of cells with potential mechanosensory functions: the blastocoelar cells, the pigment cells, the ectodermal cells and the ciliated band cells. The short FM1-43 labelling time of 30 seconds excluded the possibility of endocytosis into these cells. The structure of the FM1-43 labelled blastocoelar network closely resembles the serotonin receptor cell network (SRN) described previously (Katow et al., 2007). The motile vesicles within blastocoelar cells were not an unexpected observation. The cytoplasm of blastocoelar cells is known to contain vesicles and ER (Ryberg, 1977).

The reduction in ectodermal labelling intensity after 24hr incubation, suggested that most of the FM1-43 dye was bound to the outer membranes of plutei and partitioned out of the membranes, as expected. The persistence of blastocoelar cell labelling and retention of their fluorescence intensity suggested that FM1-43 was internalized into the cytoplasm of these cells, and that the observed labelling did not occur due to FM1-43 binding to their outer membranes. The appearance of specific ciliated band cells labelled with FM1-43 at the tips of the postoral arms, after 24 hour incubation, suggested that they were either not visible at 0hrs because of background ectodermal fluorescence, or that FM1-43 had accumulated in the cytoplasm of those

cells over night. Overall, FM1-43 labelling has identified at least two types of potential mechanosensory cells in plutei: the blastocoelar cells and specific cells in the ciliated band. The short incubation time with FM1-43 suggests that dye internalization in these cells occurred via cation channels. If this is true, then the pore properties of these channels, such as their pore diameter, are similar to those hair cell METs and TRP channels (Farris et al., 2004).

After a 24-hour incubation of live FM1-43 labelled plutei in culture, an increased amount of thin blastocoelar processes became visible. The spread of fluorescence into thin blastocoelar cell processes suggests that the dye is most likely initially concentrated within the cell bodies and then distributed away from the cell bodies into the processes. Distribution to more processes may occur over time either through connections within the blastocoelar network, or by release of dye from cells into the blastocoelar space and internalization by other cells.

Disruption of SRN development resulted in reduction of complexity of FM1-43 labelled network and reduced FM1-43 fluorescence intensity in blastocoelar cells suggesting that FM1-43 is internalized into the SRN. Reduced fluorescence intensity in blastocoelar cells of pCPA treated embryos supports speculations that FM1-43 labelling occurs through internalization into their cytoplasm, and not by simple binding to their external membranes. Disruption of the SRN development results in reduction of the number of inter-blastocoelar cell connections and blastocoelar cell processes (Katow et al., 2007), which indicates that the presence of these structures is important for FM1-43 internalization. The SRN is thought to control spatial swimming (Katow et al., 2007) and/or sense the extra-embryonic environment through its numerous processes inserted into the ectoderm (Katow et al., 2004) (refer to section 1.3.5.5). It is possible that FM1-

43 is internalized into the SRN from the external medium through mechanosensory channels located in its processes inserted into the ectoderm. FM1-43 internalization may be an indication of the physiological function of the SRN in detecting mechanical stimuli from the extra-embryonic environment, which in turn may have a role in regulating spatial swimming. TPRA1 protein is one of the candidate components of such channels.

Analysis of punctate FM1-43 labelling in the ectoderm of plutei demonstrated that FM1-43 labelled rings of lobules at the bases of cilia. The labelled lobules around the bases of cilia resembled the distribution of the components of the Golgi complex in ciliated ectodermal cells (Eldon et al., 1990), or endosomes near basal bodies of cilia. Thus, FM1-43 may be taken up by endocytosis at the bases of cilia, which may explain the labelling of motile vesicles within the pluteus ectoderm. The short incubation time with FM1-43 and an immediate washout step should have prevented the endocytosis in the ectoderm. However, due to experimental constraints the plutei were always visualized at least 5 minutes after the washout step. Since FM1-43 incorporates into membranes, it is not washed out completely. Therefore, FM1-43 may have been internalized by endocytosis into the cytoplasm of ectodermal cells during the interval between the washout step and visualization. Short incubation times of less than one minute with FM1–43 have been reported to result in uptake of FM1-43 at bases of cilia in *Tetrahymena*, accompanied by appearance of mobile vesicles in the cytoplasm of cells. It has been suggested that this FM1-43 internalization occurs via clathrin-coated pits at the bases of cilia (Elde et al., 2005). Ruthenium red, a polycationic dye, has been reported to stain granules in the microvilli of the ciliated band cells of sea urchin plutei *Psummechinus miliuris* (Ryberg and Lundgren, 1977). Therefore, FM1-43 labelling may be also be localized to microvilli within the ectoderm. Microvilli are present in the ciliated

band ectoderm, oral and aboral ectoderm, and they are not all restricted in their location to the collars around the motile cilia. Many are found randomly distributed on the surfaces in the cells in the ectoderm (Nakajima, 1986b). This may explain presence of multiple puncta in the ectoderm which are not organized into rings.

Rapid internalization and release of FM1-43 was observed in a specific group of blastocoelar cells, which were in close contact with the aboral ectoderm, in a live FM1-43 labelling assay. The initial stages of the FM1-43 internalization into the blastocoelar cell network may be mediated by this group of blastocoelar cells. The close contact of these cells with the ectoderm and the observed dynamics of FM1-43 internalization support the speculation that the blastocoelar cell network internalizes FM1-43 through its processes inserted into the ectoderm. The rapidity of dye internalization suggests that it does not occur through endocytosis, but is rather suggestive of functional cationic channels in those cells. Such channels could be mechanosensory. It appears that FM1-43 may be released into the blastocoel from these cells, where it can label the rest of the blastocoelar network. However, the rapid release, which included a rapid contraction of the cell cytoplasm, is most likely indicative of damage to the cells rather than some natural physiological function. The presence of the fluorescence void suggests that FM1-43 labelling of these cells occurs in their cytoplasm, and on their outer surfaces.

A significant difference was observed in FM1-43 labelling of plutei in the live FM1-43 labelling assay compared to plutei labelled in culture with a washout step. Rapid labelling and release of fluorescence was observed in a subpopulation of blastocoelar cells in close contact with the ectoderm, and not within the major blastocoelar cell tracts. To determine why plutei labelled in culture had different labelling patterns than the plutei labelled on a slide, plutei labelled in culture without washout

were compared to slide labelled plutei using the same laser settings. The results suggest that slow diffusion of dye on the slide results in a low dye concentration around the plutei, restricting FM1-43 labelling to cells of the ectoderm or closely associated blastocoelar cells and preventing the labelling of the rest of the blastocoelar network. Alternatively, continuous exposure of the FM1-43 dye or plutei to the laser, during the live FM1-43 labelling assay, may have resulted in labelling differences by damage to the blastocoelar network or through other unknown mechanisms. Finally, a gradual increase in dye concentration over time on a slide surrounding the plutei versus a sudden immersion of plutei in a constant concentration of the dye for 30 seconds may have blocked the dye internalization into most blastocoelar cells by an unknown mechanism.

The shape and colocalization of the rapidly labelled cells with pigment cells suggested that they might be pigment cells rather than part of the blastocoelar cell network. Explosive release of fluorescence by pigment cells in response to laser light exposure has been described previously in sea urchin larvae (Nakamura et al., 2001). A short exposure of 1-2min of sea urchin larvae to blue light (450-490nm) caused a disruption of the red pigment granules in pigment cells that then released a green fluorescent substance, and this substance filled up the cytoplasm of the pigment cells. Prolonged exposure of pigment cells to laser light caused rupture of pigment cells and spread of the green fluorescent substance in the blastocoel and the surrounding medium. The emission spectrum of the observed fluorescence was 540nm. The live FM1-43 labelling assay used similar laser settings: a 440nm laser and a 595/50 filter. The results of the live FM1-43 labelling assay closely resemble the observations in Nakamura et al. (2001). Thus, FM1-43 might not be internalized through cation channels but through the loss of integrity of pigment cell membranes in response to the laser

irradiation. However, there are several discrepancies. In Nakamura et al. (2001), the emitted fluorescence in pigment cells, in response to laser light, occurred in the absence of fluorescent dyes in the surrounding medium. It is conceivable that the presence of FM1-43 in the live FM1-43 labelling assay enhanced the visualization of this process, and this process simply went unnoticed in my untreated embryos because of low sensitivity and exposure settings on the microscope. But exposure to laser light under the conditions I used did not cause the loss of large numbers of pigment cells or their pigment granules, in spite of the apparent rupture of multiple cells that had filled with dye. In addition, the waves of fluorescence spreading away from rapidly labelled cells, observed in the live FM1-43 labelling assay, were never observed to occur outside of the pluteus body as described by Nakamura et al. (2001). Also, live embryos labelled with FM1-43 in culture with washout were visualized repeatedly for long periods of time in multiple experiments, and flashes of fluorescence have never been observed. This makes the fact that the flashes went simply unnoticed in untreated embryos very unlikely, unless FM1-43 treatment in culture prevented the pigment cells form bursting under laser light. In conclusion, the rapid uptake and release of dye may be a reflection of normal physiology of the pluteus or may be secondary consequences of the deleterious effects of laser light on the plutei. The identity of these cells remains uncertain, since no histochemical co-labelling with pigment cell specific antibody has been performed. The rapidly labelled cells resemble the Hp-ECPN positive cells described by Ooka et al. (2009) in their shape and distribution in the pluteus, which suggests an alternative identity for these cells (refer to section 1.3.5.6).

Incubation with TO-PRO-3 was used to screen for mechanosensory cells in embryos. At pluteus stage TO-PRO-3 labelling of nuclei was detected in a specific sub-

population of blastocoelar cells and at the tips of the anterolateral and postoral arms. Cells that internalized TO-PRO-3 also internalized FM1-43. Therefore, TO-PRO-3 internalization is most likely mediated by the same cation channels that mediate FM1-43 internalization, and these channels may have a mechanosensory function. Because TO-PRO-3 does not bind to membranes, unlike FM1-43, this labelling assay is able to identify more precisely the cells which internalize both fluorescent dyes. FM1-43 and TO-PRO-3 did not label other candidate sensory cells predicted by the literature survey in section 1.3.5. Most of these candidate cells were identified in other species of urchin, so they might not be present in *S. purpuratus* embryos and early larvae.

Cells with TO-PRO-3 labelled nuclei always had FM1-43 labelling in their cytoplasm, but, interestingly, not all FM1-43-labelled cells had TO-PRO-3 nuclei. This may be indicative of different channel pore properties within these cells that allow passage of the slightly wider molecule like TO-PRO-3. Alternatively, cation channels in some cells may be in a closed state at the time of labelling. This may explain the inconsistency and the lack of symmetry of labelling of nuclei with TO-PRO-3 among different plutei, although differences in developmental timing between different cultures may be an issue as well.

TO-PRO-3 nuclear labelling was never observed at stages preceding the pluteus stage. This result suggests that, at pluteus stage, a subpopulation of blastocoelar cells develops that has properties different from the blastocoelar cells at earlier stages. Similarly, a subpopulation of ciliated band cells develops that acquires properties different from the rest of the ciliated band. TO-PRO-3 labelling of nuclei at pluteus stage coincides with the beginning of active feeding where plutei react to external physical stimuli and use their cilia to direct food particles to their mouths (Nakajima,

1986b; Strathmann, 1975; Strathmann, 2007). The placement of TO-PRO-3-labelled nuclei in the tips of the larval arms, around the ciliated band and the mouth may be physiologically relevant. These cells could employ mechanosensory channels to detect external stimuli in these areas of the pluteus. TRPA1 protein could be a part of these channels since the TRPA1 pore is large enough to allow permeation of dyes like FM1-43 and TO-PRO-3 (Karashima et al., 2010; Santos et al., 2006). The ciliated band has been proposed to be a sensory organ that communicates signals to the effector organs like the ciliated aboral ectoderm and the gut (Nakajima et al., 2004). The localization of TO-PRO-3 nuclear labelling lends further support to this hypothesis.

Cells within the ciliated band make contact with the underlying axonal tracts (Nakajima, 1986b), and multiple cells within the ciliated band express synaptotagmin and project axons into the basal axonal tracts (Nakajima et al., 2004). The cells of the tips of the pluteus arms may detect signals from the external environment, like water displacement or touch, and integrate them by direct communication with the underlying axonal tract. In this way, the pluteus may change the ciliary beating pattern of the ciliated band and change swimming direction in response to external stimuli. It has been suggested that the pigment cells and the Hp-ECPN positive cells at arm tips are required for controlling the direction of swimming in response to light (Ooka et al., 2010). This suggests that the tips of larval arm may be sensory organs that mediate responses to the external environment. Plutei swim with their arm tips facing forward according to my observations and observations described in the literature (Ooka et al., 2010; Strathmann, 2007). The presence of mechanosensory cells at arm tips may allow the plutei to modulate their spatial swimming by integrating signals from four different points of reference.

FM1-43 and TO-PRO-3 labelling was assessed at earlier developmental stages. Both dyes labelled vesicles in blastocoelar cells, starting from their appearance at gastrula stage, puncta in the ectoderm at all stages, and vesicles in the ciliated band and the pigment cells at prism and pluteus stages. Lack of complete colocalization in dye labelling of the ectodermal puncta and vesicles in other cells was expected, since FM1-43 binds to membranes, while TO-PRO-3 binds to nucleic acids. The route of entry of either dye into cells described here remains unknown. The SRN is not fully developed at gastrula or prism stages. Therefore, FM1-43 and TO-PRO-3 labelling of blastocoelar cells at these stages contradicts speculations that these dyes get internalized through mechanosensory channels of blastocoelar cell processes that are inserted into the ectoderm. Conceivably, blastocoelar cell labelling could occur by permeation of fluorescent dyes from surrounding seawater into the blastocoel through "leaky" septate junctions of the ectodermal epithelium (Dan-Sohkawa et al., 1995), and not necessarily though the processes of the blastocoelar cell network that extend into the ectoderm. In this case, their internalization into blastocoelar cells at earlier stages may be mediated by mechanosensory channels that are expressed in these cells before they are used for external mechanosensation. The punctate labelling of the ectoderm and ciliated band vesicles by TO-PRO-3 may be a result of endocytosis. However, TO-PRO-3 does not bind to membranes like FM1-43, and should not be endocytosed if washed out. A possible explanation is that some excess of TO-PRO-3 dye is retained on the ectodermal cell surface after washout and is then endocytosed. Nevertheless, the possibility of internalization of both dyes via some type of cation channels, into all cell types described here, cannot be excluded.

A dye exclusion assay was performed to determine whether TO-PRO-3 dye can be internalized into cells by endocytosis. Incubation of plutei in PI for a prolonged period of time, comparable to TO-PRO-3, did not label any nuclei within the blastocoelar cells. Labelling of puncta in the ectoderm or vesicles in the ciliated band was not observed. The PI dye is wider in structure than TO-PRO-3 and FM1-43 and should not enter cationic channels with hair cell MET or TRP channel properties; and it was expected to be excluded from all live cells. Therefore, the results suggest that TO-PRO-3 is internalized into blastocoelar cells and the cells of the ciliated band via cationic channels and not via endocytosis. Therefore, the diameter of the pores of hypothetical mechanosensory channels in these cells is less than the diameter of PI. Visualization of live plutei labelled with PI may have been a better approach for this experiment, because dye diffusion could occur after fixation, as it was seen in TO-PRO-3 labelled plutei fixed in paraformaldehyde.

Although, both dyes identify mechanosensory cells and are known to be internalized via MET in hair cells and TRPA1, their internalization may occur through other types of channels. Such channels might not be necessarily mechanosensitive. The dimensions of the channel pores which may mediate FM1-43 and TO-PRO-3 internalization in sea urchin embryos, must be at least 0.8nm in diameter, what significantly limits the pool of candidate cation channels. Other types of TRP channels have been shown to internalize FM1-43, e.g. TRPV1 (Meyers et al., 2003). Another TRP channel with pore diameters large enough to internalize FM1-43 is TRPP2 (11 angstroms) (Anyatonwu and Ehrlich, 2005) , which has been predicted in the *S. purpuratus* genome and is expressed at embryonic stages (Table 1.5). FM1-43 and TO-PRO-3 can be internalized by purinergic receptors, like P2X2 and P2X7 (Chung et al.,

2008; Khakh et al., 1999; Meyers et al., 2003; Santos et al., 2006; Virginio et al., 1999), and possibly through other channels with pore properties to similar to METs of hair cells and TRP channels, e.g. cyclic nucleotide gated channels (CNGs) (Farris et al., 2004).

In conclusion, candidate mechanosensory cell candidates were not identified by investigation of spatial TRPA1 channel expression. However, specific mechanosensory cell candidates were identified by screening with fluorescent dyes FM1-43 and TO-PRO-3. These include the cells of the blastocoelar cell network and the cells within the ciliated band. Mechanosensory channels within these cells may be involved in reception of extra-embryonic stimuli and may control embryonic swimming through the regulation ciliary beating. The timing of accumulation of transcripts for TRPA1 channel proteins during embryonic development occurs around the time of acquisition of directional swimming. This suggests that TRPA1 protein may be a component of mechanosensory channels in the apical tuft region, in the blastocoelar cell network and the cells of the ciliated band, where it may participate in reception of extra-embryonic stimuli.

4: Effects of TRPA1 channel blockers on dye internalization and embryonic swimming behaviour

4.1 Introduction

Specific pharmacological inhibitors of TRPA1 (AP18 and HC030031), and non-specific inhibitors (neomycin, gadolinium chloride and excess calcium ions), have been used to block TRPA1 channels in various animal systems. Behavioural effects, such as loss of mechanosensitivity, were observed in animal behaviour in response to TRPA1 inhibitors. TRPA1 blockers have also been used to inhibit internalization of FM1-43 and YO-PRO fluorescent dyes through TRPA1 channels and hair cell METs (refer section 1.2.2.5 for details).

In Chapter 3, I proposed that Sp-TRPA1 may participate in mechanosensation within the embryonic apical tuft, the cells of the ciliated band, and the ectodermal processes of the blastocoelar cell network. In these cells, Sp-TRPA1 may be involved in integration of extra-embryonic physical signals to control directional and spatial swimming.

In this chapter, effects of various inhibitors of TRPA1 on embryonic swimming behaviour were assessed. Also, to determine if Sp-TRPA1 could be mediating fluorescent dye internalization into candidate mechanosensory cells, various TRPA1 inhibitors were used and their effects on dye internalization were investigated.

4.2 Materials and methods

All reagents were obtained from Sigma-Aldrich unless otherwise specified.

4.2.1 Animals

As described in 2.2.1

4.2.2 Culture of embryos

As described in 2.2.2

4.2.3 Fluorescent dye labelling of embryos and larvae

As described in 3.2.17

4.2.4 Pre-treatment of live embryos with non-specific and specific TRPA1 inhibitors prior to fluorescent dye labelling

To pre-treat embryos or larvae with various TRPA1 inhibitors, the culture was concentrated to 5000 embryos/ml by reverse filtration. Treatments were performed using 2ml samples in 35mmx19mm Petri dishes (Sarstedt, Cat.No. 82.1135).

To achieve the appropriate final concentrations, stock solutions of inhibitors were added to samples using 20µl pipette and mixed immediately, to uniformly distribute the drug, by swirling the plates clockwise and counter clockwise. Stock solution concentrations: Gadolinium (III) Chloride hexahydrate (Sigma, Cat.No. 203289), 0.0372g/ml in SW; FM143FX, 1µg/µl in H_2O; TO-PRO-3, 1mM in DMSO; PI, 1mg/ml in PBS-T; neomycin sulphate (Sigma, Cat.No.N6386), 100mM in SW; gentamicin sulphate (Sigma, Cat.No.G3632), 100mg/ml in SW; AP18 (4-(4-Chlorophenyl)-3-methyl-3-buten-2-one oxime), 0.01M in DMSO (Sigma, Cat.No. A7232); HC030031 (2-(1,3-Dimethyl-2,6-

dioxo-1,2,3,6-tetrahydro-7H-purin-7 -yl)-N-(4-isopropylphenyl)acetamides), 0.01M in DMSO (Sigma, Cat. No. H4415).

Samples were treated with the following final concentrations of inhibitors unless otherwise specified: 100µM Gadolinium (III) Chloride hexahydrate for 3hrs, in the dark, at 12ºC; 1mM neomycin sulphate and 1mg/ml gentamicin sulphate from 1min to 30min, in the dark, at 12ºC; 10µM AP-18 for 1hr, in the dark, at 12ºC; 10µM HC030031 for 1hr, in the dark, at 12ºC. Mock treatments with DMSO were performed by adding a volume of DMSO equal to the volume of AP18 or HC030031 solution. To increase calcium ion concentration in SW by 5mM, 200mg/L of $CaCl_2 \cdot 2H_2O$ was added to natural SW to yield a 10mM concentration as described by Marshall and Clode (2002). Embryos were pre-treated in high calcium seawater for 15 min.

After pre-treatment live embryos were labelled with FM1-43FX or TO-PRO-3 as described in section 3.2.17 with the following modifications. The SW used for dye washout step contained inhibitors at the same concentration that was used to treat the samples.

4.2.5 Short term and long term treatments of embryos and plutei with non-specific and specific TRPA1 inhibitors

Short term and long term treatments were performed using 2ml samples of 300 to 2000embryos/ml culture, in 35mmx19mm Petri dishes (Sarstedt, Cat.No. 82.1135).

To achieve the appropriate final concentrations of inhibitors, stock solutions of inhibitors were added to plates as described in section 4.2.4. Final concentrations of all inhibitors were as outlined in section 4.2.4, unless otherwise specified. Development progress and embryo behaviour were monitored using Leica MZ95 dissecting microscope.

Swimming behaviour videos were acquired in real time using 4x objective lens and brightfield settings on Vanox (Olympus, AHBS3) microscope. Videos were recorded using a Sony Power HAD Camera (Sony), Northern Eclipse V6.0 software, (http://www.empix.com/.Vanox) and CamStudio software (http://camstudio.org/).

4.2.6 Analysis of spatial swimming using a 2-chamber swim test.

A swim-test apparatus was assembled according to instructions from Yaguchi and Katow (2003). The following modifications were made to the assembly. The upper chamber was constructed using a 15ml conical polypropylene tube (17x120mm, BD Falcon, Cat.No. 352096) that had been cut at the conical end to create an opening of 3mm in diameter. A 1.5cm length of 180 PVC tubing (Nalgene, Cat.No. 80000010), with an inner diameter of 3mm and outer diameter of 5mm, was attached to the opening with Parafilm (Pechiney Plastic Packaging, Cat.No. PM-996). A plunger from 10ml syringe (Beckton Dickinson, Cat.No.309642) was inserted into the upper chamber barrel. A 14ml round bottom polypropylene tube (17x100mm, Falcon, Cat.No. 352059) was used as the lower chamber (Fig.4.1).

To assemble the apparatus for a swimming test, the lower chamber was filled with a sample of untreated or treated embryo culture to 9.5cm mark, and mixed thoroughly to evenly distribute the embryos and positioned upright on a rack. The upper chamber was filled with SW, with or without inhibitors, to the 2ml mark using the syringe plunger. Extra care was taken to ensure that no air bubbles were trapped inside the PVC tube blocking the entrance to the upper chamber. The upper chamber was mounted on top of the lower chamber making sure that the end of the PVC tube made contact with the lower chamber SW surface, and that the tube end was submerged by 2mm, so that the SW connected the two chambers (Fig. 4.1). The upper chamber was

then fixed in place, using tape, to fix the upper chamber in the upright position and prevent its displacement during the assay. A small space was left between the upper and lower chambers to allow air exchange to occur.

The swimming test was allowed to continue for 3hrs. To stop the swimming test, the upper chamber was removed, and the syringe plunger was used to expel its contents into a 35mmx19mm Petri dish (Sarstedt, Cat.No. 82.1135).

To count the embryos, a 150 x 15mm Petri dish (Fisher Scientific, Cat.No. 0875712) was lined with a 1cm square grid. This dish was filled with either the upper or lower chamber contents. Poly (ethylene oxide) (Aldrich, Cat. No. 189464) was added to the plate until the SW consistency was thickened enough to completely immobilize the embryos. Leica MZ95 dissecting microscope was used to count the embryos. The embryos in the upper and lower chambers was counted for each assembly. The upper chamber embryo percentage was then estimated, by dividing the number in the upper chamber by the total number of all embryos within the assembly and multiplying that number by 100.

All experimental samples were subjected to the assay in triplicate. The percentages of embryos in the upper chambers were compared between untreated and treated embryos. To determine if the differences in percentages were significant, Microsoft Excel was used to perform a Two Sample Independent T-test, assuming unequal variances.

Figure 4.1 Swimming test assembly

Swimming test chamber assembly is shown standing upright on a rack. Seawater (blue).

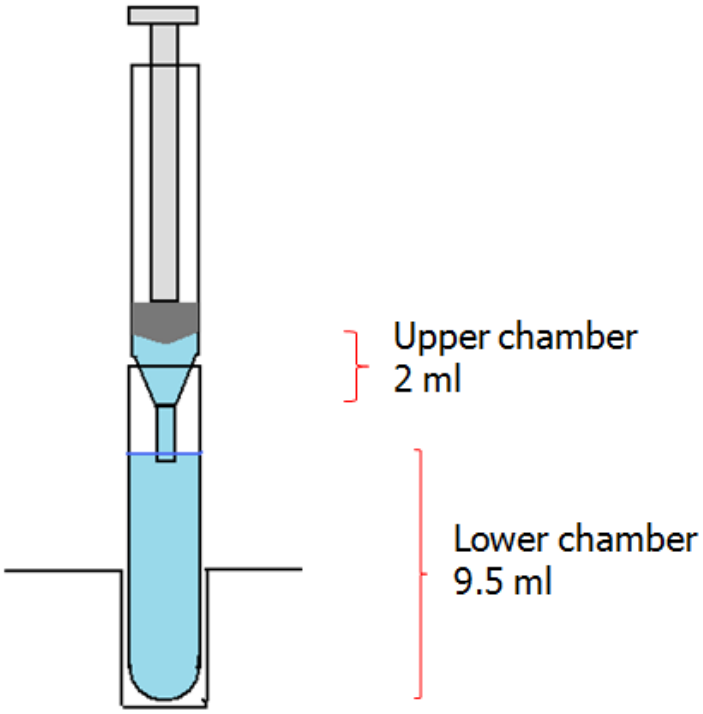

4.3 Results

4.3.1 Immediate effects of specific TRPA1 channel blockers on swimming behaviour

Swimming behaviours of embryos and early 4-arm plutei in the following experiments were assessed in 35mm Petri dishes using a dissecting microscope. The swimming behaviours were identified and categorized as "directional", "spiralling", "circling", "rotation", "slow moving" or "motionless" or "slowly moving" according to guidelines outlined in Figure 4.2. The swimming pattern of blastulae was random, not "directional", and has been described previously in Figure 5 of Maruyama et al. (1981).

Figure 4.2 Swimming behaviours of embryos and plutei

Schematic diagrams showing normal and abnormal swimming behaviours of embryos. A, B, D) Gastrula with apical tuft cilia. E) Pluteus. A) Directional swimming. Normal swimming behaviour observed in mesenchyme blastulae, gastrulae, prisms and plutei. The embryo displaces with its animal plate facing forward, as it rotates in counter clockwise direction. The blue arrow shows the embryo displacement trajectory. The red arrow shows embryo rotation around its anterior-posterior axis. B) Spiralling. Abnormal swimming behaviour observed in gastrulae, prisms and plutei in response to inhibitor treatment. The blue arrow shows the embryo displacement trajectory. The red arrow shows the path of embryo displacement as it moves forward. The animal plate of the embryo follows the red line, and the anal side of the embryo faces out and the abanal side faces inward at all times during this movement. The embryo no longer rotates around its axis as observed in directional swimming. C) Directional swimming and spiralling as seen in Petri dishes. The blue plane represents the SW surface. D) Circling. Abnormal swimming behaviour observed at hatched blastulae, gastrulae and prisms induced by inhibitor treatments. Embryo displacement occurs within the plane of the SW surface. The red arrow shows the path of embryo displacement. E) Rotation. Abnormal behaviour for mesenchyme blastula, gastrula or prism stage embryos, but is a normal behaviour of plutei. Embryos collect at SW surface and rotate around their anterior/posterior axes (red arrows) while being positioned with their anterior/posterior axes perpendicular to the SW surface. F) Circling and rotation as seen in Petri dishes. The blue plane represents the SW surface. Circling can be observed at the bottom of the dish as well. G) Motionless or slowly moving. Abnormal behaviour for all stages examined induced by inhibitor treatments. The embryos lay still or move slowly at the SW surface or at the bottom of the culture dish. The blue plane represents the SW surface.

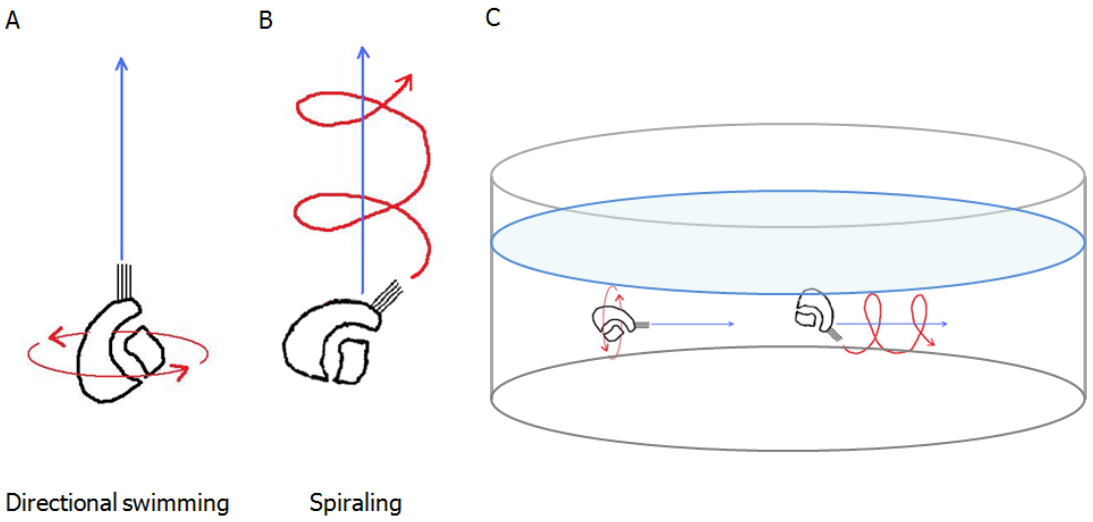
A
B
C
Directional swimming
Spiraling
D
E
F
Circling
Rotation
G

4.3.1.1 AP18

To investigate whether a specific pharmacological TRPA1 inhibitor, AP18, has an effect on swimming behaviour of embryos and plutei, hatched blastula (24 hpf), gastrula (48hpf), prism (72hpf), and early 4-arm pluteus (96hpf) stage samples were treated with 50μM AP18. The embryos were then monitored for 30 minutes (Table 4.1).

Treatment of hatched blastulae with AP18 had no effect on their swimming behaviour. For gastrulae, prisms and plutei, AP18 treatment caused a disruption of normal directional swimming (Fig. 4.2A, Supplemental video 12) resulting in distinct spiralling swimming pattern (Fig. 4.2B, Supplemental video 13) and a reduction in swimming activity, observed within the first 10 minutes of treatment. The spiralling was observed to gradually transition into circling (Fig. 4.2D) in gastrulae and prisms. By 20 minutes, the directional swimming and swimming activity level were completely restored at all stages examined. When AP18 solvent DMSO was added alone, the swimming activity of embryos was slightly reduced during the first 2 minutes but was always fully recovered by 5 minutes at all stages examined (Table 4.1).

Table 4.1 Immediate effects of AP18 on swimming behaviour of embryos and plutei

Table summarizing immediate effects on swimming behaviour of various developmental stages in response to AP18 or DMSO during the first 30 minutes of treatment. Descriptions of swimming behaviours used in this figure: directional swimming (Fig.4.2A, C), spiralling (Fig.4.2B, C), circling (Fig. 4.2D, F).

Stage	Time post AP18 and DMSO application									
	0-1min		2min		5min		10min		20min to 30min	
	AP18	DMSO	AP18	DMSO	AP18	DMSO	AP18	DMSO	AP18	DMSO
Hatched blastula 24hpf	No effect	No effect	No effect	No effect	No effect	No effect	No effect	No effect	No effect	No effect
Gastrula 24hpf	Normal speed; ~10% spiralling	Slow speed; 100% directional swimming	Normal speed; 100% spiralling or circling at the bottom	Slow speed; 100% directional swimming	Normal speed; ~90% spiralling or circling at the bottom; ~10% directional swimming	Normal speed; 100% directional swimming	Slow speed; ~10% spiralling; ~90% directional swimming	Normal speed; 100% directional swimming	Normal speed; 100% directional swimming	Normal speed; 100% directional swimming
Prism 72hpf	Normal speed; ~10% spiralling; ~90% directional swimming	Normal speed; 100% directional swimming	Slow speed; ~50% circling at the bottom; ~50% spiralling	Normal speed; 100% directional swimming	Slow speed; ~50% circling at the bottom; ~50% spiralling	Normal speed; 100% directional swimming	Slow speed; 100% move slowly or circle at the bottom	Normal speed; 100% directional swimming	Normal speed; 100% directional swimming	Normal speed; 100% directional swimming
Pluteus 96hpf	100% slow movement at the bottom	Slow speed; 100% directional swimming	100% slow movement or circling at the bottom	Normal speed; 100% directional swimming	Slow speed; ~50% directional Swimming; ~50% slow movement at the bottom	Slow speed; 100% directional swimming	Normal speed; ~50% spiralling; ~50% directional swimming	Normal speed; 100% directional swimming	Normal speed; 100% directional swimming	Normal speed; 100% directional swimming

These results suggest that AP18, but not its solvent DMSO, caused transient effects on the swimming behaviour of embryos. Since AP18 is a specific inhibitor of TRPA1, the observed swimming effects are likely caused by Sp-TRPA1 channel inhibition. No AP18 effects were seen for hatched blastulae, but were observed for gastrulae, prisms and plutei. This suggests that AP18 treatment affects specific molecules or structures that are present at these stages but are absent in blastulae, such as the apical tuft and blastocoelar cells. Sp-TRPA1 protein may be selectively expressed or active in those structures, and may be important for control of directional swimming.

4.3.1.2 HC030031

A preliminary investigation of HC030031 effects on hatched blastulae showed no effects on swimming behaviour at 10, 50 and 100μM concentrations. Preliminary investigation of HC030031 effects on gastrulae showed that 50μM concentration caused some transient spiralling, which disappeared within the first 5 minutes of treatment. When another equal dose of the drug was applied again, no effect on swimming behaviour was observed.

Lack of effect on hatched blastulae and the spiralling in gastrulae were consistent with previously observed AP18 effects (Table 4.1), suggesting that HC030031 effects were also stage specific. The similarities in effects of two different drugs specific for TRPA1 suggest that the observed effects on swimming behaviour are specific to Sp-TRPA1 channel inhibition. The results also indicate that HC030031 may be a less potent inhibitor than AP18.

4.3.2 Immediate effects of non-specific TRPA1 channel blockers on swimming behaviour

4.3.2.1 Fluorescent dyes

To determine if FM1-43 causes immediate effects on swimming behaviour, hatched blastula (24hpf), gastrula (48hpf), prism (72hpf), early 4-arm pluteus (96hpf) stage samples were continuously treated with 3μM FM1-43 without washout. The embryos were monitored for the first 30 minutes of treatment.

Continuous FM1-43 treatment caused an immediate separation of embryos at all stages into two populations: one population was confined to the culture dish bottom and another to the seawater surface (as seen in Fig.4.2G). Directional swimming and swimming activity were inhibited at all stages, and normal swimming behaviour did not recover after 30 minutes of treatment. In hatched blastulae, gastrulae, and prisms the swimming behaviour observations were similar: embryos on the bottom were motionless (Fig.4.2G) while surface-confined embryos were circling (Fig.4.2D, F). At 30 minutes after beginning of FM1-43 treatment, the separation of embryos in two populations persisted but circling on the surface slowed down. In plutei, the observations were slightly different from other stages: bottom-confined embryos were motionless while surface-confined embryos did not circle and rotated instead (Fig.4.2E, F). At 30 minutes after beginning of FM1-43 treatment, no significant changes in location or behaviour of plutei were observed (Supplemental table 3).

To determine if continuous treatment with TO-PRO-3 could affect the swimming behaviour, in the same way as FM1-43, hatched blastula (24hpf), gastrula (48hpf), prism (72hpf), and early 4-arm pluteus (96hpf) samples were continuously treated with

2μM TO-PRO-3 without washout. The embryos were monitored for the first 30 minutes of treatment.

The initial separation of embryos into two populations, bottom and surface confined, occurred at hatched blastula and gastrula stages, however, little or no circling was observed on the surface. At prism and pluteus stages, most of the embryos were immediately confined to the bottom, without circling behaviours observed. After 30 minutes, all the embryos were motionless and confined to the bottom at all stages examined (Supplemental table 3).

Propidium iodide is a fluorescent cationic dye that is wider in structure than FM1-43 and TO-PRO-3 and henceforth should not be able to penetrate cation channel pores (refer to section 3.3.9). When PI embryos were continuously treated with PI at all stages at 2μM concentration without washout, no effects were observed on their swimming activity or pattern, even after a 30-minutes of treatment (Supplemental table 3).

The results show that fluorescent cationic dyes FM1-43 and TO-PRO-3 cause immediate and severe effects on embryonic swimming behaviour at all stages. This suggests that both dyes affect the ciliated ectoderm, and not specific structures like the apical tuft or the blastocoelar cells that are present at later stages. Lack of effect of PI on swimming behaviour suggests that FM1-43 and TO-PRO-3 mediate their effects by permeating or blocking cation channels in embryos, which are likely to have structural pore properties similar to those of the hair cell METs or TRP channels.

After 30-minute observations were complete for embryos treated with FM1-43 and TO-PRO-3, the plates were incubated overnight at 12ºC in the dark. Embryos recovered full swimming activity and directional swimming overnight, in the presence of

FM1-43 and TO-PRO-3, indicating that neither of the dyes was lethal to the embryos, and that the observed effects were not due to embryonic death.

To determine if overnight dye degradation or precipitation caused the recovery of swimming in embryos, more FM1-43 dye was applied to gastrula embryos, which had been treated continuously with 3μM FM1-43 beginning at blastula stage, to a final concentration of 6μM. Preliminary observations showed that second application of FM1-43 caused an immediate familiar effect of separation into two populations and circling at the surface. However, swimming activity and directional swimming were retained within approximately 5% of the embryos. All the embryos recovered their full swimming activity and directional swimming within 30 minutes after dye application.

These results suggest that degradation and precipitation of FM1-43 dye, and likely TO-PRO-3 dye, were not the cause of embryonic swimming activity and directional swimming recovery. A resistance to the fluorescent dye effects appeared to develop in embryos.

Spiralling appears to be a form of deregulated directional swimming and circling a more severe form of spiralling (Fig. 4.2A, B, and D). To determine if circling caused by treatment with FM1-43 was a more severe form of the spiralling caused by AP-18, lower concentrations of FM1-43 were tested: 1, 0.4, 0.2, and 0.1 μM. Preliminary observations indicate that treatment with reduced FM1-43 concentrations caused a transient collection of a small fraction of embryos at the surface, while the rest of the embryos retained their directional swimming. No spiralling pattern was observed (Supplemental table 4).

These results suggest that the circling swimming behaviour caused by treatment with FM1-43 is not mediated by inhibition of Sp-TRPA1 alone, but perhaps via inhibition of other cation channels.

4.3.2.2 Neomycin, gentamicin, gadolinium chloride and calcium ions

Neomycin and gentamicin are both aminoglycoside antibiotics that are candidate non-selective inhibitors of TRPA1 and other cationic channels that have properties similar to pores of TRPA1 channels and hair cell METs (refer to section 1.2.2.5). To determine if neomycin or gentamicin had an immediate effect on embryonic swimming behaviour, the embryos were continuously treated with varying concentrations of neomycin or gentamicin at hatched blastula (24hpf), gastrula (48hpf), prism (72hpf), and early 4-arm pluteus (96hpf) stages. The embryos were monitored for the first hour after antibiotic application.

Antibiotic treatment caused an immediate inhibition of swimming activity without visible transient effects on swimming directionality like spiralling or circling. The effects on embryonic swimming activity were similar for both neomycin and gentamicin, and these effects were not stage specific. Treatment with 1mM and 0.300mM neomycin or 1mg/ml and 0.3mg/ml gentamicin caused an immediate inhibition of swimming activity, resulting in settling of all embryos to the bottom of the culture dishes. This effect persisted after 30 minutes of treatment. Addition of 0.09mM of neomycin and 0.090mg/ml of gentamicin caused partial inhibition of swimming activity, which was fully recovered to the level seen in untreated embryos within 30 minutes of treatment. Lower concentrations of antibiotics had little or no effect on swimming behaviour (Table 4.2). After 30 minute observations were complete for neomycin and gentamicin treated

embryos were incubated overnight at 12ºC in the dark. Embryos always recovered full swimming activity overnight in presence of the antibiotics.

The antibiotics inhibited swimming activity in a dose dependent manner at all stages examined. Since different types of antibiotics caused similar effects at all stages examined, the results suggest that the effect was specific to the aminoglycoside antibiotics. Therefore, the observed swimming effects were most likely due to cation channel inhibition. Lack of stage specific effects suggests that antibiotic effects are mediated through the ciliated ectoderm, as suggested for embryos treated with FM1-43 or TO-PRO-3. It appears that the embryos also develop a resistance to neomycin effects as they do for the fluorescent dye effects. Examination of embryos immobilized by the antibiotics at 40x magnification, using brightfield settings on a spinning disk confocal microscope, detected moving cilia in the ectoderm and the ciliated band. The cilia were observed to beat slower than the cilia of the untreated embryos. Thus, the immediate swimming inhibition was not due to deciliation or paralysis of cilia.

Gadolinium chloride (Gd^{3+}) at 100µM concentration has been reported to partially block TRPA1 currents (Kindt et al., 2007). Plutei were continuously treated with 100µM Gd^{3+} for up to 3hrs and observed. Gd^{3+} treatment caused an immediate immobilization of embryos and they settled to the bottom of the culture dish. None of the plutei recovered their swimming activity after Gd^{3+}treatment, even after Gd^{3+} washout. Gadolinium chloride formed a cloudy precipitate in seawater, and appeared to be toxic to plutei. To determine if elevation of calcium ion concentration could have an effect on embryonic swimming behaviour, plutei were treated in 5mM higher calcium seawater. No discernable effect was noted in the swimming behaviour of plutei.

Table 4.2 Immediate effects of antibiotics on embryonic swimming activity

Table summarizing swimming observations for three different embryo batches treated with neomycin and one batch of embryos treated with gentamycin from 0 minutes to 30minutes or 1hr. Swimming activity was scored using the following system: 0, no movement, all embryos are motionless; +, embryos are motionless or slowly moving at the bottom; ++, embryos are swimming at approximately half the speed of untreated embryos; +++, normal swimming speed equivalent to untreated embryos. Observations for separate batches of embryos are separated by a "/".

Stage	Neomycin concentration	Neomycin		Gentamicin concentration	Gentamicin	
		0 min	30min-1hr		0 min	30 min
Blastula 24hpf	1.000mM	0/0/0	0/0/0	1.000mg/ml	0	0
	0.300mM	0/0/0	0/0/0	0.300mg/ml	+	+
	0.090mM	+/+/+	+/+/+	0.090mg/ml	+++	+++
	0.025mM	++/+++/+++	++/+++/++	0.025mg/ml	+++	+++
	0.010mM	+++/+++/+++	+++/+++/+++	0.010mg/ml	+++	+++
	Untreated	+++/+++/+++	+++/+++/+++	Untreated	+++	+++
Gastrula 48hpf	1.000mM	0/0/0	0/0/0	1.000mg/ml	0	0
	0.300mM	0/0/0	0/0/0	0.300mg/ml	0	0
	0.090mM	0/+/+	0/+/+	0.090mg/ml	++	++
	0.025mM	+++/+++/+++	+++/++/++	0.025mg/ml	+++	+++
	0.010mM	+++/+++/+++	+++/+++/+++	0.010mg/ml	+++	+++
	Untreated	+++/+++/+++	+++/+++/+++	Untreated	+++	+++
Prism 72hpf	1.000mM	0/0/0	0/0/0	1.000mg/ml	0	0
	0.300mM	0/0/0	+/0/0	0.300mg/ml	0	0
	0.090mM	++/+/+	+/+/+	0.090mg/ml	+	++
	0.025mM	+++/+++/+++	+/++/++	0.025mg/ml	+++	+++
	0.010mM	+++/+++/+++	+++/+++/+++	0.010mg/ml	+++	+++
	Untreated	+++/+++/+++	+++/+++/+++	Untreated	+++	+++
Pluteus 96hpf	1.000mM	0/0/0	0/0/0	1.000mg/ml	0	0
	0.300mM	0/0/0	0/0/0	0.300mg/ml	0	0
	0.090mM	+/+++/+	+/+/+	0.090mg/ml	++	++
	0.025mM	+++/+++/+++	+++/+/++	0.025mg/ml	+++	+++
	0.010mM	+++/+++/+++	+++/+++/+++	0.010mg/ml	+++	+++
	Untreated	+++/+++/+++	+++/+++/+++	Untreated	+++	+++

4.3.3 Effects of FM1-43 on spatial swimming

The spatial swimming assay was performed in a previous study to compare swimming behaviours of pCPA treated embryos to untreated controls (Yaguchi and Katow, 2003). It was claimed to differentiate between the embryos having an ability to swim vertically from the embryos where this ability was partially inhibited (Yaguchi and Katow, 2003). A similar type of assay was performed in Ooka et al. (2009). The SRN was suggested to be required for coordination of ciliary beating that allows this vertical or "spatial" swimming to occur (Katow et al., 2007). In Chapter 3, the FM1-43 labelled blastocoelar cell network was identified as the SRN, and I suggested that FM1-43 is internalized into the SRN through mechanosensory channels in the processes inserted into the ectoderm. In addition, I suggested that cells within the ciliated band at arm tips may internalize FM1-43 through mechanosensory channels as well. Both the SRN and the ciliated band cells may be required for reception and integration of external physical stimuli to coordinate spatial swimming.

According to my observations, the embryos of all stages retained their swimming activity and directional swimming if the FM1-43 treatment was not continuous, where FM1-43 dye was washed out immediately after a 30-second treatment. Therefore, it was interesting to determine whether FM1-43 internalization into the blastocoelar network or the cells of the ciliated band had effect on spatial swimming in embryos an early 4-arm plutei. If this assay indeed measures spatial swimming, then only the embryos which are able to orchestrate their ciliary beating properly will be able to swim vertically.

To assay FM1-43 effects on spatial swimming, a 2-chamber "spatial swimming activity" assay was performed as described in Yaguchi et al. (2003). In this assay, a lower chamber was connected to an upper chamber by a narrow tube. Embryos were placed in the lower chamber, and the number of embryos in the upper chamber was calculated after a 3hr incubation period. A 2-chamber assembly was initially constructed according to the instructions in Yaguchi et al. (2003). Experiments were performed using this assembly and the suggested time, but it did not yield accurate and reproducible measurements. The entrance to the upper chamber was too narrow, so assembly was redesigned to widen the opening into the upper chamber (Fig.4.1). This modification greatly improved the accuracy and reproducibility of measurements, without changing the timing of the assay.

To perform the assay, triplicate samples of hatched blastula (24hpf), gastrula (48hpf), prism (72hpf), and early 4-arm pluteus (96hpf) stage embryos from the same batch were treated for 30 seconds with FM1-43 followed by immediate washout. The assay was performed and the percentages of embryos that swam into the upper chambers after 3hrs were calculated as described in section 4.2.6. Triplicate samples of untreated embryos were concurrently analyzed for each stage. Percentages of untreated and FM1-43-treated embryos in the upper chambers were compared using an unequal variance t-test for statistical significance. Seven different batches of embryos (or cultures) were analyzed in total. The results for each of the seven cultures are shown separately in Fig. 4.3. All the calculations are reported in Supplemental Fig. 18.

Both reductions and increases in fractions of embryos in upper chambers were observed for hatched blastulae (24hpf) treated with FM1-43 compared to untreated embryos. FM1-43 had no consistent effect on hatched blastulae among seven different

batches of embryos (Fig. 4.3A). At gastrula stage (48hpf), FM1-43 treatment caused a general decrease in the upper chamber mean percentages, observed in six out of seven cultures, and a statistically significant decrease, observed in one out of seven cultures (Fig.4.3B). At prism stage (72hpf), FM1-43 treatment caused a general decrease in the upper chamber mean percentages for all cultures, with a statistically significant decrease in four out of seven cultures (Fig. 4.3C). At pluteus stage (96hpf), it caused a general decrease in the upper mean chamber percentages, observed in six out of seven cultures, but no statistically significant decrease in any cultures (Fig. 4.3D).

This experiment did not yield enough statistically significant data to determine, with confidence, if FM1-43 has an effect on spatial swimming of embryos. However, the general trends in results suggest a stage specific effect of FM1-43 on spatial swimming. FM1-43 decreases spatial swimming among gastrulae, prisms and plutei, but has no discernable effect on hatched blastulae. Prism stage embryos were the most sensitive to the FM1-43 treatment. The observed stage specific effects suggest involvement of the blastocoelar network and possibly ciliated band cells in spatial swimming.

To determine if specific TRPA1 inhibitors can affect spatial swimming, embryos at hatched blastula (24hpf), gastrula (48hpf), prism (72hpf), and early 4-arm pluteus (96hpf) stages were treated for 30 min to 1hr with AP18 or HC030031 and then assayed in the 2-chamber swimming test assembly. Multiple experiments failed to detect differences between treated and untreated embryos.

Given that the effects on swimming of AP18 and HC030031 were observed only during the first 10 minutes of treatment the results were not surprising, suggesting that this assay was inappropriate for these inhibitors.

To determine if this assay can distinguish between SRN mediated spatial swimming and random spatial swimming activity, untreated plutei (96hpf), which have fully developed SRN, were compared to untreated blastulae (24hpf), which do not have the SRN (Fig. 4.4, Supplemental Fig. 19). Five out of seven cultures showed that more blastulae than plutei swam into the upper chambers, with that difference being statistically significant in 2 instances (Fig.4.4).

The results suggest that the capacity to swim into the upper chamber does not depend on the presence of the SRN and the assay does not appear to be an exact measure of upwardly spatial swimming, and appears to measure swimming activity as well, since blastulae are more active than plutei.

Figure 4.3 Spatial swimming activity assay of effects of treatment with FM1-43

Panels A-D show the raw data comparing the means of triplicate samples for untreated and FM1-43 treated embryos at 24, 48, 72 and 96hpf, across seven different cultures. The vertical capped bars represent the standard deviations of the means. Double asterisks show the cultures that had statistically significant differences according to the unequal variance t-test, and a two-tailed p value <0.05. A single asterisk marks cultures that did not have statistically significant differences, but had a two tailed p value very close to 0.05, within 0.05 to 0.1 range. A-D) Red bars, mean percentages for untreated embryos; Blue bars, mean percentages for FM1-43 treated embryos. A) Hatched blastula stage (24hpf). B) Gastrula stage (48hpf). C) Prism stage (72hpf). D) Early 4-arm pluteus stage (96hpf). Raw data, calculations and p values are reported in Supplemental figure 18.

A

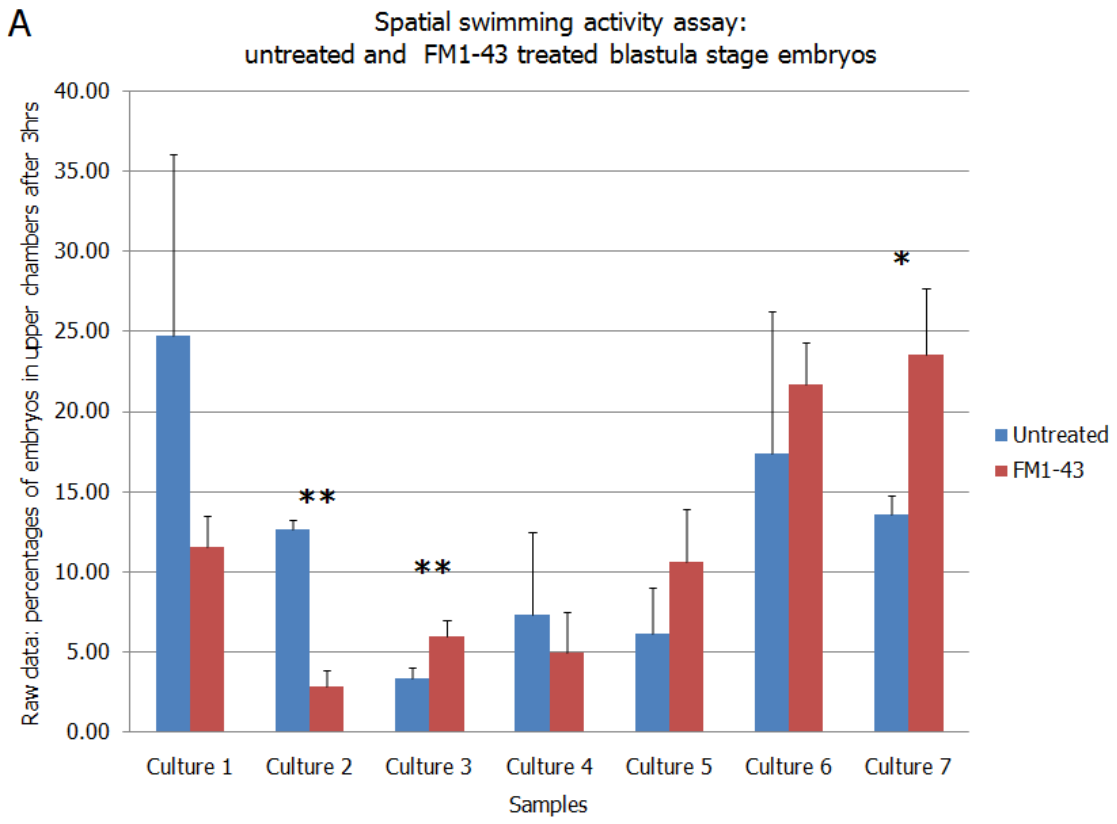
Spatial swimming activity assay:
untreated and FM1-43 treated blastula stage embryos
Raw data: percentages of embryos in upper chambers after 3hrs
40.00
35.00
30.00
25.00
20.00
15.00
10.00
5.00
0.00
**
**
*
Culture 1
Culture 2
Culture 3
Culture 4
Culture 5
Culture 6
Culture 7
Samples
Untreated
FM1-43

B

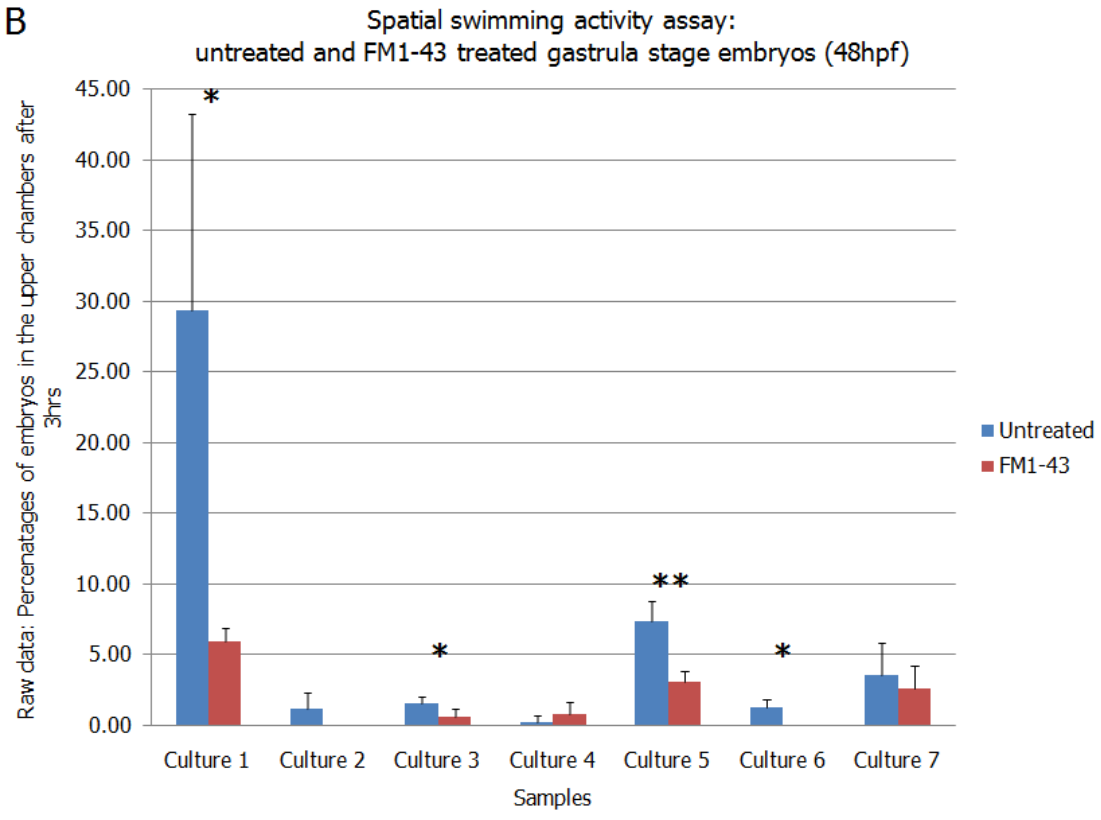
Spatial swimming activity assay:
untreated and FM1-43 treated gastrula stage embryos (48hpf)
Raw data: Percenatages of embryos in the upper chambers after 3hrs
45.00
40.00
35.00
30.00
25.00
20.00
15.00
10.00
5.00
0.00
*
*
**
*
Culture 1
Culture 2
Culture 3
Culture 4
Culture 5
Culture 6
Culture 7
Samples
Untreated
FM1-43

C

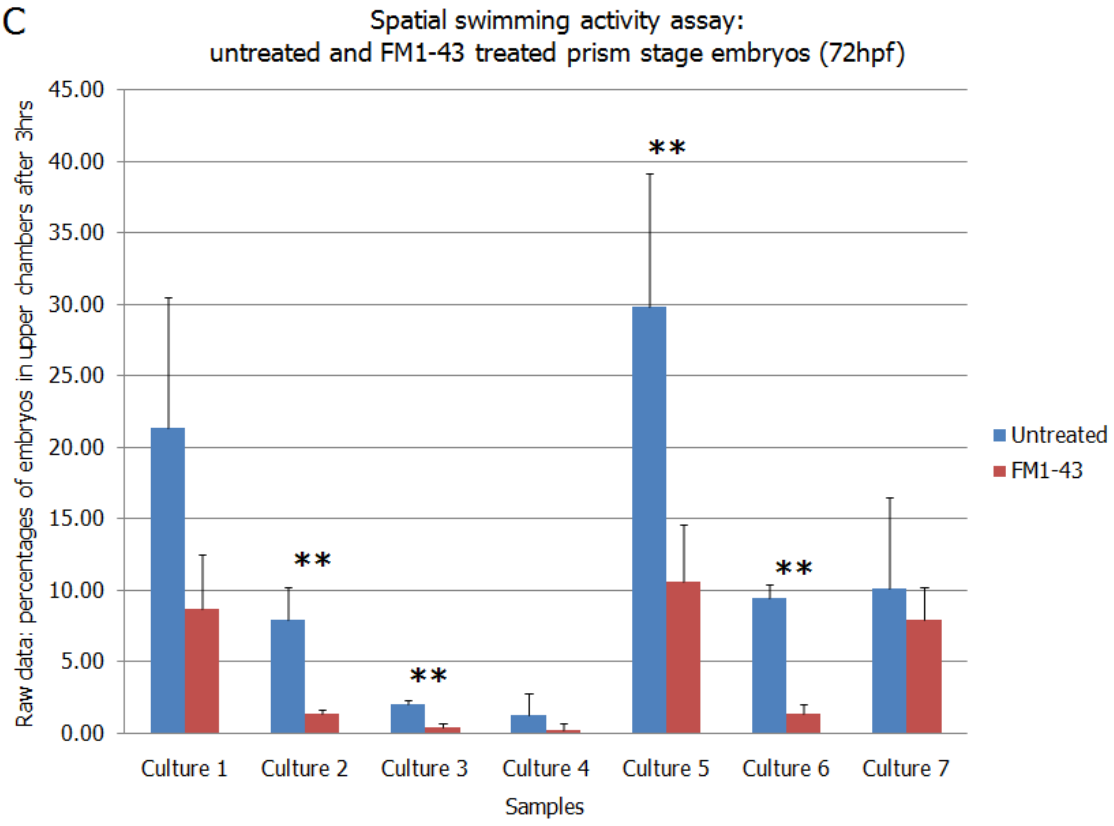
Spatial swimming activity assay:
untreated and FM1-43 treated prism stage embryos (72hpf)
Raw data: percentages of embryos in upper chambers after 3hrs
45.00
40.00
35.00
30.00
25.00
20.00
15.00
10.00
5.00
0.00
**
**
**
**
Culture 1
Culture 2
Culture 3
Culture 4
Culture 5
Culture 6
Culture 7
Samples
Untreated
FM1-43

D

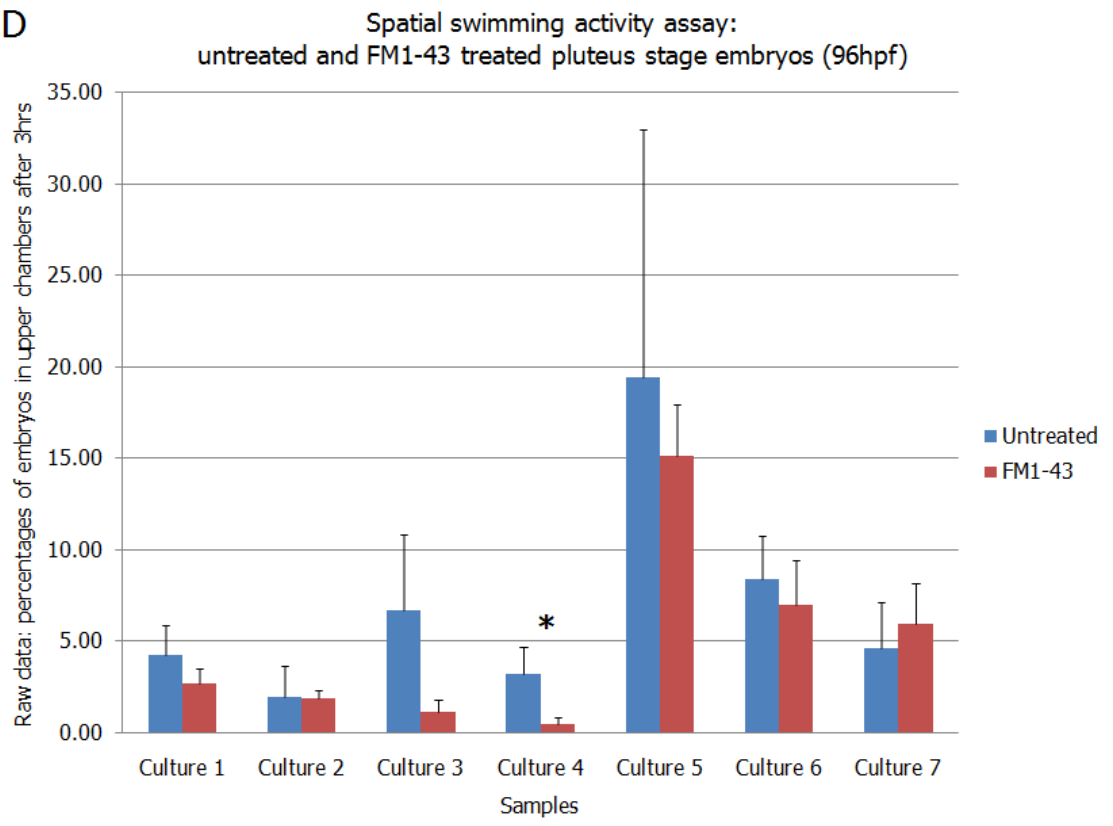
Spatial swimming activity assay:
untreated and FM1-43 treated pluteus stage embryos (96hpf)
Raw data: percentages of embryos in upper chambers after 3hrs
35.00
30.00
25.00
20.00
15.00
10.00
5.00
0.00
*
Culture 1
Culture 2
Culture 3
Culture 4
Culture 5
Culture 6
Culture 7
Samples
Untreated
FM1-43

Figure 4.4 Spatial swimming activity assay test comparing blastulae and early 4-arm plutei

The mean percentages of embryos in the upper chamber for triplicate samples of untreated 24hpf and 96hpf embryos for seven different cultures. The vertical capped bars represent the standard deviation of the means. Double asterisks mark cultures that had statistically significant differences according to the unequal variance t-test and two-tailed p value <0.05. One asterisk marks cultures that did not have statistically significant differences, but had a two tailed p value very close to 0.05, within 0.05 to 0.10 range. Red bars, hatched blastulae (24hpf); Blue bars, untreated early 4-arm plutei (96hpf). Raw data, calculations and p values are reported in Supplemental figure 19.

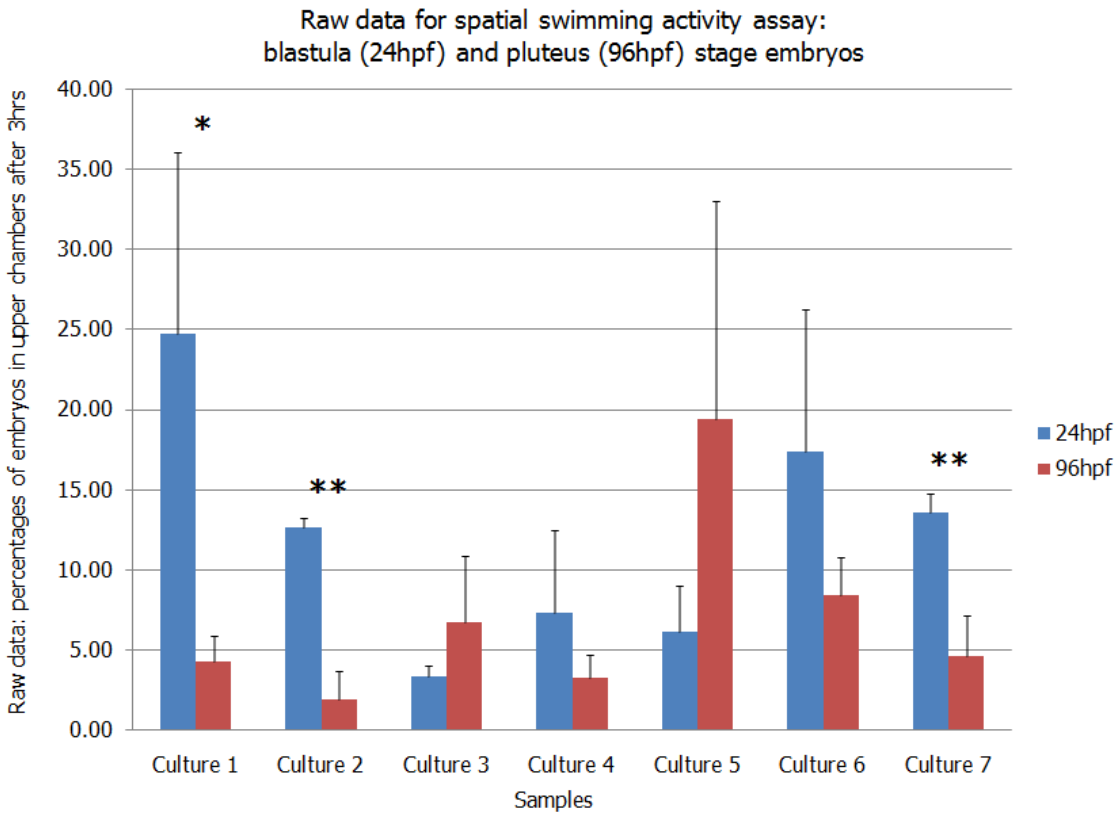
Raw data for spatial swimming activity assay:
blastula (24hpf) and pluteus (96hpf) stage embryos
Raw data: percentages of embryos in upper chambers after 3hrs
40.00
35.00
30.00
25.00
20.00
15.00
10.00
5.00
0.00
*
**
**
Culture 1
Culture 2
Culture 3
Culture 4
Culture 5
Culture 6
Culture 7
Samples
24hpf
96hpf

4.3.4 Effects of channel blockers on fluorescent dye internalization

4.3.4.1 AP18 and HC030031

AP18 and HC030031 have been reported to block YO-PRO uptake into mammalian cultured cells at half maximal inhibitory concentrations of 10.3 ± 0.8μM and 9.4 ± 0.6μM, respectively (Chen et al., 2009).

To determine if the specific pharmacological inhibitors of TRPA1 channels AP18 or HC030031 affect FM1-43 internalization into mechanosensory cell candidates, plutei were pre-treated with 10μM or 100μM concentrations of AP18 or HC030031 or with DMSO (the AP18 and HC030031 solvent) for 1hr. They were then exposed to FM1-43 for 30 seconds, washed in presence of AP18, HC030031 or DMSO, fixed with in paraformaldehyde and visualized. No effect on the intensity FM1-43 labelling was observed for either drug or DMSO compared to untreated controls (Supplemental Fig. 20).

This result suggests that FM1-43 is not internalized via Sp-TRPA1 channels alone, but more likely via other cationic channels with pore properties of hair cell METs or TRP channels. The effects of these drugs on TO-PRO-3 labelling were not investigated because of its artifactual labelling of fixed embryos and expense of the drugs.

4.3.4.2 Neomycin, gadolinium chloride and calcium ions

Various non-specific TRPA1 channel blockers were used to determine if FM1-43 or TO-PRO-3 internalization into mechanosensory cell candidates can be inhibited in early 4-arm plutei (96hpf).

Plutei were pre-treated 1mM neomycin for 30 minutes, and were then labelled with FM1-43 for 30 seconds, or TO-PRO-3 for 40 minutes, and washed in presence of neomycin. Plutei were visualized live, without fixation. Compared to untreated plutei, neomycin significantly reduced FM1-43 labelling of the entire blastocoelar cell network, but not the labelling of the ectoderm (Fig. 4.5). However, labelling of the blastocoelar cell network and nuclear labelling by TO-PRO-3 was not reduced by a 30-minute treatment with neomycin (Supplemental Fig. 21). If plutei were treated with neomycin, for a shorter period of 1 minute, no difference in labelling between untreated and treated plutei was observed (Supplemental Fig. 22). Since the washout step did not occur overnight, visualization of labelling of ciliated band cells at arm tips was impossible due to background fluorescence. Therefore, neomycin effects on their labelling were not determined.

Inhibition of FM1-43 labelling by a 30-minute treatment with neomycin suggests that FM1-43 labelling of blastocoelar cells is mediated through cation channels with pore properties of hair cell METs or TRP channels, and possibly through Sp-TRPA1 channels.

To determine if the general cation channel blocker Gd^{3+} could block FM1-43 internalization in mechanosensory cell candidates, plutei were pre-treated with 100μM of Gd^{3+} for 3hrs before FM1-43 labelling, fixed and visualized. Gd^{3+} had no effect on FM1-43 labelling. Increasing its concentration ten-fold had no effects (Supplemental Fig. 23). Gd^{3+}precipitated rapidly in seawater, and appeared to be toxic to embryos. Therefore, this result was unreliable. Plutei were incubated in high calcium seawater for 30 minutes, exposed to FM1-43 for 30 seconds, fixed and visualized. Raising the calcium ion concentration in seawater by 5mM had no effect on FM1-43 labelling (Supplemental Fig. 24).

Figure 4.5 Effects of neomycin on FM1-43 internalization into the blastocoelar cell network of early 4-arm plutei

Confocal images showing reduction of FM1-43 fluorescence intensity in the blastocoelar cell network of neomycin treated plutei compared to untreated plutei. Images were acquired using the same laser sensitivity and exposure to compare FM1-43 fluorescence intensity across samples. A scale bar of 20µm applies to all panels. A) Untreated pluteus, FM1-43 labelled body left and right rod tracts (arrowheads). B) Brightfield image corresponding to panel A). C) Untreated pluteus, FM1-43 labelled postoral rod tract (arrowhead). D) Brightfield image corresponding to panel C. E) Untreated pluteus, FM1-43 labelled body rod tracts at pluteus tip (arrowhead). F) Brightfield image corresponding to panel E. G) Neomycin treated pluteus, reduced fluorescence in left body rod tract (arrowheads) compared to panel A. H) Brightfield image corresponding to panel G. I) Neomycin treated pluteus, reduced fluorescence in postoral rod tract (arrowhead) compared to panel C. J) Brightfield image corresponding to panel I. K) Neomycin treated pluteus, reduced fluorescence in body rod tracts at pluteus tip (arrowhead) compared to panel E. L) Brightfield image corresponding to panel K.

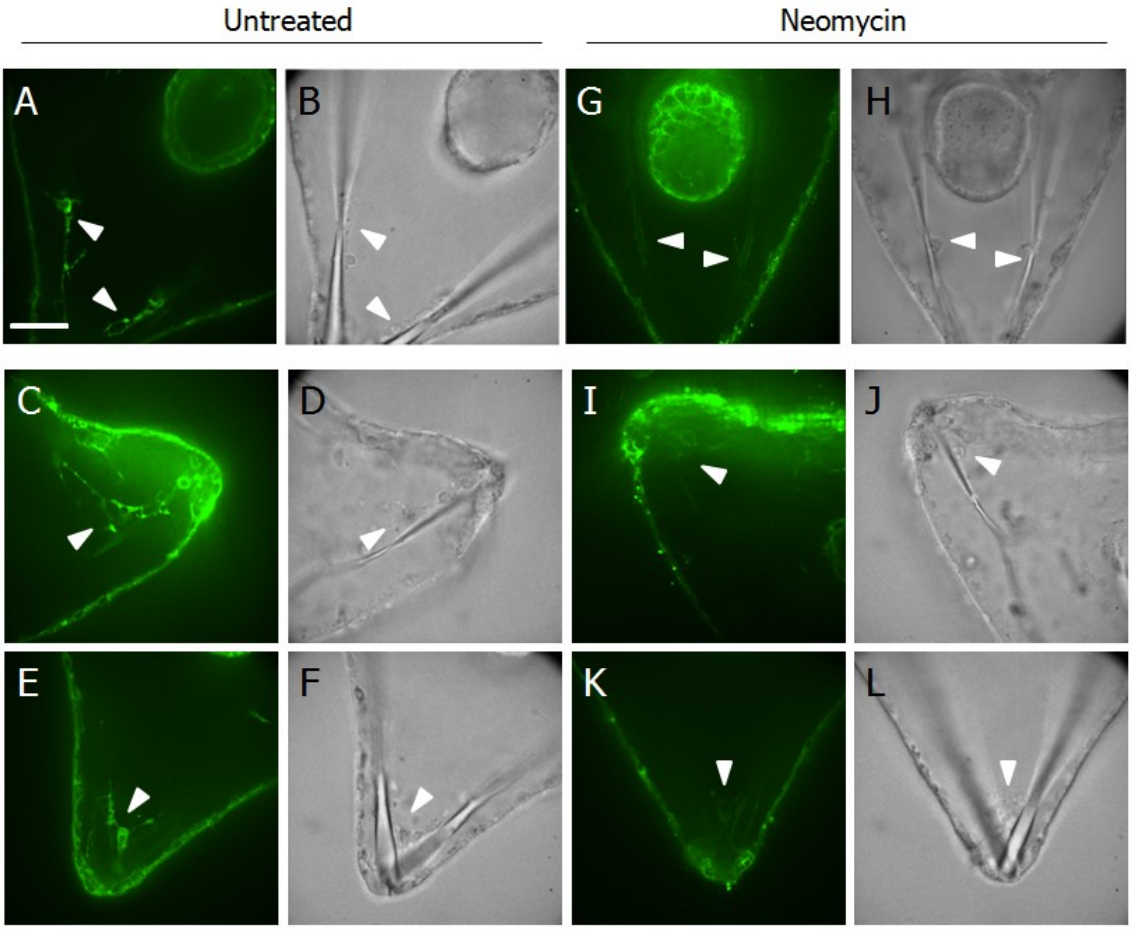
Untreated
Neomycin
A
B
G
H
C
D
I
J
E
F
K
L

4.3.5 Long term effects of TRPA1 inhibitors on development and swimming behaviour

Hatched blastula (24hpf), gastrula (48hpf), and prism (72hpf) stage embryos were treated with various non-specific and specific TRPA1 inhibitors: 3μM FM1-43, 2μM TO-PRO-3 and 2μM PI (Supplemental table 5); 1mM neomycin (Supplemental table 6); 50μM AP18 (Supplemental table 7). Embryonic development and behaviour were monitored until early 4-arm pluteus stage (96hpf). Results of a preliminary investigation of HC030031 effects are reported in Supplemental table 7.

Similarities in developmental effects and swimming behaviours were observed among different inhibitors. Developmental retardation and abnormalities, such as elevation of mesenchyme cell numbers, were seen for embryos treated with AP18 and neomycin. Spiralling was observed in AP18 and HC030031 treated embryos. An abnormal form of directional swimming, with faster spinning than the one seen in untreated embryos, was seen in response to neomycin and TO-PRO-3 treatments. The effects of the non-specific TRPA1 blocker neomycin on development and swimming were more severe than those of specific TRPA1 blockers. Blastulae were most sensitive to the effects of these inhibitors.

4.4 Discussion

The aim of this set of experiments was to investigate the effects of specific and non-specific TRPA1 channel inhibitors on embryonic swimming behaviour, and to determine whether those inhibitors can block FM1-43 or TO-PRO-3 internalization in the candidate sensory cells indentified in Chapter 3.

Treatment of gastrulae, prisms and plutei with AP18 resulted in immediate and transient spiralling and circling behaviours. Blastulae were not sensitive to AP18 treatment. The stage specific effect of AP18 suggests that the observed swimming behaviours are most likely caused by its effect on molecules or specific structures present at gastrula, prism and pluteus stages, like the apical tuft, the ciliated band or the blastocoelar cell network, all of which are lacking in blastulae. The results suggest that Sp-TRPA1 channel may be involved in control of directional swimming, but does not appear to be essential for swimming activity.

One of the explanations for spiralling and circling behaviours at gastrula and prism stages is the disruption of the hypothetical apical tuft function. In Chapter 3, I suggested that Sp-TRPA1 protein may be expressed in the immotile cilia of the apical tuft, where it may be required for sensing water flow, as the embryo swims forward, allowing orchestration of ciliary beating required for directional swimming. Upregulation of Sp-TRPA1 transcripts was observed at mesenchyme blastula stage, when the apical tuft develops. The timing and the nature of responses of embryos to AP18, Sp-TRPA1 gene expression timing, and timing of formation of the apical tuft all suggest that the Sp-TRPA1 protein is present in the apical tuft cilia or in the animal plate cells. AP18 may be directly inhibiting the Sp-TRPA1 channel or a mechanotransducer containing Sp-TRPA1 protein in the ciliary tuft or the animal plate thereby disrupting directional swimming.

An interesting difference in AP18 effects was observed between gastrulae, prisms and plutei whereby the latter shows less pronounced spiralling or circling swimming behaviours. Since the blastocoelar network is not fully developed in gastrula and prism stage embryos, compared to plutei, the difference in swimming effects may be

attributed to inhibition of Sp-TRPA1 channels in the blastocoelar network. The SRN, which is a part of the blastocoelar cell network, is thought to regulate ciliary beating and control spatial swimming (Katow et al., 2007). AP18 treatment may have inhibited Sp-TRPA1 channels in the SRN network resulting in deregulation of ciliary beating and inhibition of directional swimming in plutei.

Preliminary observations of embryonic behaviour in response to HC030031 treatment support involvement of Sp-TRPA1 in embryonic directional swimming. The evidence shows that HC030031 may be less effective than AP18 in inhibiting Sp-TRPA1.

The difference between drug effects may lie within their mode of action. The effects for both pharmacological TRPA1 inhibitors on swimming behaviour were transient. No similar observations were reported in previous studies where these compounds were used to inhibit mammalian TRPA1. Mechanism of action for HC030031 is presently unknown. The transient effect of AP18 may be explained by the proposed mechanism of inhibition of TRPA1, whereby the channel is covalently modified by this drug (DeFalco et al., 2010). Firstly, AP18 might be depleted from the seawater as it covalently modifies the cysteine residues of TRPA1, although the high concentration of AP18 in the samples does not support this idea. Alternatively, precipitation of AP18 and HC030031 may account for the transient nature of their effects, as a film of precipitate was observed immediately upon addition of AP18 to seawater, and crystal formation was noted during long term observations of HC030031 treated samples. In addition, congeners of AP18 have been reported to possess both agonist and antagonist activities, and substitution or deletion of chemical groups in AP18 resulted in conversion of AP18 into an agonist of mammalian TRPA1 (DeFalco et al., 2010). Therefore, it is possible that differences between the Sp-TRPA1 and mammalian TRPA1 protein, like their tertiary

structures, allow AP18 to switch from acting as an inhibitor to acting as an agonist within a short period of time. Finally, transient effects may be results of upregulation of protein expression of alternatively spliced forms of Sp-TRPA1, which cannot be covalently modified by AP18. In addition, other types of mechanosensitive channels may take over control of embryonic swimming behaviour and be insensitive to AP18 or HC030031.

Continuous treatments of embryos with FM1-43 and TO-PRO-3, but not PI, without washout, produced dramatic effects on directional swimming at all stages. The dyes may be directly or indirectly affecting the orchestration of ciliary beating in the ectoderm, which propels the embryos in a defined pattern. Both FM1-43 and TO-PRO-3 are known to selectively permeate channels having pore properties of hair cell METs and TRP channels (refer to section 1.2.2.4). Therefore, these dyes may be blocking multiple mechanosensory channels, including Sp-TRPA1, in the embryonic cilia resulting in the observed altered swimming behaviour.

Although FM1-43 and TO-PRO-3 should be penetrating and perhaps blocking the channels with similar pore properties, their effects on swimming behaviour were markedly different. The FM1-43-induced surface confinement and circling were not observed for TO-PRO-3 treated embryos. This is most likely attributed to structural differences between FM1-43 and TO-PRO-3. FM1-43 is a membrane dye, while TO-PRO-3 cannot intercalate into the lipid layer. Perhaps, labelling of embryonic membranes is responsible for behavioural differences observed. In addition, differences in sizes or other properties between FM1-43 and TO-PRO-3 may have resulted in inhibition of different types of cation channels, which in turn produced differences in the observed swimming behaviour. The varying responses of embryos to treatment with FM1-43,

manifesting as separation into bottom- and surface-confined populations, might be the consequence of momentary differences in local dye concentration upon addition of the dye stock to the suspension of embryos.

Full recovery of directional swimming was observed overnight, in presence of FM1-43 and TO-PRO-3, at all stages examined. Preliminary results suggest that the embryos develop a resistance to dye effects. This recovery may be attributed to the embryos using channels with smaller pore sizes, which might not be accessible for blocking by either dye.

Smaller concentrations of FM1-43 caused immediate and transient circling on the surface. The transient nature of the observed circling may be explained by transient binding and immediate washout of FM1-43 from embryo surfaces or cation channel pores. Transition from directional swimming to spiralling and eventually to circling, observed in AP18 treated embryos, was not observed in this experiment. This again suggests that more cation channels than Sp-TRPA1 are involved in control of directional swimming.

The effects of antibiotic treatment were very similar to the effects of treatments with FM1-43 and TO-PRO-3. Neomycin and gentamicin had severe effects on swimming activity, and treated embryos were able to recover their swimming activity fully over night in the presence of antibiotics. FM1-43, TO-PRO-3, and aminoglycoside antibiotics may be inhibiting the same types of cationic channels. Differences in effects between fluorescent dyes and antibiotics suggest that different populations of cation channels are involved in swimming control. Neomycin treatment slows down ciliary beating, suggesting that active cation channels in the ciliated ectoderm may be required for regulation of ciliary beating speed, which is in turn required for swimming activity.

Gadolinium chloride irreversibly inhibited swimming activity of plutei and appeared to have a toxic effect on the plutei. However, its immediate effects support the conclusion that cation channels are involved in swimming control. Calcium concentration elevation had no effect on swimming behaviour. Calcium concentration is intrinsically high in seawater; therefore, elevation of 5mM might have not been effective in inducing noticeable swimming behaviour effects.

Severe effects on swimming activity by non-specific cation channel inhibitors, observed here, are not surprising. Existence of cation channels in ciliary membranes, which modulate swimming and feeding behaviours in sea urchin larvae, has been suggested previously (Hart, 1990). In the cells of the ciliated band, contact of motile cilia with particles may elicit opening of hypothetical stretch-activated cation channels in those cilia leading to ciliary beating reversals in affected cells, which are required for directing food particles into the larval mouth (Hart, 1990; Strathmann, 2007). Earlier embryonic stages appear to have different types of cation channels which have different properties from the ones in the cilia in the ciliated band, and cation channel inhibition was observed to cause different types of responses in swimming behaviour at different embryonic stages (reviewed in Hart (1990)). This may explain why a variation in behavioural responses was observed to different types of non-specific TRPA1 inhibitors.

The 2-chamber assay was used in this study to assess spatial swimming in embryos and early 4-arm plutei. Comparing abilities of blastulae and plutei to swim into the upper chambers suggests that this assay does not exclusively measure the SRN-mediated spatial swimming as previously proposed (Katow et al., 2007; Yaguchi and Katow, 2003). The assay does not only measure an ability of embryos to coordinate ciliary beating allowing them swim vertically into the upper chambers, but most likely

also measures a combination of other factors including general swimming activity. Swimming activity and other factors are probably predominantly stage specific. Thus, this swimming assay can still be useful in assaying spatial swimming in the embryos of the same stage, what probably controls for most of these factors.

Experimental data from multiple cultures has shown that a 30-second FM1-43 treatment, with washout, generally reduced the ability of embryos to swim into the upper chamber at gastrula, prism and pluteus stages, but not at blastula stage. Since a washout step was performed before the assay, and the embryos were incubated for 3 hours, allowing ample time for ectodermal destaining, the cells that internalized the dye were the most likely candidates for the observed swimming effects. Also, the embryos retained their ability to swim directionally after this treatment, implying that ciliary beating was not significantly affected. The stage specifity of the observed FM1-43 effects suggest that such candidate cells are most likely the cells of the blastocoelar cell network or the cells of the ciliated band that internalize FM1-43 (refer to section 3.3.6). The results of this assay suggest that FM1-43 internalization into the SRN network appears to affect its function in orchestration of ciliary beating that allows upwardly spatial swimming to occur (Katow et al., 2007). These results support my proposal in Chapter 3 that FM1-43 blocks mechanosensory channels, like TRPA1, within the ectodermal processes of this network, thus impairing its ability to integrate external mechanical signals from the environment that may be required for directing spatial swimming. Similarly, FM1-43 may also affect the function of candidate mechanosensory cells in the ciliated band at arm tips.

The most pronounced effects of FM1-43 in the 2-chamber swimming assay, with most significant results, were observed at prism stage. The blastocoelar cell network and

the SRN are only partially formed at prism stage, with fewer connections than seen at pluteus stage (Katow et al., 2004; Katow et al., 2007). Participation of the gastrula stage or prism stage SRN network in spatial swimming has not been characterized. Therefore, it is not clear whether observed effect on swimming behaviour during those stages can be attributed to FM1-43 internalization into the blastocoelar network, or blocking cation channels, located elsewhere, such as the animal plate or ciliary band cells.

The general trends across seven cultures suggest that FM1-43 has an effect on embryonic swimming behaviour, but the interpretation of results was complicated by a variability between responses to treatments of embryo batches obtained from different fertilizations. Variability between different sea urchin cultures is a natural occurrence and may involve a variation in developmental rates and altered sequence of developmental events, even if the embryos are maintained in uniform conditions (Wray et al., 2004). This may explain the sometimes contradicting responses to FM1-43 treatment between different cultures. The general trends observed within the results suggest that if more experiments on different cultures are done, more statistically significant differences between untreated and FM1-43 treated embryos will be observed.

The results of the 2-chamber assay were particularly inconsistent for hatched blastulae. Sea urchin embryo cultures often develop somewhat asynchronously. At 24hpf, a significant proportion of embryos can be in unhatched form, at early blastula stage, or at mesenchyme blastula stage. This variation cannot be easily controlled. An experiment using a completely synchronous culture containing only swimming hatched early blastulae is not possible. It might be possible to filter out unhatched embryos to

improve reproducibility, but this was not done. The 3 hour long assay should minimize the effects of variation in rates of development within the culture.

To determine whether Sp-TRPA1 mediates FM1-43 or TO-PRO-3 internalization into the blastocoelar network at pluteus stage, the plutei were treated with specific and non-specific inhibitors of TRPA1 prior to fluorescent dye labelling. Specific inhibitors of TRPA1 and AP18, had no effect on FM1-43 labelling of the blastocoelar cell network, which suggests that more cation channels are involved in FM1-43 uptake into these cells. However, a non-specific inhibitor neomycin reduces FM1-43 labelling of the blastocoelar cell network providing strong evidence for cation channels that mediate FM1-43 internalization into this network. This result supports my speculations that functional Sp-TRPA1 channels or other mechanosensory channels with hair cell MET and TRP channel properties are present within the blastocoelar cell processes that contact the pluteus exterior, since neomycin should not block dye diffusion through septate junctions in the ectodermal walls. Also, inhibition of swimming activity and effects on ciliary beating, which coincide with neomycin treatment, suggest that active mechanosensory channels within the blastocoelar cell network may participate in regulation of ciliary beating and spatial swimming in plutei.

Despite its effects on FM1-43 labelling, TO-PRO-3 labelling was not noticeably reduced by neomycin. Antibiotics are bulkier molecules than fluorescent dyes, and they are reversible channel pore blockers, which compete for pore binding sites with fluorescent dyes (van Netten and Kros, 2007). Due to these properties, the block of fluorescent dye internalization was probably incomplete. Therefore, TO-PRO-3 internalization may have been reduced, but that reduction may not have been noticeable

if TO-PRO-3 is a very potent marker of nuclei. Smaller concentrations of TO-PRO-3 might be required to detect a difference in labelling similar to FM1-43.

Reduction of FM1-43 labelling in the blastocoelar network did not appear to result from damage by 30-minute neomycin treatment, since no obvious structural damage was observed, and TO-PRO-3 labelling (a dye exclusion assay for healthy cells) identified similar sets on nuclei in the blastocoelar cell network. Since 1-minute neomycin treatment did not reduce FM1-43 labelling, the most likely explanation is the insufficient time for neomycin diffusion into the pores of the cation channels.

Observations of long term effects of all TRPA1 inhibitors have shown that blastula embryos were more prone to inhibitor-induced developmental defects than other stages. Unlike immediate effects, long-term effects of specific and non-specific TRPA1 inhibitors cannot be interpreted as direct effects on Sp-TRPA1 channels. Long-term effects on development are likely to be indirect results of the inhibitors on embryonic development, and are not easily explained. Some common effects on development were observed like reduction in embryo size, morphological abnormalities, increased number of mesenchyme cells, and changes in swimming directionality and speed. Although effects on swimming behaviour were observed, causal relationships remain uncertain. Most of the time those effects were not informative. Nevertheless, similarities in morphological abnormalities and swimming behaviours hint at involvement of Sp-TRPA1 and other cation channels in similar processes including development or function of structures involved in control of swimming in the sea urchin embryos. The acquired information about the effects of TRPA1 inhibitors on embryo morphology and swimming behaviour may be useful for prediction of possible abnormalities to look for, if Sp-TRPA1 expression was knocked down using morpholino-antisense oligonucleotides.

In conclusion, different types of cation channels in the ciliated ectoderm of embryos and early 4-arm plutei, having TRP-channel or hair cell MET pore properties, appear to be involved in control of swimming behaviour. Sp-TRPA1 appears to be important for coordination of directional swimming, but is not essential for swimming activity. Multiple lines of evidence, outlined in this chapter and in Chapter 3, strongly suggest that Sp-TRPA1 channels or other hypothetical mechanosensory channels which may contain Sp-TRPA1 protein are present in the candidate sites or physiological centres for swimming control, like the apical tuft or the blastocoelar cell network.

5: Conclusions

The specific goals of my Thesis project were:

1. Characterize spatial and temporal expression of Usher genes and the TRPA1 gene in embryos and early (4-arm plutei) of *S. purpuratus* possibly identifying putative mechanosensory and photosensory cells.
2. Screen for possible mechanosensory cells using fluorescent dyes FM1-43 and TO-PRO.
3. Assess the effects of non-specific inhibitors of mechanosensory channels and specific inhibitors of TRPA1 on internalization of FM1-43 and TO-PRO dyes, and on the swimming behaviour of embryos and early pluteus larvae.

The results presented in this Thesis lead to the following conclusions.

Expression analysis did not identify candidate mechanosensory cells. In situ hybridization using riboprobes for most Usher genes and Sp-TRPA1 gene failed to identify spatial expression of these genes in embryos and plutei.

Sea urchin Usher genes do not appear to have a sensory role in embryos and early 4-arm plutei, and some of them may function in nervous system development instead. However, the timing of temporal upregulation of Sp-TRPA1 transcripts and specific effects of AP18 on swimming behaviour indicated that Sp-TRPA1 protein may be expressed in sensory structures, suggesting that sensory function of Sp-TRPA1 including

mechanosensation may conserved in sea urchins. Therefore, in sea urchins, TRPA1 may function as an analogue of invertebrate TRPN1.

Mechanosensory cell candidates were identified by screening with FM1-43 and TO-PRO-3 for uptake in cells putatively via cationic channels for the first time in sea urchins, demonstrating that fluorescent dye screening may be useful in identifying candidate mechanosensory cells in invertebrates, as it is in vertebrates (Meyers et al., 2003; Santos et al., 2006). These cells included the cells of the ciliated band at the tips of larval arms and the blastocoelar cell network. This screening method has singled out specific mechanosensory cell candidates in the ciliated band out of multiple proposed mechanosensory cell candidates (refer to section 1.3.5).

Non-specific cation channel inhibitor neomycin reduced FM1-43 internalization in the blastocoelar network of plutei, demonstrating that functional cation channels with mechanotransducer pore properties may be present in the ectodermal processes of this network. Both of these types of cells may mediate integration of external physical signals through their putative mechanosensory channels to control ciliary beating and spatial swimming. These cells may be involved in geotactic behaviours of plutei reported previously (Yoshida, 1966) and/or in feeding behaviour (Strathmann, 2007). The results in this Thesis support the hypothesis that the ciliary band is the sensory field controlling embryonic swimming behaviour (Nakajima et al., 2004).

Several non-specific TRPA1 inhibitors produced effects on swimming behaviour consistent with the effects of specific TRPA1 inhibitor AP18, suggesting involvement of multiple other cationic channels with mechanotransducer pore properties, in swimming behaviour control. This Thesis is a first report where AP18 caused specific behavioural effects in invertebrates.

Effects of AP18 suggest that Sp-TRPA1 may be regulated by electrophiles found in external environment via covalent modification of its cysteine and lysine residues at its N-terminus (Kang et al., 2010). Therefore, Sp-TRPA1 may participate in chemosensation as well as in mechanotransduction in sea urchins.

6: Future work

Several investigations may be conducted in the light of the results outlined in this Thesis. Although Usher genes do not appear to have sensory functions in embryos and early larvae, the results suggested involvement of Whirlin and VLGR1 in neuronal development. Morpholino knockdown on Sp-Whirlin or Sp-VLGR1 can be performed to look for defects in neural development or function.

Screening with fluorescent dyes has identified candidate mechanosensory cells including the blastocoelar cell network, ciliated band cells and pigment cells. Definitive identities of the mechanosensory candidate cells remain to be determined. Specific antibody markers for pigment cells, SRN network, and synaptotagmin network are available and should be used in immunostaining to detect their colocalization with cells labelled with FM1-43 or TO-PRO3 dyes.

One of the main unanswered questions in this thesis was whether fluorescent dyes were internalized into the blastocoelar cell network through the ectodermal processes, or by passing through the ectoderm, perhaps by diffusion through the septate junctions in the ectoderm. Injection of dye into the blastocoel and incubation of embryos in small fluorescent molecules of various sizes that are not expected to pass through cationic channels may help answer this question.

Although multiple lines of evidence suggest that endocytosis was not responsible for dye internalization into candidate mechanosensory cells, the possibility of endocytosis into these cells cannot be excluded at this point. One way this problem can

be addressed is by using an alternative membrane dye similar to FM1-43 called FM3-25. This dye has a wide structure, and it neither blocks or permeates the cation channels because of its structure. If the candidate mechanosensory cells internalize the dyes via cation channels, the treatment of embryos with FM3-25 should not result in labelling of these cells. Examining the labelling pattern of FM3-25 will also help to differentiate between FM1-43 background ectodermal staining and the labelling of mechanosensory cells. This dye would be a better agent in the dye exclusion assay because no literature references were found describing PI internalization or lack thereof into cells though cation channels.

Results of multiple experiments in this thesis suggest TRPA1 protein expression or activity in the apical tuft cilia, ciliated band cells and blastocoelar cells. TRPA1 protein expression should be characterized. Multiple commercial antibodies are available for TRPA1 from vertebrate and invertebrate species that may provide reagents for immunostaining for TRPA1 in urchin embryos. Alternatively, the sequence of Sp-TRPA1 could be used to produce a fusion protein suitable for raising an antiserum.

Morpholino antisense oligonucleotides (MASO) could be used to knock down expression of Sp-TRPA1. The possible effects may reflect the effects of specific TRPA1 inhibitors on swimming behaviour and development that I have reported in this Thesis. Although, more investigation of developmental effects of TRPA1 inhibitors needs to be done to provide more detailed insights into the role of Sp-TRPA1 in development. Dye uptake assays with FM1-43 and TO-PRO-3 should be useful for assessing the effects of MASO on the candidate mechanosensory cells presented in this Thesis. Swimming assays described here are also available to assay for MASO effects.

Effects of AP18 on swimming activity suggested that Sp-TRPA1 may be involved in regulation of directional swimming in embryos and early larvae. The fact that a TRPA1 antagonist was able to produce an observable swimming behaviour effect raises the question if the specific agonists of mammalian TRPA1 like allyl isothiocyanate or allicin, could also induce swimming behaviour changes in sea urchin embryos. If effects on swimming are observed it would be interesting to determine if these responses could be reversed by TRPA1 inhibitor treatments. The effects of treatment with HC030031 were similar to AP18 and should be investigated further. Other types of specific pharmacological Sp-TRPA1 inhibitors are available commercially. They can also be used to treat embryos and early larvae. All of these approaches would provide better evidence for involvement of Sp-TRPA1 in swimming behaviour regulation.

Only one potential role of Sp-TRPA1 was considered for in sea urchin embryos in this Thesis. Sp-TRPA1 is likely electrophile sensitive, and could have multiple other roles, including chemosensation and/or thermosensation. This can be investigated as well.

Fluorescent dye labelling has provided evidence for the existence of multiple cation channels with pore properties similar to hair cell METs and TRP channels. The identity and function of these channels can be investigated. TRP channels are implicated in mechanosensation in other systems, like the Sp-TRPP2, are interesting targets for investigation as they may participate in swimming behaviour regulation like Sp-TRPA1.

Only one non-specific inhibitor of TRPA1, neomycin was able to reduce FM1-43 labelling in the blastocoelar cell network suggesting that fluorescent dye internalization into this network occurs via cation channels. No such effect was observed with specific inhibitors, AP18 and HC030031. These inhibitors elicit their effects on swimming activity within the first 10 minutes of treatment, while FM1-43 labelling was performed after 1hr

of treatment. The timing of FM1-43 labelling should be adjusted to suit the time frame of AP18 and HC030031 inhibitor effects, to determine with if these inhibitors have an effect on fluorescent dye internalization. This experiment would provide more concrete evidence for Sp-TRPA1 mediating fluorescent dye internalization into the blastocoelar cell network.

The spatial swimming assay has detected changes in swimming behaviour in response to FM1-43 treatment. However, this assay was not a reliable test for mechanosensitivity of the candidate sensory cells. It may be possible to develop an assay based on touch to assess effects of TRPA1 inhibitors on embryonic and larval behaviour in response to physical stimuli. Also an assay can be developed measuring the ability of embryos and larvae to reverse direction of swimming in response to obstacles. I made some preliminary effort to develop such assays, but quantitation presents a challenge.

Inhibition of development of Hp-ECPN positive cells was detected when embryos were cultured in the dark according to Ooka et al (2009). It appears that lack of specific environmental stimuli, like light, may have an effect on development of specific structures required for detection of these stimuli. Identification of specific sensory structures in sea urchin larvae may require culturing of embryos in an environment where such sensory stimuli are available. In this Thesis embryos were not exposed to light, but were exposed to mechanical stimulation in culture.

Appendix: Electronic files

Electronic data and files listed below and appended as a DVD, form part of this work.

All the supplemental figure and table files can be opened with Adobe Acrobat. The supplemental video QuickTime Movie files (MOV) were created with Volocity V5.0 and can be opened with Apple QuickTime player. The Audio Video Interleave (AVI) files were created using CamStudio software and can be opened with Windows Media Player. Both types of video files can be opened by any other video program that supports the MOV or AVI file formats.

PDF Files:

- MariaVolnoukhin_Supplemental figure 1.pdf 186 KB
- MariaVolnoukhin_Supplemental figure 2.pdf 1.11 MB
- MariaVolnoukhin_Supplemental figure 3.pdf 160 KB
- MariaVolnoukhin_Supplemental figure 4.pdf 156 KB
- MariaVolnoukhin_Supplemental figure 5.pdf 228 KB
- MariaVolnoukhin_Supplemental figure 6.pdf 138 KB
- MariaVolnoukhin_Supplemental figure 7.pdf 189 MB
- MariaVolnoukhin_Supplemental figure 8.pdf 160 KB
- MariaVolnoukhin_Supplemental figure 9.pdf 165 KB
- MariaVolnoukhin_Supplemental figure 10.pdf 163 KB
- MariaVolnoukhin_Supplemental figure 11.pdf 161 KB
- MariaVolnoukhin_Supplemental figure 12.pdf 183 KB
- MariaVolnoukhin_Supplemental figure 13.pdf 174 KB
- MariaVolnoukhin_Supplemental figure 14.pdf 690 KB
- MariaVolnoukhin_Supplemental figure 15.pdf 187 KB
- MariaVolnoukhin_Supplemental figure 16.pdf 297 KB
- MariaVolnoukhin_Supplemental figure 17.pdf 155 KB
- MariaVolnoukhin_Supplemental figure 18.pdf 290 KB
- MariaVolnoukhin_Supplemental figure 19.pdf 171 KB
- MariaVolnoukhin_Supplemental figure 20.pdf 236 KB
- MariaVolnoukhin_Supplemental figure 21.pdf 161 KB
- MariaVolnoukhin_Supplemental figure 22.pdf 196 KB
- MariaVolnoukhin_Supplemental figure 23.pdf 180 KB

- MariaVolnoukhin_Supplemental figure 24.pdf 156 KB
- MariaVolnoukhin_Supplemental table 1.pdf 252 KB
- MariaVolnoukhin_Supplemental table 2.pdf 118 KB
- MariaVolnoukhin_Supplemental table 3.pdf 156 KB
- MariaVolnoukhin_Supplemental table 4.pdf 137 KB
- MariaVolnoukhin_Supplemental table 5.pdf 114 KB
- MariaVolnoukhin_Supplemental table 6.pdf 147 KB
- MariaVolnoukhin_Supplemental table 7.pdf 185 KB

AVI and MOV files

- MariaVolnoukhin_Supplemental video 1.mov 765 KB
- MariaVolnoukhin_Supplemental video 2.mov 540 KB
- MariaVolnoukhin_Supplemental video 3.mov 1.06 MB
- MariaVolnoukhin_Supplemental video 4.mov 853 KB
- MariaVolnoukhin_Supplemental video 5.mov 959 KB
- MariaVolnoukhin_Supplemental video 6.mov 1.29 MB
- MariaVolnoukhin_Supplemental video 7.mov 5.30 MB
- MariaVolnoukhin_Supplemental video 8.mov 31.0 MB
- MariaVolnoukhin_Supplemental video 9.mov 53.0 MB
- MariaVolnoukhin_Supplemental video 10.mov 12.3 MB
- MariaVolnoukhin_Supplemental video 11.mov 24.7 MB
- MariaVolnoukhin_Supplemental video 12.avi 25.3 MB
- MariaVolnoukhin_Supplemental video 13.avi 23.4 MB

References

Adato, A., Lefevre, G., Delprat, B., Michel, V., Michalski, N., Chardenoux, S., Weil, D., El-Amraoui, A. and Petit, C. (2005a). Usherin, the Defective Protein in Usher Syndrome Type IIA, is Likely to be a Component of Interstereocilia Ankle Links in the Inner Ear Sensory Cells. *Hum. Mol. Genet.* 14, 3921-3932.

Adato, A., Michel, V., Kikkawa, Y., Reiners, J., Alagramam, K. N., Weil, D., Yonekawa, H., Wolfrum, U., El-Amraoui, A. and Petit, C. (2005b). Interactions in the Network of Usher Syndrome Type 1 Proteins. *Hum. Mol. Genet.* 14, 347-356.

Adato, A., Vreugde, S., Joensuu, T., Avidan, N., Hamalainen, R., Belenkiy, O., Olender, T., Bonne-Tamir, B., Ben-Asher, E., Espinos, C. et al. (2002). USH3A Transcripts Encode Clarin-1, a Four-Transmembrane-Domain Protein with a Possible Role in Sensory Synapses. *Eur. J. Hum. Genet.* 10, 339-350.

Ahmed, Z. M., Riazuddin, S., Riazuddin, S. and Wilcox, E. R. (2003). The Molecular Genetics of Usher Syndrome. *Clin. Genet.* 63, 431-444.

Aizenberg, J., Tkachenko, A., Weiner, S., Addadi, L. and Hendler, G. (2001). Calcitic Microlenses as Part of the Photoreceptor System in Brittlestars. *Nature* 412, 819-822.

Alagramam, K. N., Murcia, C. L., Kwon, H. Y., Pawlowski, K. S., Wright, C. G. and Woychik, R. P. (2001). The Mouse Ames Waltzer Hearing-Loss Mutant is Caused by Mutation of Pcdh15, a Novel Protocadherin Gene. *Nature Genetics* 27, 99-102.

Al-Anzi, B., Tracey, W. D. and Benzer, S. (2006). Response of Drosophila to Wasabi is Mediated by Painless, the Fly Homolog of Mammalian TRPA1/ANKTM1. *Curr. Biol.* 16, 1034-1040.

Amemiya, S., Akasaka, K. and Terayama, H. (1979). Reversal of Polarity in Ciliated Cells of the Isolated Sea Urchin Pluteus Gut. *J. Exp. Zool.* 210, 177-182.

Anand, U., Otto, W. R., Facer, P., Zebda, N., Selmer, I., Gunthorpe, M. J., Chessell, I. P., Sinisi, M., Birch, R. and Anand, P. (2008). TRPA1 Receptor Localisation in the Human Peripheral Nervous System and Functional Studies in Cultured Human and Rat Sensory Neurons. *Neurosci. Lett.* 438, 221-227.

Andre, E., Campi, B., Materazzi, S., Trevisani, M., Amadesi, S., Massi, D., Creminon, C., Vaksman, N., Nassini, R., Civelli, M. et al. (2008). Cigarette Smoke-Induced Neurogenic Inflammation is Mediated by Alpha,Beta-Unsaturated Aldehydes and the TRPA1 Receptor in Rodents. *J. Clin. Invest.* 118, 2574-2582.

Angerer, L. M. and Angerer, R. C. (2000). Animal-Vegetal Axis Patterning Mechanisms in the Early Sea Urchin Embryo. *Dev. Biol.* 218, 1-12.

Angerer, L. M. and Angerer, R. C. (2003). Patterning of Sea Urchin Embryo: Gene Regulatory Networks, Signaling Pathways, and Cellular Interactions. *Curr. Top. Dev. Biol.* 53, 159-198.

Anyatonwu, G. I. and Ehrlich, B. E. (2005). Organic Cation Permeation through the Channel Formed by Polycystin-2. *J. Biol. Chem.* 280, 29488-29493.

Arden, G. B. and Fox, B. (1979). Increased Incidence of Abnormal Nasal Cilia in Patients with Retinitis Pigmentosa. *Nature* 279, 534-536.

Arenas-Mena, C., Cameron, A. and Davidson, E. (2000). Spatial Expression of Hox Cluster Genes in the Ontogeny of a Sea Urchin. *Development* 127, 4631-4643.

Auclair, W. and Siegel, B. W. (1966). Cilia Regeneration in the Sea Urchin Embryo: Evidence for a Pool of Ciliary Proteins. *Science* 154, 913-915.

Bailey, T. J., El-Hodiri, H., Zhang, L., Shah, R., Mathers, P. H. and Jamrich, M. (2004). Regulation of Vertebrate Eye Development by Rx Genes. *Int. J. Dev. Biol.* 48, 761-770.

Balak, K. J., Corwin, J. T. and Jones, J. (1990). Regenerated Hair Cells can Originate from Supporting Cell Progeny: Evidence from Phototoxicity and Laser Ablation Experiments in the Lateral Line System. *J. Neurosci.* 10, 2502-2512.

Bandell, M., Story, G. M., Hwang, S. W., Viswanath, V., Eid, S. R., Petrus, M. J., Earley, T. J. and Patapoutian, A. (2004). Noxious Cold Ion Channel TRPA1 is Activated by Pungent Compounds and Bradykinin. *Neuron* 41, 849-857.

Bandell, M., Macpherson, L. J. and Patapoutian, A. (2007). From Chills to Chilis: Mechanisms for Thermosensation and Chemesthesis Via thermoTRPs. *Curr. Opin. Neurobiol.* 17, 490-497.

Baris, B., Ataman, M., Sener, C. and Kalyoncu, F. (1994). Bronchial Asthma in a Patient with Usher Syndrome: Case Report. *J. Asthma* 31, 487-490.

Barrong, S. D., Chaitin, M. H., Fliesler, S. J., Possin, D. E., Jacobson, S. G. and Milam, A. H. (1992). Ultrastructure of Connecting Cilia in Different Forms of Retinitis Pigmentosa. *Arch. Ophthalmol.* 110, 706-710.

Bautista, D. M., Movahed, P., Hinman, A., Axelsson, H. E., Sterner, O., Heogesteatt, E. D., Julius, D., Jordt, S. E. and Zygmunt, P. M. (2005). Pungent Products from Garlic Activate the Sensory Ion Channel TRPA1. *Proc. Natl. Acad. Sci. U.S.A.* 102, 12248-12252.

Bautista, D. M., Jordt, S. E., Nikai, T., Tsuruda, P. R., Read, A. J., Poblete, J., Yamoah, E. N., Basbaum, A. I. and Julius, D. (2006). TRPA1 Mediates the Inflammatory Actions of Environmental Irritants and Proalgesic Agents. *Cell* 124, 1269-1282.

Beer, A. J., Moss, C. and Thorndyke, M. (2001). Development of Serotonin-Like and SALMFamide-Like Immunoreactivity in the Nervous System of the Sea Urchin Psammechinus Miliaris. *Biol. Bull.* 200, 268-280.

Bennett, V. and Chen, L. (2001). Ankyrins and Cellular Targeting of Diverse Membrane Proteins to Physiological Sites. *Curr. Opin. Cell Biol.* 13, 61-67.

Bessac, B. F., Sivula, M., von Hehn, C. A., Caceres, A. I., Escalera, J. and Jordt, S. E. (2008). Transient Receptor Potential Ankyrin 1 Antagonists Block the Noxious Effects of Toxic Industrial Isocyanates and Tear Gases. *FASEB J* 23, 1102-1114.

Betz, W. J. and Bewick, G. S. (1992). Optical Analysis of Synaptic Vesicle Recycling at the Frog Neuromuscular Junction. *Science* 255, 200-203.

Betz, W. J., Mao, F. and Smith, C. B. (1996). Imaging Exocytosis and Endocytosis. *Curr. Opin. Neurobiol.* 6, 365-371.

Betz, W. J., Mao, F. and Bewick, G. S. (1992). Activity-Dependent Fluorescent Staining and Destaining of Living Vertebrate Motor Nerve Terminals. *J. Neurosci.* 12, 363-375.

Bisgrove, B. M. and Burke, R. D. (1986). Development of Serotonergic Neurons in Embryos of the Sea Urchin, *Strongylocentrotus Purpuratus*. *Dev. Growth Differ.* 28, 569-574.

Bisgrove, B. M. and Burke, R. D. (1987). Development of the Nervous System of the Pluteus Larva of *Strongylocentrotus Droebachiensis*. *Cell Tissue Res.* 248, 335-343.

Blackshaw, S. and Snyder, S. H. (1999). Encephalopsin: A Novel Mammalian Extraretinal Opsin Discretely Localized in the Brain. *J. Neurosci.* 19, 3681-3690.

Blevins, E. and Johnsen, S. (2004). Spatial Vision in the Echinoid Genus Echinometra. *J. Exp. Biol.* 207, 4249-4253.

Boeda, B., El-Amraoui, A., Bahloul, A., Goodyear, R., Daviet, L., Blanchard, S., Perfettini, I., Fath, K. R., Shorte, S., Reiners, J. et al. (2002). Myosin VIIa, Harmonin and Cadherin 23, Three Usher I Gene Products that Cooperate to Shape the Sensory Hair Cell Bundle. *EMBO J.* 21, 6689-6699.

Bonneau, D., Raymond, F., Kremer, C., Klossek, J. M., Kaplan, J. and Patte, F. (1993). Usher Syndrome Type I Associated with Bronchiectasis and Immotile Nasal Cilia in Two Brothers. *J. Med. Genet.* 30, 253-254.

Boolootian, R. A. (1966). Reproductive Physiology. In *Physiology of Echinodermata* (ed. R. A. Boolootian), pp. 561-614. New York: Interscience.

Burke, R. D. (1983). Development of the Larval Nervous System of the Sand Dollar, Dendraster Excentricus. *Cell Tissue Res.* 229, 145-154.

Burke, R. D., Brand, D. G. and Bisgrove, B. W. (1986). Structure of the Nervous System of the Auricularia Larva of *Parasticopus Californicus*. *Biol. Bull.* 170, 450-460.

Burke, R. D. (1978). The Structure of the Nervous System of the Pluteus Larva of *Strongylocentrotus Purpuratus*. *Cell Tissue Res.* 191, 233-247.

Burke, R. D., Angerer, L. M., Elphick, M. R., Humphrey, G. W., Yaguchi, S., Kiyama, T., Liang, S., Mu, X., Agca, C., Klein, W. H. et al. (2006). A Genomic View of the Sea Urchin Nervous System. *Dev. Biol.* 300, 434-460.

Buznikov, G. A., Peterson, R. E., Nikitina, L. A., Bezuglov, V. V. and Lauder, J. M. (2005). The Pre-Nervous Serotonergic System of Developing Sea Urchin Embryos and Larvae: Pharmacologic and Immunocytochemical Evidence. *Neurochem. Res.* 30, 825-837.

Byrne, M., Nakajima, Y., Chee, F. C. and Burke, R. D. (2007). Apical Organs in Echinoderm Larvae: Insights into Larval Evolution in the *Ambulacraria*. *Evol Dev.* 9, 432-445.

Caceres, A. I., Brackmann, M., Elia, M. D., Bessac, B. F., del Camino, D., D'Amours, M., Witek, J. S., Fanger, C. M., Chong, J. A., Hayward, N. J. et al. (2009). A Sensory Neuronal Ion Channel Essential for Airway Inflammation and Hyperreactivity in Asthma. *Proc. Natl. Acad. Sci. U. S. A.* 106, 9099.

Cai, X. (2008). Unicellular Ca2+ Signaling 'Toolkit' at the Origin of Metazoa. *Mol. Biol. Evol.* 25, 1357-1361.

Calestani, C., Rast, J. P. and Davidson, E. H. (2003). Isolation of Pigment Cell Specific Genes in the Sea Urchin Embryo by Differential Macroarray Screening. *Development* 130, 4587-4596.

Cameron, R. A., Fraser, S. E., Britten, R. J. and Davidson, E. H. (1991). Macromere Cell Fates during Sea Urchin Development. *Development* 113, 1085-1091.

Cameron, A. R., Smith, L. C., Britten, R. J. and Davidson, E. H. (1994). Ligand-Dependent Stimulation of Introduced Mammalian Brain Receptors Alters Spicule Symmetry and Other Morphogenetic Events in Sea Urchin Embryos. *Mech. Dev.* 45, 31-47.

Casano, C., Gianuzza, F., Roccheri, M. C., DiGiorgi, R., Maenza, L. and Ragusa, M. A. (2003). Hsp40 is Involved in Cilia Regeneration in Sea Urchin Embryos. *J. Histochem. Cytochem.* 51, 1581-1587.

Castiglioni, A. J. and García-Añoveros, J. (2007). MechanoTRPs and TRPA1. In *Current Topics in Membranes* (ed. Owen P. Hamill), pp. 171-189: Academic Press.

Caterina, M. J. (2007). Transient Receptor Potential Ion Channels as Participants in Thermosensation and Thermoregulation. *Am. J. Physiol. Regul. Integr. Comp. Physiol.* 292, R64-76.

Cavanaugh, G. M. (1975). Formulae and Methods VI. In *The Marine Biological Laboratory*, pp. 84. Massachusetts: Woods Hole.

Cebi, M. and Koert, U. (2007). Reactivity Recognition by TRPA1 Channels. *ChemBioChem* 8, 979-980.

Chen, J., Kim, D., Bianchi, B. R., Cavanaugh, E. J., Faltynek C.R., Kym, P. R. and Reilly, R. M. (2009). Pore Dilation Occurs in TRPA1 but Not in TRPM8 Channels. *Mol. Pain* 5, 3.

Chia, F. (1977). Scanning Electron Microscopic Observations of the Mesenchyme Cells in the Larvae of the Starfish Pisaster Ochraceus. *Acta Zool.* 58, 45-51.

Chia, F. S. and Burke, R. D. (1978). Echinoderm Metamorphosis: Fate of Larval Structures. In *Settlement and Metamorphosis of Marine Invertebrate Larvae* (ed. F. S. Chia and M. S. Rice), pp. 219-234. New York: Elsevier-North Holland.

Christensen, A. P. and Corey, D. P. (2007). TRP Channels in Mechanosensation: Direct Or Indirect Activation? *Nat. Rev. Neurosci.* 8, 510-521.

Christopher, K., Chang, J. and Goldberg, J. (1996). Stimulation of Cilia Beat Frequency by Serotonin is Mediated by a Ca2+ Influx in Ciliated Cells of Helisoma Trivolvis Embryos. *J. Exp. Biol.* 199, 1105-1113.

Chung, M. K., Guler, A. D. and Caterina, M. J. (2008). TRPV1 shows Dynamic Ionic Selectivity during Agonist Stimulation. *Nat. Neurosci. 2008*, 555-564.

Clapham, D. E. (2003). TRP Channels as Cellular Sensors. *Nature* 426, 517-524.

Cobb, J. L. S. and Pentreath, V. W. (1977). Anatomical Studies of Simple Invertebrate Synapses Utilizing Stage Rotation Electron Microscopy and Densitometry. *Tissue Cell* 9, 125-135.

Cochilla, A. J., Angelson, J. K. and Betz, W. J. (1999). Monitoring Secretory Membrane with FM1-43 Fluorescence. *Ann. Rev. Neurosci.* 22, 1-10.

Collazo, A., Fraser, S. E. and Mabee, P. M. (1994). A Dual Embryonic Origin for Vertebrate Mechanoreceptors. *Science* 264, 426-430.

Corey, D. P. (2006). What is the Hair Cell Transduction Channel? *J. Physiol.* 576, 23-28.

Corey, D. P., Garcia-Anoveros, J., Holt, J. R., Kwan, K. Y., Lin, S. Y., Vollrath, M. A., Amalfitano, A., Cheung, E. L., Derfler, B. H., Duggan, A. et al. (2004). TRPA1 is a Candidate for the Mechanosensitive Transduction Channel of Vertebrate Hair Cells. *Nature* 432, 723-730.

Cosgrove, D. E., Bhattacharya, G., Meehan, D., Delimont, D., Gratton, M. A., Kimberling, W. and Birch, D. (2004). Usherin Binds Integrins on RPE Cells and may Mediate Adhesion and Cellular Homeostasis. *ARVO Meeting Abstracts* 45, 2483.

Crawford, B. J., Campbell, S. S. and Reimer, C. L. (1997). Ultrastructure and Synthesis of the Extracellular Matrix of Pisaster Ochraceus Embryos Preserved by Freeze Substitution. *J. Morphol.* 232, 133-153.

Cruz-Orengo, L., Dhaka, A., Heuermann, R. J., Young, T. J., Montana, M. C., Cavanaugh, E. J., Kim, D. and Story, G. M. (2008). Cutaneous Nociception Evoked by 15-Delta PGJ2 Via Activation of Ion Channel TRPA1. *Mol. Pain.* 4, 30.

Cui, K. and Yuan, X. (2007). TRP Channels and Axon Pathfinding. In *TRP Ion Channel Function in Sensory Transduction and Cellular Signaling Cascades* (ed. S. Heller and W. B. Liedtke), pp. 55-67. Boca Raton: CRC Press.

Czerny, T. and Busslinger, M. (1995). DNA-Binding and Transactivation Properties of Pax-6: Three Amino Acids in the Paired Domain are Responsible for the Different Sequence Recognition of Pax-6 and BSAP (Pax-5). *Mol. Cell. Biol.* 15, 2858-2871.

D'Alterio, C., Tran, D. D., Yeung, M. W., Hwang, M. S., Li, M. A., Arana, C. J., Mulligan, V. K., Kubesh, M., Sharma, P., Chase, M. et al. (2005). Drosophila Melanogaster Cad99C, the Orthologue of Human Usher Cadherin PCDH15, Regulates the Length of Microvilli. *J. Cell Biol.* 171, 549-558.

Damann, N., Voets, T. and Nilius, B. (2008). TRPs in our Senses. *Curr. Biol.*18, R880-R889.

Dan, K. and Okazaki, K. (1956). Cyto-Embryological Studies of Sea Urchins III. Role of Secondary Mesenchyme Cells in the Formation of the Primitive Gut in Sea Urchin Larvae. *Biol. Bull.* 110, 29-42.

Dan-Sohkawa, M., Kaneko, H. and Noda, K. (1995). Paracellular, Transepithelial Permeation of Macromolecules in the Body Wall Epithelium of Starfish Embryos. *J. Exp. Zool.* 271, 264-272.

Davidson, E. H., Cameron, R. A. and Ransick, A. (1998). Specification of Cell Fate in the Sea Urchin Embryo: Summary and some Proposed Mechanisms. *Development* 125, 3269-3290.

Davidson, E. H., Rast, J. P., Oliveri, P., Ransick, A., Calestani, C., Yuh, C., Minokawa, T., Amore, G., Hinman, V., Arenas-Mena, C. et al. (2002). A Provisional Regulatory Gene Network for Specification of Endomesoderm in the Sea Urchin Embryo. *Dev. Biol.* 246, 162-190.

DeFalco, J., Steiger, D., Gustafson, A., Emerling, D. E., Kelly, M. G. and Duncton, M. A. J. (2010). Oxime Derivatives Related to AP18: Agonists and Antagonists of the TRPA1 Receptor. *Bioorg. Med. Chem. Lett.* 20, 276-279.

Delprat, B., Michel, V., Goodyear, R., Yamasaki, Y., Michalski, N., El-Amraoui, A., Perfettini, I., Legrain, P., Richardson, G., Hardelin, J. P. et al. (2005). Myosin XVa and Whirlin, Two Deafness Gene Products Required for Hair Bundle Growth, are Located at the Stereocilia Tips and Interact Directly. *Hum. Mol. Genet.* 14, 401-410.

Delsuc, F. l., Brinkmann, H., Chourrout, D. and Philippe, H. (2006). Tunicates and Not Cephalochordates are the Closest Living Relatives of Vertebrates. *Nature* 439, 965-968.

Deutch, A. Y. and Roth, R. H. (1999). Neurotransmitters. In *Fundamental Neuroscience*, pp. 193-234. San Diego: Academic Press.

Di Palma, F., Holme, R. H., Bryda, E. C., Belyantseva, I. A., Pellegrino, R., Kachar, B., Steel, K. P. and Noben-Trauth, K. (2001). Mutations in Cdh23, Encoding a New Type of Cadherin, Cause Stereocilia Disorganization in Waltzer, the Mouse Model for Usher Syndrome Type 1D. *Nat. Genet.* 27, 103-107.

Di Palma, F., Belyantseva, I. A., Kim, H. J., Vogt, T. F., Kachar, B. and Noben-Trauth, K. (2002). Mutations in Mcoln3 Associated with Deafness and Pigmentation Defects in Varitint-Waddler (Va) Mice. *PNAS* 99, 14994-14999.

Doerner, J. F., Gisselmann, G., Hatt, H. and Wetzel, C. H. (2007). Transient Receptor Potential Channel A1 is Directly Gated by Calcium Ions. *J. Biol. Chem.* 282, 13180-13189.

Doran, S. A., Koss, R., Tran, C. H., Christopher, K. J., Gallin, W. J. and Goldberg, J. I. (2004). Effect of Serotonin on Ciliary Beating and Intracellular Calcium Concentration in Identified Populations of Embryonic Ciliary Cells. *J. Exp. Biol.* 207, 1415-1429.

Drew, L. J. and Wood, J. N. (2007). FM1-43 is a Permeant Blocker of Mechanosensitive Ion Channels in Sensory Neurons and Inhibits Behavioural Responses to Mechanical Stimuli. *Mol. Pain* 3, 1.

Drew, L. J., Wood, J. N. and Cesare, P. (2002). Distinct Mechanosensitive Properties of Capsaicin-Sensitive and -Insensitive Sensory Neurons. *J. Neurosci.* 22, RC228.

Eid, S. R., Crown, E. D., Moore, E. L., Liang, H. A., Choong, K. C., Dima, S., Henze, D. A., Kane, S. A. and Urban, M. O. (2008). HC-030031, a TRPA1 Selective Antagonist, Attenuates Inflammatory- and Neuropathy-Induced Mechanical Hypersensitivity. *Mol. Pain* 4, 48.

Elde, N. C., Morgan, G., Winey, M., Sperling, L. and Turkewitz, A. P. (2005). Elucidation of Clathrin-Mediated Endocytosis in Tetrahymena Reveals an Evolutionarily Convergent Recruitment of Dynamin. *PLoS Genet.* 1, e52.

Eldon, E. D., Montpetit, I. C., Nguyen, T., Decker, G., Valdizan, M. C., Klein, W. H. and Brandhorst, B. P. (1990). Localization of the Sea Urchin Spec3 Protein to Cilia and Golgi Complexes of Embryonic Ectoderm Cells. *Genes Dev.* 4, 111-122.

Erler, I., Hirnet, D., Wissenbach, U., Flockerzi, V. and Niemeyer, B. A. (2004). Ca^{2+}selective Transient Receptor Potential V Channel Architecture and Function Require a Specific Ankyrin Repeat. *J. Biol. Chem*. 279, 34456-34463.

Ernest, S., Rauch, G., Haffter, P., Geisler, R., Petit, C. and Nicolson, T. (2000). Mariner is Defective in Myosin VIIA: A Zebrafish Model for Human Hereditary Deafness. *Hum. Mol. Genet.* 9, 2189-2196.

Ettensohn, C. A. (1992). Cell Interactions and Mesodermal Cell Fates in the Sea Urchin Embryo. *Dev. Suppl.*, 43-51.

Ettensohn, C. A. and McClay, D. R. (1986). The Regulation of Primary Mesenchyme Cell Migration in the Sea Urchin Embryo: Transplantations of Cells and Latex Beads. *Dev. Biol.* 117, 380-391.

Ettensohn, C. A. and Ingersoll, E. P. (1992). Morphogenesis of Sea Urchin Embryo. In *Morphogenesis* (ed. K. M. Rossomando and S. Alexander). New York: Marcel Dekker, Inc.

Ettensohn, C. A. and Sweet, H. C. (2000). Patterning the Early Sea Urchin Embryo. *Curr. Top. Dev. Biol.* 50, 1-44.

Fajardo, O., Meseguer, V., Belmonte, C. and Viana, F. (2008). TRPA1 Channels Mediate Cold Temperature Sensing in Mammalian Vagal Sensory Neurons: Pharmacological and Genetic Evidence. *J. Neurosci.* 28, 7863-7875.

Farris, H. E., LeBlanc, C. L., Goswami, J. and Ricci, A. J. (2004). Probing the Pore of the Auditory Hair Cell Mechanotransducer Channel in Turtle. *J. Physiol.* 558, 769-792.

Fell, H. B. and Pawson, D. L. (1966). The General Biology of Echinoderms. In *Physiology of Echinoderms.* (ed. R. A. Boolootian), pp. 1-48. New York: Interscience.

Flockerzi, V. (2007). An Introduction on TRP Channels. In *Transient Receptor Potential (TRP) Channels* (ed. V. Flockerzi and B. Nilius), pp. 1-19: Springer Berlin Heidelberg.

Forge, A. and Schacht, J. (2000). Aminoglycoside Antibiotics. *Audiol. Neurootol.* 5, 3-22.

Furukawa, R., Takahashi, Y., Nakajima, Y., Dan-Sohkawa, M. and Kaneko, H. (2009). Defense System by Mesenchyme Cells in Bipinnaria Larvae of the Starfish, Asterina Pectinifera. *Dev. Comp. Immunol.* 33, 205-215.

Futter, C. E., Ramalho, J. S., Jaissle, G. B., Seeliger, M. W. and Seabra, M. C. (2004). The Role of Rab27a in the Regulation of Melanosome Distribution within Retinal Pigment Epithelial Cells. *Mol. Biol. Cell* 15, 2264-2275.

Gale, J. E., Marcotti, W., Kennedy, H. J., Kros, C. J. and Richardson, G. P. (2001). FM1-43 Dye Behaves as a Permeant Blocker of the Hair-Cell Mechanotransducer Channel. *J. Neurosci.* 21, 7013-7025.

Garcia-Anoveros, J. and Nagata, K. (2007). TRPA1. In *Transient Receptor Potential (TRP) Channels* (ed. V. Flockerzi and B. Nilius), pp. 347-362: Springer Berlin Heidelberg.

Garcia-Martinez, C., Morenilla-Palao, C., Planells-Cases, R., Merino, J. M. and Ferrer-Montiel, A. (2000). Identification of an Aspartic Residue in the P-Loop of the Vanilloid Receptor that Modulates Pore Properties. *J. Biol. Chem.* 275, 32552-32558.

Garson, M. J. (1989). Biosynthetic Studies on Marine Natural Products. *Nat. Prod. Rep.* 6, 143-170.

Garstang, W. (1894). Preliminary Note on a New Theory of the Phyogeny of the Chordata. *Zool. Anz.* 27, 1.

Gehring, W. J. (2005). New Perspectives on Eye Development and the Evolution of Eyes and Photoreceptors. *J. Hered.* 96, 171-184.

Geleoc, G. S. G. and Holt, J. R. (2003). Developmental Acquisition of Sensory Transduction in Hair Cells of the Mouse Inner Ear. *Nat. Neurosci.* 6, 1019-1020.

Geng, R., Geller, S. F., Hayashi, T., Ray, C. A., Reh, T. A., Bermingham-McDonogh, O., Jones, S. M., Wright, C. G., Melki, S., Imanishi, Y. et al. (2009). Usher Syndrome IIIA Gene Clarin-1 is Essential for Hair Cell Function and Associated Neural Activation. *Hum. Mol. Genet.* 18, 2748-2760.

Gibbs, D., Azarian, S. M., Lillo, C., Kitamoto, J., Klomp, A. E., Steel, K. P., Libby, R. T. and Williams, D. S. (2004). Role of Myosin VIIa and Rab27a in the Motility and Localization of RPE Melanosomes. *J. Cell. Sci.* 117, 6473-6483.

Gibbs, D., Kitamoto, J. and Williams, D. S. (2003). Abnormal Phagocytosis by Retinal Pigmented Epithelium that Lacks Myosin VIIa, the Usher Syndrome 1B Protein. *Proc. Natl. Acad. Sci. U. S. A.* 100, 6481-6486.

Gibson, A. W. and Burke, R. D. (1985). The Origin of Pigment Cells in Embryos of the Sea Urchin *Strongylocentrotus Purpuratus*. *Dev. Biol.* 107, 414-419.

Gibson, F., Walsh, J., Mburu, P., Varela, A., Brown, K. A., Antonio, M., Beisel, K. W., Steel, K. P. and Brown, S. D. (1995). A Type VII Myosin Encoded by Mouse Deafness Gene Shaker-1. *Nature* 374, 62-64.

Gibson, A. W. and Burke, R. D. (1987). Migratory and Invasive Behavior of Pigment Cells in Normal and Animalized Sea Urchin Embryos. *Exp. Cell Res.* 173, 546-557.

Giese, A. C. and Farmanfarmanian, A. (1963). Resistance of the Purple Sea Urchin to Osmotic Stress. *Biol. Bull.* 124, 182-192.

Gilbert, S. F. (2000). *Developmental Biology, 6th Edition*. Sunderland (MA): Sinauer Associates.

Gillespie, P. G. and Walker, R. G. (2001). Molecular Basis of Mechanosensory Transduction. *Nature* 413, 194-202.

Glazer, A. N. and Rye, H. S. (1992). Stable dye–DNA Intercalation Complexes as Reagents for High-Sensitivity Fluorescence Detection. *Nature* 359, 859-861.

Gong, Z. Y. and Brandhorst, B. P. (1987). Stimulation of Tubulin Gene Transcription by Deciliation of Sea Urchin Embryos. *Mol. Cell. Biol.* 7, 4238-4246.

Gosens, I., van Wijk, E., Kersten, F. F., Krieger, E., van der Zwaag, B., Märker, T., Letteboer, S. J., Dusseljee, S., Peters, T., Spierenburg, H. A. et al. (2007). MPP1 Links the Usher Protein Network and the Crumbs Protein Complex in the Retina. *Hum. Mol. Genet.* 16, 1993-2003.

Gras, H. and Weber, W. (1977). Light-Induced Alterations in Cell Shape and Pigment Displacement in Chromatophores of the Sea Urchin *Centrostephanus Longispinus*. *Cell. Tiss. Res.* 182, 165-176.

Griffiths, M. (1965). A Study of the Synthesis of Naphthaquinone Pigments by the Larvae of Two Species of Sea Urchins and their Reciprocal Hybrids. *Dev. Biol.* 11, 433-447.

Gustafson, T., Lundgren, B. and Treufeldt, R. (1972a). Serotonin and Contractile Activity in the Echinopluteus. A Study of the Cellular Basis of Larval Behaviour. *Exp.Cell Res.* 72, 115-39.

Gustafson, T., Ryberg, E. and Treufeldt, R. (1972b). Acetylcholine and Contractile Activity in the Echinopluteus. A Study of the Cellular Basis of Larval Behaviour. *Acta Embryol.*, 199-223.

Gustafson, T. and Toneby, M. I. (1971). How Genes Control Morphogenesis. the Role of Serotonin and Acetylcholine in Morphogenesis. *Am. Sci.* 59, 452-462.

Gustafson, T. and Wolpert, L. (1963). Studies on the Cellular Basis of the Morphogenesis in the Sea Urchin Embryo. *Exp. Cell Res.* 29, 561-582.

Gustafson, T. and Wolpert, L. (1967). Cellular Movement and Contact in Sea Urchin Morphogenesis. *Biol. Rev. Camb. Philos. Soc.* 42, 442-498.

Hamada, F. N., Rosenzweig, M., Kang, K., Pulver, S. R., Ghezzi, A., Jegla, T. J. and Garrity, P. A. (2008). An Internal Thermal Sensor Controlling Temperature Preference in *Drosophila*. *Nature* 454, 217-220.

Hardie, R. C. and Raghu, P. (2001). Visual Transduction in Drosophila. *Nature* 413, 186-193.

Hardin, J. D. (1990). Context-Dependent Cell Behaviors during Gastrulation. *Semin. Dev. Biol.* 1, 335-345.

Hardin, J. and McClay, D. R. (1990). Target Recognition by the Archenteron during Sea Urchin Gastrulation. *Dev Biol.* 142, 86-102.

Hardin, J. D. (1988). The Role of Secondary Mesenchyme Cells during Sea Urchin Gastrulation Studied by Laser Ablation. *Development* 103, 317-324.

Harlow, P. and Nemer, M. (1987). Developmental and Tissue-Specific Regulation of B-Tubulin Gene Expression in the Embryo of the Sea Urchin *Strongylocentrotus Purpuratus*. *Genes Dev.* 1, 147-160.

Harris, P. J., Waters, R. E. and Taylor, F. J. R. (1980). A Broad Spectrum Artificial Medium for Coastal and Open Ocean Phytoplankton. *J. Phycol.* 16, 28-35.

Hart, M. W. (1990). Manipulating External Ca^{2+} Inhibits Particle Capture by Planktotrophic Echinoderm Larvae. *Can. J. Zool.* 68, 2610-2615.

Hasson, T., Hintzelman, M. B., Santos-Sacchi, J., Corey, D. P. and Mooseker, M. S. (1995). Expression in Cochlea and Retina of Myosin VIIa, the Gene Product Defective in Usher Syndrome Type 1B. *Proc. Natl Acad. Sci. U.S.A.* 92, 9815-9819.

Hasson, T., Walsh, J., Cable, J., Mooseker, M. S., Brown, S. D. and Steel, K. P. (1997). Effects of Shaker-1 Mutations on Myosin-VIIa Protein and mRNA Expression. *Cell Motil. Cytoskeleton* 37, 127-138.

Haughland, R. P. (1992-1994). Handbook of Fluorescent Probes and Research Chemicals.

Hay-Schmidt, A. (2000). The Evolution of the Serotonergic Nervous System. *Proc. Biol. Sci.* 267, 1071-1079.

Henkel, A. W., Lubke, J. and Betz, W. J. (1996). FM1-43 Dye Ultrastructural Localization in and Release from Frog Motor Nerve Terminals. *Proc. Natl. Acad. Sci. U. S. A.* 93, 1918-1923.

Hibino, T., Loza-Coll, M., Messier, C., Majeske, A. J., Cohen, A. H., Terwilliger, D. P., Buckley, K. M., Brockton, V., Nair, S. V., Berney, K. et al. (2006). The Immune Gene Repertoire Encoded in the Purple Sea Urchin Genome. *Dev. Biol.* 300, 349-365.

Hinman, A., Chuang, H., Bautista, D. M. and Julius, D. (2006). TRP Channel Activation by Reversible Covalent Modification. *Proc. Natl. Acad. Sci. U.S.A.* 103, 19564-19568.

Hinman, V. F., Nguyen, A. T. and Davidson, E. H. (2003). Expression and Function of a Starfish Otx Ortholog, AmOtx: A Conserved Role for Otx Proteins in Endoderm Development that Predates Divergence of the Eleutherozoa. *Mech. Dev.* 120, 1165-1176.

Hoenderop, J. G., Voets, T., Hoefs, S., Weidema, F., Prenen, J., Nilius, B. and Bindels, R. J. (2003). Homo and Heterotetrameric Architecture of the Epithelial Ca2+ Channels TRPV5 and TRPV6. *EMBO*, 776-785.

Horstadius, S. (1973). *Experimental Embryology of Echinoderms*. London: Oxford University Press.

Howard, J. and Bechstedt, S. (2004). Hypothesis: A Helix of Ankyrin Repeats of the NOMPC-TRP Ion Channel is the Gating Spring of Mechanoreceptors. *Curr. Biol.* 14, R224-R226.

Hoyer, D., Hannon, J. P. and Martin, G. R. (2002). Molecular, Pharmacological and Functional Diversity of 5-HT Receptors. *Pharmacol. Biochem. Behav.* 71, 533-554.

Hoyer, D. and Martin, G. (1997). 5-HT Receptor Classification and Nomenclature: Towards a Harmonization with the Human Genome. *Neuropharmacology* 36, 419-428.

Hudspeth, A. J. (1997). How Hearing Happens. *Neuron* 19, 947-950.

Hunter, D. G., Fishman, G. A., Mehta, R. S. and Kretzer, F. L. (1986). Abnormal Sperm and Photoreceptor Axonemes in Usher's Syndrome. *Arch. Ophthalmol.* 104, 385-389.

Hyman, L. H. (1955). *The Invertebrates: Echinodermata*. New York: McGraw-Hill.

Jacobson, S. G., Cideciyan, A. V., Aleman, T. S., Sumaroka, A., Roman, A. J., Gardner, L. M., Prosser, H. M., Mishra, M., Bech-Hansen, N. T., Herrera, W. et al. (2008). Usher Syndromes due to MYO7A, PCDH15, USH2A Or GPR98 Mutations Share Retinal Disease Mechanism. *Hum. Mol. Genet.*

Jahnel, U., Nawrath, H., Rupp, J. and Ochi, R. (1993). L-Type Calcium Channel Activity in Human Atrial Myocytes as Influenced by 5-HT. *Naunyn Schmiedebergs Arch. Pharmacol.* 348, 396-402.

Jaquemar, D., Schenker, T. and Trueb, B. (1999). An Ankyrin-Like Protein with Transmembrane Domains is Specifically Lost After Oncogenic Transformation of Human Fibroblasts. *J. Biol. Chem.* 274, 7325-7333.

Johnson, K. R., Gagnon, L. H., Webb, L. S., Peters, L. L., Hawes, N. L., Chang, B. and Zheng, Q. Y. (2003). Mouse Models of USH1C and DFNB18: Phenotypic and Molecular Analyses of Two New Spontaneous Mutations of the Ush1c Gene. *Hum. Mol. Geneti.* 12, 3075-3086.

Jordt, S. E., Bautista, D. M., Chuang, H. H., McKemy, D. D., Zygmunt, P. M., Hogestatt, E. D., Meng, I. D. and Julius, D. (2004). Mustard Oils and Cannabinoids Excite Sensory Nerve Fibres through the TRP Channel ANKTM1. *Nature* 427, 260-265.

Jorgensen, F. (1989). Evolution of Octavolateralis Sensory Cells. In *The Mechanosensory Lateral Line: Neurobiology and Evolution.* (ed. P. G. S. Coombs and H. Muenz), pp. 115-145. New York: Springer.

Kahn-Kirby, A. H. and Bargmann, C. I. (2006). TRP Channels in *C. elegans*. *Annu. Rev. Physiol.* 68, 719-736.

Kaneko, H., Kawahara, Y. and Dan-Sohkawa, M. (1995). Primary Culture of Mesodermal and Endodermal Cells of the Starfish Embryo. *Zool. Sci.* 12, 551-558.

Kaneko, H., Okai, M., Murabe, N., Shimizu, T., Ikegami, S. and Dan-Sohkawa, M. (2005). Fibrous Component of the Blastocoelic Extracellular Matrix Shapes Epithelia in Concert with Mesenchyme Cells in Starfish Embryos. *Dev. Dyn.* 232, 915-927.

Kang, K., Pulver, S. R., Panzano, V. C., Chang, E. C., Griffith, L. C., Theobald, D. L. and Garrity, P. A. (2010). Analysis of *Drosophila* TRPA1 Reveals an Ancient Origin for Human Chemical Nociception. *Nature* 464, 597-600.

Kanzaki, M., Nagasawa, M., Kojima, I., Sato, C., Naruse, K., Sokabe, M. and Iida, H. (1999). Molecular Identification of a Eukaryotic, Stretch-Activated Nonselective Cation Channel. *Science* 285, 882-886.

Karashima, Y., Prenen, J., Talavera, K., Janssens, A., Voets, T. and Nilius, B. (2010). Agonist-Induced Changes in Ca(2+) Permeation through the Nociceptor Cation Channel TRPA1. *Biophys J.* 98, 773-783.

Karashima, Y., Damann, N., Prenen, J., Talavera, K., Segal, A., Voets, T. and Nilius, B. (2007). Bimodal Action of Menthol on the Transient Receptor Potential Channel TRPA1. *J. Neurosci.* 27, 9874-9884.

Katow, H. and Aizu, G. (2002). Essential Role of Growth Factor Receptor-Mediated Signal Transduction through the Mitogen-Activated Protein Kinase Pathway in Early Embryogenesis of the Echinoderm. *Dev. Growth Differ.* 44, 437-455.

Katow, H., Yaguchi, S. and Kyozuka, K. (2007). Serotonin Stimulates [Ca2+]i Elevation in Ciliary Ectodermal Cells of Echinoplutei through a Serotonin Receptor Cell Network in the Blastocoel. *J. Exp. Biol.* 210, 403-412.

Katow, H., Yaguchi, S., Kiyomoto, M. and Washio, M. (2004). The 5-HT Receptor Cell is a New Member of Secondary Mesenchyme Cell Descendants and Forms a Major Blastocoelar Network in Sea Urchin Larvae. *Mech. Dev.* 121, 325-337.

Kedei, N., Szabo, T., Lile, J. D., Treanor, J. J., Olah, Z., Iadarola, M. J. and Blumberg, P. M. (2001). Analysis of the Native Quaternary Structure of Vanilloid Receptor 1. *J. Biol. Chem.* 276, 28613-28619.

Keller, R. E., Danilchik, M., Gimlich, R. and Shih, J. (1985). The Function and Mechanism of Convergent Extension during Gastrulation of *Xenopus Laevis*. *Embryol. Exp. Morph.* 89, 185-209.

Kelley, M. W., Ochiai, C. K. and Corwin, J. T. (1992). Maturation of Kinocilia in Amphibian Hair Cells: Growth and Shortening Related to Kinociliary Bulb Formation. *Hear. Res.* 59, 108-115.

Kennedy, B. G., Torabi, A. J., Kurzawa, R., Echtenkamp, S. F. and Mangini, N. J. (2010). Expression of Transient Receptor Potential Vanilloid Channels TRPV5 and TRPV6 in Retinal Pigment Epithelium. *Mol. Vis.* 16, 665-675.

Keren, H., Lev-Maor, G. and Ast, G. (2010). Alternative Splicing and Evolution: Diversification, Exon Definition and Function. *Nat. Rev. Genet.* 11, 345-355.

Kerstein, P. C., del Camino, D., Moran, M. M. and Stucky, C. L. (2009). Pharmacological Blockade of TRPA1 Inhibits Mechanical Firing in Nociceptors. *Mol. Pain* 5, 19.

Khakh, B. S., Bao, X. R., Labarca, C. and Lester, H. A. (1999). Neuronal P2X Transmittergated Cation Channels Change their Ion Selectivity in Seconds. *Nat. Neurosci.* 2, 322-330.

Kiehart, D. P., Franke, J. D., Chee, M. K., Montague, R. A., Chen, T. L., Roote, J. and Ashburner, M. (2004). Drosophila Crinkled, Mutations of which Disrupt Morphogenesis and Cause Lethality, Encodes Fly Myosin VIIA. *Genetics* 168, 1337-1352.

Kikkawa, Y., Shitara, H., Wakana, S., Kohara, Y., Takada, T., Okamoto, M., Taya, C., Kamiya, K., Yoshikawa, Y., Tokano, H. et al. (2003). Mutations in a New Scaffold Protein Sans Cause Deafness in Jackson Shaker Mice. *Hum. Mol. Genet.* 12, 453-461.

Kimitsuki, T., Nakagawa, T., Hisashi, K., Komune, S. and Komiyama, S. (1996). Gadolinium Blocks Mechano-Electric Transducer Current in Chick Cochlear Hair Cells. *Hear. Res.* 101, 75-80.

Kindt, K. S., Viswanath, V., Macpherson, L., Quast, K., Hu, H., Patapoutian, A. and Schafer, W. R. (2007). Caenorhabditis Elegans TRPA-1 Functions in Mechanosensation. *Nat. Neurosci.* 10, 568-577.

Klionsky, L., Tamir, R., Gao, B., Wang, W., Immke, D. C., Nishimura, N. and Gavva, N. R. (2007). Species-Specific Pharmacology of Trichloro(Sulfanyl)Ethyl Benzamides as Transient Receptor Potential Ankyrin 1 (TRPA1) Antagonists. *Mol. Pain* 3, 39.

Klomp, A. E., Teofilo, K., Legacki, E. and Williams, D. S. (2007). Analysis of the Linkage of MYRIP and MYO7A to Melanosomes by RAB27A in Retinal Pigment Epithelial Cells. *Cell Motil. Cytoskeleton* 64, 474-487.

Kobayashi, K., Fukuoka, T., Obata, K., Yamanaka, H., Dai, Y., Tokunaga, A. and Noguchi, K. (2005). Distinct Expression of TRPM8, TRPA1, and TRPV1 mRNAs in Rat Primary Afferent Neurons with adelta/c-Fibers and Colocalization with Trk Receptors. *J. Comp. Neurol.* 493, 596-606.

Kominami, T., Takata, H. and Takaichi, M. (2001). Behavior of Pigment Cells in Gastrula-Stage Embryos of Hemicentrotus Pulcherrimus and Scaphechinus Mirabilis. *Dev. Growth Differ.* 43, 699-707.

Kremer, H., van Wijk, E., Marker, T., Wolfrum, U. and Roepman, R. (2006). Usher Syndrome: Molecular Links of Pathogenesis, Proteins and Pathways. *Hum. Mol. Genet.* 15, R262-270.

Kroese, A. B., Das, A. and Hudspeth, A. J. (1989). Blockage of the Transduction Channels of Hair Cells in the Bullfrog's Sacculus by Aminoglycoside Antibiotics. *Hear. Res.* 37, 203-217.

Kros, C. J. (1996). Physiology of Mammalian Cochlear Hair Cells. In *The Cochlea* (ed. P. Dallos, A. N. Popper and R. R. Fay), pp. 318-385. New York: Springer-Verlag.

Kros, C. J., Marcotti, W., van Netten, S. M., Self, T. J., Libby, R. T., Brown, S. D. M., Richardson, G. P. and Steel, K. P. (2002). Reduced Climbing and Increased Slipping Adaptation in Cochlear Hair Cells of Mice with Myo7a Mutations. *Nat. Neurosci.* 5, 41-47.

Kros, C. J., Rusch, A. and Richardson, G. P. (1992). Mechano-electrical Transducer Currents in Hair Cells of the Cultured Neonatal Mouse Cochlea. *Proc. R. Soc. Lond.* B249, 185-193.

Kuhn, R. and Wallenfells, K. (1940). Echinochrome Als Prosthetische Gruppen Hochmolekularern Symplexe in Den Eiern Von Arbacia Pustulosa. *Ber. Dt. Chem. Ges.* 73, 458-464.

Kung, C. (2005). A Possible Unifying Principle for Mechanosensation. *Nature* 436, 647-654.

Kussel-Andermann, P., El-Amraoui, A., Safieddine, S., Nouaille, S., Perfettini, I., Lecuit, M., Cossart, P., Wolfrum, U. and Petit, C. (2000). Vezatin, a Novel Transmembrane Protein, Bridges Myosin VIIA to the Cadherin-Catenins Complex. *EMBO J.* 19, 6020-6029.

Kwan, K. Y., Glazer, J. M., Corey, D. P., Rice, F. L. and Stucky, C. L. (2009). TRPA1 Modulates Mechanotransduction in Cutaneous Sensory Neurons. *J. Neurosci.* 29, 4808-4819.

Kwan, K. Y., Allchorne, A. J., Vollrath, M. A., Christensen, A. P., Zhang, D. S., Woolf, C. J. and Corey, D. P. (2006). TRPA1 Contributes to Cold, Mechanical, and Chemical Nociception but is Not Essential for Hair-Cell Transduction. *Neuron* 50, 277-289.

Lacalli, T. C., Holland, N. D. and West, J. E. (1994). Landmarks in the Anterior Central Nervous System of Amphioxus Larvae. *Philos. Trans. R. Soc. Lond.* B 344, 165-185.

Lagziel, A., Ahmed, Z. M., Schultz, J. M., Morell, R. J., Belyantseva, I. A. and Friedman, T. B. (2005). Spatiotemporal Pattern and Isoforms of Cadherin 23 in Wild Type and Waltzer Mice during Inner Ear Hair Cell Development. *Dev. Biol.* 280, 295-306.

Lee, G., Abdi, K., Jiang, Y., Michaely, P., Bennett, V. and Marszalek, P. E. (2006). Nanospring Behaviour of Ankyrin Repeats. *Nature* 440, 246-249.

Lee, Y., Lee, Y., Lee, J., Bang, S., Hyun, S., Kang, J., Hong, S. T., Bae, E., Kaang, B. K. and Kim, J. (2005). Pyrexia is a New Thermal Transient Receptor Potential Channel Endowing Tolerance to High Temperatures in *Drosophila Melanogaster.* . *Nat. Genet.* 37, 305-310.

Lepage, T., Sardet, C. and Gache, C. (1992). Spatial Expression of the Hatching Enzyme Gene in the Sea Urchin Embryo. *Dev. Biol.* 150, 23-32.

Letunic, I., Doerks, T. and Bork, P. (2009). SMART 6: Recent Updates and New Developments. *Nucleic Acids Res.* 37, D229-D232.

Leys, S. P., Mackie, G. O. and Meech, R. W. (1999). Impulse Conduction in a Sponge. *The J. Exp.Biol.* 202, 1139-1150.

Li, W., Feng, Z., Sternberg, P. W. and Shawn-Xu, X. Z. (2006). A *C. Elegans* Stretch Receptor Neuron Revealed by a Mechanosensitive TRP Channel Homologue. *Nature* 440, 684-687.

Liedtke, W. (2008). Molecular Mechanisms of TRPV4-Mediated Neural Signaling. . *Ann. N.Y Acad. Sci.* 1144, 42-52.

Liedtke, W. and Kim, C. (2005). Functionality of the TRPV Subfamily of TRP Ion Channels: Add Mechano-TRP and Osmo-TRP to the Lexicon! *Cell. Mol. Life Sci.* 62, 2985-3001.

Lishko, P. V., Procko, E., Jin, X., Phelps, C. B. and Gaudet, R. (2007). The Ankyrin Repeats of TRPV1 Bind Multiple Ligands and Modulate Channel Sensitivity. *Neuron* 54, 905-918.

Liu X., Vansant G., Udovichenko I.P., Wolfrum U. and Williams D.S. (1997). Myosin VIIa, the Product of the Usher 1B Syndrome Gene, is Concentrated in the Connecting Cilia of Photoreceptor Cells. *Cell Motil. Cytoskeleton* 37, 240-252.

Liu, L., Li, Y., Wang, R., Yin, C., Dong, Q., Hing, H., Kim, C. and Welsh, M. J. (2007a). *Drosophila* hygrosensation Requires the TRP Channels Water Witch and Nanchung. *Nature* 450, 294-298.

Liu, X., Bulgakov, O. V., Darrow, K. N., Pawlyk, B., Adamian, M., Liberman, M. C. and Li, T. (2007b). Usherin is Required for Maintenance of Retinal Photoreceptors and Normal Development of Cochlear Hair Cells. *Proc. Natl. Acad. Sci. U. S. A.* 104, 4413-4418.

Logan, C. Y. and McClay, D. R. (1999). Lineages that Give Rise to Endoderm and Mesoderm in the Sea Urchin Embryo. In *Cell Lineage and Determination.* (ed. S. A. Moody), pp. 41-58. New York: Academic Press.

Logan, C. Y. and McClay, D. R. (1997). The Allocation of Early Blastomeres to the Ectoderm and Endoderm is is Variable in the Sea Urchin Embryo. *Development* 124, 2213-2223.

Lopes, V. S., Ramalho, J. S., Owen, D. M., Karl, M. O., Strauss, O., Futter, C. E. and Seabra, M. C. (2007). The Ternary Rab27a-Myrip-Myosin VIIa Complex Regulates Melanosome Motility in the Retinal Pigment Epithelium. *Traffic* 8, 486-499.

Lumpkin, E. A., Marquis, R. E. and Hudspeth, A. J. (1997). The Selectivity of the Hair Cell's Mechanoelectrical-Transduction Channel Promotes Ca2+ Flux at Low Ca2+ Concentrations. *Proc. Natl. Acad. Sci. U.S.A.* 94, 10997-11002.

Lyman, J. and Fleming, R. H. (1940). Composition of Seawater. *J. Mar. Res.* 3, 134-146.

MacBride, E. W. (1903). The Development of Echinus Esculentus, Together with some Points in the Development of E. Miliaris and E. Acutus. *Philosophical Transactions of the Royal Society of London.Series B, Containing Papers of a Biological Character* 195, 285-327.

Mackie, G. O., Spencer , A. N. and Strathmann, R. (1969). Electrical Activity Associated with Ciliary Reversal in an Echinoderm Larva. *Nature* 223, 1384-1385.

Macpherson, L. J., Dubin, A. E., Evans, M. J., Marr, F., Schultz, P. G., Cravatt, B. F. and Patapoutian, A. (2007). Noxious Compounds Activate TRPA1 Ion Channels through Covalent Modification of Cysteines. *Nature* 445, 541-542.

Macpherson, L. J., Geierstanger, B. H., Viswanath, V., Bandell, M., Eid, S. R., Hwang, S. W. and Patapoutian, A. (2005). The Pungency of Garlic: Activation of TRPA1 and TRPV1 in Response to Allicin. *Curr. Biol.* 15, 929-934.

Macpherson, L. J., Hwang, S. W., Miyamoto, T., Dubin, A. E., Patapoutian, A. and Story, G. M. (2006). More than Cool: Promiscuous Relationships of Menthol and Other Sensory Compounds. *Mol. Cell Neurosci.* 32, 335-343.

Maerker, T., van Wijk, E., Overlack, N., Kersten, F. F. J., McGee, J., Goldmann, T., Sehn, E., Roepman, R., Walsh, E. J., Kremer, H. et al. (2007). A Novel Usher Protein Network at the Periciliary Reloading Point between Molecular Transport Machineries in Vertebrate Photoreceptor Cells. *Hum. Mol. Genet.*

Marchuk, D., Drumm, M., Saulino, A. and Collins, F. S. (1991). Construction of T-Vectors, a Rapid and General System for Direct Cloning of Unmodified PCR Products. *Nucl. Acids Res.* 19, 1154.

Marcotti, W., van Netten, S. M. and Kros, C. J. (2005). The Aminoglycoside Antibiotic Dihydrostreptomycin Rapidly Enters Mouse Outer Hair Cells through the Mechano -Electrical Transducer Channels. *J. Physiol.* 567, 505-521.

Marshall, A. T. and Clode, P. L. (2002). Effect of Increased Calcium Concentration in Sea Water on Calcification and Photosynthesis in the Scleractinian Coral Galaxea Fascicularis. *J. Exp. Biol.* 205, 2107-2113.

Martins, G. G., Summers, R. G. and Morril, J. B. (1998). Cells are Added to the Archenteron during and Following Secondary Invagination in the Sea Urchin *Lytechinus Variegatus*. *Dev. Biol.* 198, 330-342.

Maruyama, Y. K. (1981). Development of Swimming Behavior in Sea Urchin Embryos. I. *J. Exp. Zool.* 215, 163-171.

Mastrangelo, A. M., Belloni, S., Barilli, S., Ruperti, B., Di Fonzo, N., Stanca, A. M. and Cattivelli, L. (2005). Low Temperature Promotes Intron Retention in Two e-Cor Genes of Durum Wheat. *Planta* 221, 705-715.

Masuda, M. and Sato, H. (1984). Asynchronization of Cell Divisions is Concurrently Related with Ciliogenesis in Sea Urchin Blastulae. *Dev. Growth. Diff.* 26, 281-294.

Matta, J.A., Cornett, P.M., Miyares, R.L., Abe, K., Sahibzada, N., Ahern, G.P. (2008). General Anesthetics Activate a Nociceptive Ion Channel to Enhance Pain and Inflammation. *Proc. Natl. Acad. Sci. U.S.A.* 105, 8784-8789.

Mburu, P., Mustapha, M., Varela, A., Weil, D., El-Amraoui, A., Holme, R. H., Rump, A., Hardisty, R. E., Blanchard, S., Coimbra, R. S. et al. (2003). Defects in Whirlin, a PDZ Domain Molecule Involved in Stereocilia Elongation, Cause Deafness in the Whirler Mouse and Families with DFNB31. *Nat. Genet.* 34, 421-428.

McClay, D. R., Armstrong, N. A. and Hardin, J. (1992). Pattern Formation during Gastrulation in Sea Urchin Embryo. *Dev. Suppl.* 1992, 33-41.

McClay, D. R., Gross, G. M., Rnage, R., Peterson, R. E. and Bradham, C. (2004). Sea Urchin Gastrulation. In *Gastrulation: From Cells to Embryos* (ed. C. D. Stern), pp. 123-137.

McGee, J., Goodyear, R. J., McMillan, D. R., Stauffer, E. A., Holt, J. R., Locke, K. G., Birch, D. G., Legan, P. K., White, P. C., Walsh, E. J. et al. (2006). The very Large G-Protein-Coupled Receptor VLGR1: A Component of the Ankle Link Complex Required for the Normal Development of Auditory Hair Bundles. *J. Neurosci.* 26, 6543-6553.

McLendon, J. F. (1912). Echinochrome, a Red Substance in Sea Urchins. *J. Biol. Chem.* 11, 435-441.

McNamara, C. R., Mandel-Brehm, J., Bautista, D. M., Siemens, J., Deranian, K. L., Zhao, M., Hayward, N. J., Chong, J. A., Julius, D., Moran, M. M. et al. (2007). TRPA1 Mediates Formalin-Induced Pain. *Proc. Natl. Acad. Sci. U.S.A.* 104, 13525-13530.

Merlino, G. T., Chamberlain, J. P. and Kleinsmith, L. J. (1978). Effects of Deciliation of Tubulin Messenger RNA Activity in Sea Urchin Embryos. *J. Biol. Chem.* 253, 7078-7085.

Metchnikoff, E. (1891). *Lectures on the Comparative Pathology of Inflammation Delivered at Pasteur Institute in 1891*. New York: Dover.

Meyers, J. R., MacDonald, R. B., Duggan, A., Lenzi, D., Standaert, D. G., Corwin, J. T. and Corey, D. P. (2003). Lighting Up the Senses: FM1-43 Loading of Sensory Cells through Nonselective Ion Channels. *J. Neurosci.* 23, 4054-4065.

Michalski, N., Michel, V., Bahloul, A., Lefevre, G., Barral, J., Yagi, H., Chardenoux, S., Weil, D., Martin, P., Hardelin, J. P. et al. (2007). Molecular Characterization of the Ankle-Link Complex in Cochlear Hair Cells and its Role in the Hair Bundle Functioning. *J. Neurosci.* 27, 6478-6488.

Michel, V., Goodyear, R. J., Weil, D., Marcotti, W., Perfettini, I., Wolfrum, U., Kros, C. J., Richardson, G. P. and Petit, C. (2005). Cadherin 23 is a Component of the Transient Lateral Links in the Developing Hair Bundles of Cochlear Sensory Cells. *Dev. Biol.* 280, 281-294.

Minokawa, T., Rast, J. P., Arenas-Mena, C., Franco, C. B. and Davidson, E. H. (2004). Expression Patterns of Four Different Regulatory Genes that Function during Sea Urchin Development. *Gene Expr. Patterns* 4, 449-456.

Mogensen, M. M., Rzadzinska, A. and Steel, K. P. (2007). The Deaf Mouse Mutant Whirler Suggests a Role for Whirlin in Actin Filament Dynamics and Stereocilia Development. *Cell Motil. Cytoskeleton* 64, 496-508.

Montell, C. (1999). Visual Transduction in Drosophila. *Annu. Rev. Cell. Dev. Biol.* 15, 231-268.

Montell, C. (2005). The TRP Superfamily of Cation Channels. *Sci. STKE* 2005, re3.

Montell, C. and Caterina, M. (2007). Thermoregulation: Channels that are Cool to the Core. *Curr.Biol.* 17, R885-R887.

Moran, M. M., Fanger, C., Chong, J. A., Mcnamara, C., Zhen, X. and Mandel-Brehm, J. (2007). WO2007073505. *Chem. Abstr.* 147, 118074.

Moss, C., Burke, R. D. and Thorndyke, M. C. (1994). Immunocytochemical Localization of the Neuropeptide S1 and Serotonin in Larvae of the Starfish *Pisaster Ochraceus* and *Asterias Rubens*. *J. Mar. Biol.* 74, 61-71.

Muller, U. (2008). Cadherins and Mechanotransduction by Hair Cells. *Curr. Opin. Cell Biol.* 20, 557-566.

Murakami, A. (1983). Control of Ciliary Beat Frequency in *Mytillus*. *J. Submicrosc. Cytol.* 15, 313-316.

Murakami, A. (1987). Control of Ciliary Beat Frequency in the Gill of Mytilus—I. Activation of the Lateral Cilia by Cyclic AMP. *Comp. Biochem. Physiol. C* 86, 273-279.

Mutai, H. and Heller, S. (2003). Vertebrate and Invertebrate TRPV-Like Mechanoreceptors. *Cell Calcium* 33, 471-478.

Nagata, K., Duggan, A., Kumar, G. and Garcia-Anoveros, J. (2005). Nociceptor and Hair Cell Transducer Properties of TRPA1, a Channel for Pain and Hearing. *J. Neurosci.* 25, 4052-4061.

Nagatomo, K. and Kubo, Y. (2008). Caffeine Activates Mouse TRPA1 Channels but Suppresses Human TRPA1 Channels. *Proc. Natl. Acad. Sci. U.S.A.* 105, 17373-17378.

Nakajima, Y. (1987). Localization of Catecholaminergic Nerves in Larval Echinoderms. *Zool. Sci.* 4, 293-299.

Nakajima, Y. (1986a). Presence of a Ciliary Patch in Preoral Epithelium of Sea Urchin Plutei. *Dev. Growth Differ.* 28, 243-249.

Nakajima, Y. (1986b). Development of the Nervous System of Sea Urchin Embryos: Formation of Ciliary Bands and the Appearance of Two Types of Ectoneural Cells in the Pluteus. 28, 531-542.

Nakajima, Y., Kaneko, H., Murray, G. and Burke, R. D. (2004). Divergent Patterns of Neural Development in Larval Echinoids and Asteroids. *Evol. Dev.* 6, 95-104.

Nakamura, S., Mikamori, M., Hiramatsu, M., Eura, S., Takamoto, H. and Watanabe, M. (2001). Spectacular Fluorescence Emission in Sea Urchin Larvae. *Zool. Sci.* 18, 807-810.

Neya, T. (1965). Photic Behavior of Sea Urchin Larvae, Hemicentrotus Pulcherrimus. *Zool. Mag.* 74, 11-16.

Ng, H., Weigele, M., Moran, M., Chong, J., Fanger, C., Larsen, G. R., Del Camino, D., Hayward, N., Adams, S. and Ripka, A. (2009). WO2009002933. *Chem. Abstr.* 150, 9804.

Nguyen, T., Chin, W., O'Brien, J. A., Verdugo, P. and Berger, A. J. (2001). Intracellular Pathways Regulating Ciliary Beating of Rat Brain Ependymal Cells. *J. Physiol.* 531, 131-140.

Nicolson, T., Rusch, A., Friedrich, R. W., Granato, M., Ruppersberg, J. P. and Nusslein-Volhard, C. (1998). Genetic Analysis of Vertebrate Sensory Hair Cell Mechanosensation: The Zebrafish Circler Mutants. *Neuron* 20, 271-283.

Niehrs, C. and Pollet, N. (1999). Synexpression Groups in Eukaryotes. *Nature* 402, 483-487.

Nilius, B., Vennekens, R., Prenen, J., Hoenderop, J. G., Droogmans, G. and Bindels, R. J. (2001). The Single Pore Residue Asp542 Determines Ca^{2+} Permeation and Mg^{2+} Block of the Epithelial Ca^{2+} Channel. *J. Biol. Chem.* 276, 1020-1025.

Nishikawa, S. and Sasaki, F. (1996). Internalization of Styryl Dye FM1-43 in the Hair Cells of Lateral Line Organs in Xenopus Larvae. *J. Histochem. Cytochem.* 44, 733-741.

Norrander, J. M., Linck, R. W. and Stephens, R. E. (1995). Transcriptional Control of Tektin A mRNA Correlates with Cilia Development and Length Determination during Sea Urchin Embryogenesis. *Development* 121, 1615-1623.

O'Neil, R. G. and Heller, S. (2005). The Mechanosensitive Nature of TRPV Channels. *Pflugers. Archiv.* 451, 193-203.

Oberwinkler, J., Lis, A., Giehl, K. M., Flockerzi, V. and Philipp, S. E. (2005). Alternative Splicing Switches the Divalent Cation Selectivity of TRPM3 Channels. *J. Biol. Chem.* 280, 22540-22548.

Ohmori, H. (1985). Mechano-electrical Transduction Currents in Isolated Vestibular Hair Cells of the Chick. *J. Physiol.* 359, 189-217.

Okazaki, K. (1975). Spicule Formation by Isolated Micromeres of the Sea Urchin Embryo. *Am. Zool.* 15, 567-581.

Oliveri, P. and Davidson, E. H. (2004). Gene Regulatory Network Controlling Embryonic Specification in the Sea Urchin. *Curr. Opin. Genet. Dev.* 14, 351-360.

Ooka, S., Katow, T., Yaguchi, S., Yaguchi, J. and Katow, H. (2010). Spatiotemporal Expression Pattern of an Encephalopsin Orthologue of the Sea Urchin Hemicentrotus Pulcherrimus during Early Development, and its Potential Role in Larval Vertical Migration. *Dev. Growth Differ.* 52, 195-207.

Overlack, N., Maerker, T., Latz, M., Nagel-Wolfrum, K. and Wolfrum, U. (2008). SANS (USH1G) Expression in Developing and Mature Mammalian Retina. *Vision Res.* 48, 400-412.

Owsianik, G., Talavera, K., Voets, T. and Nilius, B. (2006). Permeation and Selectivity of Trp Channels. *Annu. Rev. Physiol*. 68, 685-717.

Ozaki, H. (1974). Localization and Multiple Forms of Acetylcholinesterase in Sea Urchin Embryos. *Dev. Growth Differ.* 16, 267-279.

Patapoutian, A. and Jegla, T. J. (2007). WO2007098252. *Chem. Abstr.* 147, 292253.

Pazour, G. J., San Agustin, J. T., Follit, J. A., Rosenbaum, J. L. and Witman, G. B. (2002). Polycystin-2 Localizes to Kidney Cilia and the Ciliary Level is Elevated in Orpk Mice with Polycystic Kidney Disease. *Curr.Biol.* 12, R378-R380.

Pedersen, S. F. and Nilius, B. (2007). Transient Receptor Potential Channels in Mechanosensing and Cell Volume Regulation. *Methods Enzymol.* 428, 183-207.

Pennington, J. T. and Emlet, R. B. (1986). Ontogenetic and Diel Vertical Migration of a Planktonic Echinoid Larva, DendrasterExentricus (Eschscholtz): Occurrence, Causes, and Probable Consequences. *J. Exp. Mar. Biol. Ecol.* 104, 69-95.

Peterson, R. E. and McClay, D. R. (2003). Primary Mesenchyme Cell Patterning during the Early Stages Following Ingression. *Dev. Biol.* 254, 68-78.

Petrus, M., Peier, A. M., Bandell, M., Hwang, S. W., Huynh, T., Olney, N., Jegla, T. and Patapoutian, A. (2007). A Role of TRPA1 in Mechanical Hyperalgesia is Revealed by Pharmacological Inhibition. *Mol. Pain* 3, 40.

Petty, J. T., Bordelon, J. A. and Robertson, M. E. (2000). Thermodynamic Characterization of the Association of Cyanine Dyes with DNA. *J. Phys. Chem. B* 104, 7221-7227.

Phillips, J., Chiem, J. L. and Westerfield, M. (2007). Zebrafish Usher Genes are Necessary for Retinal Cell Function and Survival. *ARVO abstracts* 4494,.

Prevette, L. E., Mullen, D. G. and Banaszak Holl, M. M. (2010). Polycation-Induced Cell Membrane Permeability does Not Enhance Cellular Uptake Or Expression Efficiency of Delivered DNA. *Mol. Pharm.* 7, 870-883.

Price, N. M., Thompson, P. A. and Harrison, P. J. (1987). Selenium: An Essential Element for Growth of the Coastal Marine Diatom *Thalassiosira Pseudonana* (*Bacillariophyceae*). *J. Phycol.* 23, 1-9.

Prober, D. A., Zimmerman, S., Myers, B. R., McDermott, B. M.,Jr, Kim, S., Caron, S., Rihel, J., Solnica-Krezel, L., Julius, D., Hudspeth, A. J. et al. (2008). Zebrafish TRPA1 Channels are Required for Chemosensation but Not for Thermosensation Or Mechanosensory Hair Cell Function. *J. Neurosci.* 28, 10102-10110.

Raible, F., Tessmar-Raible, K., Arboleda, E., Kaller, T., Bork, P., Arendt, D. and Arnone, M. I. (2006). Opsins and Clusters of Sensory G-Protein-Coupled Receptors in the Sea Urchin Genome. *Dev.Biol.* 300, 461-475.

Raisinghani, M. and Premkumar, L. S. (2005). Block of Native and Cloned Vanilloid Receptor 1 (TRPV1) by Aminoglycoside Antibiotics. *Pain* 113, 123-133.

Reese, E. S. (1966). The Complex Behavior of Echinoderms. In *Physiology of Echinoderms* (ed. R. A. Boolootian), pp. 15-218. New York: Interscience.

Reiners, J., Marker, T., Jurgens, K., Reidel, B. and Wolfrum, U. (2005). Photoreceptor Expression of the Usher Syndrome Type 1 Protein Protocadherin 15 (USH1F) and its Interaction with the Scaffold Protein Harmonin (USH1C). *Mol. Vis.* 11, 347-355.

Reiners, J., Nagel-Wolfrum, K., Jurgens, K., Marker, T. and Wolfrum, U. (2006). Molecular Basis of Human Usher Syndrome: Deciphering the Meshes of the Usher Protein Network Provides Insights into the Pathomechanisms of the Usher Disease. *Exp. Eye Res.* 83, 97-119.

Reiners, J., Reidel, B., El-Amraoui, A., Boeda, B., Huber, I., Petit, C. and Wolfrum, U. (2003). Differential Distribution of Harmonin Isoforms and their Possible Role in Usher-1 Protein Complexes in Mammalian Photoreceptor Cells. *Invest. Ophthalmol. Vis. Sci.* 44, 5006-5015.

Reiners, J., van Wijk, E., Marker, T., Zimmermann, U., Jurgens, K., te Brinke, H., Overlack, N., Roepman, R., Knipper, M., Kremer, H. et al. (2005). Scaffold Protein Harmonin (USH1C) Provides Molecular Links between Usher Syndrome Type 1 and Type 2. *Hum. Mol. Genet.* 14, 3933-3943.

Reiners, J. and Wolfrum, U. (2006). Molecular Analysis of the Supramolecular Usher Protein Complex in the Retina. Harmonin as the Key Protein of the Usher Syndrome. *Adv. Exp. Med. Biol.* 572, 349-353.

Ricci, A. J., Crawford, A. C. and Fettiplace, R. (2003). Tonotopic Variation in the Conductance of the Hair Cell Mechanotransducer Channel. *Neuron* 40, 983-990.

Rosenbaum, J. L. and Witman, G. B. (2002). Intraflagellar Transport. *Nat. Rev. Mol. Cell. Biol.* 3, 813-825.

Rosenzweig, M., Brennan, K. M., Tayler, T. D., Phelps, P. O., Patapoutian, A. and Garrity, P. A. (2005). The *Drosophila* ortholog of Vertebrate TRPA1 Regulates Thermotaxis. *Genes Dev.* 19, 419-424.

Ruffins, S. W. and Ettensohn, C. A. (1996). A Fate Map of the Vegetal Plate of the Sea Urchin (Lytechinus Variegatus) Mesenchyme Blastula. *Development* 122, 253-263.

Ryan, T. A. (2001). Presynaptic Imaging Techniques. *Curr. Opin. Neurobiol.* 11, 544-549.

Ryberg, E. (1973). The Localization of Cholinesterase and Nonspecific Esterase in the Echinopluteus. *Zool. Scripta* 2, 163-170.

Ryberg, E. (1974). Localization of Biogenic Amines in Echinopluteus. *Acta Zoologica* 55, 179-189.

Ryberg, E. (1977). The Nervous System of the Early Echinopluteus. *Cell Tissue Res.* 179, 157-167.

Ryberg, E. and Lundgren, B. O. (1977). Extra-Ectodermal Strands in the Ciliated Bands of the Echinopluteus. *Dev.Growth Differ.* 19, 299-308.

Rzadzinska, A. K., Derr, A., Kachar, B. and Noben-Trauth, K. (2005). Sustained Cadherin 23 Expression in Young and Adult Cochlea of Normal and Hearing-Impaired Mice. *Hear. Res.* 208, 114-121.

Sahly, I., El Amraoui, A., Abitbol, M., Petit, C. and Dufier, J. L. (1997). Expression of Myosin VIIA during Mouse Embryogenesis. *Anat. Embryol.* 196, 159-170.

Saihan, Z., Webster, A. R., Luxon, L. and Bitner-Glindzicz, M. (2009). Update on Usher Syndrome. *Curr. Opin. Neurol.* 22, 19-27.

Saino, T., Matsuura, M. and Satoh, Y. (2002). Application of Real-Time Confocal Microscopy to Intracellular Calcium Ion Dynamics in Rat Arterioles. *Histochem. Cell Biol.* 117, 295-305.

Samanta, M. P., Tongprasit, W., Istrail, S., Cameron, R. A., Tu, Q., Davidson, E. H. and Stolc , V. (2006). The Transcriptome of the Sea Urchin Embryo. *Science* 314, 960-962.

Sammeth, M., Foissac, S. and Guigó, R. (2008). A General Definition and Nomenclature for Alternative Splicing Events. *PLoS Comput. Biol.* 4, e1000147.

Sankila, E. M., Pakarinen, L., Kääriäinen, H., Aittomäki, K., Karjalainen, S., Sistonen, P. and de la Chapelle, A. (1995). Assignment of an Usher Syndrome Type III (USH3) Gene to Chromosome 3q. *Hum. Mol. Genet.* 4, 93-98.

Santos, F., MacDonald, G., Rubel, E. W. and Raible, D. W. (2006). Lateral Line Hair Cell Maturation is a Determinant of Aminoglycoside Susceptibility in Zebrafish (Danio Rerio). *Hear. Res.* 213, 25-33.

Sawada, Y., Hosokawa, H., Hori, A., Matsumura, K. and Kobayashi, S. (2007). Cold Sensitivity of Recombinant TRPA1 Channels. *Brain Res.* 1160, 39-46.

Schaefer, M. (2005). Homo- and Heteromeric Assembly of TRP Channel Subunits. *Pflugers Arch.* 451, 35-42.

Schliwa, M. and Bereiter-Hahn, J. (1973). Pigment Movements in Fish Melanophores: Morphological and Physiological Studies. III. the Effects of Colchicine and Vinblastine. *Z. Zellforsch.* 147, 127-148.

Schote, U. and Seelig, J. (1998). Interaction of the Neuronal Marker Dye FM1-43 with Lipid Membranes. Thermodynamics and Lipid Ordering. *Biochim. Biophys. Acta.* 1415, 135-146.

Schroder, J., Raiber, S., Berger, T., Schmidt, A., Schmidt, J., Soares-Sello, A. M., Bardshiri, E., Strack, D., Simpson, T. J., Veit, M. et al. (1998). Plant Polyketide Synthases: A Chalcone Synthase-Type Enzyme which Performs a Condensation Reaction with Methylmalonyl-CoA in the Biosynthesis of C-Methylated Chalcones. *Biochemistry* 37, 8417-8425.

Schroeder, T. (1981). Development of a "primitive" Sea Urchin (*Eucidaris Tribuloides*): Irregularities in the Hyaline Layer, Micromeres, and Primary Mesenchyme. *Biol. Bull.* 161, 141-151.

Schultz, J., Milpetz, F., Bork, P. and Ponting, C. P. (1998). SMART, a Simple Modular Architecture Research Tool: Identification of Signaling Domains. *Proc. Natl. Acad. Sci. U.S.A.* 95, 5857-5864.

Sea Urchin Genome Sequencing Consortium, Sodergren, E., Weinstock, G. M., Davidson, E. H., Cameron, R. A., Gibbs, R. A., Angerer, R. C., Angerer, L. M., Arnone, M. I., Burgess, D. R. et al. (2006). The Genome of the Sea Urchin Strongylocentrotus Purpuratus. *Science* 314, 941-952.

Seiler, C., Finger-Baier, K. C., Rinner, O., Makhankov, Y. V., Schwarz, H., Neuhauss, S. C. and Nicolson, T. (2005). Duplicated Genes with Split Functions: Independent Roles of protocadherin15 Orthologues in Zebrafish Hearing and Vision. *Development* 132, 615-623.

Seiler, C. and Nicolson, T. (1999). Defective Calmodulin-Dependent Rapid Apical Endocytosis in Zebrafish Sensory Hair Cell Mutants. *J. Neurobiol.* 41, 424-434.

Senften, M., Schwander, M., Kazmierczak, P., Lillo, C., Shin, J. B., Hasson, T., Geleoc, G. S. G., Gillespie, P. G., Williams, D., Holt, J. R. et al. (2006). Physical and Functional Interaction between Protocadherin 15 and Myosin VIIa in Mechanosensory Hair Cells. *J. Neurosci.* 26, 2060-2071.

Service, M. and Wardlaw, A. C. (1984). Echinochrome-A as a Bactericidal Substance in the Coelomic Fluid of *Echinus Esculentus*. *Comp. Biochem. Physiol.* 79B, 161-165.

Sharif-Naeini, R., Dedman, A., Folgering, J. H., Duprat, F., Patel, A., Nilius, B. and Honore, E. (2008). TRP Channels and Mechanosensory Transduction: Insights into the Arterial Myogenic Response. *Pflugers. Archiv.* 456, 529-540.

Shin, J., Adams, D., Paukert, M., Siba, M., Sidi, S., Levin, M., Gillespie, P. G. and Gründer, S. (2005). Xenopus TRPN1 (NOMPC) Localizes to Microtubule-Based Cilia in Epithelial Cells, Including Inner-Ear Hair Cells. *Proc. Natl. Acad. Sci. U.S.A.* 102, 12572-12577.

Si, F., Brodie, H., Gillespie, P. G., Vazquez, A. E. and Yamoah, E. N. (2003). Developmental Assembly of Transduction Apparatus in Chick Basilar Papilla. *J. Neurosci.* 23, 10815-10826.

Sidi, S., Friedrich, R. W. and Nicolson, T. (2003). NompC TRP Channel Required for Vertebrate Sensory Hair Cell Mechanotransduction. *Science* 301, 96-99.

Siemens, J., Kazmierczak, P., Reynolds, A., Sticker, M., Littlewood-Evans, A. and Müller, U. (2002). The Usher Syndrome Proteins Cadherin 23 and Harmonin Form a Complex by Means of PDZ-Domain Interactions. *Proc. Natl. Acad. Sci. U.S.A.* 99, 14946-14951.

Siemens, J., Lillo, C., Dumont, R. A., Reynolds, A., Williams, D. S., Gillespie, P. G. and Muller, U. (2004). Cadherin 23 is a Component of the Tip Link in Hair-Cell Stereocilia. *Nature* 428, 950-955.

Silva, J. R. (2000). The Onset of Phagocytosis and Identity in the Embryo of *Lytechinus Variegatus*. *Dev. Comp. Immunol.* 24, 733-739.

Smith, L. C. (2005). Host Responses to Bacteria: Innate Immunity in Invertebrates. In *Advances in Molecular and Cellular Microbiology* (ed. M. McFall-Ngai and B. H. N. Ruby), pp. 2: Cambridge Univ. Press.

Smith, R. J., Berlin, C. I., Hejtmancik, J. F., Keats, B. J., Kimberling, W. J., Lewis, R. A., Möller, C. G., Pelias, M. Z. and Tranebjaerg, L. (1994). Clinical Diagnosis of the Usher Syndromes. Usher Syndrome Consortium. *Am. J. Med. Genet.* 50, 32-38.

Smith, M. M., Cruz Smith, L., Cameron, R. A. and Urry, L. A. (2008). The Larval Stages of the Sea Urchin, Strongylocentrotus Purpuratus. *J. Morphol.* 269, 713-733.

Sobkowicz, H. M., Slapnick, S. M. and August, B. K. (1995). The Kinocilium of Auditory Hair Cells and Evidence for its Morphogenetic Role during the Regeneration of Stereocilia and Cuticular Plates. *J. Neurocytol.* 24, 633-653.

Sokabe, T., Tsujiuchi, S., Kadowaki, T. and Tominaga, M. (2008). *Drosophila* painless is a Ca^{2+}-Requiring Channel Activated by Noxious Heat. *J. Neurosci.* 28, 9929-9938.

Sollner, C., Rauch, G. J., Siemens, J., Geisler, R., Schuster, S. C., Muller, U., Nicolson, T. and Tubingen 2000 Screen Consortium. (2004). Mutations in Cadherin 23 Affect Tip Links in Zebrafish Sensory Hair Cells. *Nature* 428, 955-959.

Soni, L. E., Warren, C. M., Bucci, C., Orten, D. J. and Hasson, T. (2005). The Unconventional Myosin-VIIa Associates with Lysosomes. *Cell. Motil. Cytoskeleton* 62, 13-26.

Sotomayor, M., Corey, D. P. and Schulten, K. (2005). In Search of the Hair-Cell Gating Spring Elastic Properties of Ankyrin and Cadherin Repeats. . *Structure* 13, 669-682.

Spencer, A. N. (1974). Non-Nervous Conduction in Invertebrates and Embryos. *Amer. Zool.* 14, 917-929.

Steel, K. P. and Kros, C. J. (2001). A Genetic Approach to Understanding Auditory Function. *Nat. Genet.* 27, 143-149.

Stepanyan, R., Boger, E. T., Friedman, T. B. and Frolenkov, G. L. (2006). TRPA1, a Hair Cell Channel with Unknown Function? *Abstr. Midwinter. Res. Meet. Assoc. Res. Otolaryngol.*, 211-212.

Stephens, R. E. (1995). Ciliogenesis in Sea Urchin Embryos: A Subroutine in the Program of Development. *BioEssays* 17, 331-340.

Stephens, R. E. (2008). Ciliogenesis, Ciliary Function, and Selective Isolation. *ACS Chem. Biol.* 3, 84-86.

Stephens, R. and Prior, G. (1992). Dynein from Serotonin-Activated Cilia and Flagella: Extraction Characteristics and Distinct Sites for cAMP-Dependent Protein Phosphorylation. *J. Cell. Sci.* 103, 999-1012.

Story, G. M., Peier, A. M., Reeve, A. J., Eid, S. R., Mosbacher, J., Hricik, T. R., Earley, T. J., Hergarden, A. C., Andersson, D. A., Hwang, S. W. et al. (2003). ANKTM1, a TRP-Like Channel Expressed in Nociceptive Neurons, is Activated by Cold Temperatures. *Cell* 112, 819-829.

Strathmann, R. R. (1975). Larval Feeding in Echinoderms. *Amer. Zool.* 15, 717-730.

Strathmann, R. R. (2007). Time and Extent of Ciliary Response to Particles in a Non-Filtering Feeding Mechanism. *Biol. Bull.* 212, 93-103.

Strathmann, R. R. (1971). The Feeding Behavior of Planktotrophic Echinoderm Larvae: Mechanisms, Regulation, and Rates of Suspensionfeeding. *J. Exp. Mar. Biol. Ecol.* 6, 109-160.

Sukharev, S. and Corey, D. P. (2004). Mechanosensitive Channels: Multiplicity of Families and Gating Paradigms. *Sci.STKE* 219, re4.

Takata, H. and Kominami, T. (2003). Behavior and Differentiation Process of Pigment Cells in a Tropical Sea Urchin Echinometra Mathaei. *Dev. Growth Differ.* 45, 473-483.

Takata, H. and Kominami, T. (2004). Behavior of Pigment Cells Closely Correlates the Manner of Gastrulation in Sea Urchin Embryos. *Zool. Sci.* 21, 1025-1035.

Taura, A., Kojima, K., Ito, J. and Ohmori, H. (2006). Recovery of Hair Cell Function After Damage Induced by Gentamicin in Organ Culture of Rat Vestibular Maculae. *Brain Res.* 1098, 33-48.

Taylor-Clark, T. E., Undem, B. J., MacGlashan, D. W., Ghatta, S., Carr, M. A. and McAlexander, M. J. (2008). Prostaglandin-Induced Activation of Nociceptive Neurons Via Direct Interaction with Transient Receptor Potential A1 (TRPA1). *Mol. Pharmacol.* 73, 274.

Thorndyke, M. C., Crawford, B. D. and Burke, R. D. (1992). Localization of a SALMFamide Neuropeptide in the Larval Nervous System of the Sand Dollar *Dendraster Excentricus*. *Acta. Zool.* 73, 207-212.

Tian, G., Zhou, Y., Hajkova, D., Miyagi, M., Dinculescu, A., Hauswirth, W. W., Palczewski, K., Geng, R., Alagramam, K. N., Isosomppi, J. et al. (2009). Clarin-1, Encoded by the Usher Syndrome III Causative Gene, Forms a Membranous Microdomain: Possible Role of Clarin-1 in Organizing the Actin Cytoskeleton. *J. Biol. Chem.* 284, 18980-18993.

Tierney, A. J. (2001). Structure and Function of Invertebrate 5-HT Receptors: A Review. *Comp. Biochem. Physiol. A. Mol. Integr. Physiol.* 128, 791-804.

Tobin, D. M. and Bargmann, C. I. (2004). Invertebrate Nociception: Behaviors, Neurons and Molecules. *J. Neurobiol.* 61, 161-174.

Todi, S. V., Sharma, Y. and Eberl, D. F. (2004). Anatomical and Molecular Design of the Drosophila Antenna as a Flagellar Auditory Organ. *Microsc. Res. Tech.* 63, 388-399.

Todi, S. V., Franke, J. D., Kiehart, D. P. and Eberl, D. F. (2005). Myosin VIIA Defects, which Underlie the Usher 1B Syndrome in Humans, Lead to Deafness in Drosophila. *Curr.Biol.* 15, 862-868.

Toneby, M. (1973). Detection of 5-Hydroxytryptamine in Developing Sea Urchin Embryos. *Dev. Genes Evol.* 172, 258-261.

Toneby, M. (1977). Functional Aspects of 5-Hydroxytryptamine in Early Embryogenesis of the Sea urchin *Paracentrotus Lividus*. *Dev. Genes Evol.* 181, 247-259.

Tracey Jr., W., Wilson, R. I., Laurent, G. and Benzer, S. (2003). Painless, a Drosophila Gene Essential for Nociception. *Cell* 113, 261-273.

Trevisani, M., Siemens, J., Materazzi, S., Bautista, D. M., Nassini, R., Campi, B., Imamachi, N., Andrè, E., Patacchini, R., Cottrell, G. S. et al. (2007). 4-Hydroxynonenal, an Endogenous Aldehyde, Causes Pain and Neurogenic Inflammation through Activation of the Irritant Receptor TRPA1. *Proc. Natl. Acad. Sci. U.S.A.* 104, 13519-13524.

Tsilou, E. T., Rubin, B. I., Caruso, R. C., Reed, G. F., Pikus, A., Hejtmancik, J. F., Iwata, F., Redman, J. B. and Kaiser-Kupfer, M. I. (2002). Usher Syndrome Clinical Types I and II: Could Ocular Symptoms and Signs Differentiate between the Two Types? *Acta. Ophthalmol. Scand.* 80, 196-201.

Tsunozaki, M. and Bautista, D. M. (2009). Mammalian Somatosensory Mechanotransduction. *Curr. Opin. Neurobiol.* 19, 362-369.

van Netten, S. M. and Kros, C. J. (2007). Insights into the Pore of the Hair Cell Transducer Channel from Experiments with Permeant Blockers. In *Current Topics in Membranes* (ed. Owen P. Hamill), pp. 375-398: Academic Press.

van Wijk, E., van der Zwaag, B., Peters, T., Zimmermann, U., Te Brinke, H., Kersten, F. F., Marker, T., Aller, E., Hoefsloot, L. H., Cremers, C. W. et al. (2006). The DFNB31 Gene Product Whirlin Connects to the Usher Protein Network in the Cochlea and Retina by Direct Association with USH2A and VLGR1. *Hum. Mol. Genet.* 15, 751-765.

van Wijk, E., Pennings, R. J. E., te Brinke, H., Claassen, A., Yntema, H. G., Hoefsloot, L. H., Cremers, F. P. M., Cremers, C. W. R. J. and Kremer, H. (2004). Identification of 51 Novel Exons of the Usher Syndrome Type 2A (USH2A) Gene that Encode Multiple Conserved Functional Domains and that are Mutated in Patients with Usher Syndrome Type II. *Am. J. Hum. Genet.* 74, 738-744.

Vennekens, R., Owsianik, G. and Nilius, B. (2008). Vanilloid Transient Receptor Potential Cation Channels: An Overview. *Curr. Pharm. Des.* 14, 18-31.

Virata, M. J. and Zeller, R. W. (2010). Ascidians: An Invertebrate Chordate Model to Study Alzheimer's Disease Pathogenesis. *Dis. Model. Mech.*, [Epub ahead of print].

Virginio, C., MacKenzie, A., Rassendren, F. A., North, R. A. and Surprenant, A. (1999). Pore Dilation of Neuronal P2X Receptor Channels. *Nat. Neurosci.* 2, 315-321.

Viswanath, V., Story, G. M., Peier, A. M., Petrus, M. J., Lee, V. M., Hwang, S. W., Patapoutian, A. and Jegla, T. (2003). Opposite Thermosensor in Fruitfly and Mouse. *Nature* 423, 822-823.

Voets, T., Talavera, K., Owsianik, G. and Nilius, B. (2005). Sensing with TRP Channels. *Nat. Chem. Biol.* 1, 85-92.

Wada, Y., Mogami, Y. and Baba, S. (1997). Modification of Ciliary Beating in Sea Urchin Larvae Induced by Neurotransmitters: Beat-Plane Rotation and Control of Frequency Fluctuation. *J. Exp. Biol.* 200, 9-18.

Wagenaar, M., van Aarem, A., Huygen, P., Pieke-Dahl, S., Kimberling, W. and Cremers, C. (1999). Hearing Impairment Related to Age in Usher Syndrome Types 1B and 2A. *Arch Otolaryngol. Head. Neck. Surg.* 125, 441-445.

Waguespack, J. R. and Ricci, A. J. (2005). Aminoglycoside Ototoxicity: Permeant Drugs Cause Permanent Hair Cell Loss. *J. Physiol.* 567, 359-360.

Walker, R. G., Willingham, A. T. and Zuker, C. S. (2000). A Drosophila Mechanosensory Transduction Channel. *Science* 287, 2229-2234.

Weber, W. and Dambach, M. (1974). Light-Sensitivity of Isolated Pigment Cells of the Sea Urchin *Centrostephanus Longispinus*. *Cell Tiss. Res.* 148, 437-440.

Weber, W. and Gras, H. (1980). Ultrastructural Observations on Changes in Cell Shape in Chromatophores of the Sea Urchin *Centrostephanus Longispinus*. *Cell Tiss. Res.* 206, 21-33.

Wei, Z., Angerer, R. C. and Angerer, L. M. (2006). A Database of mRNA Expression Patterns for the Sea Urchin Embryo. *Dev. Biol.* 300, 476-484.

Wersall, J., Bjorkroth, B., Flock, A. and Lundquist, P. G. (1973). Experiments on Ototoxic Effects of Antibiotics. *Adv. Otorhinolaryngol.* 20, 14-41.

Weston, M. D., Luijendijk, M. W. J., Humphrey, K. D., Möller, C. and Kimberling, W. J. (2004). Mutations in the VLGR1 Gene Implicate G-Protein Signaling in the Pathogenesis of Usher Syndrome Type II. *Am. J. Hum. Genet.* 74, 357-366.

Whittaker, C. A., Bergeron, K., Whittle, J., Brandhorst, B. P., Burke, R. D. and Hynes, R. O. (2006). The Echinoderm Adhesome. *Dev. Biol.* 300, 252-266.

Williams, D. S. (2008). Usher Syndrome: Animal Models, Retinal Function of Usher Proteins, and Prospects for Gene Therapy. *Vision Res.* 48, 433-441.

Winkel-Shirley, B. (2002). Biosynthesis of Flavonoids and Effects of Stress. *Curr. Opin. Plant Biol.* 5, 218-223.

Wise, G. E. (1969). Ultrastructure of Amphibian Melanophores After Light-Dark Adaptation and Hormonal Treatment. *J. Ultrastruct. Res.* 27, 472-485.

Wolfrum, U. (2003). The Cellular Function of the Usher Gene Product Myosin VIIa is Specified by its Ligands. *Adv. Exp. Med. Biol.* 533, 133-142.

Wolfrum, U., Liu, X., Schmitt, A., Udovichenko, I. P. and Williams, D. S. (1998a). Myosin VIIa as a Common Component of Cilia and Microvilli. *Cell Motil. Cytoskeleton* 40, 261-271.

Wolfrum, U., Liu, X., Schmitt, A., Udovichenko, I. P. and Williams, D. S. (1998b). Myosin VIIa as a Common Component of Cilia and Microvilli. *Cell Motil. Cytoskeleton* 40, 261-271.

Wolfrum, U. and Schmitt, A. (2000). Rhodopsin Transport in the Membrane of the Connecting Cilium of Mammalian Photoreceptor Cells. *Cell Motil. Cytoskeleton* 46, 95-107.

Woodley, J. D. (1982). Photosensitivity in *Diadema Antillarum*: Does it show Scototaxis?. In *The International Echinoderm Conference* (ed. J. M. Lawrence), pp. 61. Rotterdam: Balkema.

Wray, G. A. (1999). Introduction to Sea Urchins. In *Cell Lineage and Determination.* (ed. S. A. Moody), pp. 3-9. New York: Academic Press.

Wray, G. A., Kitazawa, C. and Miner, B. (2004). Culture of Echinoderm Larvae through Metamorphosis. In *Development of Sea Urchins, Ascidians, and Other Invertebrate Deuterostomes: Experimental Approaches* (ed. C. A. Ettensohn, G. M. Wessel and G. A. Wray), pp. 75-84. London: Elsevier Academic Press.

Xiao, B., Dubin, A. E., Bursulaya, B., Viswanath, V., Jegla, T. J. and Patapoutian, A. (2008). Identification of Transmembrane Domain 5 as a Critical Molecular Determinant of Menthol Sensitivity in Mammalian TRPA1 Channels. *J. Neurosci.* 28, 9640-9651.

Yaguchi, S., Kanoh, K., Amemiya, S. and Katow, H. (2000). Initial Analysis of Immunochemical Cell Surface Properties, Location and Formation of the Serotonergic Apical Ganglion in Sea Urchin Embryos. *Dev. Growth Differ.* 42, 479-488.

Yaguchi, S. and Katow, H. (2003). Expression of Tryptophan 5-Hydroxylase Gene during Sea Urchin Neurogenesis and Role of Serotonergic Nervous System in Larval Behavior. *J. Comp. Neurol.* 466, 219-229.

Yaguchi, S., Nakajima, Y., Wang, D. and Burke, R. D. (2006). Embryonic Expression of Engrailed in Sea Urchins. *Gene Expr. Patterns* 6, 566-571.

Yang, X. C. and Sachs, F. (1990). Characterization of Stretch-Activated Ion Channels in Xenopus Oocytes. *J. Physiol.* 431, 103-122.

Yerramilli, D. and Johnsen, S. (2010). Spatial Vision in the Purple Sea Urchin Strongylocentrotus Purpuratus (Echinoidea). *J. Exp. Biol.* 213, 249-255.

Yin, J. and Kuebler, W. M. (2010). Mechanotransduction by TRP Channels: General Concepts and Specific Role in the Vasculature. *Cell Biochem. Biophys.* 56, 1-18.

Yoder, B. K., Hou, X. and Guay-Woodford, L. M. (2002). The Polycystic Kidney Disease Proteins, Polycystin-1, Polycystin-2, Polaris, and Cystin, are Co-Localized in Renal Cilia. *J. Am. Soc. Nephrol.* 13, 2508-2516.

Yoshida, M. (1966). Photosensitivity. In *Physiology of Echinoderms*, pp. 435. New York: Interscience.

Zrada, S. E., Braat, K., Doty, R. L. and Laties, A. M. (1996). Olfactory Loss in Usher Syndrome: Another Sensory Deficit? *Am. J. Med. Genet.* 64, 602-603.

Zurborg, S., Yurgionas, B., Jira, J. A., Caspani, O. and Heppenstall, P. A. (2007). Direct Activation of the Ion Channel TRPA1 by Ca2+. *Nat. Neurosci.* 10, 277-279.